INOSITOL 1,3-ACETALS AS VERSATILE INTERMEDIATES FOR THE SYNTHESIS OF CYCLITOL DERIVATIVES

THESIS

SUBMITTED TO

SAVITRIBAI PHULE PUNE UNIVERSITY

FOR THE DEGREE OF

DOCTOR OF PHILOSOPHY

IN

CHEMISTRY

BY

RICHA SHARADCHANDRA SARDESSAI

RESEARCH SUPERVISOR

Dr. M. S. SHASHIDHAR

DIVISION OF ORGANIC CHEMISTRY

CSIR-NATIONAL CHEMICAL LABORATORY

PUNE 411 008, INDIA

FEBRUARY 2017

Dedicated to
Mamma, Pop and
Manik Kaka

CERTIFICATE

This is to certify that the work incorporated in the thesis entitled "**Inositol 1,3-acetals as versatile intermediates for the synthesis of cyclitol derivatives**" submitted by **Richa S. Sardessai** was carried out by her under my supervision at the National Chemical Laboratory, Pune, India. Such materials, obtained from other sources have been duly acknowledged in the thesis.

Date:

Division of Organic Chemistry
National Chemical Laboratory
Pune-411 008, India

(Dr. M. S. SHASHIDHAR)
Research Supervisor

National Chemical Laboratory, Pune (India)

DECLARATION

I hereby declare that the thesis entitled **"Inositol 1,3-acetals as versatile intermediates for the synthesis of cyclitol derivatives"** submitted for Ph.D. degree to the University of Pune has been carried out at National Chemical Laboratory, under the supervision of **Dr. M. S. Shashidhar**. This work is original and has not been submitted in part or full by me for any degree or diploma to any university.

Date:

Division of Organic Chemistry,
National Chemical Laboratory,
Pune-411 008

(RICHA S. SARDESSAI)

Acknowledgements

On completion of one of the most significant academic endeavour I have undertaken, I wish to thank all the people who have supported and encouraged me.

At the outset I wish to express my deep sense of gratitude and profound thanks to my research supervisor Dr.M. S. Shashidhar for not only mentoring me but for going above and beyond the call of duty. His meticulous and thorough style of working, kind heartedness, endless patience and humanitarianism are attributes I strive to take forward with me along with the chemistry that I learnt from him.

I would like to thank X-ray crystallography group, Dr. R. G. Gonnade and Dr. (Mrs.) Shobhana Krishnaswamy for their great help in determining the x-ray structures. I wish to express my gratitude to Dr. Kumar Vanka for teaching me theoretical (DFT) calculations. I would like to thank Prof. D. D. Dhavale for his valuable suggestions and scientific discussion during assessment of my Ph.D. work.

My sincere thanks to scientists of the division; Dr. P.K. Tripathi,(HOD) Dr. G. Pandey, Dr. N. N. Joshi, , Dr. S. P. Chavan, Dr. U. R. Kalkote, Dr. R. A. Joshi, Dr.(Mrs.) V. A. Kumar, Dr. N. P. Argade, Dr. G. J. Sanjayan, Dr. H. V. Thulasiram, Dr. C. V. Ramana, Dr. D. S. Reddy, Dr. R. P. Singh, Dr. Santosh Mhaske, Dr. S. Iyer, Dr.(Mrs.) A. P. Likhithe, Dr. (Mrs.) S. P. Maybhate, Dr. Muthukrishnan, Dr. A. T. Biju and others. I wish to thank Dr. P. A. Joy, Mrs. Puranik and Mrs. Kolhe (SAC office) for their help. Help from analytical units for characterization of compounds is gratefully acknowledged. I thank Dr. Rajmohanan for NMR, Mrs. Damse, for IR facility Mrs. S. P. Kunte, for HPLC, Dr. P. L. Joshi (and Mrs. Sawant, Mrs. Sanas) for microanalysis Dr.(Mrs.) Shanthakumari, Pranali Jadhav and Bhushan for HRMS.

I am forever indebted to my from school teachers, Mrs. Maragaret and Mrs. Lopes; college teachers, Dr. Udai Naik, Dr. Vrinda Borkar, Varsha Ma'am, Sonia Ma'am, Suchana Ma'am, Deepa Ma'am; M. Sc. teachers, Prof. Tilve, Prof. S. P. Kamat, and Prof. V. P. Kamat, for their impeccable teaching.

It gives me immense pleasure to express my sincere thanks to my senior colleagues; Dr. (Mrs.) Madhuri Patil, Dr. Rajendra Jagdhane, Dr. Shailesh Dixit, Dr. Bharat Gurale, Dr. Alson Mart, and especially Dr. Tamboli Majid for their friendly nature,and for the excellent training, valuable discussion and support I received from them. I am also deeply grateful to Dr. Manmath Patil, Dr. Ravi Jagtap and Dr. Revannath Sutar for their help. I am thankful to my labmates Veer, Nivedita, Nitai, Nilesh, Niharika, Rohit, Santosh, Amartyo, Priyadarshini, Parmeshwari, Aleena, and Archana, for maintaining cheerful atmosphere in the lab. I also am grateful to my extended lab members Ekta, Sridhar, Samir, Pranaya, Debamitra, Rupesh for all their help in crystallography. I would like to thank Moreji for help and lab maintenance.

I would like to thank Dr. (Mrs.) Vidya Shashidhar, Mrs. Vaishali Gonnade, Dr. (Mrs.)Vedavati Puranik and Mrs. Nandini Dixit for their advices and help.

I am most grateful to my friends from NCL, Dr. Roshana and Dr. Remya (fellow tea enthusiast) for their support, encouragement and friendship. I wish to thank all my friends at NCL, Dr. Gouri Priya, Dr. Priyanka, Kiran Jawade, Dr.Atul, Dr. Pravat, Dr. Kiran, Dr. Kailash, Dr. Bhausaheb, Dr. Deepak , Dr. Ankush, Dr. Seema, Rincy Raju, Nilofer, Kritika, Shiva Kumara, Krishna Prasad, Suresh, Ragini, Manisha,Vishwnadh (adopted junior), Nishamole, Arati, Shakuntala, Reema, Rashmi, Sneha B. Sanjeev, Sachin, Rahul, Akshay, Vasudevan, Kashinath, Gajanan, Vidya, Rohini, Sneha, Bindu Baby, Anshu, Jaya, Pushpanjali, Leena, and my room mates Soumya, Rubina,Prajitha, Meenal, Himani, Monika, Sumana, for keeping my spirits up outside the lab.

I wish to thank my friends Nancy, Shawn, Archit, Pranay, Sonali, Mira, Sandesh, Amit, Hari and seniors Dr. Gayatri and Dr. Priyanka for always being with me through thick and thin.

I wish to sincerely thank Sawant kaka and family for their never ending support at each and every step. I also wish to thank Uday kaka, Anna and (late)Naveen kaka and their families for their love.

Words will never be enough to appreciate the love and blessings I have received from my family: (late) Kashi kaka, Sucha Baba, Jyotsna atya, (late) Pendya baba, Vinod atya, Raghu Mauso, Lalu maushi, Anand Mama, Vishnudas Mauso, Shobha Maushi, Sunil Mauso, Utai, Baburao Mama, Neelam Mami, Nandan Mauso, Mitai , Sucha, Ujja, Pondu, Parag Bhaiyya, Vinda, Vishwesh, Laxmi, Suraj, Sujay, Raunak, Parth, Ved and Agastya.

I wish to especially thank Manik kaka for his constant support, advise, love, and encouragement at every juncture. I am indescribably indebted to Mamma and Pop for their selfless love, hardships, sacrifice, encouragement, support and for teaching me that a strong will and an optimistic outlook can move mountains. They have been the wind beneath my wings and pushed me to pursue my dreams without inhibitions.

Finally, though I may not be of a large enough stature, I wish to thank the Prime Mover in the grand scheme of life for both; the blessings and the blessings in disguise.

February 2017 *Richa*

CONTENTS

Abbreviations

Ac	Acetyl
AcBr	Acetyl bromide
Ac_2O	Acetic anhydride
AcCl	Acetyl chloride
AIBN	Azobisisobutyronitrile
All	Allyl
Anhd.	Anhydrous
aq.	Aqueous
Bn	Benzyl
BnBr	Benzyl bromide
BuLi	Butyl lithium
Calcd	Calculated
Cat.	Catalytic
Concd	Concentration
CSA	Camphorsulfonic acid
COSY	Correlation Spectroscopy
DCC	N,N'-Dicyclohexylcarbodiimide
D_2O	Deuterium Oxide
DCM	Dichloromethane
DDQ	2,3-Dichloro-5,6-dicyano-1,4-benzoquinone
DFT	Density Functional Theory
DIBAL-H	Diisobutyl aluminium Hydride
dil.	Dilute
DIPEA	Di-isopropyl ethyl amine
DMAP	*N, N*-dimethylamino pyridine
DMF	*N, N*-Dimethylformamide
DMSO	Dimethyl sulfoxide
eq.	Equivalent
EDC·HCl	1-Ethyl-3-(3-dimethyllaminopropyl)carbodiimide hydrochloride
Et_3N	Triethylamine

g	Gram
GPI	Glycophosphatidylinositol
h	Hour (s)
Hz	Hertz
*i*BuNH$_2$	*iso*-Butyl amine
IBX	2-Iodoxybenzoic acid
IR	Infrared
LC-MS	Liquid chromatography-mass spectrometry
Mp	Melting point
Me	Methyl
MeOH	Methanol
MeI	Methyliodide
Mes	Mesityl
mg	Milli gram
min.	Minute(s)
mL	Milliliter
mmol	Milli moles
$NaBH_4$	Sodium borohydride
NaN_3	Sodium azide
NaOMe	Sodium methoxide
NMR	Nuclear magnetic Resonance
ORTEP	Oak Ridge Thermal Ellipsoid Plot Program
$Pd(PPh_3)_4$	Tetrakis(triphenylphosphine)palladium
Ph	Phenyl
PI-PLC	Phosphatidylinositol-specific phospholipase C
PMB	4-Methoxy benzyl
PCB	4-Chloro benzyl
PBB	4-Bromo benzyl
PIP_3	Phosphatidylinositol-3,4,5-tris-phosphate
Py	Pyridine
rac-	Racemic
rt	Room temperature (23–30 ^oC)

TMS	Trimethylsilyl
TMSOTf	Trimethylsilyl triflate
TFA	Trifluoroacetic acid
TFAA	Trifluroacetic anhydride
Tf_2O	Trifluoromethanesulfonic anhydride
THF	Tetrahydrofuran
TLC	Thin layer chromatography
TsCl	4-Toluene sulfonyl chloride
TsOH	4-Toluene sulfonic acid

SYNOPSIS OF THE THESIS

Introduction:

The thesis entitled '**Inositol 1,3 acetals as versatile intermediates for the synthesis of cyclitol derivatives**' consists of four chapters. Chapter 1 is a review of literature reports on the synthetic potential and utility of 1,3-acetals, with emphasis on *myo*-inositol 1,3-acetals. The latter have been used for the synthesis of biologically or medicinally relevant natural products, natural and unnatural inositol derivatives such as phosphoinositols and their analogs. Chapter 2 deals with the study of the effect of the orthoester moiety on regioselective reductive cleavage of *myo*-inositol orthoesters to the corresponding 1,3-acetals by DIBAL-H. Chapter 3 investigates the role of the 1,3-acetal bridge during the selective nucleophilic addition to the ketone in *myo*-inositol-1,3-acetal derivatives. Chapter 4 highlights the stabilization of racemic 4-*O*-benzyl-*myo*-inositol-1,3,5-orthoformate molecules in their crystal; this benzyl ether is a key intermediate for the synthesis of phosphoinositols, and other inositol derivatives.

Chapter 1. A review on the synthetic utility of inositol 1,3-acetals.

myo-Inositol and its derivatives / analogs have become conspicuous in the literature related to chemistry and biology due to the involvement of phosphoinositols in cellular signal transduction mechanisms and anchoring of certain proteins to cell membranes.[1] However, the intricacies and biological implications of the *myo*-inositol cycle are not yet fully unraveled. Many synthetic methodologies and techniques have been developed in the recent past for the synthesis of inositol derivatives useful in the study of the inositol cycle. Some of these methods have also been used for the synthesis of natural products (other than inositol derivatives) and their analogs.[2]

1,2 acetal derivatives **2**–**4** (Scheme 1) of *myo*-inositol have been frequently used as early intermediates for the synthesis of various classes of compounds mentioned above, although the acetalization of *myo*-inositol (**1**) often leads to the formation of isomeric acetals **2**-**4**, which have to be separated by chromatography.

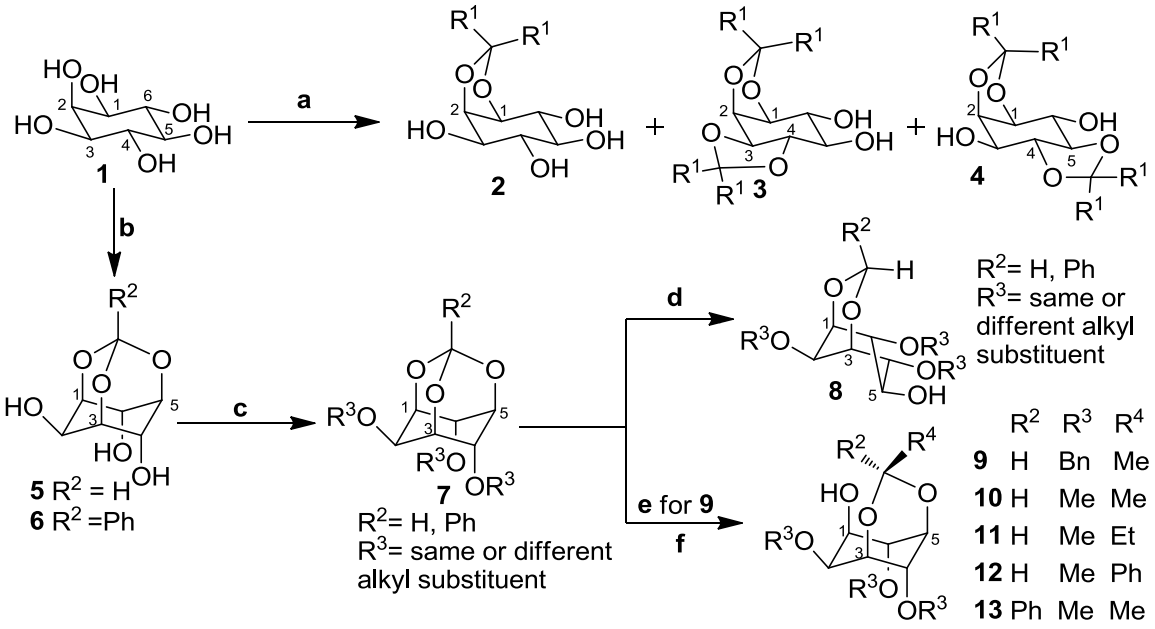

Scheme 1. (a) DMF, R^1COR^1, TsOH; (b) DMF, $R^2C(OEt)_3$ or $R^2C(OMe)_3$, TsOH, 110-140 °C; (c) DMF, NaH or LiH, alkyl halide; (d) DCM, DIBAL-H (2.2 eq), rt; (e) DCM, Me_3Al, rt; (f) benzene, R^4MgX (2 eq), reflux.

In contrast, the *myo*-inositol orthoesters **7** can be prepared as sole products in good yields. The differentially protected *myo*-inositol 1,3-acetals **8**–**13** can be obtained *via* the reductive cleavage of *O*-protected orthoester derivatives of *myo*-inositol. The acetals **8** can be obtained by reduction[3,4] of **7** with DIBAL-H while acetals **9**-**13** can be obtained by cleavage of **7** with trimethylaluminium[4] or Grignard reagents.[5] There does not appear to be any report on the preparation of *myo*-inositol derived 1,3-acetals from the corresponding 1,3-diols by classical acid catalyzed ketalization reactions. These bridged acetals provide opportunities (Figure 1) for new selective reactions (of the inositol hydroxyl groups) since conformation of the two six membered rings deviate from the normal chair conformation.

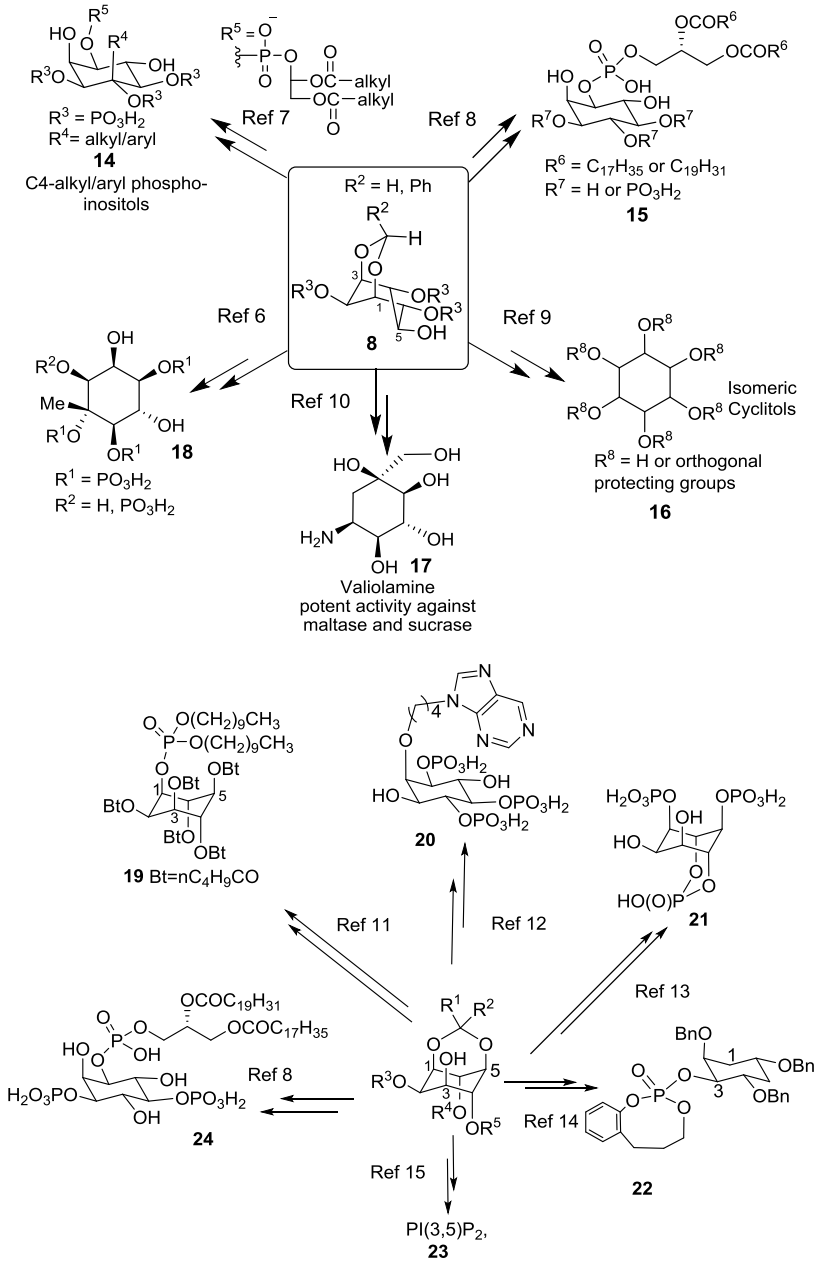

Figure 1. Synthetic utility of *myo*-inositol derived 1,3 acetals

Hence, 1,3-acetals of *myo*-inositol derivatives have the potential to emerge as useful intermediates for the preparation of many biologically relevant inositol derivatives.

The contents of this chapter have been published. B. P. Gurale, R. S. Sardessai, M. S. Shashidhar, *myo*-Inositol *1,3*-acetals as early intermediates during the synthesis of cyclitol derivatives, *Carbohydr. Res.* **2014**, *399*, 8-14. http://dx.doi.org/10.1016/j.carres.2014.08.010

Chapter 2. A study of the regioselectivity of the reductive cleavage of *myo*-inositol orthoesters with DIBAL-H.

As discussed in chapter 1 the cleavage of *myo*-inositol orthoformate by trimethyl aluminium or Grignard reagent generates the 1,3-acetals **34-42** whereas cleavage by DIBAL-H generates the 1,3 acetals **43-51** as major products.[4,16-22]

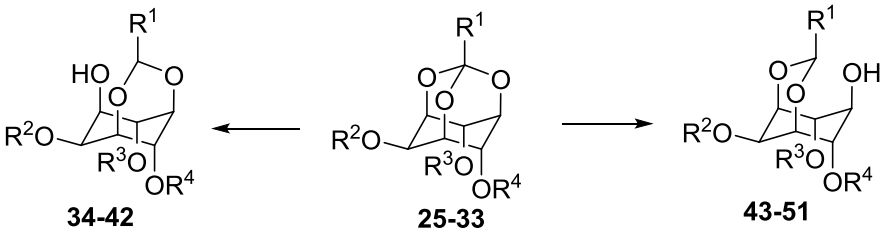

25, **34**, **43** R^1=H, R^2= R^3= R^4=Bn
26, 35, **44** R^1=H ,R^2=TBDMS, R^3=R^4=Bn
27, **36**, **45** R^1=H, R^2=R^3=Bn, R^4=PMB
28, **37**, **46** R^1=Ph, R^2=R^3=R^4=Bn
29, **38**, **47** R^1=H, R^2=R^3= R^4=PMB
30, **39**, **48** R^1=Ph, R^2=R^3=R^4=All
31, **40**, **49** R^1=H, R^2=PMB, R^3=R^4=Bn
32, **41**, **50** R^1=Ph,R^2=PMB, R^3=R^4=Bn
33, **42**, **51** R^1=Ph, R^2=PBB, R^3=PMB, R^4=All

Scheme 2: Reductive cleavge of *myo*-inositol orthoesters.

Close scrutiny of the reports indicated (due to lack of material balance) that in most reports the 1,3-acetals **43-51** may not have formed exclusively. The results could not be compared to get an insight into the regioselectivity of this reductive cleavage since the experimental conditions were not comparable. Hence in order to obtain a deeper insight into this aspect, *myo*-inositol orthoesters which vary only at the apical orthoester substituent were prepared and their reductive cleavage with DIBAL-H studied under comparable conditions. *myo*-inositol orthoesters **56-58** were prepared and subjected to cleavage by DIBAL-H and the results are shown in Scheme 3.

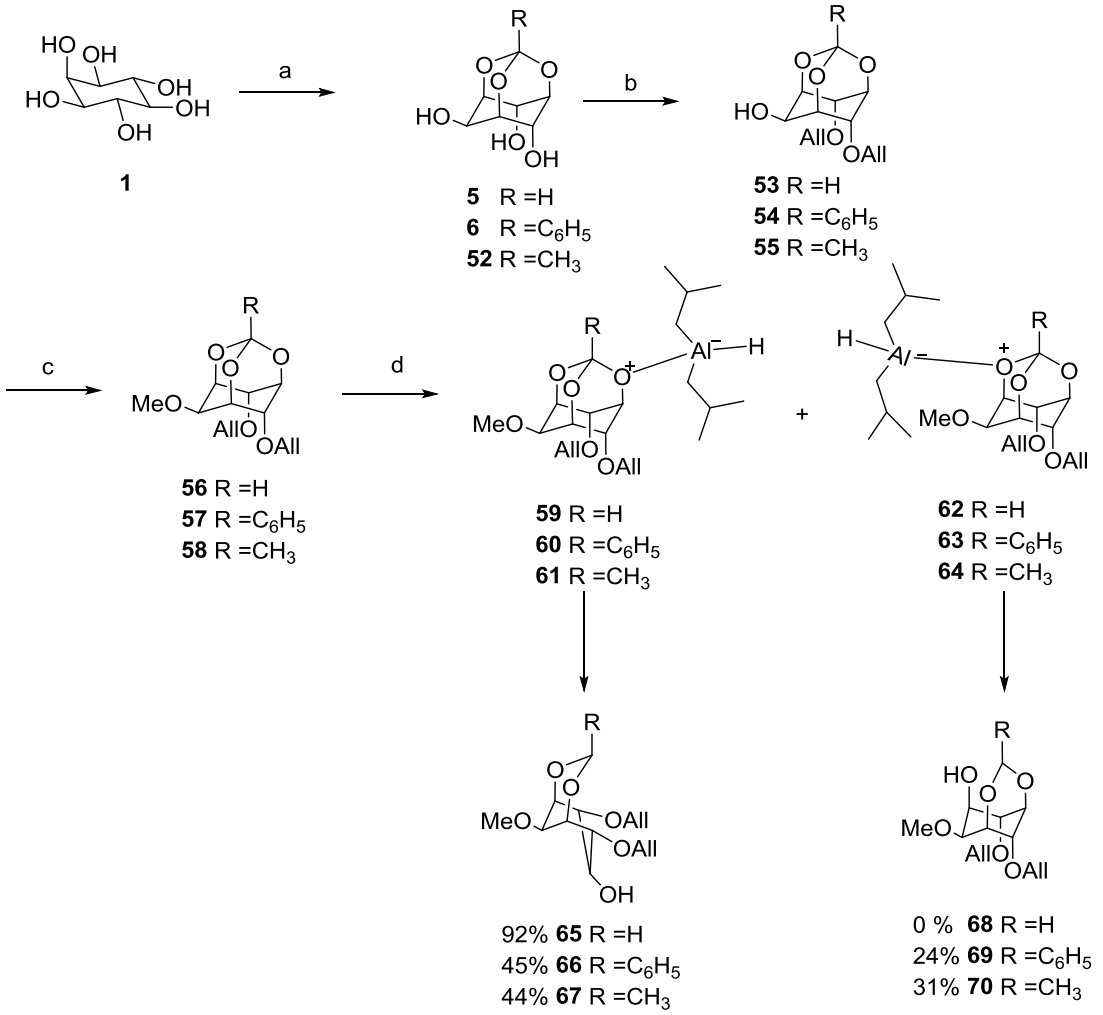

Scheme 3. (a) DMF, $RC(OEt)_3$ or $RC(OMe)_3$, TsOH, 110-140 °C, 70-90%; (b) DMF, LiH, AllBr, 24h, 60-80% ; (c) DMF, NaH, MeI, 24h, 60-80% (d) dry DCM, DIBAL-H (2.5eq), 2.5h, 0 °C TO RT, 65-92 %.

The results clearly indicated that selectivity for the formation of the 1,3-acetals **65-67** decreased on going from orthoformate to orthobenzoate to orthoacetate. DFT calculations were carried out to estimate the relative stability of the possible DIBAL-H complexes **59-64** that lead to the isomeric 1,3-acetals (Scheme 3). The results revealed that the difference in stability between the two different complexes increases as the orthoester group changes from orthoformate to orthobenzoate to orthoacetate (Figure 2). This is in concurrence with the trend of the decreasing regioselectivity observed. This implies that as the orthoester group becomes streically challenged the regioselctivity of the reduction suffers.

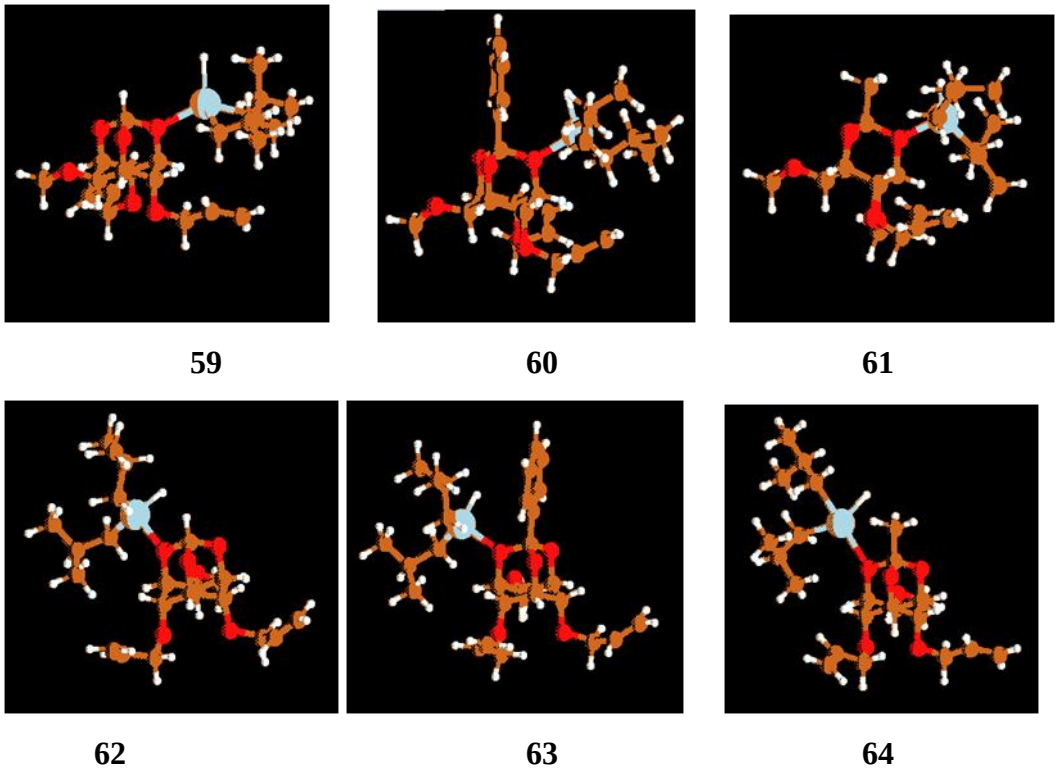

Figure 2: Energy minimized structures of the DIBAL-H complexes of the orthoesters. $\Delta E_{59\text{-}62}$= 1.5 Kcals/mole; $\Delta E_{60\text{-}63}$ = 2.1Kcals/mole; $\Delta E_{61\text{-}64}$ =2.6 Kcals/mole**.**

For the orthoacetate, since the difference in energy between the two DIBAL-H complexes is higher, the rate of inter- convertibility is much less, and each intermediate perhaps has enough time to form the respective cleavage product, giving rise to the almost equitable mixture. In contrast, for the orthoformate, since the difference in energy between the two DIBAL-H complexes is lower, the rate of inter-convertibility is much higher, and if one DIBAL-H complex (**59**) gets reduced faster than the other (**62**), the reductive cleavage can result in very high regio-selectivity. The effective bulk of the phenyl ring being intermediate between that of H and Me (owing to its planarity), the observed selectivity for the reductive cleavage of the orthobenzoate is between that of the orthoformate and the orthoacetate.

Chapter 3. **Investigations to delineate the role of the 1,3 acetal bridge in inososes for nucleophilic addition to the carbonyl group.**

Inososes form important intermediates for the synthesis of many biologically important cyclitol derivatives (**Figure 3).**

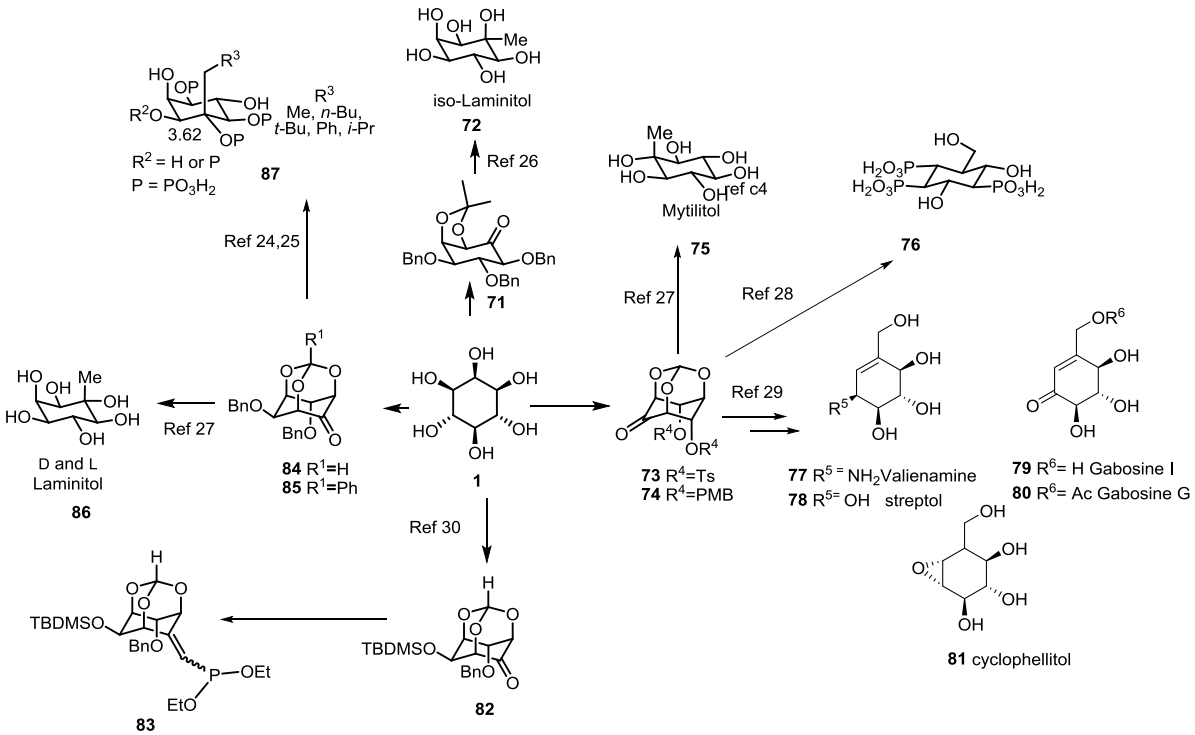

Figure 3: Synthetic utility of the inositol derived ketones.

Previous work in our laboratory had shown that the addition to inositol derived ketones containing a 1,3 acetal bridge led to the formation of a single product (Scheme 4). This chapter seeks to investigate the role played by the 1,3-acetal bridge in this highly selective addition reaction.

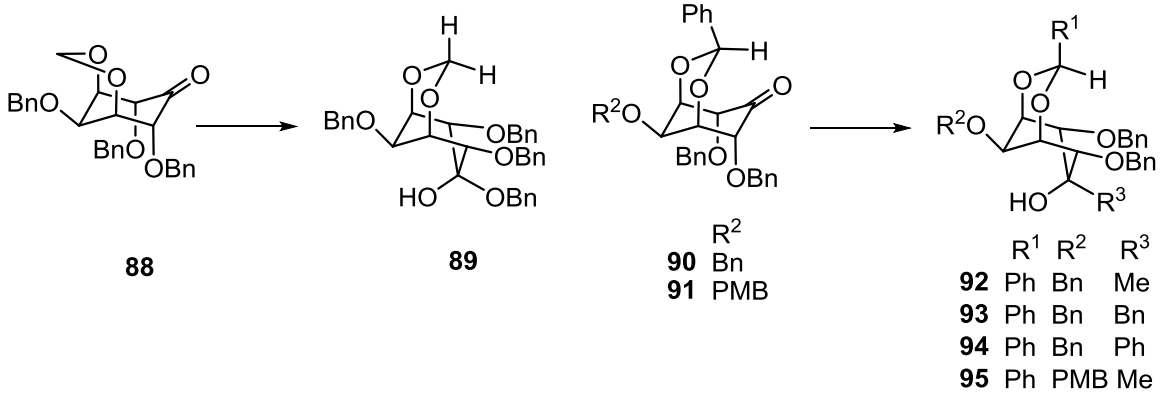

Scheme 4. Diethyl ether, R^3MgBr, -10 °C, 2 h, 90-94%

In order to ascertain the role of the 1,3 acetal bridge, the the ketone **101** without the 1,3 acetal bridge was prepared and subjected to hydride reduction as well as Grignard reaction.

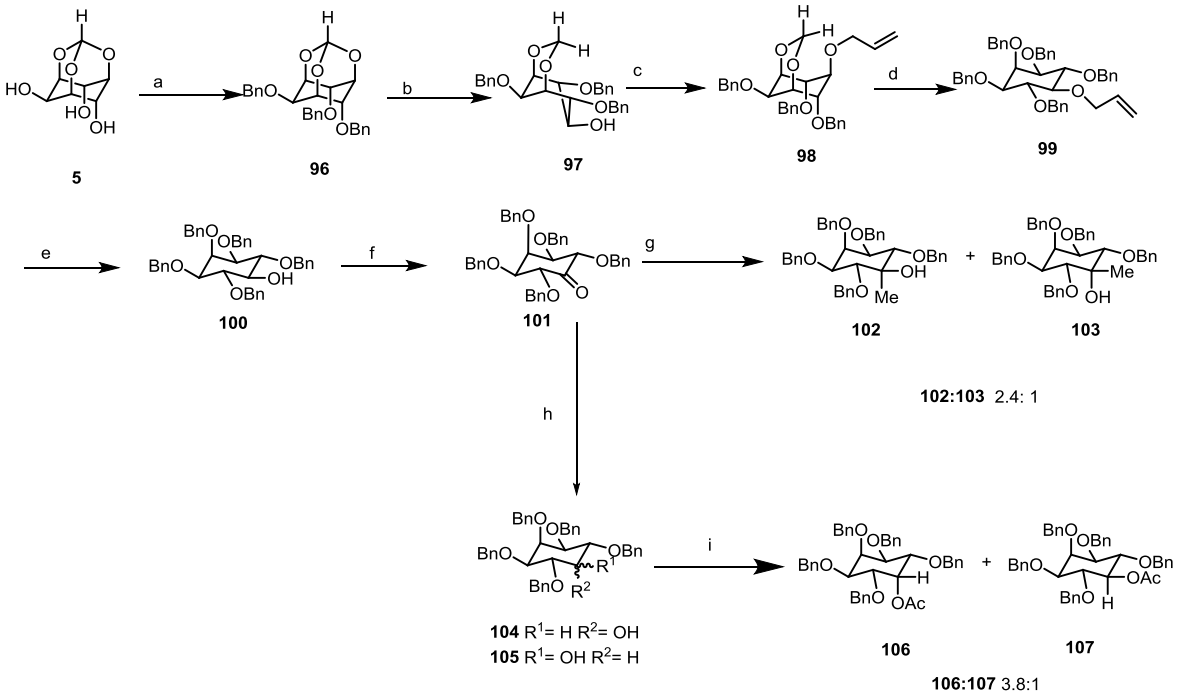

Scheme 5 (a) DMF, NaH, BnBr, rt, 3 h, 92%; (b) DCM, DIBAL-H, 0 °C-rt, 90%; (c) DMF, NaH, AllBr, rt, 3 h, 92%; (d) (i) HCl, MeOH, 12h; (ii) DMF, NaH, BnBr, rt, 3 h, 82% over 2 steps; (e)ethanol, anhy. K_2CO_3, $Pd(PPh_3)_4$, reflux, 48h, 86%, (f) EtOAc, IBX, 6h, 96%; (g) toluene, MeMgI, rt, 1h, (h)MeOH, $NaBH_4$, reflux, 24h; (i)Pyridine, Ac_2O, DMAP, 48h, RT.

As shown in Scheme 5, both these reactions resulted in the formation of a mixture of products. These results conclusively established the role of the acetal bridge in directing selective addition to the carbonyl group. The precursor **100** for the ketone **101** was extremely difficult to generate from the allyl ether **99**. Various attempts to cleave the allyl ether were unsuccessful due to the steric crowding around the allyl group, as revealed by single crystal X-ray diffraction analysis (of **99** and **100**). In some experiments, the cleavage of the allyl ether in **99** was concomitant with the cleavage of the benzyl group to yield a complex mixture of products.

Chapter 4. Achieving molecular stability of racemic 4-O-benzyl-*myo*-inositol-1,3,5-orthoformate through crystallization.

This chapter describes the stabilization of racemic 4-O-benzyl-*myo*-inositol orthoformate (**108**) through crystal formation. The racemic monobenzyl ether **108** is an important intermediate in the synthesis of many biologically important inositol derivatives (Figure 4).

However racemic **108** (a gummy compound as reported in the literature) is inherently unstable when left in the gummy state and hence cannot be stored over long periods of time without compromising on its purity. We needed to prepare bulk quantities of **108** as a part of an ongoing program on the study of regioselective reactions in *myo*-inositol orthoesters. A survey of the literature reports indicated that most of the 4-O-substituted *myo*-inositol orthoformates were stable solids. Hence we wondered whether the stability of racemic **108** would improve if it could be coaxed to form crystals. We also carried out experiments to investigate the cause of instability of racemic **108** in the gummy state. This required the comparison of the stability of the orthoacetate and orthobenzoate analogs of **108**. Gist of all these experiments is shown in Scheme 6. Our investigations revealed that in the gummy state orthoester moiety is cleaved, to form the corresponding hydroxyl esters. These esters prevent crystallization of racemic **108** and hence cause further decomposition. However, in the crystalline state racemic **108** is stable and can be stored over extended period of time.

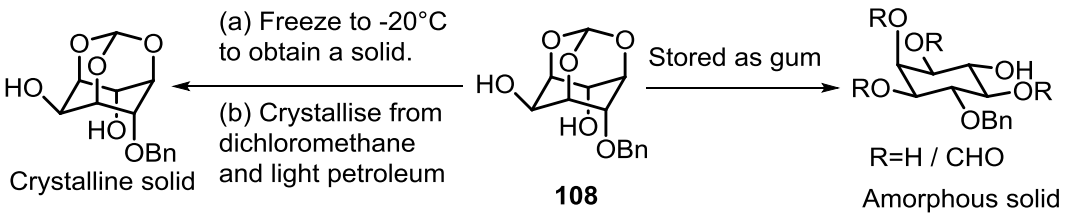

Scheme 6.

Results presented in this chapter are published. R. Sardessai, S. Krishnaswamy, M. S. Shashidhar, Achieving molecular stability of racemic 4-*O*-benzyl-*myo*-inositol-1,3,5-orthoformate through crystal formation, *CrystEngComm*, **2012**, *14*, 8010 - 8016. DOI: 10.1039/C2CE26199E

Results presented in this chapter are published. R. Sardessai, S. Krishnaswamy, M. S. Shashidhar, Achieving molecular stability of racemic 4-*O*-benzyl-*myo*-inositol-1,3,5-orthoformate through crystal formation, *CrystEngComm*, **2012**, *14*, 8010 - 8016. DOI: 10.1039/C2CE26199E

References :

1. a) B. V. L. Potter, *Comprehensive Medicinal Chemistry*, Vol 4, Pergamon Press 1990; b) D. C. Billington, *The Inositol Phosphates: Chemical synthesis and biological significance*. VCH, New York, N.Y. 1993; c) K. Hinchliffe, R. Irvine, *Nature*, **1997**, *390*, 123; d) M. A. J. Ferguson, A. F. Williams, *Annu. Rev. Biochem.* **1988**, *57*, 285; e) *Phosphoinositides: chemistry, biochemistry and biochemical applications*, K. S. Bruzik, Ed.; ACS symposium series 718. American chemical society, Washington D.C. USA, 1999.
2. a) J. Duchek, D. R. Adams, T. Hudlicky, *Chem. Rev.* **2011**, *111*, 4223 and references cited there in; b) S. Pilgrim, G. Kociok-K€ohn, M. D. Lloyd, S. E. Lewis, *Chem. Commun.* **2011**, *47*, 4799.
3. I. H. Gilbert, A. B. Holmes, M. J. Pestchanker, R. C. Young, *Carbohydr. Res.* **1992**, *234*, 117.
4. C. Murali, M. S. Shashidhar, C. S. Gopinath, *Tetrahedron*, **2007**, *63*, 4149.
5. S-M. Yeh, G. H. Lee, Y. Wang, T-Y. Luh, *J. Org. Chem.* **1997**, *62*, 8315.
6. Swarbrick, J. M.; Gaffney, P. R. J. *J. Org. Chem.* **2010**, *75*, 4376–4386.
7. Swarbrick, J. M.; Cooper, S.; Bultynck, G.; Gaffney, P. R. J. *Org. Biomol. Chem.* **2009**, *7*, 1709–1715.
8. Conway, S. J.; Gardiner, J.; Grove, S. J. A.; Johns, M. K.; Lim, Z.-Y.; Painter, G. F.; Robinson, D. E. J. E.; Schieber, C.; Thuring, J. W.; Wong, L. S. M.; Yin, M.-X.; Burgess, A. W.; Catimel, B.; Hawkins, P. T.; Ktistakis, N. T.; Stephens, L. R.; Holmes, A. B. *Org. Biomol. Chem.* **2010**, *8*, 66–74
9. Jagdhane, R. C.; Shashidhar, M. S. *Eur. J. Org. Chem.* **2010**, 2945–2953.
10. Jagdhane, R. C.; Shashidhar, M. S. *Tetrahedron*, **2011**, *67*, 7963–7970.
11. Song, F.; Zhang, J.; Zhao, Y.; Chen, W.; Lib, L.; Xi, Z. *Org. Biomol. Chem.* **2012**, *10*, 3642-3654.
12. Moris, M. A.; Caron, A. Z.; Guillemette, G.; Rognan, D.; Schmitt, M.; Schlewer, G. *J. Med. Chem.* **2005**, *48*, 1251–1255.
13. Garrett, S. W.; Liu, C.; Riley, A. M.; Potter, B. V. L. *J. Chem. Soc. Perkin Trans 1*, **1998**, 1367–1368.
14. Ballereau, S.; Poirier, S. N.; Guillemette, G.; Spiess, B.; Schlewer, G. *J. Chem.Soc., Perkin Trans. 1*, **1998**, 1859–1864.
15. Eisch, J. J.; Rhee, S. G. *J. Am. Chem. Soc.*, **1974**, *96*, 7276–7284.

16. Gilbert, I. H.; Holmes, A. B.; Young, R. C. *Tetrahedron Lett*. **1990**, *31*, 2633–2634.

17. Gilbert, I. H.; Holmes, A. B.; Pestchanker, M. J.; Young R. C. *Carbohydr. Res.* **1992**, *234*, 117–130.

18. Grove, S. J. A.; Gilbert, I. H.; Holmes, A. B.; Painter, G. F.; Hill, M. L. *Chem. Commun.* **1997**, 1633–1634.

19. Capolicchio, S.; Thakor, D. T.; Linden, A.; Jessen, H. J. *Angew. Chem. Int. Ed.* **2013**, *52*, 6912-6916.

20. Mart, A; Shashidhar, M. S. *Tetrahedron*, **2012**, *68*, 9769-9776.

21. Jagdhane, R. C.; Shashidhar, M. S. *Tetrahedron*, **2011**, *67*, 7963–7970.

22. Gurale, B. P.; Krishnaswamy, S.; Vanka, K.; Shashidhar, M. S. *Tetrahedron*, **2011**, *67*, 7280-7288.

23. Jagdhane, R. C.; Shashidhar, M. S. *Eur. J. Org. Chem.* **2010**, 2945–2953.

24. Swarbrick, J. M.; Cooper, S.; Bultynck, G.; Gaffney, P. R. J. *Organic & Biomolecular Chemistry*, **2009**, *7*, 1709.

25. Swarbrick, J. M.; Gaffney, P. R. J. *The Journal of Organic Chemistry*, **2010**, *75*, 4376.

26. Gigg, J.; Gigg, R. *Carbohydrate Research*, **1997**, *299*, 77.

27. Sarmah, M. P.; Shashidhar, M. S.; Sureshan, K. M.; Gonnade, R. G.; Bhadbhade, M. M. *Tetrahedron*, ***2005***, *61*, 4437.

28. Riley, A. M.; Murphy, C. T.; Lindley, C. J.; Westwick, J.; Potter, B. V. L. *Bioorganic & Medicinal Chemistry Letters*, **1996**, *6*, 2197.

29. Mondal, S.; Prathap, A.; Sureshan K. M. *J. Org. Chem.*, **2013**, *78*, 7690−7700.

30. Song, F.; Zhang, J.; Cui, Q., Wang, T.; Chen, W.; Li, L.; Xi Z. *Tetrahedron Lett.*, **2012**, *53*, 1102–1104.

31. Baudin, G.; Glänzer, B. I.; Swaminathan, K. S.; Vasella, A. *Helv. Chim. Acta*, **1988**, *71*, 1367-1378.

32. Kim, S.; Lee, S.l; Cheong, C. *Bull. Korean Chem. Soc.*, **2004**, *25*, 1578-1580.

33. Sato, K.; Akai, S.i; Sugita, N.; Ohsawa, T.; Kogure, T.; Shoji, H.; Yoshimura, J. *J. Org. Chem.*, **2005**, *70*, 7496-7504.

List of publications and posters

1. **Sardessai, R. S.**; Krishnaswamy, S.; Shashidhar, M. S. 'Achieving molecular stability of racemic 4-*O*-benzyl-*myo*-inositol-1,3,5-orthoformate through crystal formation' *CrystEngComm*, **2012**, **DOI:** 10.1039/C2CE26199E.

2. Gurale, B. P.; **Sardessai, R. S**.; Shahsidhar, M. S. ' *myo*-Inositol *1,3*-acetals as early intermediates during the synthesis of cyclitol derivatives. ' *Carbohydr Res.* **2014** http://dx.doi.org/10.1016/j.carres.2014.08.010

3. **Sardessai, R. S.**; Shashidhar, M. S. ' A study of the regioselectivity of the reductive cleavage of *myo*-inositol orthoesters with DIBAL-H. ', *manuscript under preparation.*

Poster Presentations

1. Achieving molecular stability of racemic 4-*O*-benzyl-*myo*-inositol-1,3,5-orthoformate through crystal formation. **Richa S. Sardessai**, Mysore S. Shashidhar, presented at National Science Day, NCL, 2013.

2. Study of the regioselectivity of DIBAL cleavage of inositol orthoesters
   Richa S. Sardessai, Mysore S. Shashidhar , presented at National Science Day, NCL, 2014 and 10th J-NOST Conference held at IIT Madras 2014.

Chapter 1

A review on the synthetic utility of inositol *1,3*-acetals

This chapter is published in– Gurale, B. P; Sardessai, R. S., *Carbohydr. Res.* **2014**, *399*,8-14. http://dx.doi.org/10.1016/j.carres.2014.08.010

1.1. Introduction

myo-Inositol and its derivatives / analogs have become conspicuous in the literature related to chemistry and biology due to the involvement of phosphoinositols in cellular signal transduction mechanisms and anchoring of certain proteins to cell membranes.[1-5] Realization of the fact that the production and destruction of pyrophosphates of inositol are highly regulated by enzymes in living cells (bacteria to mammals) has recently augmented the interest in the synthesis of phosphorylated inositol derivatives and their analogs.[6-8] Phosphatidylinositol (**1.2**) is a component of mammalian cell membranes. Phosphorylated derivatives of **1.2** play fundamental role in a multitude of cellular processes.[9] Derivatives of inositols other than phosphoinositols are also important since several of them occur in nature. Amino derivatives of inositols are present in antibiotics[10-13] and a few others act as glycosidase inhibitors.[14-16] Illustrative examples of natural products and biologically active compounds containing cyclitol moiety as the main core are shown in Chart 1.

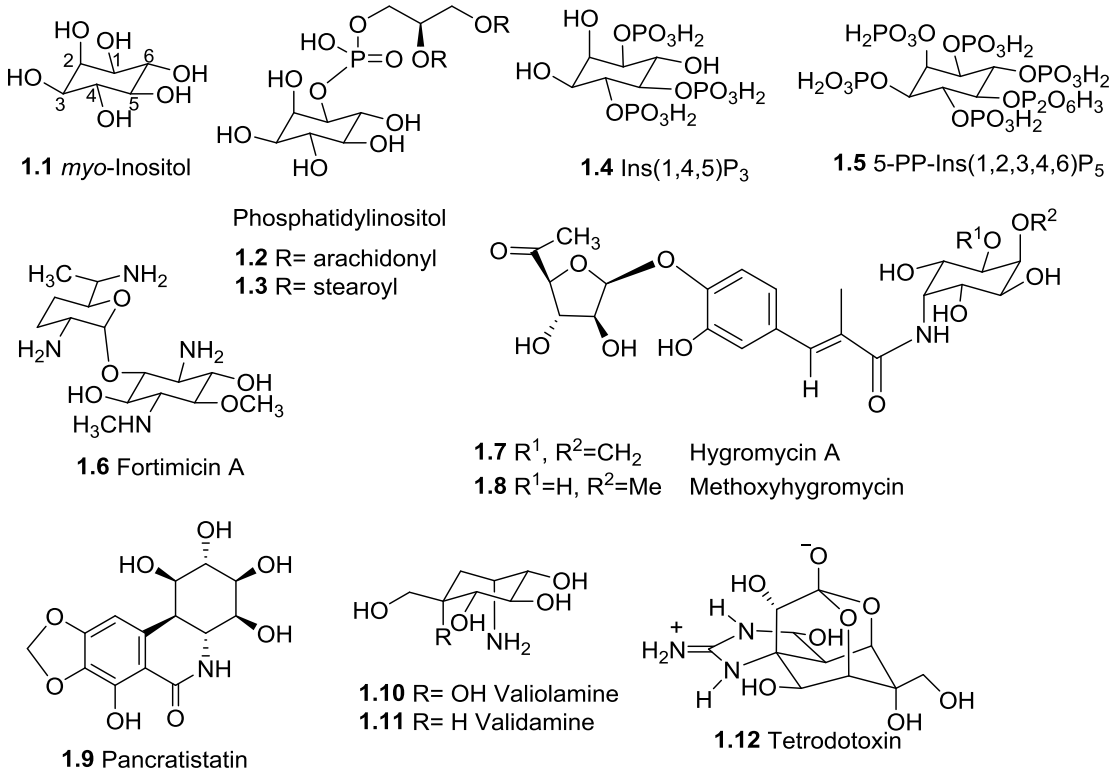

Chart 1. Structure of natural products containing inositol moieties.

Interestingly, *myo*-inositol does not occur in the free-state in nature. Perhaps, the most abundant naturally occurring *myo*-inositol derivative is phytic acid (*myo*-inositol hexakisphosphate), which is present in larger quantities in plants. Nine isomers of

inositol (1,2,3,4,5,6-hexahydroxy cyclohexane) are reported in the literature (Chart 2). All of them, except the *chiro*-inositol have the *meso*-configuration. Enantiomeric derivatives of *chiro*-inositol (pinitol and quebrachitol) occur in nature. *myo*-Inositol (**1.1)**, has five equatorial hydroxyl groups and an axial hydroxyl group with a plane of symmetry passing through two carbon atoms.

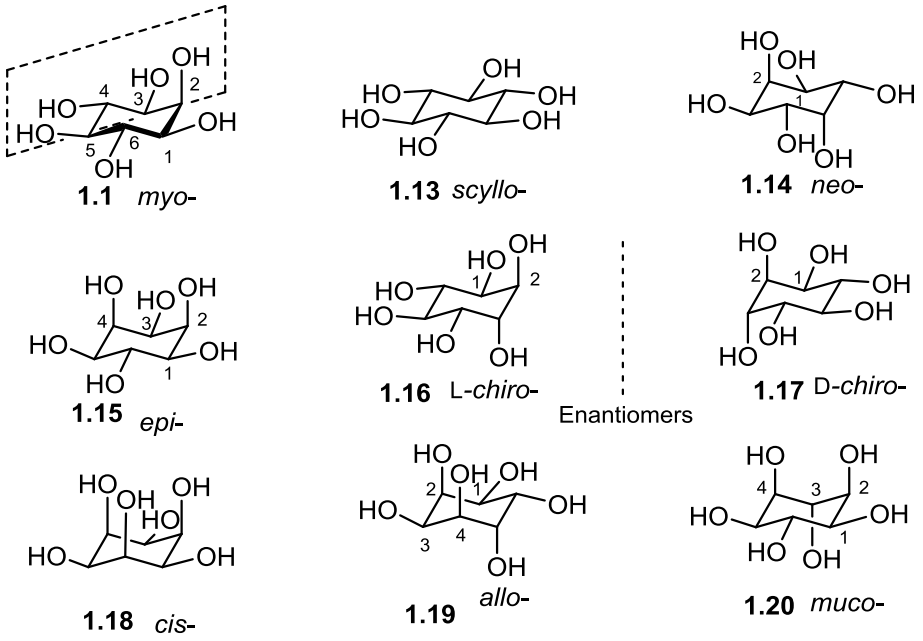

Chart 2. Reported isomers of inositol.

According to convention,[17] anti-clockwise numbering in an unsymmetrically substituted *myo*-inositol leads to the configurational D-prefix and clockwise numbering gives the substituted *myo*-inositol an L-prefix. An IUBAC recommendation allowing all biologically relevant compounds to be denoted as D-isomers has also been proposed (Chart 3).[18]

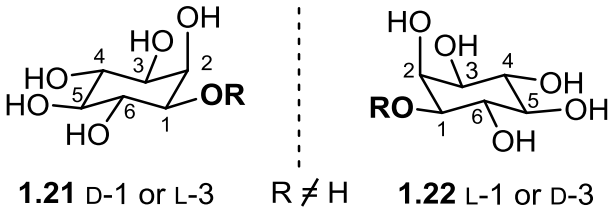

Chart 3. Ring C-atom numbering in unsymmetrical *myo*-inositol derivatives. All the asymmetrically substituted *myo*-inositol derivatives reported are racemic; however, only one of the enantiomers is shown in all the schemes.

Cyclitols and their derivatives have been synthesized from different kinds of starting materials, such as naturally occurring inositols (*myo*- and *chiro*-inositols and

their derivatives, Chart 4),[19, 20, 21] sugars (glucose, ribose etc.)[22-28] benzene and its derivatives (toluene, naphthalene, benzoquinone),[29] and norbornyl derivatives (Chart 5).[30-32]

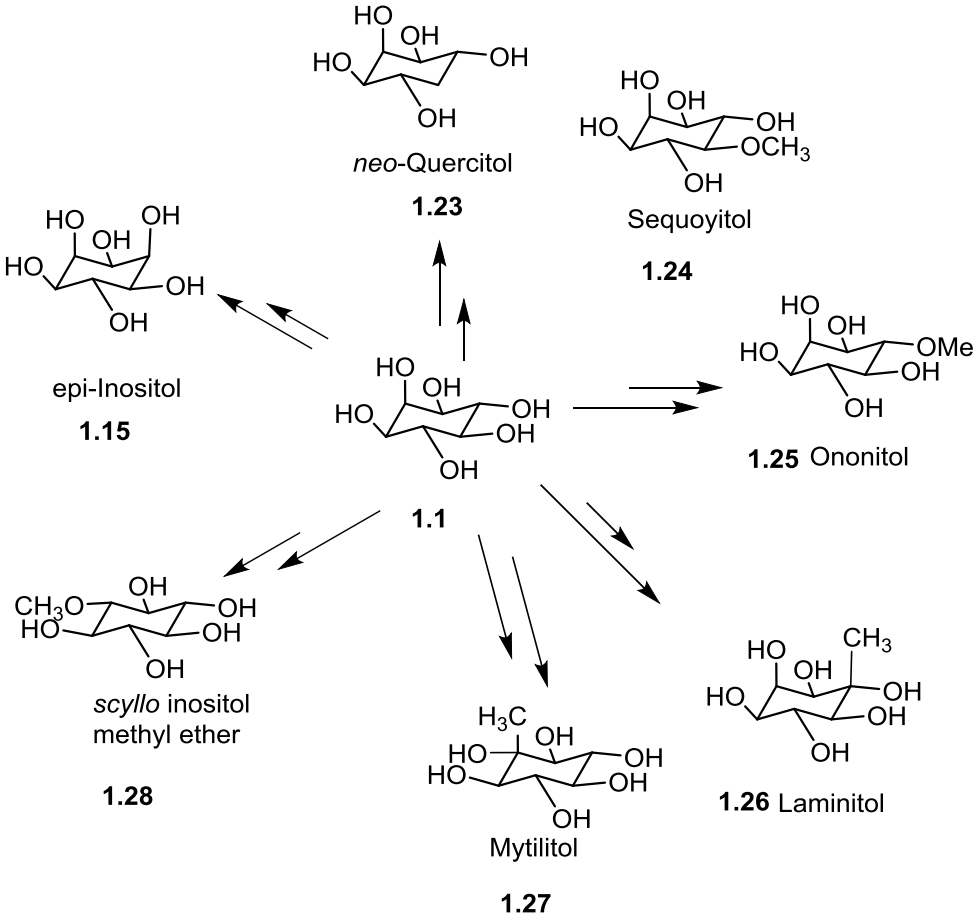

Chart 4. Illustrative examples of inositol derivatives synthesized from *myo*-inositol. See references 19, 20, 21 for details.

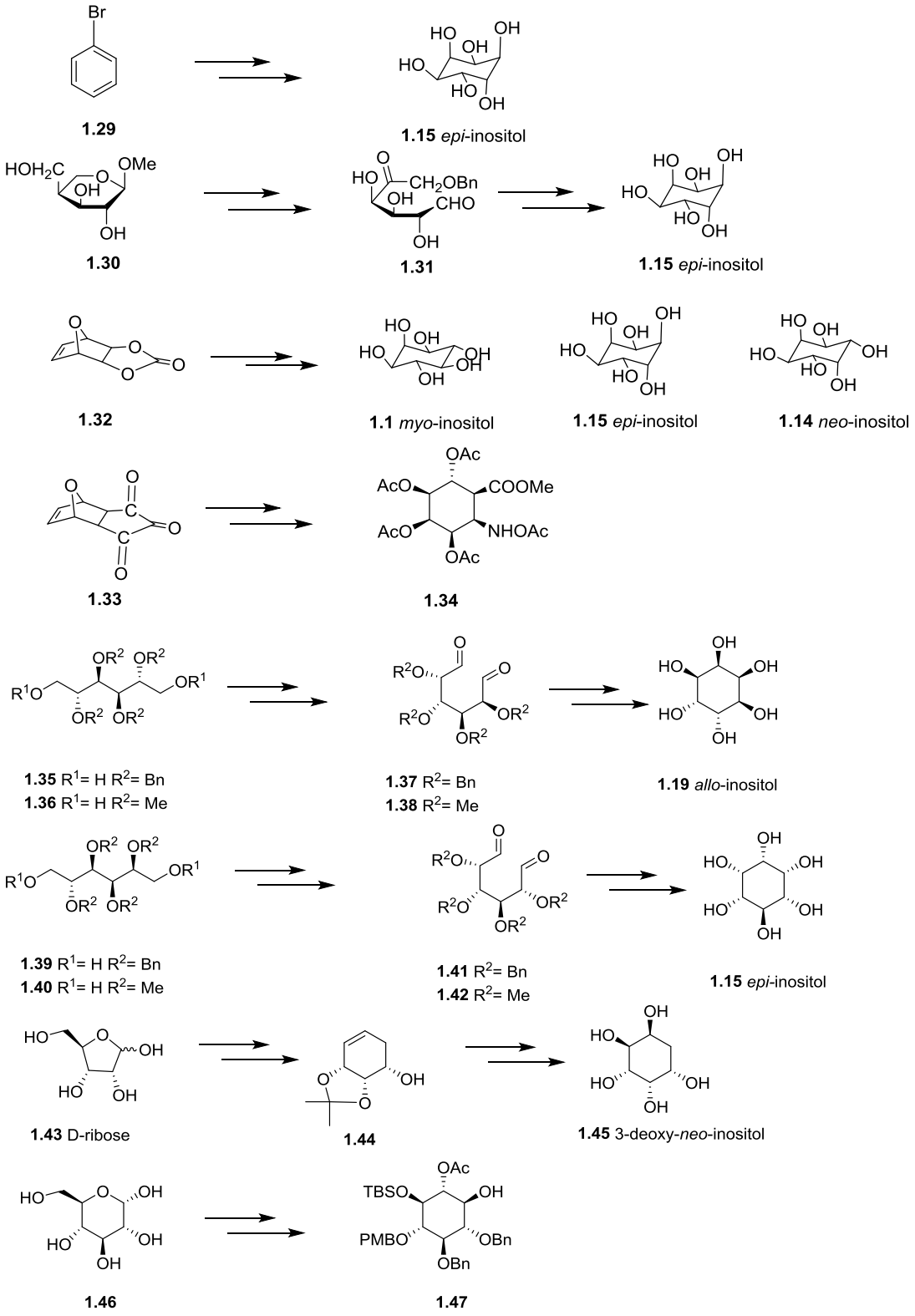

Chart 5. Illustrative examples for the preparation of inositol derivatives from non–inositol sources. See references 22, 24-26, 29, 30, 32 for details.

myo-Inositol (**1.1**) is perhaps the most frequently used starting material for the synthesis of phosphoinositols and their analogs. This is because *myo*-inositol is relatively inexpensive due to its abundance and the relative reactivity of its hydroxyl

groups as well as many of its derivatives is quite well understood.[17,18] The stereochemical structure and its consequences on the derivatization of the hydroxyl groups of *myo*-inositol is well documented in the literature (Chart 3). *myo*-Inositol has also been utilized for the synthesis of several natural products (other than phosphoinsitols) and their analogs (Chart 6). [33-36]

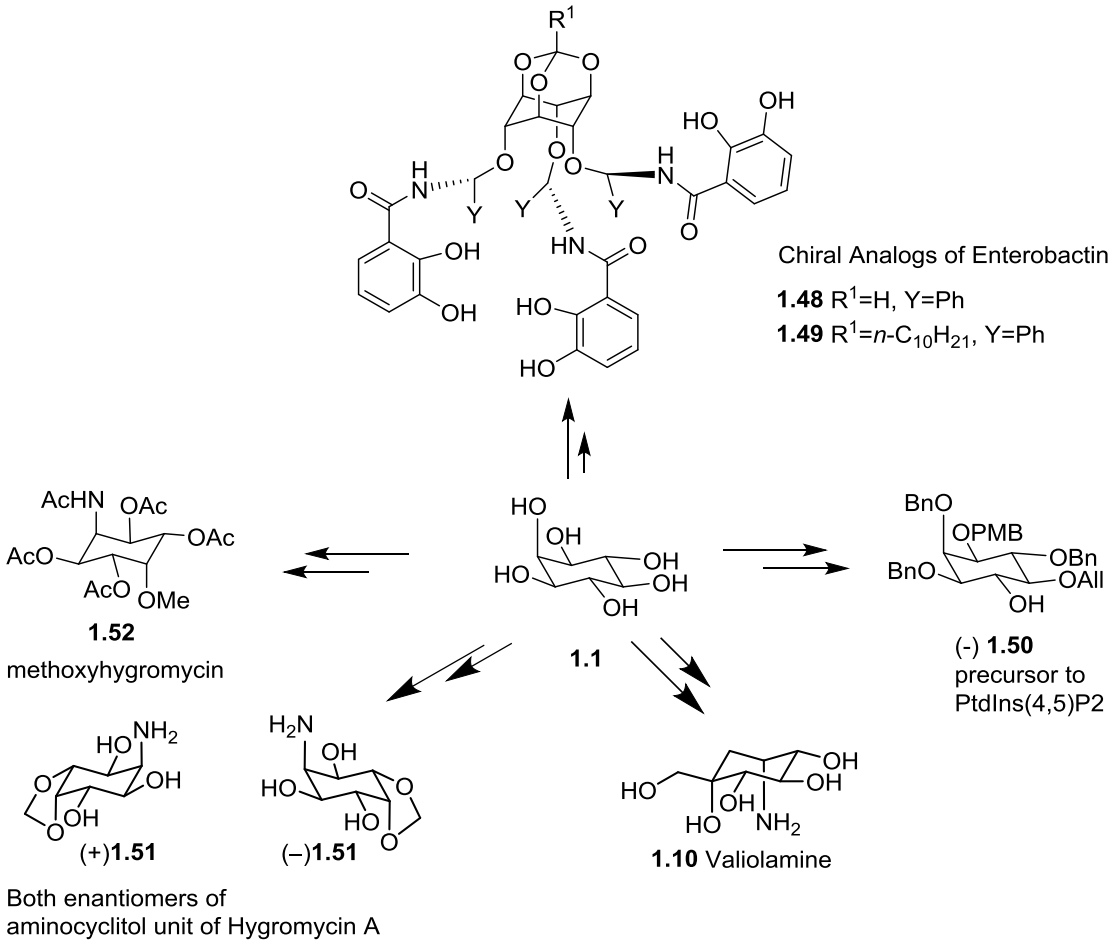

Chart 6. Illustrative examples of natural products and their analogues synthesized from *myo*-inositol.

As is evident from the structure of *myo*-inositol, any synthetic sequence utilizing it as the starting material, requires extensive protection and deprotection of its hydroxyl groups. Regioselective protection of *myo*-inositol hydroxyl groups is an arduous task since all the hydroxyl groups are secondary and the reactivity differences between them is subtle. Hence, reaction of *myo*-inositol (or its partially protected derivatives) with most reagents leads to the formation of a mixture of products; formation of acetals **1.53-1.56** of *myo*-inositol is shown in Scheme 1 as an example.

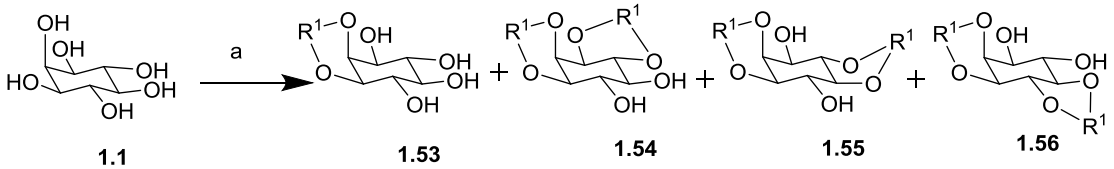

Scheme 1. (a) $R^1(OMe)_2$ / mineral acid; R^1 = isopropylidene or cyclohexylidene.

Acetalization of *myo*-inositol leads to the formation of *1,2*-acetals of its hydroxyl groups (vicinal diols, numbers *1* and *2* refer to the relative position of the hydroxyl groups rather than conventional numbering of *myo*-inositol ring carbon atoms which are not *italicized* – see **1.1** in Chart 2) and there is no report on the formation of inositol-*1,3*-bridged acetals (from *1,3*-diols, numbers *1* and *3* refer to the relative position of the hydroxyl groups) in any of these reactions. The latter acetals can only be obtained by the partial cleavage of *myo*-inositol-1,3,5-orthoesters (see below). Preparation and the use of *1,3*-acetals of polyols and carbohydrates, other than inositols, have been reported (Chart7).[37-47] However, as expected, such instances are relatively rare compared to those of *1,2*-acetals.

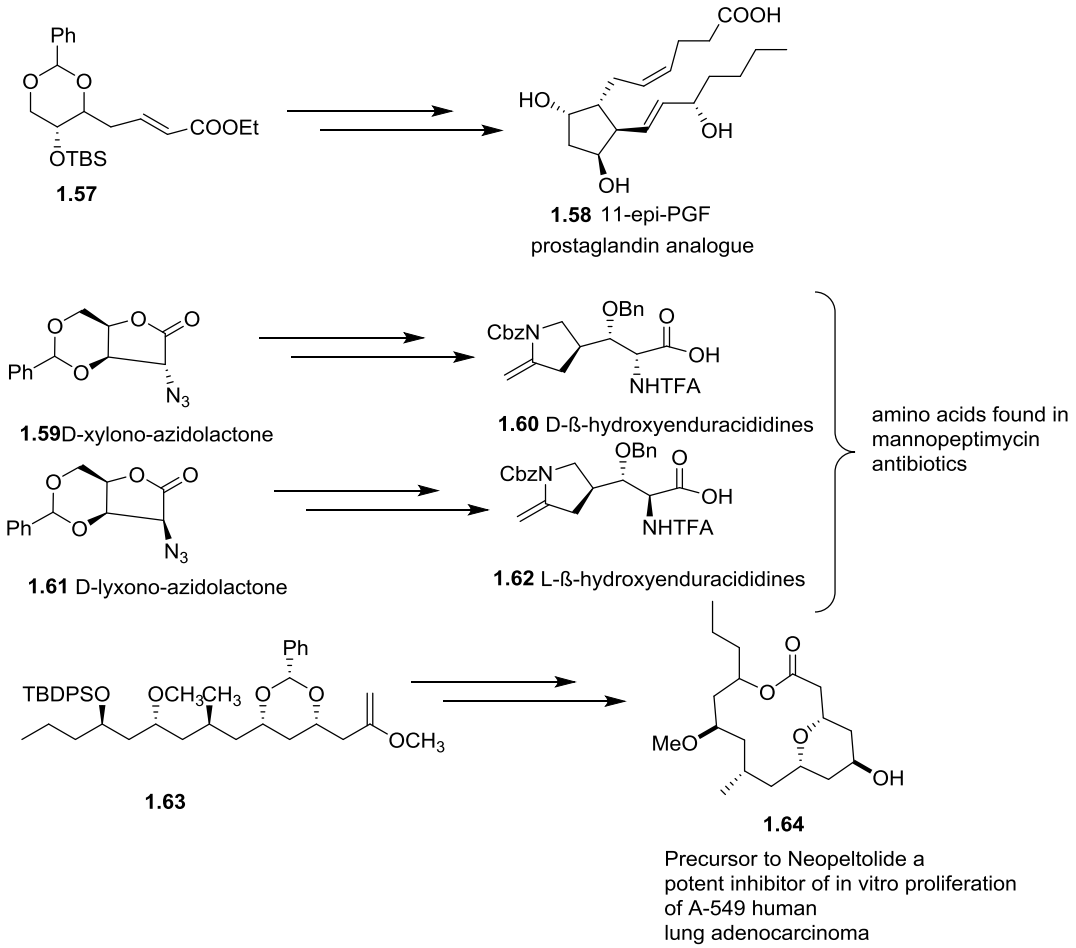

Chart 7. Illustrative examples of 1,3 acetals derived from polyols other than inositol. See references 45-47 for details.

Since acetalization of *myo*-inositol leads to the formation of at least three isomeric products (Scheme 1, and perhaps oligomeric acetals as well) the isolated yield of each of these acetals is seldom more than 35%. Hence these acetals are not good as early intermediates in syntheses starting from *myo*-inositol, since the yield of the final product is compromised right in the beginning of the synthetic scheme. A way around this is to use orthoesters of *myo*-inositol, which can be obtained as single products, often in yields excess of 90%. Reaction of *myo*-inositol with trialkyl-orthoesters results in the formation of *myo*-inositol-1,3,5-orthoesters as the sole product in high yield (**1.66**–**1.69**, Scheme 2), wherein three hydroxyl groups are protected simultaneously.[48-53]

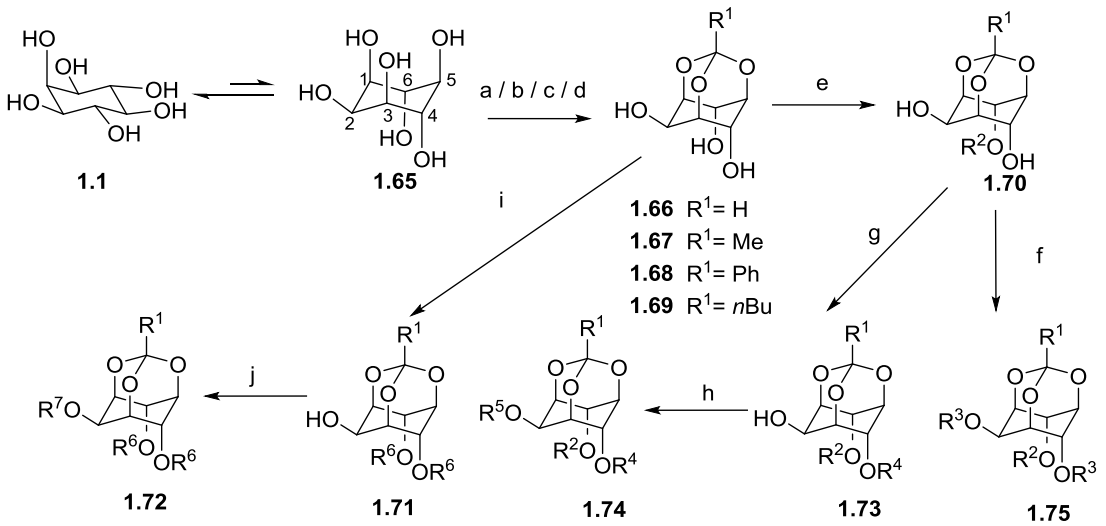

Scheme 2. (a) $HC(OEt)_3$, TsOH, DMF, 110 ^oC, 4 h; (b) $MeC(OEt)_3$, TsOH, DMF, 90–100 ^oC, 4 h; (c) $PhC(OMe)_3$, CSA, DMSO, 85 ^oC, 5 h; (d) *n*-$BuC(OMe)_3$, CSA, DMSO, 60 ^oC. (e) R^2X, NaH, DMF; (f) R^3X, NaH, DMF; (g) R^4X in DMF, *n*-BuLi, THF; (h) R^5X, NaH, DMF; (i) R^6X, LiH, DMF; (j) R^7X, NaH, DMF. R^2-R^7= combination of Me, Allyl, Bn, PMB, PBB.

Due to the strong intramolecular hydrogen bonding between the C4- and C6-hydroxyl groups of *myo*-inositol orthoesters **1.66-1.69**, and differences in the ability of the hydroxyl groups of diols **1.70** to form chelates with metal ions, reaction of the hydroxyl groups of these orthoesters with alkyl halides can be controlled to obtain mono-, di- or triethers exclusively (Scheme 2).[54-56]

Hence a variety of orthogonally protected *myo*-inositol derivatives can be obtained in a short time. Reductive cleavage of these orthoesters results in the formation of *1,3* acetals (consequently releasing one of the three hydroxyl groups of the orthoester moiety), which are fast becoming early intermediates for

phosphoinositol synthesis. Similarly regioselective acylation of *myo*-inositol orthoesters can also be carried out to obtain a variety of mono-, di- and tri-esters.[57-58] However, they are not generally useful for the preparation of *1,3*-acetals, since esters are not stable to reductive cleavage conditions required to obtain *1,3*-acetals from orthoesters.

1.2. Preparation of *myo*-inositol-*1,3*-acetals by the reductive cleavage of orthoesters

1.2a. Reductive cleavage of inositol orthoesters with DIBAL-H

Reductive cleavage of *myo*-inositol orthoesters carrying different groups at the 2-*O*, 4-*O* and 6-*O*-positions of the inositol ring with DIBAL-H affords the corresponding *myo*-inositol-*1,3*-acetal (Scheme 3) liberating the C5-hydroxyl group, predominantly.[8,35,58-63]

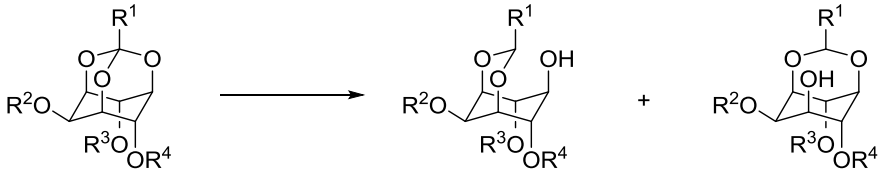

R^1=H, R^2= R^3= R^4=Bn	**1.76**	**1.85**	**1.94**
R^1=H, R^2=TBDMS, R^3= R^4=Bn	**1.77**	**1.86**	**1.95**
R^1=H, R^2= R^3=Bn, R^4=PMB	**1.78**	**1.87**	**1.96**
R^1=Ph, R^2= R^3= R^4=Bn	**1.79**	**1.88**	**1.97**
R^1=H, R^2= R^3= R^4=PMB	**1.80**	**1.89**	**1.98**
R^1=Ph, R^2= R^3= R^4=All	**1.81**	**1.90**	**1.99**
R^1=H, R^2=PMB, R^3= R^4=Bn	**1.82**	**1.91**	**1.100**
R^1=Ph, R^2=PMB, R^3=, R^4=Bn	**1.83**	**1.92**	**1.101**
R^1=Ph, R^2=PBB, R^3=PMB, R^4=All	**1.84**	**1.93**	**1.102**

Scheme 3. Cleavage of *myo*-inositol orthoesters with DIBAL-H (2.2 – 2.7 equivalents, -78 to 0 °C). The *1,3*-acetals shown are to illustrate the orthoester bond cleaved; the conformation of these molecules could vary from those shown. See end of section for a discussion on the conformational aspects of inositol *1,3*-acetals.

Use of excess of DIBAL-H resulted in complete cleavage of the orthobenzoate **1.79** to the diol **1.104** (Scheme 4).[62 ,64, 65] Since reduction of **1.79** with two equivalents of DIBAL-H results in the formation of the C5-alcohol, it is clear that the 1,3-acetal **1.103** formed undergoes further reduction to form the racemic diol **1.104**.

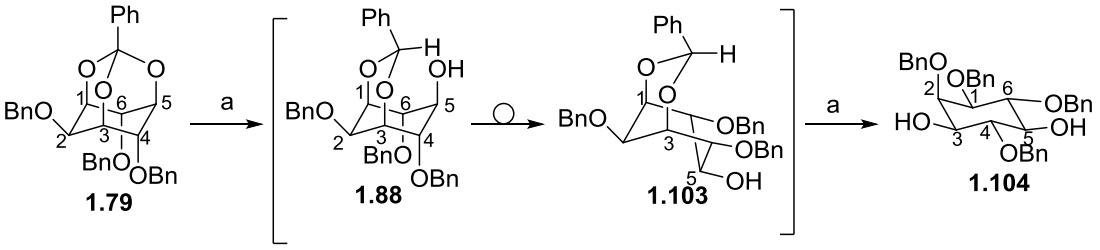

Scheme 4. (a) DIBAL-H (excess), dichloromethane, 93-100%.

The observed selectivity in this reductive cleavage reaction (Scheme 3) is thought to be due to the steric bulk of the organometallic reducing reagent.[59,62,65] The stereoselectivity of the reductive cleavage of the orthoformate **1.76** has been investigated and the mechanisms proposed. [66-68] In the DIBAL-H reduction of **1.76** to **1.85** it was determined that at least 2 molar equivalents of DIBAL-H are required for the reaction to proceed to completion (Scheme 5). It was proposed that the first equivalent of DIBAL-H acts as a Lewis acid, coordinating to the C5-oxygen, perhaps the most sterically accessible oxygen in **1.76**. Subsequent cleavage of the orthoformate affords the oxocarbenium ion **1.106**, the unfavorable 1,3-steric interactions in which can be accommodated by a ring-flip to the boat conformation **1.107**. Reduction of this oxocarbenium ion by a second equivalent of DIBAL-H from the less hindered face produces the 1,3-acetal **1.85** exclusively. Deuterium labeling experiments with **1.76** ruled out the delivery of hydride to **1.105** resulting in the cleavage of the orthoester moiety.[68]Although the experimental results available so far cannot distinguish between the delivery of hydride to **1.106** and **1.107** the delivery of hydride to **1.107** seems more likely, due to the 1,3-diaxial strain present in **1.106** (which results in a conformational change to **1.107**).

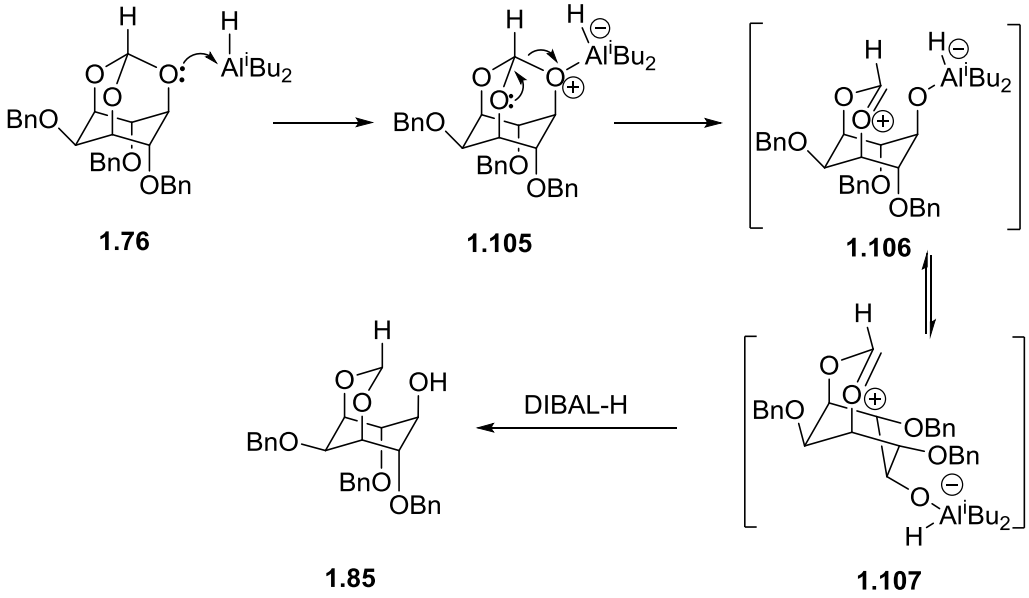

Scheme 5. Proposed mechanism for the cleavage of the symmetrically substituted *myo*-inositol orthoformates by DIBAL-H.[66, 68]

The DIBAL-H mediated cleavage of symmetrically substituted orthoesters always resulted in almost exclusive cleavage (see below) at the C5-positon of *myo*-inositol (Scheme 5). However, regioselectivity of the reductive cleavage of *myo*-inositol orthoesters carrying unsymmetrical substituents could not be ascertained clearly.[56 ,68] Reduction of the un-symmetrically *O*-substituted orthoformate racemic **1.78** gave the C5-alcohol **1.87** as a single isolated product[69] while, reduction of the orthobenzoate moiety in **1.84** resulted in the formation of a mixture of products from which the benzylidene acetal **1.93** was isolated in 60% yield.[56]

Reduction of **1.84** with an excess of DIBAL-H gave a mixture of isomeric diols **1.109** and **1.110**,[56] but this result is not sufficient to conclude the sole intermediacy of the 1,3-acetal **1.108** (Scheme 6). This is because no data on the regioselectivity of the reductive cleavage of *1,3*-acetals or the relative ease of reduction of the *myo*-inositol 1,3- and 1,5-acetals (such as **1.93** , **1.102** and **1.108**) are available.

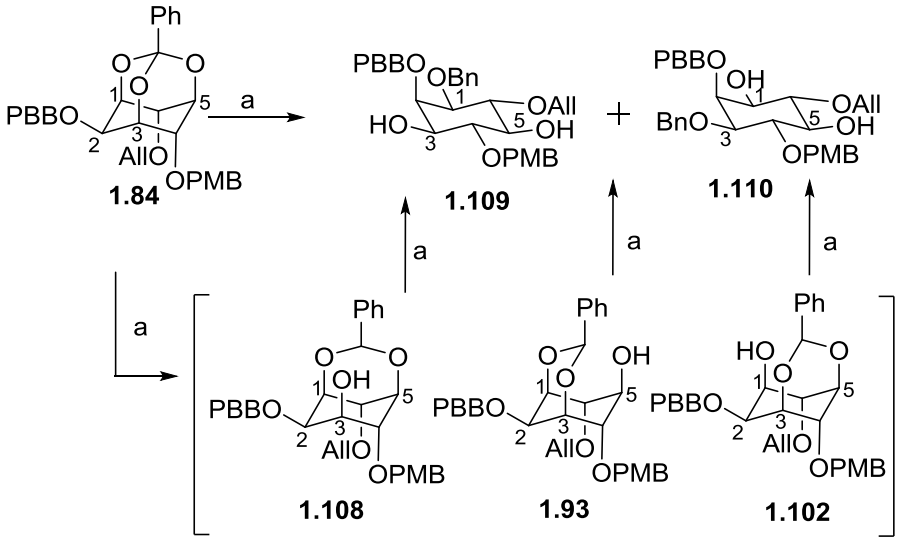

Scheme 6. (a) Excess DIBAL-H, dichloromethane, 73% (mixture of **1.109** and **1.110**).

Results on the cleavage of the ring C-substituted *myo*-inositol orthoesters (Scheme 7) showed that the nature of the product formed was dependent on the inositol ring C-substituent. Most of these orthoesters yielded a mixture of the 3,5-acetal **1.112** and the triol **1.113** on reaction with DIBAL-H. Generation of the 3,5-*O*-benzylidene acetal shows that the initial attack of DIBAL-H need not necessarily occur at the 5-O position as observed for symmetric inositol orthoesters (Scheme 3).[64,65]

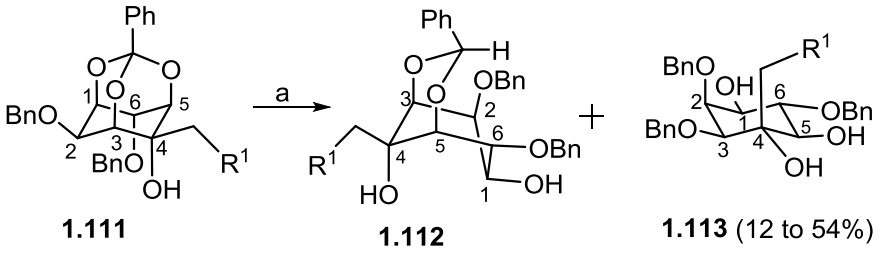

Scheme 7. (a) DIBAL-H, dichloromethane. R^1 = H, Me, *n*-Bu, *t*-Bu, Ph, *i*-Pr

1.2b. Reductive cleavage of inositol orthoesters with trimethyl aluminium

In contrast to the DIBAL-H cleavage of inositol orthoesters (Scheme 3), the trimethylaluminium-mediated cleavage of inositol orthoesters exclusively afforded the corresponding racemic 1,5-acetal, which results from the cleavage of either the C1-O or the C3-O bond in the *myo*-inositol orthoester (Scheme 8).[51,59,66,70]

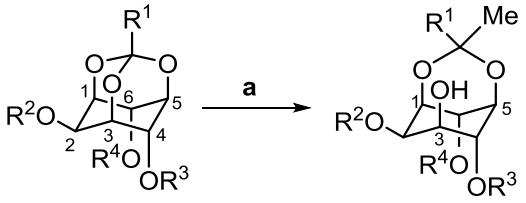

1.76, 1.114-1.116 **1.117-1.120**

1.76, 1.117 R^1 = H; R^2 = R^3 = R^4 = Bn
1.114, 1.118 R^1 = H; R^2 =Bn; R^3 = R^4 = All
1.115, 1.119 R^1 = Me; R^2 = R^3 = R^4 = Bn
1.116, 1.120 R^1 = H; R^2 = $(CH_2)_4$OTBS; R^3=All, R^4=Bn

Scheme 8. Cleavage of *myo*-inositol orthoesters with trimethylaluminum; (a) $AlMe_3$ (2.5 equivalents), 0 °C.

This outcome indicated that trimethylaluminium is presumably sufficiently small to coordinate to one or both of the equivalent oxygen atoms at the C1- or C3-position, resulting in the oxocarbenium ion **1.122**. Delivery of a methyl group to the *exo*-face of the oxocarbenium **1.123** affords the corresponding racemic 1,5-acetal **1.117** (Scheme 9).

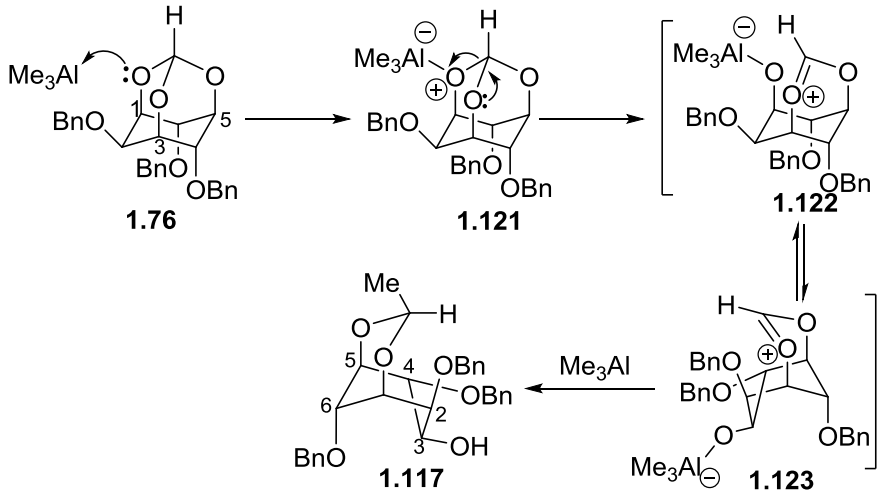

Scheme 9. Proposed mechanism for the regioselective cleavage of the orthoformate **1.76** by Me_3Al.[66]

The orthoformate derivative **1.124** on reaction with trimethylaluminium led to the formation of a mixture of epimeric acetals **1.125** and **1.126** (Scheme 10).[70] However, only one of these epimers (**1.125**) was expected according to the mechanism proposed (Scheme 9).[66]

Trimethylaluminium mediated cleavage of orthogonally protected orthoformate **1.127** led to the formation of a mixture of acetals **1.128** and **1.129** (Scheme 10).[71]

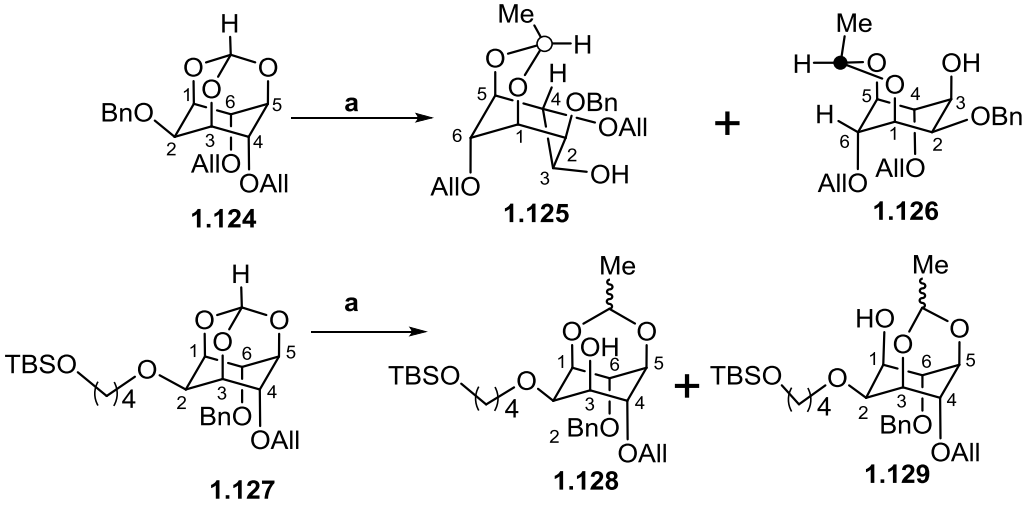

Scheme 10. (a) $AlMe_3$, dichloromethane, –78 °C to 0 °C.

Whether the epimeric acetals (eg., **1.125** and **1.126**) were formed directly from an intermediate such as **1.123** (Scheme 9) or they were formed due to epimerization (as observed in the 1,3-benzylidene derivatives, Scheme 11) of one of the acetals, subsequent to its formation, is not clear. The 1,3-benzylidene acetals **1.130**, **1.131** and **1.134** underwent epimerization at the acetal carbon on heating, in the molten state, just above their melting point. Interestingly, the same epimerization reaction did not proceed either in the crystalline state or in solution. DFT calculations suggested that the epimeric acetals **1.132**, **1.133** and **1.135** obtained by this thermal process are relatively more stable than the 1,3-acetals **1.130**, **1.131** and **1.134** obtained by the reductive cleavage of the corresponding orthobenzoate.[72]

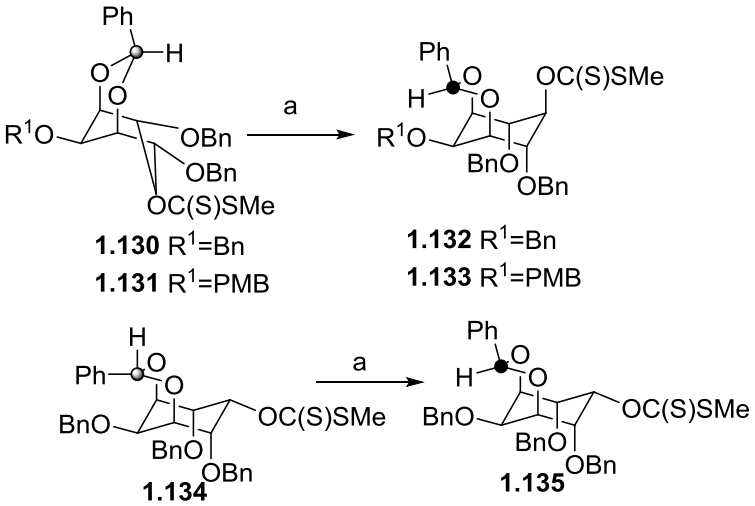

Scheme 11. Epimerization of *myo*-inositol derived 1,3-acetals. (a) 120 °C, 12 h for **1.130**, **1.131** and 30 h for **1.134**.

1.2c. Reductive cleavage of inositol orthoesters with Grignard reagents

Selective cleavage of the orthoester moiety in *myo*-inositol orthoesters at C1–O bond could also be effected with Grignard reagents (Scheme 12).[73] The observed regioselectivity for the cleavage of the orthoester was rationalized owing to the presence of the equatorial oxygen at the C2 position which could serve as an auxiliary to form a chelate such as **1.142**. This mechanism was supported by the reaction of methylmagnesium iodide with **1.143** which resulted in cleavage of the orthoester moiety; whereas in the reaction of the analogous *scyllo*-inositol orthoester derivative **1.145** with methylmagnesium iodide, a diastereomeric mixture of **1.146** (2:1) was obtained in 56% yield. No C–O bond cleavage at the orthoester moiety in **1.145** was observed. The methoxy group in **1.145** apparently directs the selectivity of the ring opening reaction at the benzylidene moiety. As observed with the reduction of DIBAL-H (Scheme 5), inositol *1,3*-acetals initially produced could be cleaved with excess of the Grignard reagent to the corresponding diols.[73]

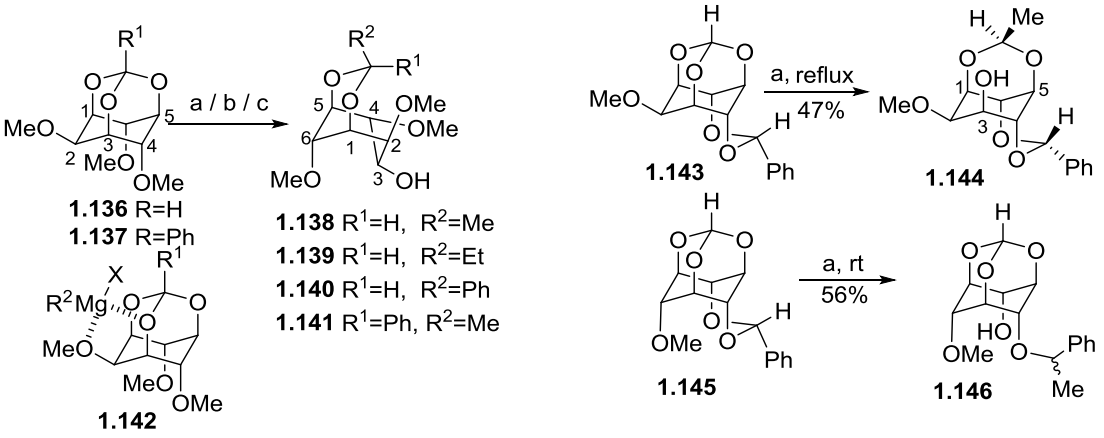

Scheme 12. (a) MeMgI in diethylether, benzene, room temperature to reflux, 16 h; (b) EtMgBr in diethylether, benzene; (c) PhMgBr in diethylether, benzene.

1.3. Structure and conformation of inositol derived 1,3-acetals

Since inositol derived *1,3*-acetals are bridged bicyclic systems, in principle, the conformation of the two rings (the inositol carbocyclic ring and the heterocyclic acetal ring) could vary depending on the substitution on the ring carbon atoms as well as phase (solid, solution, vapor) in which these molecules are present. For example, in the *1,3*-acetal **1.130** (Scheme 13), inositol ring can be in chair form or boat form and

so is the acetal ring. Hence there are four possible representations for **1.130**: both rings chair **1.130CC**; both rings boat **1.130BB**; inositol ring chair and acetal ring boat **1.130CB**; inositol ring boat and acetal ring chair **1.130BC**.

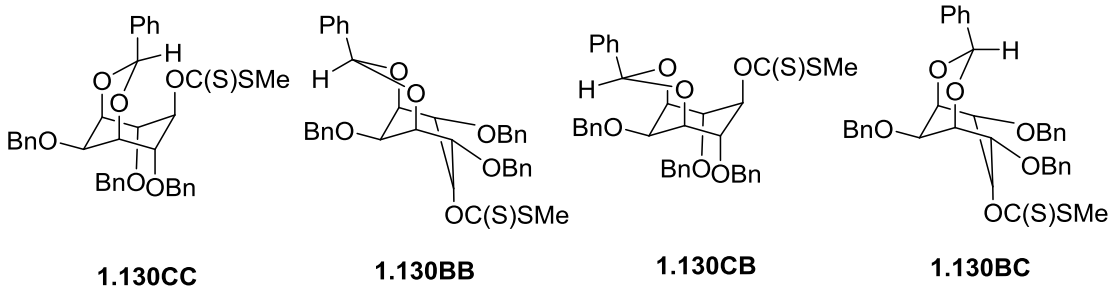

Scheme 13. Four possible ring conformations for inositol derived *1,3*-acetals.

DFT calculations on a few *1,3*-acetals has shown that conformation in which both rings are boat has very high energy and hence flips to one of the other three conformations. All the other three conformations have been experimentally observed, [36,66,72,74] although the difference in energy between them is not very high (as suggested by DFT calculations).

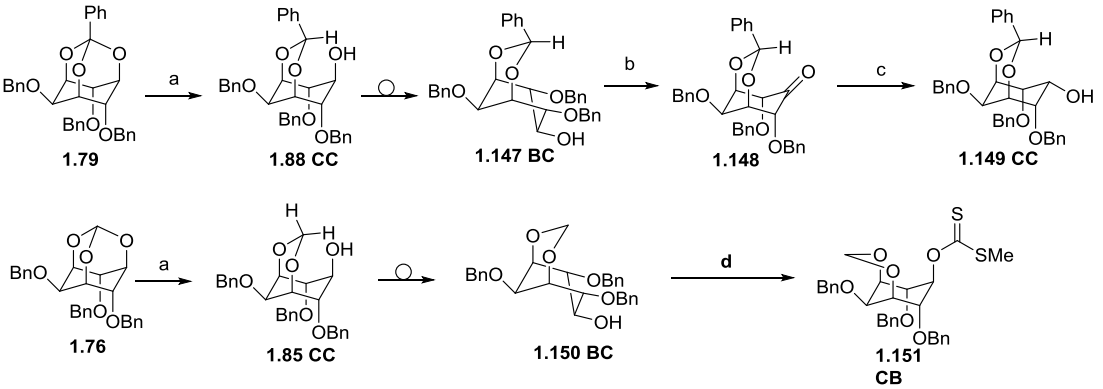

Scheme 14. (a) DIBAL-H (excess), dichloromethane, 93-100% (b) EtOAc, IBX, reflux (c) THF/MeOH, $NaBH_4$, RT, 1h 94% (d) THF, NaH, CS_2,reflux, 1h,MeI, rt, 16h, 98%

For example **1.79** when cleaved with DIBAL-H forms the alcohol **1.88** that has the inositol ring in the boat conformation whereas the acetal bridge has a chair conformation. Oxidation of **1.147** to **1.148** and subsequent reduction gives the *neo*-inositol derivative **1.149** which has the chair conformation in both the rings implying the release of strain leads the inositol ring to revert to the chair form. In contrast, in the case of **1.150** the conversion to its xanthate forces the acetal bridge to flip to the boat conformation.[74] Moreover the existence of a 1,3-acetal in different conformations in solid and solution state (Chart 8) is also reported.[36, 66, 74]

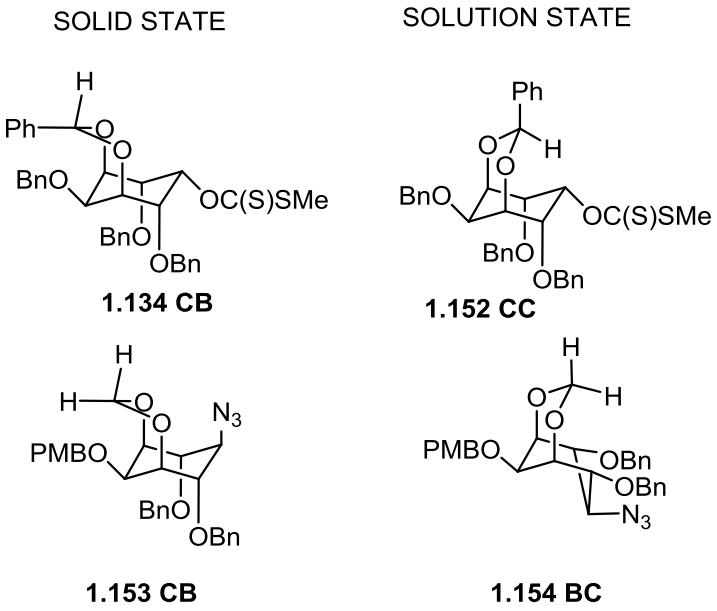

Chart 8. Examples of 1,3- accetals that exist in conformations in solid and solution states.

Hence it is likely that especially in the solution state, these conformations (Chart 8) could coexist. To the best of our knowledge, there is no report on in depth investigation of conformational aspects of these *1,3*-acetals. But there are reports of similar *myo*-inositol-*1,3*-acetals portrayed to be existing in different conformations. Compound **1.117** was reported to exist in the CC conformation whereas it actually exists in BC conformation (Chart 9).[66, 75]

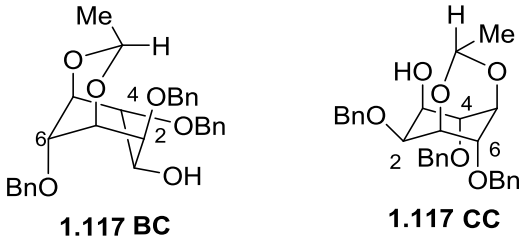

Chart 9. Examples of inositol derived *1,3*-acetals which are shown to exist in different conformations in different publications.

However such representations of the molecular structure generally do not have serious consequences since most *1,3*-acetals are used as transient protecting groups in long synthetic schemes that leave the structure of the inositol ring unperturbed. However, the conformational aspects of *1,3*-acetals do become important in reactions which lead to modifications on the inositol ring.[36,74,76]

1.4. Syntheses involving *myo*-inositol-*1,3*-acetals

Scheme 15 demonstrates the synthetic utility of *myo*-inositol-*1,3*-acetals. Derivatives from *1,3*-acetals were utilized for the synthesis of unsymmetric diphospho-inositol polyphosphates.[8] Some of these acetals were also used for the synthesis of affinity probes **1.156 (a** to **h)** which were useful in the identification of proteins in the PI-3 kinase signaling pathway;[68] inhibitors toward human inositol monophosphatase;[76] and analogs to investigate the structure activity relationship on the interaction of the second-messenger, D-Ins(1,4,5)P_3 with its receptor.[70] In higher eukaryotes, the PP-InsPs are critical components in cancer cell migration and metastasis insulin secretion, insulin sensitivity, and host-cell immune response during viral invasion. The PP-InsPs **1.165** could be easily accessed through 1,3-acetal **1.160**.[77] The purinyl analog **1.167** of Ins(1,4,5)P_3 behaved as a potent full agonist at the Ins(1,4,5)P_3-receptor.[71] Recent developments on the synthesis and biological utility of synthetic phosphoinositols and their analogs have been reviewed.[78-80]

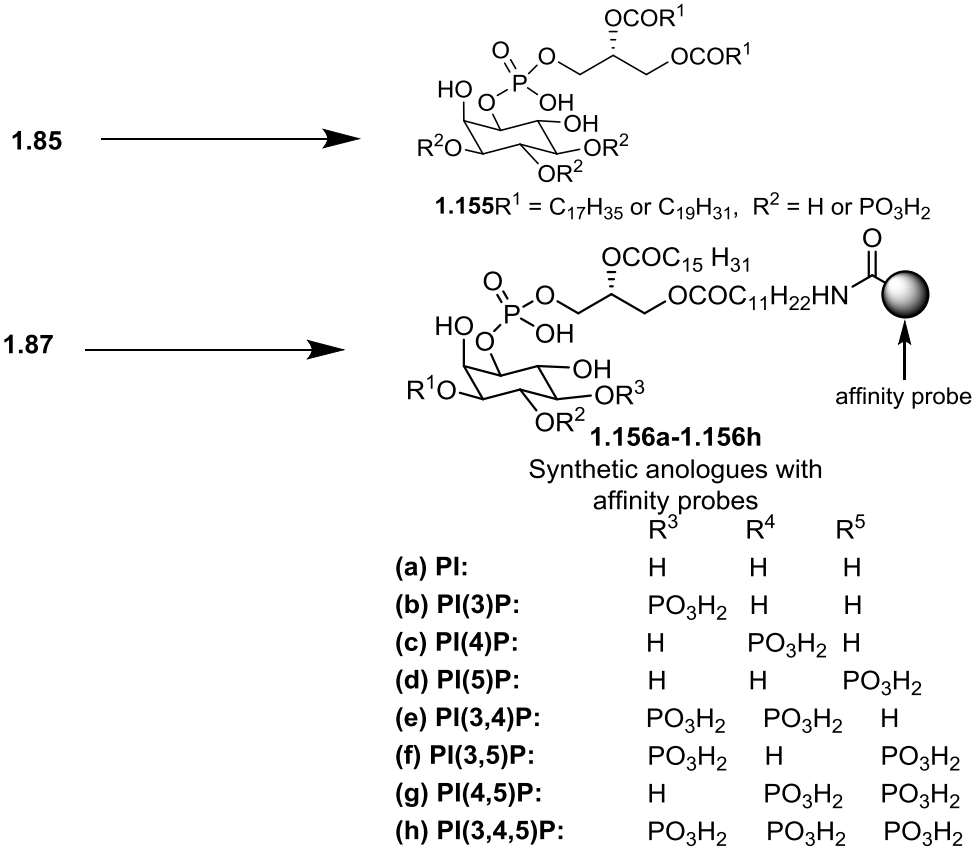

	R^3	R^4	R^5
(a) PI:	H	H	H
(b) PI(3)P:	PO_3H_2	H	H
(c) PI(4)P:	H	PO_3H_2	H
(d) PI(5)P:	H	H	PO_3H_2
(e) PI(3,4)P:	PO_3H_2	PO_3H_2	H
(f) PI(3,5)P:	PO_3H_2	H	PO_3H_2
(g) PI(4,5)P:	H	PO_3H_2	PO_3H_2
(h) PI(3,4,5)P:	PO_3H_2	PO_3H_2	PO_3H_2

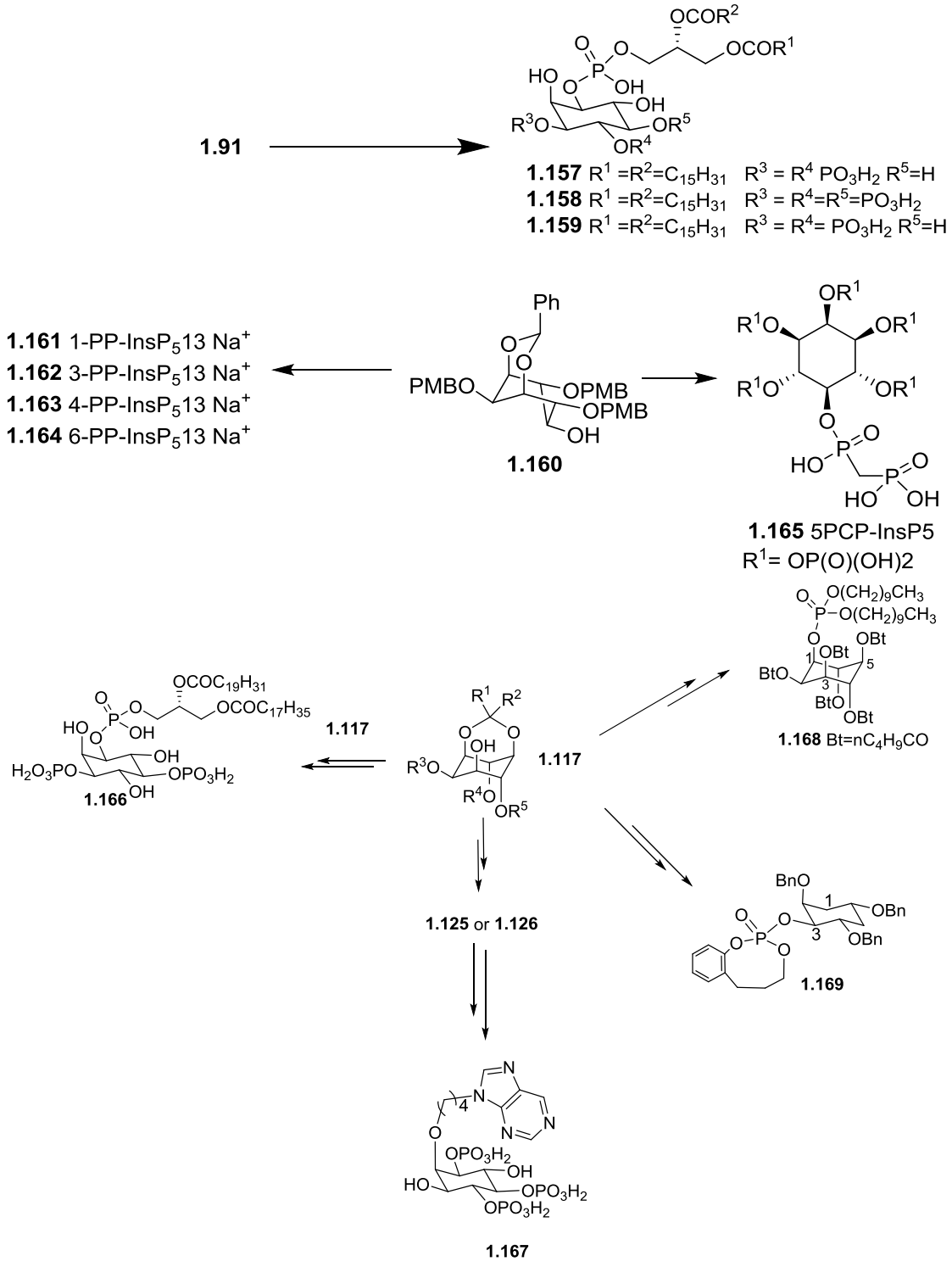

Scheme 15. Phosphoinositols and their analogs synthesized from *1,3*-acetals of *myo*-inositol. Numbers (in bold) on arrows represent the *1,3*-acetal intermediate used in the respective synthesis; these structures have appeared in earlier schemes. [8, 51, 68-70, 75]

Acetal **1.82** was converted to both the enantiomers of the aminocyclitol unit of hygromycin A (Scheme 16).

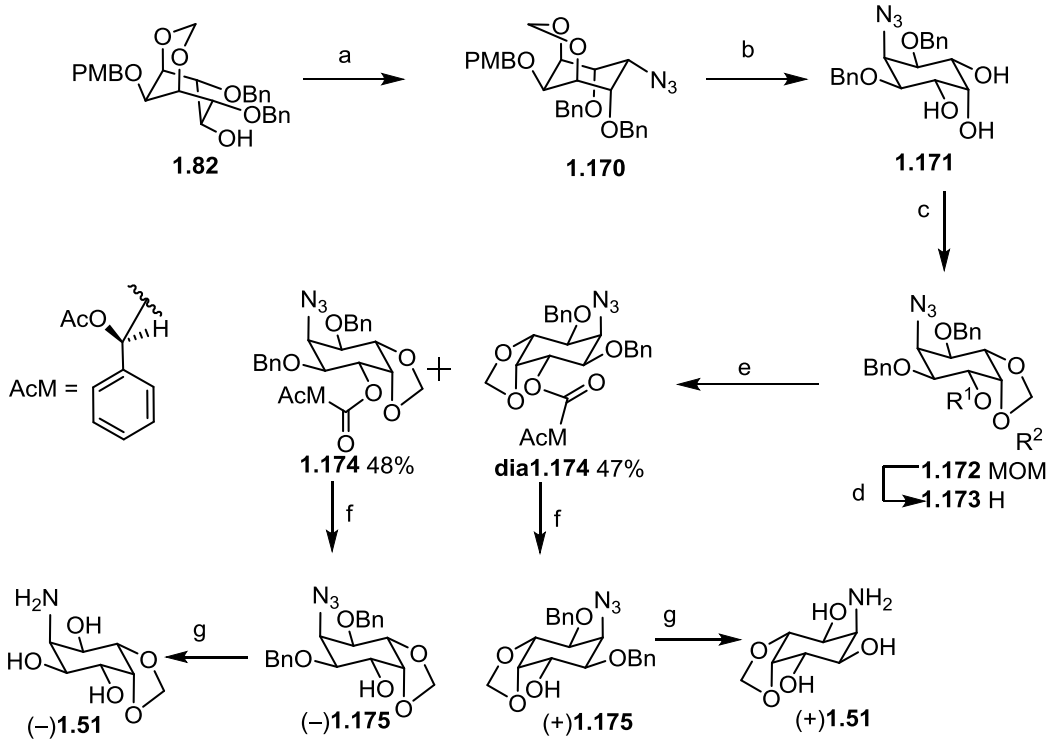

Scheme 16. (a) (i) DCM, py., Tf_2O, 0 °C, 30 min; (ii) HMPA, NaN_3, rt, 12 h, 94% (starting from **1.1**); (b) THF:MeOH, HCl, reflux, 1 h, 98%; (c) $H_2C(OMe)_2$, TMSOTf, 2,6-Lutidine, 0 °C–rt; (d) MeOH, TsOH (cat), reflux, 12 h, 94% (for 2 steps); (e) DCM, R(–)-*O*-acetylmandelic acid, DCC, rt, 3 h; (f) MeOH, KOH, rt, 2 h, 98–99%; (g) MeOH, AcOH, H_2 (400 psi), 20% Pd/C, RT, 40 h, 92–94%.

Similarly the acetal **1.147** (Scheme 17) served as a versatile intermediate and was converted to various inositol derivatives like sequoyitol (**1.24**)[51] *neo*-inositol hexaacetate (**1.176**), *myo*-inosamine hexaacetate (**1.181**) and *neo*-inosamine hexaacetate(**1.179**).[21]

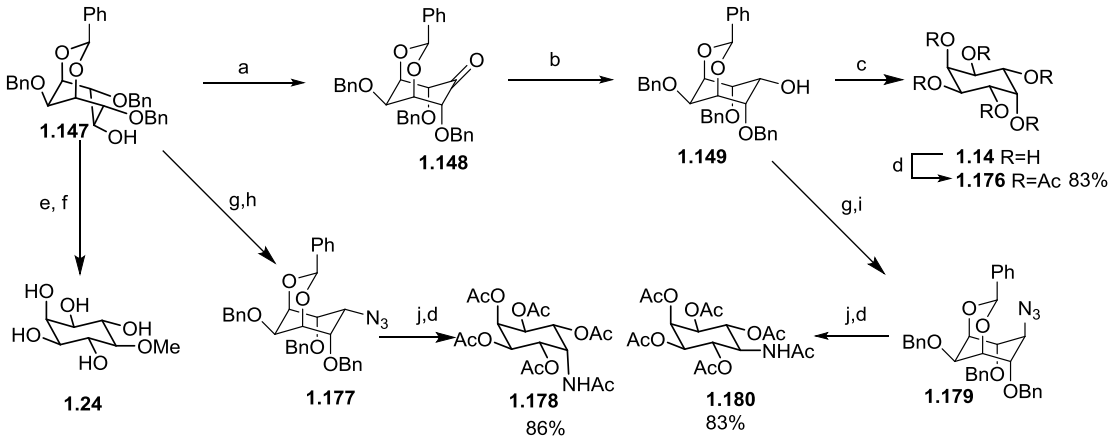

Scheme 17. (a) IBX, EtOAc, 2.5h, 98%; (b) THF/MeOH, $NaBH_4$,RT, 1h, 94% (c) EtOH, 20% $Pd(OH)_2/C$, H_2, RT, 6h; (d) Pyridine, Ac_2O, RT,40h; (e) NaH, MeI, DMF, rt, 1 h, 98% ; (f) MeOH,

$Pd(OH)_2$, reflux, 20h, 94%; (g) DCM, py., Tf_2O, 0 °C, 30 min; (h) HMPA, NaN_3, rt, 12 h, 94%; (i) DMF, NaN_3, rt, 12 h, 88%; (j)TFA, EtOH, H_2, 20%, $Pd(OH)_2$,RT, 44h.

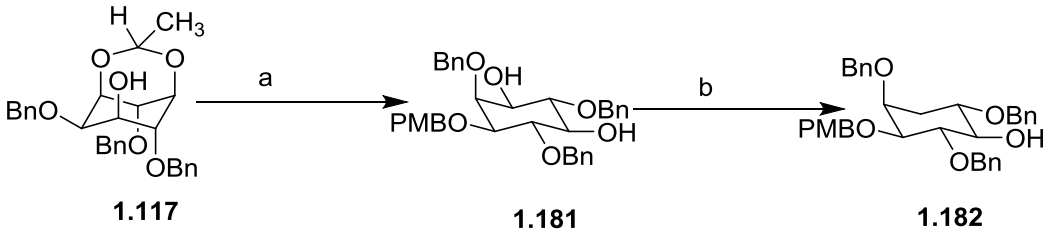

Scheme 18. (a)(i) DMF, NaH, PMBCl, 0 ° C to RT 1h, 98% over two steps; (ii)TFA, EtOH-H_2O, reflux, 2h, 93%; (b)(i)C_6H_5OSCCl, DMAP, MeCN, 20h, (ii)Bu_3SnH, AIBN, 4h, 96% over two steps.

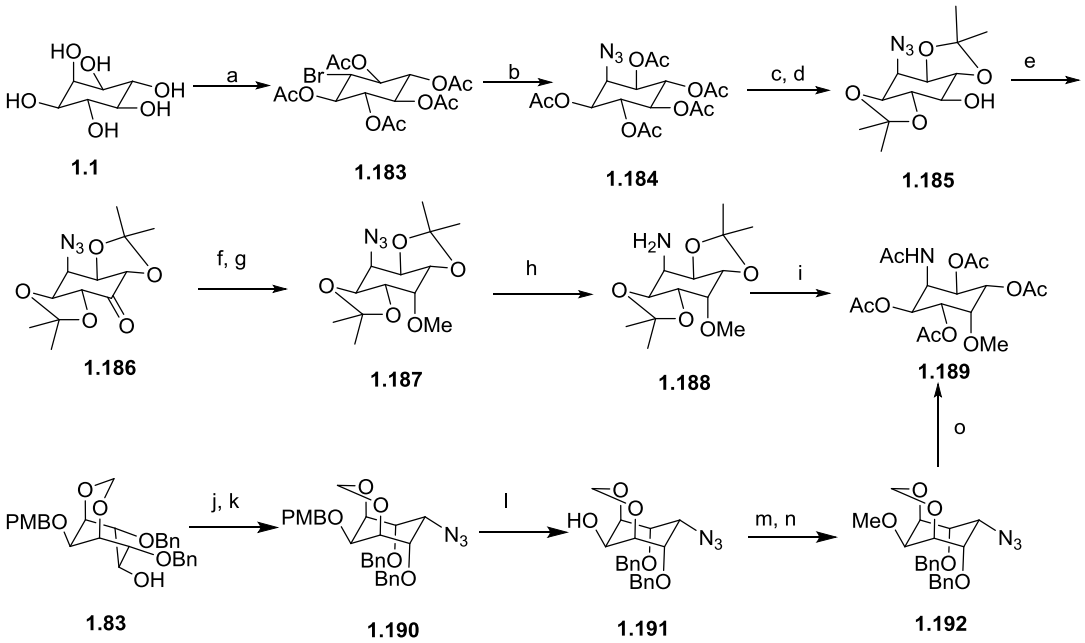

Scheme 19: (a)AcBr, Ac_2O, 120°C,6h 11%; (b)NaN_3, 10% aq. DMF, 90°C then Ac_2O/pyridine, 80% (c) 2M HCl, EtOH 92% (d) 2,2-dimethoxypropane, *p*-TsOH, DMF, 30%,(e) RuO_2, K_2CO_3, $BnN(Et)_3Cl$, $NaIO_4$, $CHCl_3$-H_2O, 88%; (f) L-selectride, THF, 75% (g) DMF, NaH, MeI , RT, 3h 86% (h)Raney-Ni, H_2, EtOH, 84%; (i) aq.AcOH 11%; (j)DCM, py., Tf_2O, 0 °C, 30 min(k) DMF, NaN_3, rt, 12 h (l) DCM-H_2O, DDQ, RT, 2.5h , 88%; (m)DMF, NaH, MeI, rt, 3h (n) MeOH, HCl, 20%, Pd/C, H_2, (400psi) 55 °C, 12h (o) Pyridine, DMAP, AC_2O, 60 °C, 12h 81% over 3 steps.

Comparison of the overall yields and the number of steps involved in converting *myo*-inositol to some of its derivatives (shown in Schemes 15 -19) via *1,3*-acetals and other intermediates is given below for illustration. Yield of Ins(1,2,3)P_3 in the *1,3*-acetal mediated synthesis was 23%[68] while the synthesis not mediated by *1,3*-acetal was 12%.[81] The overall yield obtained for the conversion of *myo*-inositol to *neo*-inositol (**1.14**) through the intermediacy of a *1,3*-acetal was 68% (six steps),[21] while the yield not involving *1,3*-acetal was 14-43%.[82, 83] Racemic valiolamine (**1.10**) could be

obtained in 8% overall yield (15 steps) from *myo*-inositol[35] while the overall yield involving intermediates other than *1,3*-acetals was 0.5% (10 steps).[84] The aminocyclitol unit of methoxyhygromycin could be obtained in 61% yield (7 steps) from *myo*-inositol via its *1,3*-acetal;[36] the yield of the same aminocyclitol was much lower (11%) using other intermediates (four steps).[83] (See scheme 19). These comparisons clearly illustrate the advantage and economy of using *myo*-inositol *1,3*-acetals as early intermediates for the synthesis of cyclitol derivatives.

1.5. Conclusions

Although the chemistry of inositols has been investigated for the past several decades, the use of inositol *1,3*-acetals in synthesis is a fairly recent phenomenon and the synthetic utility of these *1,3*-acetals has not been exploited to the full extent possible. Since many of the inositol *1,3*-acetals can be obtained as single products from *myo*-inositol, synthetic sequences involving these early intermediates are often high yielding and economical. These *1,3*-acetals being bicyclic and conformationally flexible, reveal unusual and interesting structural aspects, that could be exploited for synthesis. Inositol *1,3*-acetals allow convenient access to isomeric inositols and their analogs, natural and unnatural phosphoinositols as well as cyclitol moieties of natural products, hopefully opening up new avenues for the total synthesis of these natural products. The next two chapters of this thesis present detailed investigations on the formation of inositol-*1,3*-acetals from *myo*-inositol orthoesters by reductive cleavage with DIBAL-H and the role played by the *1,3*-acetal bridge during nucleophilic addition to inosose derivatives.

1.6. References

1. Ferguson, M. A. J.; Williams, A. F. *Annu. Rev. Biochem.* **1988**, *57*, 285–320.
2. Schmittberger, T.; Waldmann, H. *Synlett.* **1988**, 574–584.
3. Hinchliffe, K; Irvine, R. *Nature* **1997**, *390*, 123–124.
4. *Phosphoinositides: Chemistry, Biochemistry and Biomedical Applications*; Bruzik, K. S., Ed.; ACS Symposium Series 718; American Chemical Society: Washington, DC, **1999**.
5. *Cell Signaling*, Hancock, J. T., Oxford University Press, **2005**.
6. Zhang, H.; Thompson, J.; Prestwich, G. D. *Org. Lett.* **2009**, *11***,** 1551-1554.
7. Koumbis, A. E.; Duarte, C. D.; Nicolau, C.; Lehn, J. *ChemMedChem* **2011**, *6*, 169-180.
8. Capolicchio, S.; Thakor, D. T.; Linden, A.; Jessen, H. J. *Angew. Chem. Int. Ed.* **2013**, *52*, 6912-6916.
9. Di Paolo, G.; De Camilli, P. *Nature* **2006**, *443*, 651–657.
10. Walker, J. B. *Appl. Environ. Microbiol.* **2002**, *68*, 2404–2410.
11. Busscher, G. F.; Rutjes, F. P. J. T.; van Delft, F. L. *Chem. Rev*. **200**5, *105*, 775–791 and references cited therein.
12. Delgado, A. *Eur. J. Org. Chem.* **2008**, 3893–3906.
13. Diaz, L.; Casas, J.; Bujons, J.; Llebaria, A.; Deglado, A. *J. Med. Chem.* **2011**, *54*, 2069–2079.
14. Asano, N. *J. Enzyme Inhib.* **2000**, *15*, 215–234.
15. Egido-Gabás, M.; Serrano, P.; Casas, J.; Llebaria, A.; Delgado, A. *Org. Biomol. Chem.* **2005**, *3*, 1195–1201.
16. Mehta, G.; Ramesh, S. S. *Can. J. Chem.* **2005**, *83*, 581–594.
17. Parthasarathy, R.; Eisenberg, F. *Biochem. J.* **1986**, *235*, 313–322.
18. Nomenclature committee – IUB, *Biochem. J.* **1989**, *258*, 1–2.
19. Sarmah, M. P.; Shashidhar, M. S.; Sureshan, K. M.; Gonnade, R. G.; Bhadbhade, M. M. *Tetrahedron* **2005**, *61*, 4437–4446. 20.
20. Patil, M. T.; Krishnaswamy, S.; Sarmah, M. P.;Shashidhar, M. S. *Tetrahedron Lett.* **2011**, *52*, 3756–3758.
21. Murali, C.; Gurale, B. P.; Shashidhar, M. S. *Eur. J. Org. Chem.*, **2010**, 755–764.

22. Pistara, V.; Barili, P. L.; Catelani, G.; Corsaro, A.; D'Andrea, F.; Fisichella, S. *Tetrahedron Lett.* **2000**, *41*, 3253–3256.
23. Takahashi, H.; Kittaka, H.; Ikegami, S. *J. Org. Chem.* **2001**, *6*, 2705–2716.
24. Stockton, K. P; Greatrex, B. W.; Taylor D. K. *J. Org. Chem.* **2014**, *79*, 5088−5096.
25. Rodriguez, J.; Walczak, M. A. *Tetrahedron Lett* **2016**, *57*, 3281–3283.
26. Panda, A.; Biswas, R. G.; Pal, S. *Tetrahedron Lett*, **2016**, *57*, 3625–3628.
27. Luchetti, G.; Ding, K.; Ornienko, A.; d'Alarcao, M. *Synthesis* **2008**, 3148–3154
28. Catelani, G.; D'Andrea, F.; Griselli, A.; Guazzelli, L.; Legnani, L.; Toma, L. *Tetrahedron Lett.* **2008**, *49*, 4534–4536.
29. Vitelio, C.; Bellomo, A.; Brovett, M.;Seoane, G.; Gonzalez, D. *Carbohydr. Res.* **2004**, *339*, 1773–1778.
30. Kowarski, C. R.; Sarel, S. *J. Org. Chem.* **1973**, *38*, 117–119.
31. Mehta, G.; Lakshminath, S. *Tetrahedron Lett.* **2000**, *41*, 3509–3512;
32. Chola, J.; Masesane I. B. *Tetrahedron Lett.* **2008**, *49*, 5680–5682.
33. Tse, B.; Kishi, Y. *J. Am. Chem. Soc.* **1993**, *115*, 7892–7893.
34. Chida, N.; Ogawa, S. *Chem. Commun.* **1997**, 807–813.
35. Jagdhane, R. C.; Shashidhar, M. S. *Tetrahedron*, **2011**, *67*, 7963–7970.
36. Gurale, B. P. Shashidhar, M. S. and Gonnade, R. G., *J. Org. Chem.* **2012**, *77*, 5801−5807 and references cited therein.
37. Zemplen, G.; Csiiros, Z.; Angyal, S. *Ber. Dtsch. Chem. Ges.* **1937**, *70*, 1848.
38. Garegg, J.; Hultberg, H.; Oscarson, S. *J. Chem. Soc., Perkin Trans. I*, **1982**, 2395– 2397.
39. Stork, G.; Rychnovsky, S. D. *J. Am. Chem. Soc.* **1987**, *109*, 1565–1567.
40. Wipf, P.; Tsuchimoto, T.; Takahashi, H. *Pure Appl. Chem.* **1990**, *71*, 415–421.
41. Zhang, Z.; Magnusson, G. *J. Org. Chem.* **1996**, *61*, 2383–2393.
42. Guiso, M.; Procacoio, C.; Fizzano, M. R.; Piccioni, F. *Tetrahedron Lett*. **1997**, *38*, 4291–4294.
43. Ghosh, A. K.; Liu, C. *Chem. Commun.* **1999**, 1743–1744.
44. Honda, T.; Endo, K.; Ono, S. *Chem. Pharm. Bull.* **2000**, *48*, 1545–1548.
45. Johann Mulzer *Chem. Commun*. **2007**, 2107-2120.
46. Lin, C.; Hou, C.; Guo, Y.; Cheng, W . *Org. Lett.* **2016**, *18*, 5216−5219
47. Martinez-Solorio, D.; Jennings, M. P. *J. Org. Chem*. **2010**, *75*, 4095–4104.

48. Garrett, S. W.; Liu, C.; Riley, A. M.; Potter, B. V. L. *J. Chem. Soc. Perkin Trans 1*, **1998**, 1367–1368.
49. Lee, H. W.; Kishi, Y. *J. Org. Chem.* **1985**, *50*, 4402–4404.
50. Biomonte, M. A.; Vasella, A. *Helv. Chim. Acta.* **1998**, *81*, 688–694.
51. Riley, A. M.; Potter, B. V. L. *Tetrahedron Lett.* **1998**, *39*, 6769–6772.
52. Praveen, T.; Shashidhar, M. S. *Carbohydr. Res.* **2001**, *330*, 409–411.
53. Bhosekar, G.; Murali, C.; Gonnade, R. G.; Shashidhar, M. S.; Bhadbhade, M. M. *Cryst. Growth. Design* **2005**, *5*, 1977–1982.
54. Billington, D. C.; Baker, R.; Kulagowski, J. J.; Mawer, I. M.; Vacca, J. P.; de Solms, S. J.; Huff, J. R. *J. Chem. Soc. Perkin Trans. 1* **1989**, 1423–1429.
55. Devaraj, S.; Shashidhar, M. S.; Dixit, S. S. *Tetrahedron* **2005**, *61*, 529–536.
56. Jagdhane, R. C.; Shashidhar, M. S. *Eur. J. Org. Chem.* **2010**, 2945–2953.
57. Sureshan, K. M.; Shashidhar, M. S.; Praveen, T.; Das, T. *Chem. Rev*. **2003**, *103*, 4477–4503.
58. Laxmansingh, T. P.; Yuh-Sheng, W.; Shang-Cheng, H. *Chem. Commun.* **2010**, *46*, 5524-5526 and references cited therein.
59. Gilbert, I. H.; Holmes, A. B.; Young, R. C. *Tetrahedron Lett*. **1990**, *31*, 2633–2634.
60. Šala, M.; Kolar, J.; Strlič, M.; Kočevarb, M. *Carbohydr. Res.* **2006**, *341*, 897–902.
61. Grove, S. J. A.; Gilbert, I. H.; Holmes, A. B.; Painter, G. F.; Hill, M. L. *Chem. Commun.* **1997**, 1633–1634.
62. Murali, C.; Shashidhar, M. S.; Gopinath, C. S. *Tetrahedron* **2007**, *63*, 4149–4155.
63. Mart, A; Shashidhar, M. S. *Tetrahedron* **2012**, *68*, 9769-9776.
64. Swarbrick, J. M.; Cooper, S.; Bultynck, G.; Gaffney, P. R. J. *Org. Biomol. Chem.* **2009**, *7*, 1709–1715.
65. Swarbrick, J. M.; Gaffney, P. R. J. *J. Org. Chem.* **2010**, *75*, 4376–4386.
66. Gilbert, I. H.; Holmes, A. B.; Pestchanker, M. J.; Young R. C. *Carbohrydr. Res.* **1992**, *234*, 117–130.
67. Eisch, J. J.; Rhee, S. G. *J. Am. Chem. Soc.* **1974**, *96*, 7276–7284.
68. Conway, S. J.; Gardiner, J.; Grove, S. J. A.; Johns, M. K.; Lim, Z.-Y.; Painter, G. F.; Robinson, D. E. J. E.; Schieber, C.; Thuring, J. W.; Wong, L. S. M.; Yin, M.-X.; Burgess, A. W.; Catimel, B.; Hawkins, P. T.; Ktistakis, N. T.;

Stephens, L. R.; Holmes, A. B. *Org. Biomol. Chem*. **2010**, *8*, 66–74 and references cited therein.

69. Painter, G. F.; Grove S. J. A.; Gilbert, I. H.; Holmes, A. B.; Raithby, P. R.; Hill, M. L.; Hawkins, P. T.; Stephens, L. R. *J. Chem. Soc., Perkin Trans. 1* **1999**, 923–935.
70. Ballereau, S.; Poirier, S. N.; Guillemette, G.; Spiess, B.; Schlewer, G. *J. Chem. Soc., Perkin Trans. 1* **1998**, 1859–1864.
71. Moris, M. A.; Caron, A. Z.; Guillemette, G.; Rognan, D.; Schmitt, M.; Schlewer, G. *J. Med. Chem.* **2005**, *48*, 1251–1255.
72. Gurale, B. P.; Krishnaswamy, S.; Vanka, K.; Shashidhar, M. S. *Tetrahedron* **2011**, *67*, 7280-7288.
73. Yeh, S. M.; Lee, G. H.; Wang, Y.; Luh, T. Y. *J. Org. Chem.* **1997**, *62*, 8315–8318.
74. Gurale, B. P.; Kumar V.; Shashidhar, M. S. *Carbohydr. Res.* **2012**, *351*, 26–34.
75. Song, F.; Zhang, J.; Zhao, Y.; Chen, W.; Lib, L.; Xi, Z. *Org. Biomol. Chem.* **2012**, *10*, 3642-3654.
76. Schmitt, L.; Spiess, B.; Schlewer, G. *Tetrahedron Lett.* **1998**, *39*, 4817–4820.
77. Hager, A.; Wu, M.; Wang, H.; Brown, Jr. N. W.; Shears, S. B.; Veiga, N.; D. Fiedler, D. *Chem. Eur. J.* **2016**, *22*, 12406 – 12414.
78. Conway, S. J.; Miller, G. *J. Nat. Prod. Rep.* **2007**, *24*, 687–707.
79. Best, M. D.; Zhang, H.; Prestwich, G. D. *Nat. Prod. Rep.* **2010**, *27*, 1403–1430.
80. Jessen, H. J.; Capolicchio, S.; Pavlovic, I.; Thakor, D. T. *Synlett* **2014**, 1494–1498.
81. Spiers, I.D.; Freeman, S.; Poyner, D. R.; Schwalbe, C. H. *Tetrahedron Lett.*, **1995**, *36* 2125-2128.
82. Riley, A. M.; Jenkins, D. J.; Potter, B. V. L. *Carbohydr. Res*. **1998**, *314*, 277-281.
83. Chida, N.; Nakazawa, N.; Ohtsuka, M.; Suzuki, M.; Ogawa, S. *Chem. Lett.* **1990**, 423–426.
84. Ogawa, S.; Ohishi, Y.; Asada, M.; Tomoda, A.; Takahashi, A.; Ooko, Y.; Mori, M.; Itoh, M.; Korenaga, T. *Org. Biomol. Chem.* **2004**, *2*, 884–889.

Chapter 2

A study of the regioselectivity of reductive cleavage of *myo*-inositol orthoesters with DIBAL-H

2.1. Introduction

myo-Inositol, its derivatives and analogs frequently figure in the contemporary literature of chemistry and biology. Most of these reports pertain directly or indirectly, towards unraveling the intricacies of the *myo*-inositol cycle in eukaryotic cells. Impairment of the *myo*-inositol cycle has been implicated in the cause of several diseases including sleeping sickness, cancer, diabetes and manic depression.[1-9] Understandably, these developments in biology and medicine led to optimism about the pharmacological intervention of the *myo*-inositol cycle for the treatment of several diseases. Consequently, several synthetic methodologies and techniques to generate natural inositol derivatives and their analogs were developed, perhaps the most common being the use of abundantly available *myo*-inositol as the starting material.[10-14] Since *myo*-inositol has six secondary hydroxyl groups which have subtle differences in reactivity, regioselective functionalization of one of these hydroxyl groups is an arduous task. Hence most early synthetic sequences starting from *myo*-inositol resorted to initial (and transient) protection of the *myo*-inositol hydroxyl groups as the corresponding 1,2-acetals (Scheme 1, **2.1**, **2.2**, **2.3**). This step invariably generated several regio-isomers, which had to be separated before further synthetic transformations.

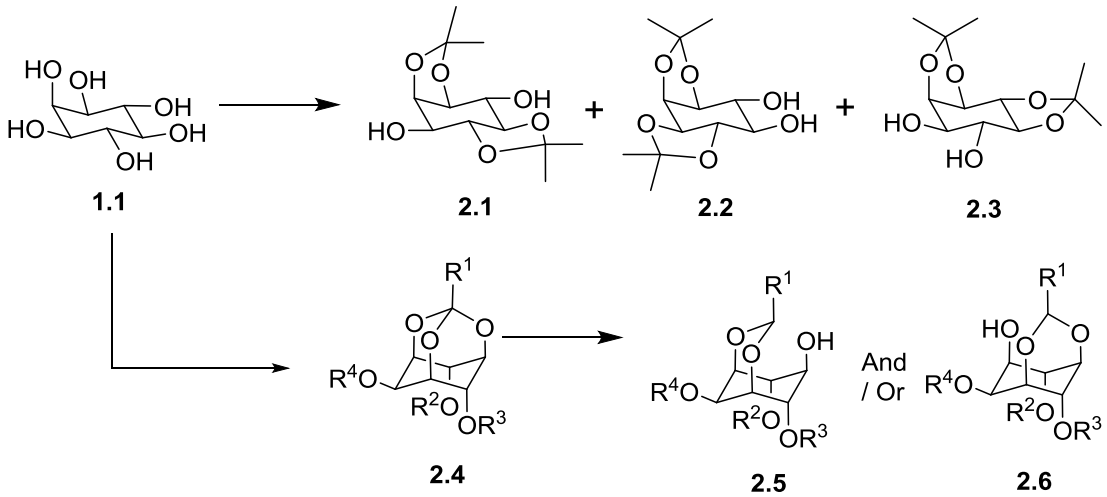

Scheme 1. Protection of *myo*-inositol hydroxyl groups as *1,2*-acetals and orthoesters.

Subsequently, methods for the simultaneous protection of three *myo*-inositol hydroxyl groups as the corresponding orthoester were developed. These orthoester derivatives are obtained as single products and hence laborious separation procedures are circumvented. Reductive cleavage of *myo*-inositol orthoesters generates *1,3*-acetals

and these appear to have potential to be key intermediates for the synthesis of inositol derivatives (Chapter 1).[15] Although, the reductive cleavage of inositol orthoesters can give rise to two isomeric *1,3*-acetals, conditions for the selective cleavage of certain *myo*-inositol orthoesters are reported.[16] Incidentally, in contrast to *1,2*-acetals, which have rigid molecular frames, the *1,3*-acetals are relatively flexible and (in principle) can exist in different conformations.[17] Hence they are interesting from the point of view of synthesis as well as molecular structure. Substitution of the orthoformate hydrogen with methyl and phenyl groups respectively generates the corresponding orthoacetate and orthobenzoate derivatives. Reductive cleavage of an orthoformate, orthoacetate and orthobenzoate respectively generate the corresponding methylidene, ethylidene and benzylidene derivatives (Scheme 1, **2.5** / **2.6** R^1 = H, Methyl, Phenyl respectively).[16, 18] These acetals have varying hydrolytic stabilities (methylidene > ethylidene > benzylidene) and (unlike the methylidene and ethylidene acetals) the benzylidene acetal on further reduction generates the corresponding benzyl ether, which is a common protecting group for alcohols. The present chapter delineates our attempts to understand the regioselectivity of the reductive cleavage of *myo*-inositol orthoesters with DIBAL-H due to variation in the apical orthoester substituent. Mechanism and selectivity of the cleavage of orthoesters by DIBAL-H have been investigated.[13, 14, 16]

2.2. Results and discussion

Although *myo*-inositol orthoesters can be cleaved with metal-organic reagents [16, 18] the most convenient and frequently encountered cleaving reagent is DIBAL-H.[18] The mechanism of the cleavage with DIBAL-H, to explain the composition of the products formed has been discussed in detail in Chapter 1. As already mentioned the substitution on the orthoester may hold bearing on the regioselectivity. (See Chapter 1, Scheme 4 and Scheme 5). This implies that the symmetry (or rather the lack of it) with regards to the *O*-substitution in *myo*-inositol orthoesters does not account for the ratio of the products formed. Hence it was speculated that the orthoester moiety might be playing a determining factor for the observed selectivity. However, the selectivity data in the literature reports on the DIBAL-H mediated cleavage of in *myo*-inositol

orthoestrs preclude any conclusion since the experimental conditions and the associated data are neither uniform nor consistent.

Hence we prepared *myo*-inositol orthoformate, orthobenzoate and orthoaceate derivatives carrying the same ethers at C2, C4, and C6-positions on the inositol ring, and subjected them to cleavage with DIBAL-H, under comparable conditions, and the results are shown in Scheme 2.

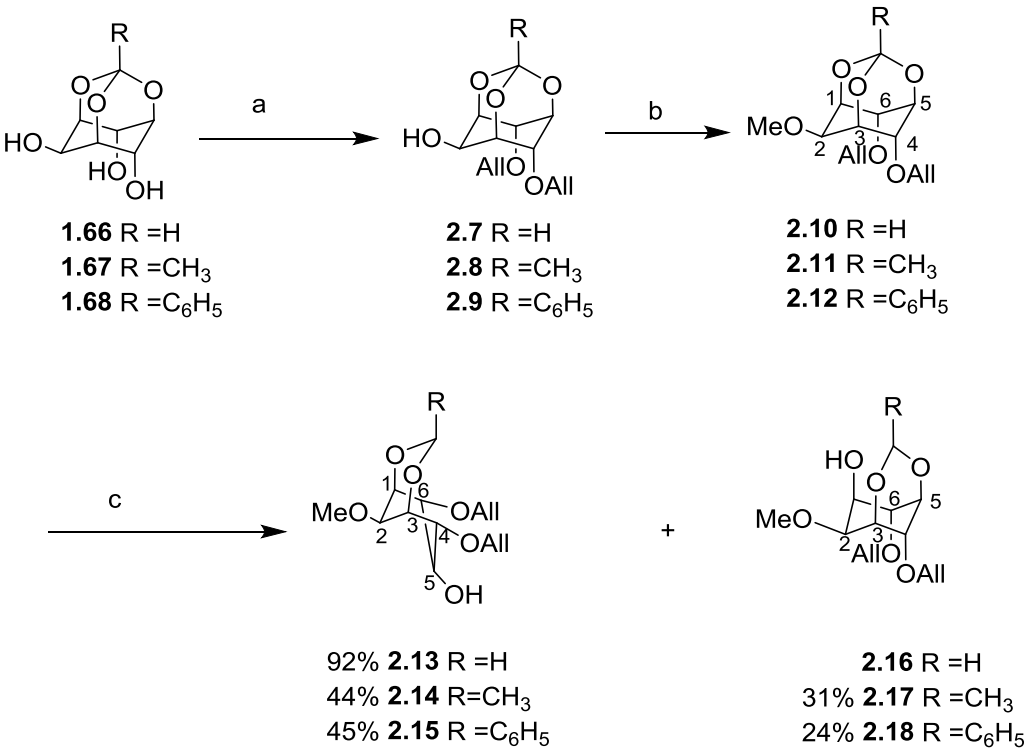

Scheme 2. a) DMF, LiH, AllBr, 24h, 0 °C to RT ,69-77 % b) NaH, MeI, DMF, 2h, 0 °C, 85 - 95 % c) DIBAL-H (2.5eq), dry DCM, 2.5h, 0 °C to RT.

The triols **1.66**-**1.68** were allylated selectively at the 4-*O*- and 6-*O*-positions, using allyl bromide and lithium hydride. We had shown earlier that this reaction is highly selective due to chelation of the C4- and C6-oxygen atoms with lithium ions.[19] The C2- hydroxyl group was then methylated to obtain the corresponding methyl ethers **2.10**-**2.12**. All the three orthoesters were subjected to reductive cleavage by DIBAL-H under comparable conditions. The results of cleavage of the three orthoesters **2.10**-**2.12** (Scheme 2) clearly show that the steric bulk of the substitutent at the apical orthoester carbon contributes significantly to the observed regioselectivity of the reductive cleavage reaction. The selectivity towards formation of the 1,3-acetals **2.13**-**2.15** decreases on going from orthoformate to orthobenzoate to orthoacetate. We could isolate the 1,3-methylidene acetal **2.13** in 92% yield as a single product, on

reduction of the orthofomate **2.10** and hence we presume that the corresponding 1,5-methylidene acetal **2.16** was either not formed or the yield was low to be isolated. Cleavage of the orthobenzoate **2.13** yielded the two isomeric benzylidene acetals **2.15** and **2.18** in the ratio 1.9:1. The structures of the isomeric products were established by the single crystal X-ray diffraction analysis of the C5-alcohol **2.15** and the *p*-nitrobenzoate ester (**2.19**) of the C3-alcohol **2.18**. The ratio of the 1,3- to 1,5-acetals on reductive cleavage of the orthoacetate **2.11** was 1.4:1. Hence the selectivity towards the formation of the 1,3-acetal on cleavage of *myo*-inositol orthoesters with DIBAL-H reduces as the bulk of the substituent at the apical orthoester carbon increases (H > Ph > Me). It is pertinent to note that though the phenyl ring might appear larger compared to a methyl group, by virtue of its planarity, phenyl ring could offer less steric hindrance (compared to the non-planar methyl group) to the incoming reducing agent.

It is apposite to mention that although the isomeric *1,3*-benzylidene acetals **2.15** and **2.18** could be separated establishing the structure of **2.18** took some effort. The 1,3-acetal **2.15** was stable and also afforded good crystals suitable for single crystal X-ray diffraction studies, which unequivocally established its structure [Figure 1(a)]. The 1,5-benzylidene acetal **2.18** on the other hand was prone to hydrolysis (see below) and failed to crystallize. Hence it was converted to the corresponding *p*-nitrobenzoate **2.19** (Scheme 3) which could be crystallized and structure determined by single crystal X-ray diffraction experiments. [Figure 1(b)]

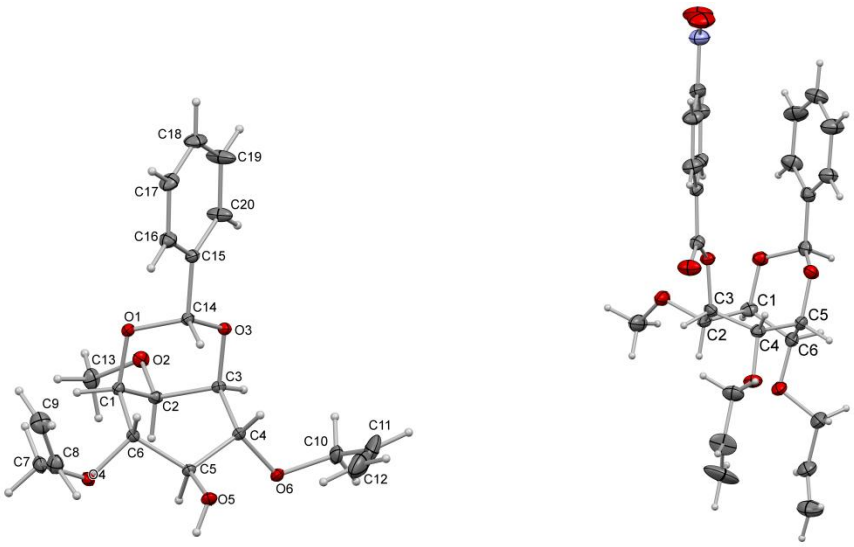

(a) (b)

Figure 1. ORTEP of (a) **2.15** (b) **2.19**. Thermal ellipsoids are drawn at 50% probability level. Hydrogen atoms are depicted as small spheres of arbitrary radii.

A $CDCl_3$ solution of **2.19** rapidly hydrolysed (perhaps due to the presence of traces of acid in $CDCl_3$) to yield the corresponding diol and benzladehyde (see Appendix for NMR spectrum). However, a good NMR spectrum could be obtained by recording the spectrum of a freshly prepared solution of **2.19**.

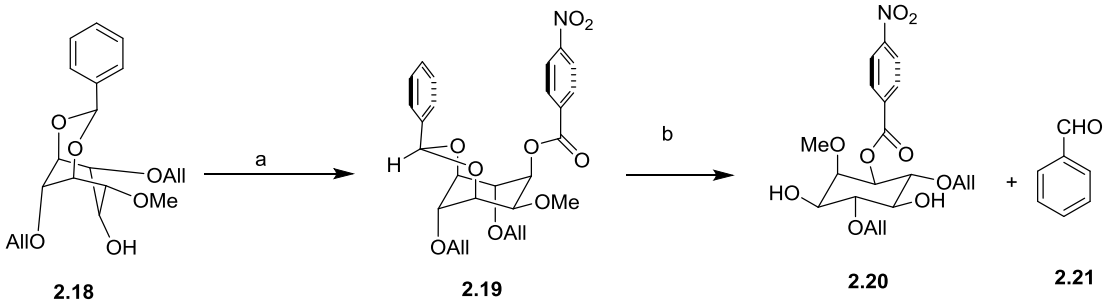

Scheme 3. a) Pyridine, *p*-nitrobenzoyl chloride, DMAP, 34 h, 0 °C to RT, 77%; (b) $CDCl_3$

The detailed mechanism explaining the formation of **2.13** to **2.18** is shown in Scheme 4.

We carried out DFT calculations to estimate the relative stability of the intermediate complexes (**2.22-2.24** and **2.31-2.33**) to gain insight into the cause of observed selectivity during the cleavage of *myo*-inositol orthoesters (Scheme 4 and Figure 2).

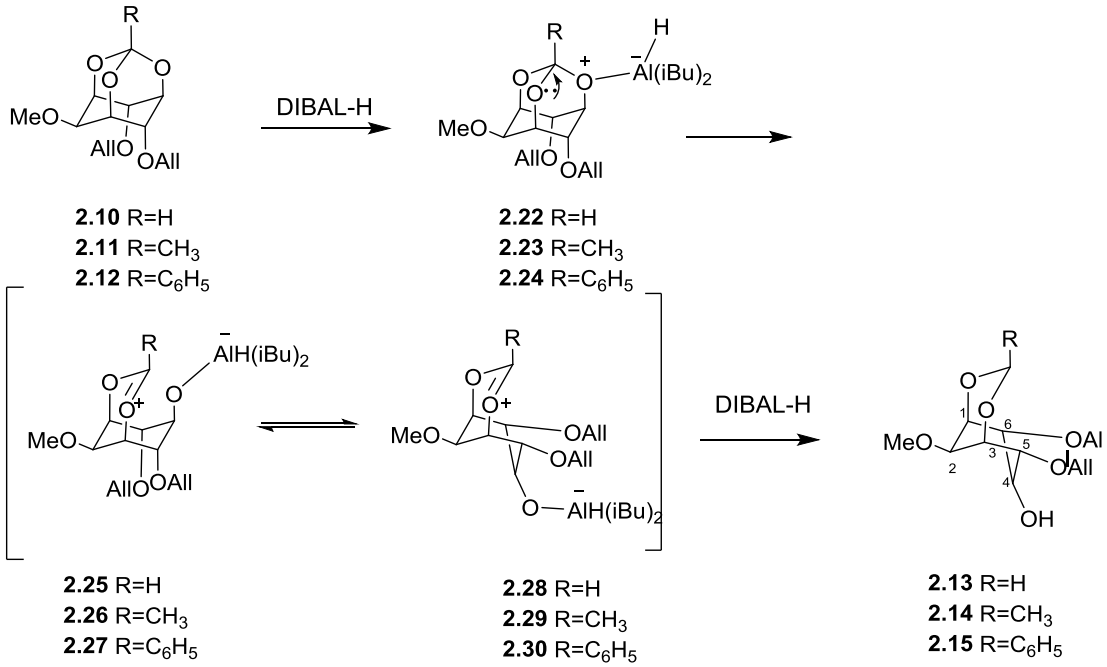

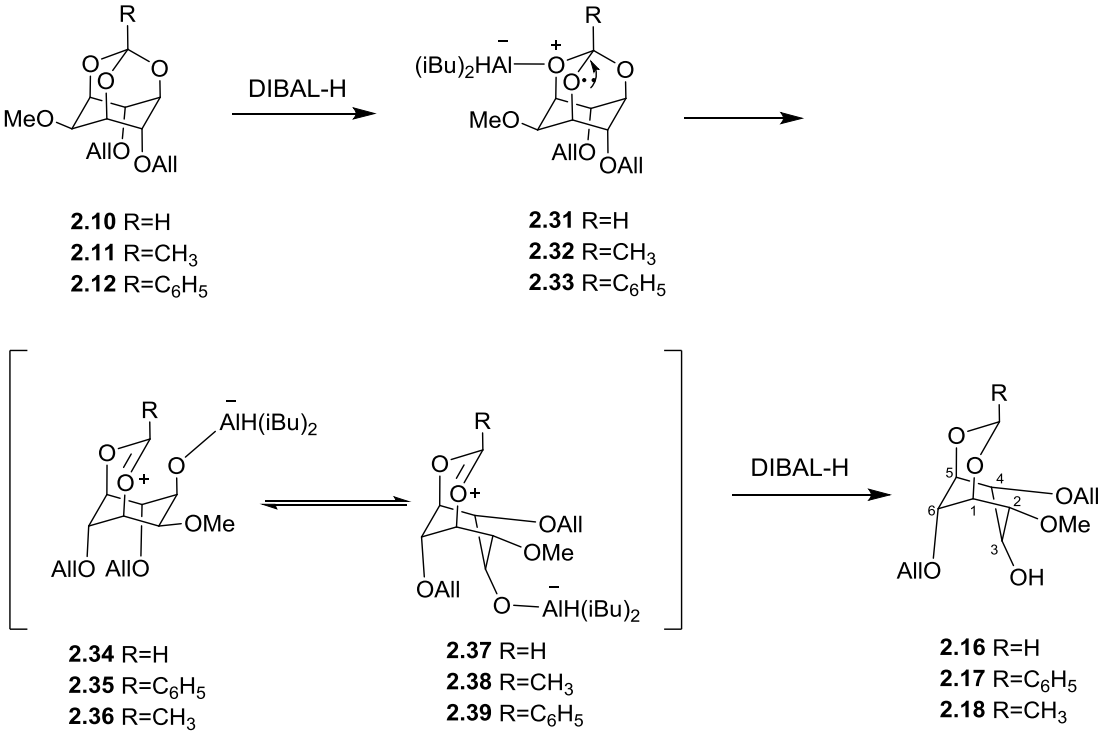

2.10 R=H
2.11 R=CH_3
2.12 R=C_6H_5

2.31 R=H
2.32 R=CH_3
2.33 R=C_6H_5

2.34 R=H
2.35 R=C_6H_5
2.36 R=CH_3

2.37 R=H
2.38 R=CH_3
2.39 R=C_6H_5

2.16 R=H
2.17 R=C_6H_5
2.18 R=CH_3

Scheme 4. Plausible mechanism for the formation of 1,3- and 1,5-acetals of *myo*-inositol by reductive cleavage of the corresponding orthoester.

The results of the DFT calculations suggested that the difference in energy between the regioisomeric DIBAL-H – orthoester complexes is in the order orthoformate (1.5 Kcal/ mol) < orthobenzoate (2.1 Kcal/ mol) < orthoacetate (2.6 Kcal/ mol). In each of these pairs, the DIBAL-H complex where the C5-oxygen atom is involved is relatively more stable than the complex where the C3 (or C1)-oxygen atom is involved. This could explain the predominant cleavage of the C5-O bond in all the three orthoesters leading to the formation of the corresponding 1,3-acetals in higher yields. These differences in energy values also imply that the ease of inter-conversion between the two isomeric complexes is in the order orthoformate > orthobenzoate > orthoacetate. These are in the increasing order of the steric bulk of the substituent at the apical carbon of the orthoester moiety. These results taken together with the experimentally observed ratio of the two cleavage (C3 and C5 of the inositol ring) products appear to suggest that the rate of formation of C5 cleavage products (**2.13-2.15**) is higher than the rate of formation of C3 cleavage products (**2.16-2.18**).

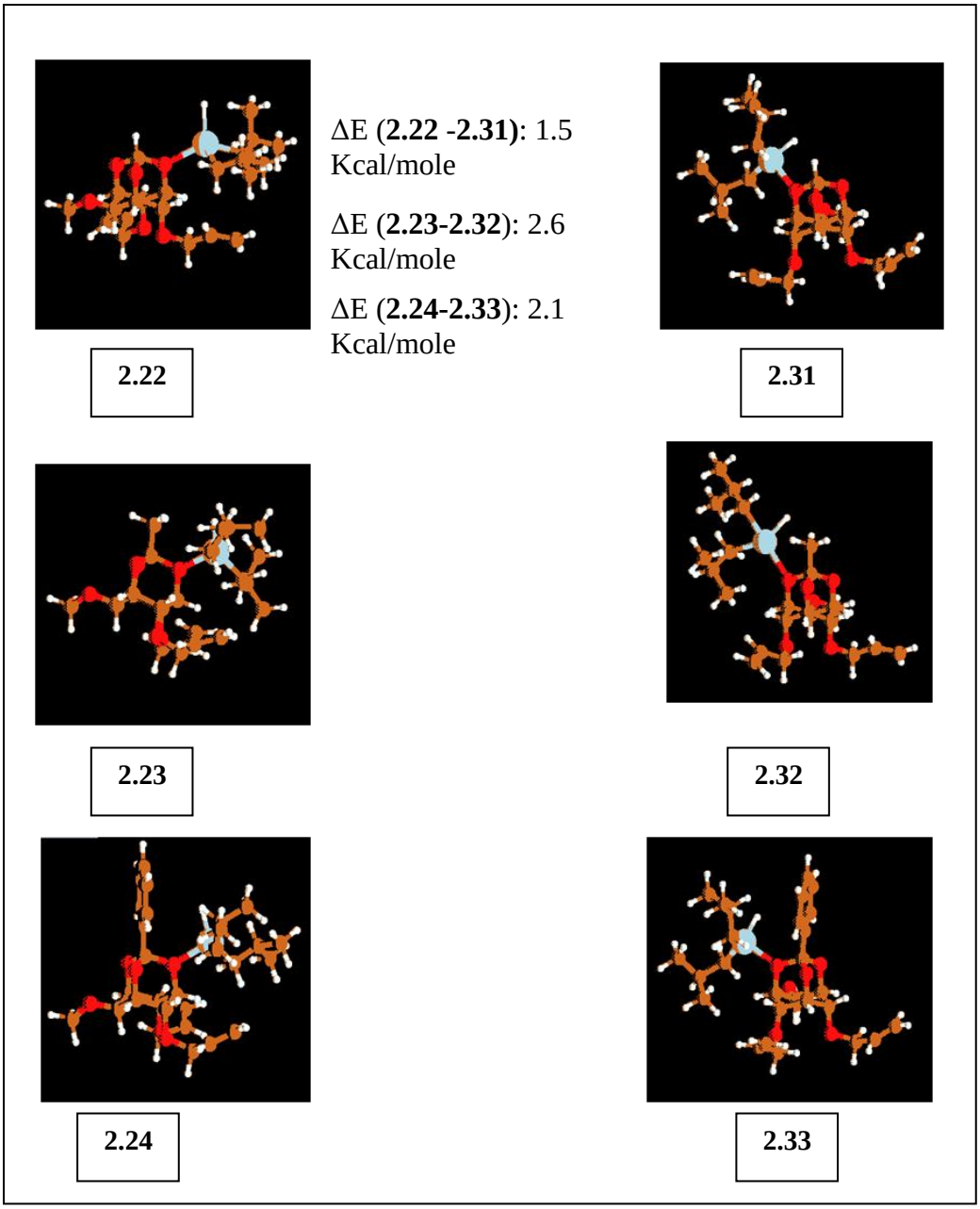

Figure 2. The optimized geometries for the intermediate DIBAL-H complexes with *myo*-inositol orthoesters that lead to the formation of 1,3- and 1,5-acetals. The energy difference ΔE represents the relative stability of the isomeric complexes.

Hence observed selectivity for the cleavage of the orthoformate is highest, while that of the orthoacetate is lowest and the orthobenzoate is between these two extremes. In other words, for the orthoacetate, since the difference in energy between the two intermediates is higher, the rate of inter- convertibility is much less, and each intermediate perhaps has enough time to form the respective cleavage product, giving rise to the almost equitable mixture. In contrast, for the orthoformate, since the

difference in energy between the two intermediates is lower, the rate of inter-convertibility is much higher, and if one DIBAL-H complex (**2.22**) gets reduced faster than the other (**2.31**), the reductive cleavage can result in very high regio-selectivity (Scheme 4). The bulk of the phenyl ring (owing to its planarity) being intermediate between that of H and Me, the observed selectivity for the reductive cleavage of the orthobenzoate is between that of the orthoformate and the orthoacetate.

It is pertinent to note at this point that in the case of the orthobenzoate and orthoacetate derivatives, there are four possible products that may be formed (Chart 1, two pairs of enantiomers – **2.40**, **2.41** and **2.42**, **2.43**).

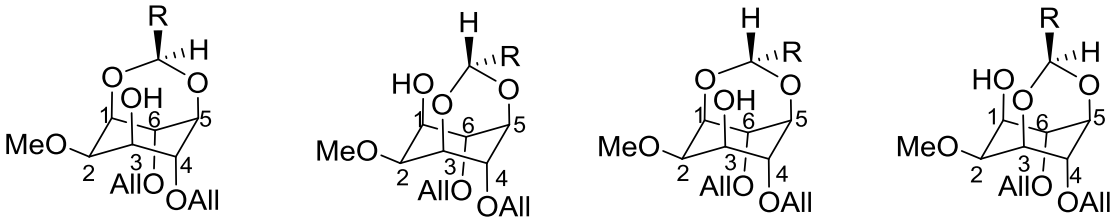

R= C_6H_5 /CH_3

Chart 1: The possible diastereomers formed by the cleavage of the orthoester.

The existence of diastereomers was suggested by the fact that in the NMR spectra of **2.17** and **2.18** broadening of the signals was observed (see Appendix). However we were not able to estimate the relative ratios or isolate the diastereomers formed. This anyway does not have bearing on the conclusions of this chapter.

2.2a. DFT Analysis of miscellaneous compounds

Since we had also observed differences in the cleavage pattern of *myo*-inositol orthoformate depending on the O-alkyl groups at 2-, 4- and 6-positions we carried out DFT calculations for the cleavage of the trimethyl ether **1.136** and tribenzyl ether **1.76** with DIBAL-H (Scheme 5, Figure 3).

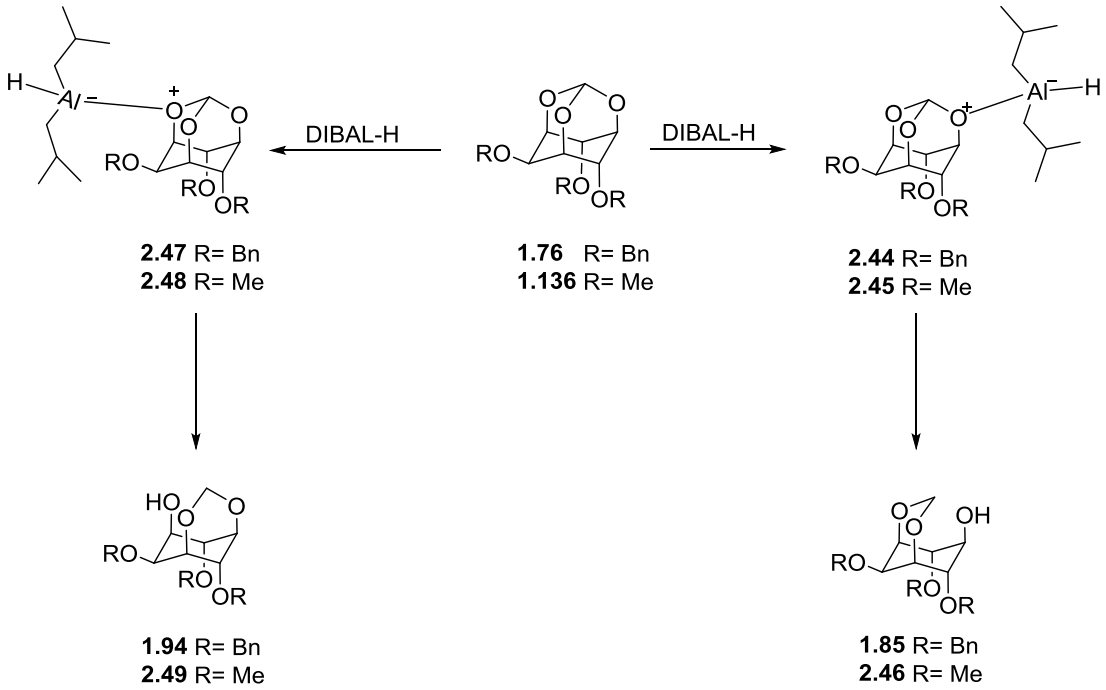

Scheme 5. The reduction of **1.136** and **1.76** with DIBAL-H

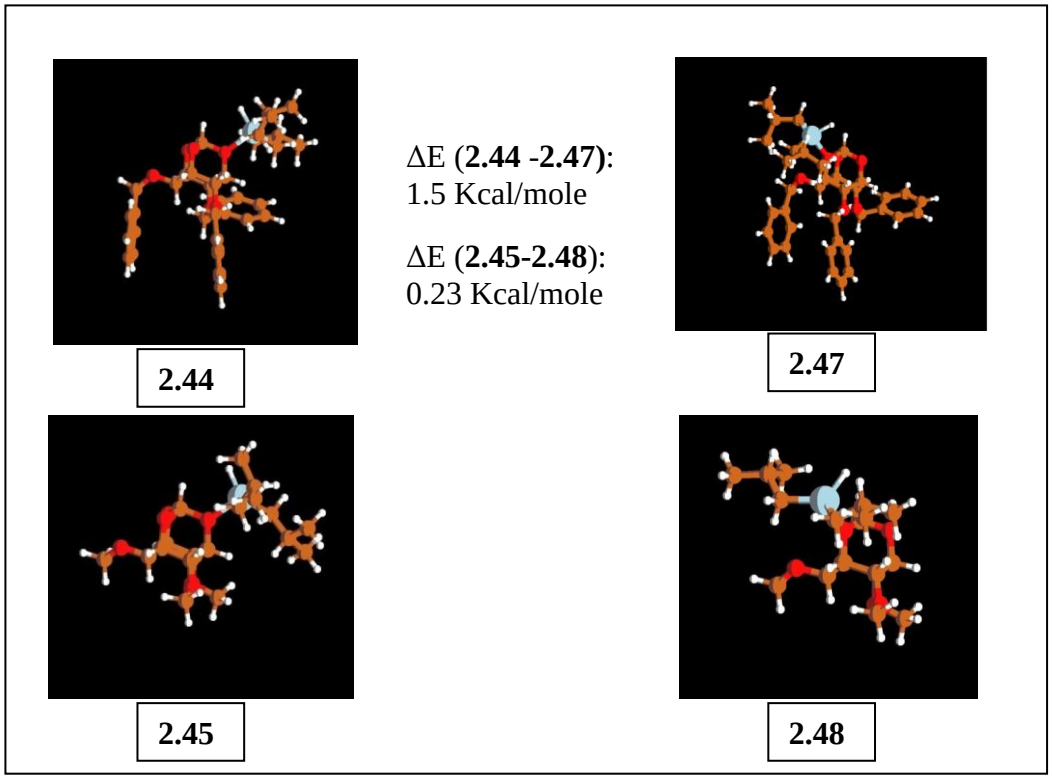

Figure 3. The optimized geometries for the intermediate DIBAL-H complexes with *myo*-inositol **1.136** and **1.76** orthoesters The energy difference ΔE represents the relative stability of the isomeric complexes.

Results of these calculations substantiate that the observed selectivity in the orthoester cleavage could also depend on the substituent at the C2, C4 and C6-hydroxyl groups, although they are far removed from the site of DIBAL-H cleavage.

Following in the same vein, we were curious to see whether the Grignard reduction of the orthoester could also be rationalized on the basis of DFT analysis. As mentioned earlier in Chapter 1 (Section 1.2c), the orientation of the C2-methoxyl group played a decisive role during the reaction of the orthoester **1.143** with Grignard reagents.

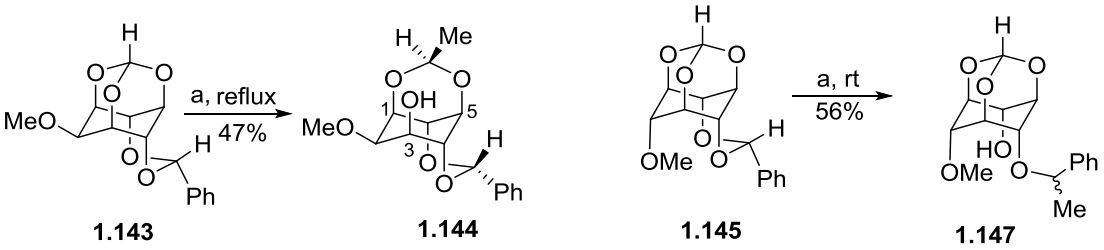

Scheme 6. (a) MeMgI in diethylether, benzene, RT to reflux, 16 h.

There are three possible chelates that could be involved during the reaction of inositol orthoformate with Grignard reagents (reaction of **1.76** and **1.136** with methylmagnesium bromide is shown in scheme 7 as an example): (a) between the C3 and C5 oxygens (**2.50** and **2.51**); (b) between the C1 and C3 oxygens (**2.54** and **2.55**) and (c) between the C1 and C2 oxygens (**2.56** and **2.57**). During geometrical optimization we observed that the chelates **2.54** and **2.55** inherently rearranged to **2.56** and **2.57** suggesting that **2.54** and **2.55** were not energetically favored (and hence were probably not involved in the reaction). From the energy differences (Figure 4) it was amply clear that the intermediates **2.56** and **2.57** were decidedly more stable than **2.50** and **2.51**.

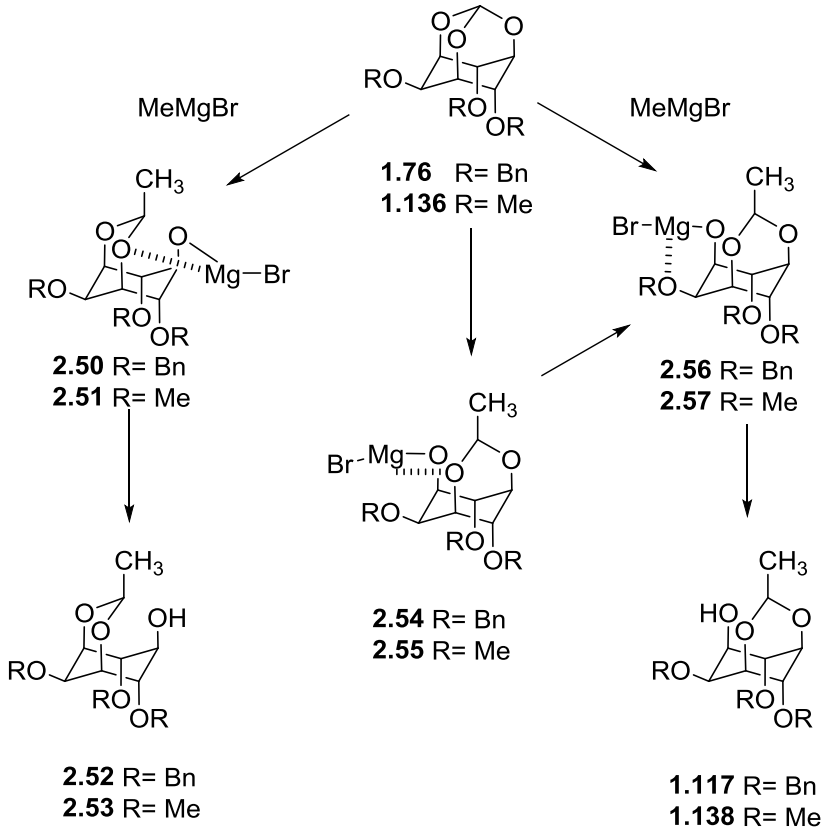

Scheme 7. The reduction of **1.136** and **1.76** with Grignard reagent MeMgBr.

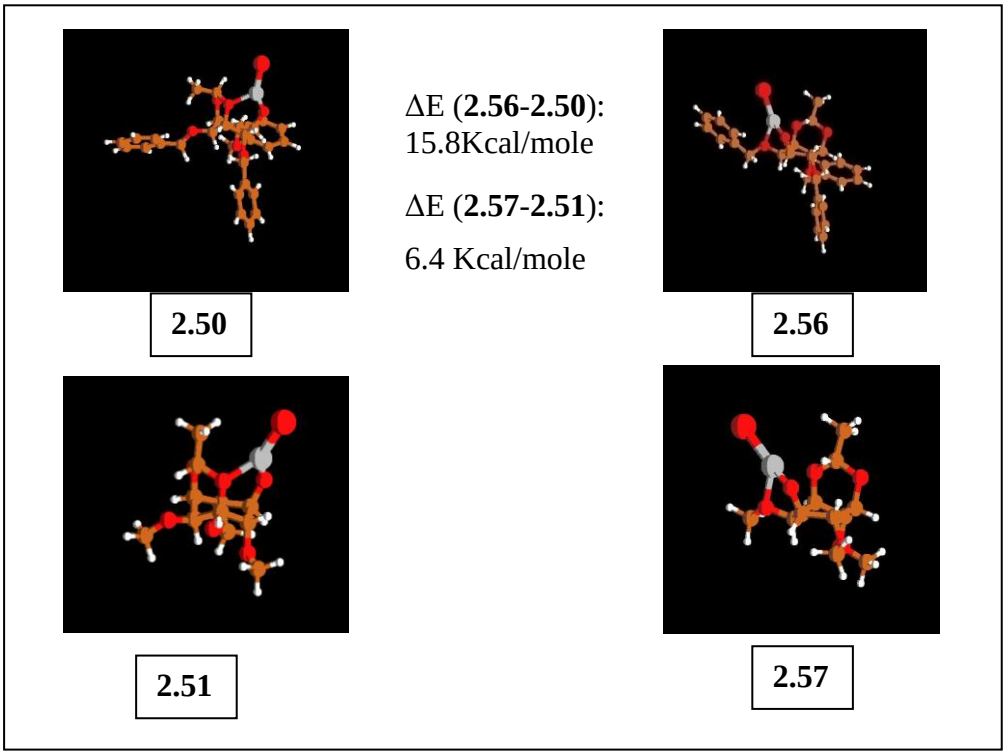

Figure 4. The optimized geometries for the intermediate MeMgBr. complexes with *myo*-inositol **1.136** and **1.76** orthoesters. The energy difference ΔE represents the relative stability of the isomeric complexes.

Hence results of DFT calculations are in good agreement with the results obtained by experiment. This reinforces the credibility of DFT calculations and the associated interpretation of the experimental results of the reductive cleavage of inositol orthoesters presented in this chapter.

2.3. Conclusion

From the experimental observations as well DFT analysis it was concluded that the orthoester group influences the regioselctivity of DIBAL- H reduction. As the bulk of the orthoesester group from increases H to phenyl to methyl, the selectivity decreases. The effect of the substituting groups was also discussed. The DFT analysis of the reaction of the orthoesters with the Grignard reaction also highlight the involvement of the C2- hydroxyl group in influencing the regio-selectivity. Hence it may not be easy to arrive at experimental conditions to attain selectivity during the cleavage of *myo*-inositol orthoesters with DIBAL-H, so as to obtain either 1,3-acetal or 1.5-acetal exclusively.

2.4. Experimental

2.4.1. X-ray Data (Collection, Structure Solution and Refinement)

Single crystal X-ray studies were carried out on a Bruker SMART APEX single crystal X-ray CCD diffractometer with graphite-monochromatized (Mo K_α= 0.71073Å) radiation. The X-ray generator was operated at 50 kV and 30 mA. Diffraction data were collected with ω scan width of 0.3° at different settings of φ (0°, 90°, 180° and 270°) keeping the sample-to-detector distance fixed at 6.145 cm and the detector position (2θ) fixed at -28°. The X-ray data acquisition was monitored by SMART program (Bruker, 2003).[20] All the data were corrected for Lorentzian and polarization effects using SAINT programs (Bruker, 2003).[20] A semi-empirical absorption correction (multiscan) based on symmetry equivalent reflections was applied by using the SADABS program (Bruker, 2003).[20] Lattice parameters were determined from least squares analysis of all reflections. The structure was solved by direct method and refined by full matrix least-squares, based on F^2, using SHELX-97 software package.[21] Molecular diagrams were generated using SHELXTL and ORTEP-32.[22]

2.4.2. Computational details

All the density functional theory calculations were carried out using the Turbomole suite of programs.[23] The DFT Geometry optimizations were performed using the B-P 86 functional.[24] The electronic configuration of the atoms was described by a triple-zeta basis set augmented by a polarization function (TURBOMOLE basis set TZVP)[25] along with the multipole accelerated resolution of identity (marij)[26] approximations were employed for an accurate and efficient treatment of the electronic Coulomb term in the density functional calculations. Solvent effects have been incorporated using the COSMO model, 44 with toluene (epsilon = 2.38)[27] as the solvent.

2.4.3. General Experimental Methods

All the solvents were purified according to the literature procedure[28] before use. All air or moisture sensitive reactions were carried out in an atmosphere of argon or nitrogen. Dry DMF and dry THF were used as solvents in all the experiments involving metal hydrides. Sodium hydride used in experiments was 60% suspension in mineral oil. Thin layer chromatography was performed on E. Merck pre-coated 60 F_{254} plates and the spots were rendered visible either by shining UV light or by

charring the plates with chromic acid solution. Column chromatographic separations (silica gel, 100–200 mesh) and flash column chromatographic separations (silica gel, 230–400 mesh) were carried out with light petroleum–ethyl acetate mixtures as eluent. 'Usual work-up' implies washing of the organic layer with water followed by brine, drying over anhydrous sodium sulfate, and removal of the solvent under reduced pressure using a rotary evaporator. IR spectra were recorded (in $CHCl_3$ solution, or as a Nujol mull or as a neat film) with a Shimadzu FTIR-8400 or Perkin–Elmer spectrophotometer. NMR spectra (200 MHz for ^1H and 50.3 MHz for ^{13}C) were recorded with a Bruker ACF 200 spectrometer unless otherwise mentioned. Chemical shifts (δ, ppm) reported are referred to internal tetramethylsilane (0 ppm) for ^1H NMR and $CDCl_3$ (77 ppm) for ^{13}C NMR. Microanalytical data were obtained using a Carlo-Erba CHNS-0 EA 1108 elemental analyzer. HRMS data was collected on Thermo Fischer Scientific Q- Exactive. All the melting points reported are uncorrected and were recorded using a Büchi B-540 electro-thermal melting point apparatus. Yields refer to chromatographically and spectroscopically pure compounds. All the asymmetrically substituted *myo*-inositol derivatives reported are racemic; however only one of the enantiomers is shown in all the schemes for convenience and clarity. Compounds previously reported in the literature were characterized by comparison of their melting points and/or ^1H NMR spectra with the reported data.

4, 6-Di-O-allyl-*myo*-inositol-1, 3, 5-orthoacetate (2.8): To a solution of orthoacetate triol **1.67** (0.518 g, 2.539 mmol), in dry DMF (30mL), lithium hydride (0.121 g, 15.234 mmol) was added at 0°C and stirred subsequently for 1 hour at ambient temperature. To the above solution (thick slurry) allyl bromide (0.231 mL, 2.64 mmol) was added and stirred for 12 h. Ice was added to the reaction mixture and stirred for 2 h, solvents were removed under reduced pressure and the residue worked up with ethyl acetate and dried over anhydrous sodium sulphate to obtain **2.8** as gum. The crude product was purified by column chromatography (eluent: 30 % ethyl acetate in light petroleum, 100-200 mesh) to afford **2.8** (0.400 g, 69%) as a gum. TLC *Rf* = 0.3 (in 25% ethyl acetate/light petroleum.)

Data for **2.8**: **IR** (Chloroform): *v* 3550–3400 cm^{-1}; **^1H NMR** (500 MHz, $CDCl_3$) δ = 5.81 - 5.91 (m, 2 H), 5.28 (dd, *J*=17.36, 1.72 Hz, 2 H), 5.16 - 5.20 (m, 2 H), 4.31 - 4.35 (m, 1 H), 4.18 - 4.25 (m, 4 H), 4.00 - 4.12 (m, 5 H), 2.96 (d, *J*=11.83 Hz, 1 H,

OH, D_2O exchangeable), 1.43 (3 H, s) ppm;**^{13}C NMR** (126 MHz, $CDCl_3$) δ = 133.8 (CH_2=*C*H), 117.2 (*C*H_2=CH), 108.9 (CH_3CO_3), 73.3 (Ins C), 73.0 (Ins C), 70.3 (*C*H_2-O), 67.6 (Ins C), 60.2 (CH_3), 24.1 (CH_3) ppm; **HRMS**: *m*/*z* calcd for $C_{14}H_{20}O_6Na^+$: 307.1152 [*M*+ Na^+]; found: 307.1157.

4,6-Di-*O*-allyl-*myo*-inositol-1,3,5-orthobenzoate (2.9): To a solution of orthobenzoate triol **1.68** (7 g, 26.3 mmol) in dry DMF (350 mL), lithium hydride (0.836 g, 105 mmol) was added at 0°C and stirred subsequently for 1 hour at ambient temperature. To the above solution (thick slurry) allyl bromide (5 mL, 58 mmol) was added and stirred for 12 h. Ice was added to the reaction mixture and stirred for 2 h, solvents were removed under reduced pressure and the residue worked up with ethyl acetate and dried over anhydrous sodium sulphate. The solvent was removed under reduced pressure to obtain the crude to obtain **2.9** as gum. The crude product was purified by column chromatography (eluent: 18% ethyl acetate in light petroleum, silica 100-200 mesh) to afford **2.9** (7 g, 77% yield) as a gum. TLC *Rf* = 0.3 (in 25% ethyl acetate/light petroleum.)

Data for **2.9**: **IR** (Chloroform): *v* 3400 cm^{-1} **^{1}H NMR** (500 MHz, $CDCl_3$) δ = 7.59 - 7.67 (m, 2 H), 7.31 - 7.43 (m, 3 H), 5.91 (m, *J*=17.09, 10.53, 5.42, 5.42 Hz, 2H), 5.32 (m, *J*=17.24, 1.58 Hz , 2 H), 5.21 (m, *J*=10.38, 1.32 Hz, 2 H), 4.53 (m, *J*=3.32, 1.72 Hz, 1 H), 4.39 - 4.43 (m,4 H), 4.07 - 4.19 (m,5 H), 3.08 (d, *J*=11.90 Hz , 1 H, OH, D_2O exchangeable) ppm; **^{13}C NMR** (126 MHz, $CDCl_3$**)** δ = 136.67 (Ph*C*O3), 133.82 (CH_2=*C*H), 129.4 (C_{arom}), 127.8(C_{arom}), 124.9 (C_{arom}), 117.3 (*C*H_2=CH), 74.1 (Ins C), 73.15 (Ins C), 70.5 (*C*H_2-O), 68.4 (Ins C), 60.4 (Ins C) ppm; **HRMS**: *m*/*z* calcd for $C_{19}H_{23}O_6Na^+$: 347.1489 [*M*+ Na^+]; found: 347.1485.

4, 6-Di-*O*-allyl-2-methyl-*myo*-inositol-1,3,5-orthoacetate (2.11): To a solution of the alcohol **2.8** (0.396 g, 1.4 mmol), in dry DMF (21 mL), sodium hydride (0.083 g, 2.1 mmol), was added and stirred for 10 min. Methyl iodide (0.13 mL, 2.1 mmol) was then added drop-wise and the reaction mixture was stirred for 3 h ambient temperature. Excess of sodium hydride was quenched by the addition of ice-cold water. The solvent was evaporated under reduced pressure and the residue was worked up with ethyl acetate and dried over anhydrous sodium sulphate. The solvent was removed under reduced pressure to afford the crude ether **2.11** which was then purified by column chromatography (eluent 25% ethyl acetate/light petroleum , silica 100-200 mesh) to obtain **2.11** as a gum (0.4 g, 96%) purified by column TLC *Rf*= 0.35 (in 25% ethyl acetate/light petroleum).

Data for **2.11**: **IR** (Chloroform): *v* 3600–3200 cm^{-1}; **^{1}H NMR** (200 MHz, $CDCl_3$) δ = 5.75 - 6.03 (m, 2 H), 5.13 - 5.44 (m, 4 H), 4.35 (d, *J*=3.03 Hz, 3 H), 4.20 - 4.30 (m, 2 H), 3.98 - 4.20 (m, 4 H), 3.67 (s, 1 H), 3.52 (s, 3 H), 1.47 (s, 1H) ppm; **^{13}C NMR (126 MHz, $CDCl_3$)** δ = 134.2 (CH_2=*C*H), 117.6 (*C*H_2=CH), 109.0 (CH_3*C*O_3), 73.5 (Ins C), 70.7 (O*C*H_2-CH=), 70.6 (Ins C), 68.5 (Ins C), 68.1 (Ins C), 56.9 (*C*H_3CO3), 24.3 (OCH_3) ppm; **HRMS**: *m*/*z* calcd for $C_{15}H_{22}O_6Na^+$: 321.1309 [*M*+ Na^+]; found: 321.1302.

4,6-Di-*O*-allyl-2-methyl-*myo*-inositol-1, 3,5-orthobenzoate (2.12): To a solution of the alcohol **2.9** (8.341 g, 24.1 mmol) in dry DMF (100 mL) , sodium hydride (1.444 g, 36.12 mmol) was added and stirred for 10 min. Methyl iodide (2.251 mL, 36.12 mmol) was then added drop-wise and the reaction mixture was stirred for 3 h at ambient temperature. Excess of sodium hydride was quenched by the addition of ice-cold water. The solvent was evaporated under reduced pressure and the residue was worked up with ethyl acetate and dried over anhydrous sodium sulphate. The solvent was removed under reduced pressure to afford the crude ether **2.12** which was then purified by column chromatography (eluent 20% ethyl acetate in light petroleum, silica 100-200 mesh) as a colorless solid (8.6 g, 84%). TLC *Rf*= 0.3 (in 15% ethyl acetate/light petroleum).

Data for **2.12**: **M.p.** 59-63 °C. (Crystallized from ethyl acetate-light petroluem); **IR** (Chloroform): *v* 3405 cm^{-1};**^{1}H NMR** (200 MHz, $CDCl_3$) δ = 7.59 - 7.70 (m , 2 H), 7.28 - 7.39 (m , 3 H), 5.82 - 6.04 (m, 2H), 5.18 - 5.40 (m, 4 H), 4.51 - 4.59 (m, 3 H), 4.38 - 4.47 (m, 2 H), 4.04 - 4.25 (m, 4 H), 3.79 (s, 1 H), 3.54 (s, 3 H) ppm; **^{13}C NMR** (126MHz, $CDCl_3$) δ = 137.1 (C_{arom}), 134.1 (CH), 129.3 (C_{arom}), 127.8 (C_{arom}), 125.3 (C_{arom}), 117.6 (*C*H_2=CH), 107.8 (Ph*C*O_3), 73.6 (Ins C), 71.0 (Ins C), 70.84 (O*C*H_2-CH=), 68.8 (Ins C), 68.5 (Ins C), 56.8 (CH_3) ppm; **HRMS**: *m*/*z* calcd for $C_{20}H_{24}O_6Na^+$: 383.1465 [*M*+ Na^+]; found: 383.1458.

Reductive cleavage of the orthoformate 2.10 with DIBAL-H: 1 M solution of DIBAL-H in toluene (9.5 mL, 9.5 mmol) was added drop-wise over a period of 15 min to a solution of the orthoformate **2.10** (1.071 g, 3.6mmol) in dry dichloromethane (25 mL) at 0 °C and then stirred at room temperature for 2.5 h. The reaction mixture was poured into a stirred solution of sodium potassium tartrate (35 mL) and saturated solution of ammonium chloride (28.5 mL) and stirred for 12 h. The mixture was extracted with ethyl acetate, washed with brine and dried over anhydrous sodium sulphate. The solvent was removed under reduced pressure to obtain the crude

alcohol. **2.13** (0.916 g , 85%) as a gum which was then purified by column chromatography (eluent 20% ethyl acetate in light petroleum, silica 100-200 mesh) to obtain **2.13** as a gum.

Data for **2.13**: **IR** (Chloroform): *v* 3600–3200 cm^{-1}; **^{1}H NMR** (200 MHz, $CDCl_3$) δ = 5.73 - 6.11 (m, 2 H), 5.11 - 5.42 (m, 4 H), 4.85 - 5.01 (m, 2 H), 4.44 - 4.57 (m, 1 H), 4.06 - 4.36 (m, 6 H), 3.75 - 4.04 (m, 3 H), 3.53 (s ,3 H), 3.20 (d, *J*=6.69 Hz, 1 H, D_2O exchangeable) ppm; **^{13}C NMR** (126MHz, $CDCl_3$) δ = 134.23 (CH_2=*C*H), 117.44 (*C*H_2=CH), 85.36 (CH_2), 80.82 (Ins C), 71.93 (Ins C), 71.07 (*C*H_2-CH=), 70.20 (Ins C), 56.04 (4 C, s) ppm; **HRMS**: *m*/*z* calcd for $C_{14}H_{22}O_6Na^+$: 309.1309 [*M*+ Na^+]; found: 309.1313.

Reductive cleavage of the orthoacetate 2.11 with DIBAL-H:1 M solution of DIBAL-H in toluene (1.9 mL, 1.9 mmol), was added drop-wise over a period of 15 min to a solution of **2.11** (0.232 g , 0.77 mmol), in dry dichloromethane (6 mL) at 0 °C and then stirred at room temperature for 2.5 h. Saturated solutions of sodium potassium tartrate (7.32 mL) and ammonium chloride (6 mL) to obtain a mixture of **2.14** and **2.17** which were separated using column chromatography (eluent 20-30% ethyl acetate in light petroleum, silica 230-400 mesh) to obtain **2.14** (0.051 g, 44%; TLC *Rf*= 0.3 (in 25% ethyl acetate/light petroleum) and **2.17** (0.036 g, 31%; TLC *Rf*= 0.4 in 25% ethyl acetate/light petroleum) in the ratio of 1.4:1. (0.116 g, starting material recovered.)

Data for **2.14**: **IR** (Chloroform): *v* 3500–3200 cm^{-1}; **^{1}H NMR** (200MHz ,$CDCl_3$) δ = 6.09 - 5.80 (m, 2 H), 5.42 - 5.17 (m, 4 H), 4.95 (d, *J* = 4.9 Hz, 1 H), 4.32 - 4.05 (m, 6 H), 3.82 - 3.61 (m, 3 H), 3.48 (s, 3 H), 3.24 (t, *J* = 2.4 Hz, 1 H), 2.55 (d, *J* = 2.7 Hz, 1 H), 1.34 (d, *J* = 4.9 Hz, 3 H) ppm; **^{13}C NMR** (126MHz ,CHLOROFORM-d) δ = 134.0(CH_2=*C*H), 118.0(*C*H_2=CH), 89.8(CH_3*C*H), 81.5(Ins C), 73.9(Ins C), 72.6(Ins C), 70.7(O*C*H_2-CH=), 70.2(Ins C), 56.9 (OCH_3), 21.2 (*C*H_3CO) ppm; **HRMS**: *m*/*z* calcd for $C_{15}H_{24}O_6Na^+$: 323.1465 [*M*+Na^+]; found: 323.1468.

Data for **2.17**: **IR** (Chloroform): *v* 3500–3200 cm^{-1}; **^{1}H NMR** (200MHz , $CDCl_3$) δ = 6.02 - 5.70 (m, 2 H), 5.49 (q, *J* = 4.8 Hz, 1 H), 5.39 - 5.13(m, 4 H), 4.74 - 3.61 (m, 10 H), 3.52 (s, 3 H), 2.21 (d, *J* = 2.9 Hz, 1 H), 1.36 - 1.11 (m, 3 H) ppm;**^{13}C NMR** (50MHz ,$CDCl_3$) δ = 134.5(CH_2=*C*H), 134.0(CH_2=*C*H), 117.8(*C*H_2=CH), 117.3(*C*H_2=CH), 90.16 (CH_3*C*H), 81.6(Ins C), 74.4(Ins C), 73.0(Ins C), 71.8(O*C*H_2-CH=), 70.6 (O*C*H_2-CH=), 68.8(Ins C), 67.8(Ins C), 56.4(OCH_3), 21.69(*C*H_3CO_3) ppm.; **HRMS**: *m*/*z* calcd for $C_{15}H_{24}O_6Na^+$: 323.1465 [*M*+Na^+]; found: 323.1465.

Reductive cleavage of the orthobenzoate 2.12 with DIBAL-H: 1 M solution of DIBAL-H in toluene (7.45 mL,), was added drop-wise over a period of 15 min to a solution of **2.12** (1 g, 2.98 mmol), in dry dichloromethane(24 mL) at -5 °C and then stirred for 3h 30min at room temperature. The reaction mixture was poured into a stirred solution of sodium potassium tartrate (24 mL) and saturated solution of ammonium chloride (22 mL) and stirred for 12 h. The mixture was extracted with ethyl acetate, washed with brine and dried over anhydrous sodium sulphate. The solvent was removed under reduced pressure to obtain a mixture of **2.15** and **2.18** (0.797 g) which were separated using column chromatography (eluent 25-30% ethyl acetate in light petroleum, silica 230-400 mesh) to obtain **2.15** (0.322 g, 45%; TLC *Rf*= 0.3 in 20 % ethyl acetate/light petroleum) and **2.17** (0.144 g, 24%; TLC *Rf*= 0.3 in 10% ethyl acetate/light petroleum) in the ratio of in the ratio 1.9: 1. (0.089 g of starting material was recovered.)

Data for **2.15**: **M.p.** 84-86°C (Crystallized from ethyl acetate-light petroluem); **IR (**Chloroform**)**: *v* 3300-3550 cm^{-1} (broad); **^{1}H NMR** (500MHz , $CDCl_3$) δ = 7.54 - 7.49 (m, 2 H), 7.40 - 7.33 (m, 3 H), 5.95 (m, *J* = 5.5, 10.9, 16.8 Hz, 2 H), 5.73 (s, 1 H), 5.38 - 5.32 (m, 2 H), 5.25 (m, *J* = 1.5, 10.4 Hz, 2 H), 4.31 (d, *J* = 2.4 Hz, 2 H), 4.30 - 4.25 (m, 2 H), 4.15 (m, *J* = 6.1, 12.8 Hz, 2 H), 3.96 (d, *J* = 8.5 Hz, 2 H), 3.79 - 3.73 (m, 1 H), 3.51 (s, 3 H), 3.36 (t, *J* = 2.4 Hz, 1 H) 2.65 (1 H, d, *J*=2.53 Hz, D_2O exchangeable) ppm; **^{13}C NMR** (126MHz, $CDCl_3$) δ = 137.8(C_{arom}), 133.9 (CH_2=*C*H), 129.2 (C_{arom}), 128.3(C_{arom}), 126.3(C_{arom}), 118.0(*C*H_2=CH), 92.6 (Ph*C*H), 81.2(Ins C), 73.5(Ins C), 73.0(Ins C), 70.7(O*C*H_2-CH=), 70.1(Ins C), 56.5(CH_3) ppm; **HRMS**: *m*/*z* calcd for $C_{20}H_{26}O_6Na^+$: 385.1622 [*M*+ Na^+]; found: 385.1613

Data for **2.18**: **IR** (Chloroform): *v* 3500–3200 cm^{-1}; **^{1}H NMR** (200MHz , $CDCl_3$) δ = 7.50-7.40 (d, *J* = 2.0 Hz, 2 H), 7.40 - 7.27 (m, 3 H), 6.06 (s, 1 H), 5.89 (m, *J* = 4.8 Hz, 2 H), 5.41 - 5.13 (m, 4 H), 4.60 (m, 1 H), 4.45 - 4.17 (m, 4 H), 4.17 - 3.81 (m, 5 H), 4.17-3.83 (d, *J* = 14.1 Hz, 5 H), 3.57 (s, 3 H), 3.22 (d, 1 H D_2O exchangeable) ppm; **^{13}C NMR** (50 MHz, $CDCl_3$) δ = 135.61 (C_{arom}), 135.08 (CH_2=*C*H), 130.37 (C_{arom}), 129.62 (C_{arom}), 117.91 (*C*H_2=CH), 82.25 (Ins C), 81.75 (Ins C), 75.42 (Ins C), 74.59 (Ins C), 73.15 (*C*H_2-CH=), 62.58 (CH_3) ppm; **HRMS**: *m*/*z* calcd for $C_{20}H_{26}O_6Na^+$: 385.1622 [*M*+H^+]; found: 385.1626.

***p*-nitrobenzoyl derivative of racemic 1(3)**, **5-*O*-Benzylidene-2-*O*-methyl-4,6-di-*O*-allyl-*myo*-5-inositol (2.19)**:To a solution of 0.5 g, 1.38 mmol) of **2.18** in pyridine

(5mL) *p*-nitrobenzoyl chloride (0.384 g, 2.071 mmol) at 0 °C and then stirred at ambient temperature for 34 h. The reaction mixture was quenched with ice and solvents evaporated in vacuo. The resulting solid was extracted with ethyl acetate, washed with brine and dried over anhydrous sodium sulphate. The solvent was removed under reduced pressure to obtain pale yellow solid which was then purified by column chromatography (eluent 17% ethyl acetate in light petroleum) to obtain **2.19** as a gum (0.512 g, 78%) TLC *Rf*= 0.3 (25% ethyl acetate in light petroleum). **M.p.** 87-90 °C; **IR** (Chloroform): 1712 cm^{-1}; **^{1}H NMR** (200 MHz, CHLOROFORM-*d*) δ = 8.38 - 8.18 (m, 4 H), 7.56 - 7.41 (m, 2 H), 7.42 - 7.29 (m, 3 H), 6.04 (s, 1 H), 6.02 - 5.78 (m, 2 H), 5.69 - 5.56 (m, 1 H), 5.42 - 5.13 (m, 4 H), 4.75 - 4.63 (m, 1 H), 4.52 - 3.99 (m, 8 H), 3.42 (s, 3 H) ppm; **^{13}C NMR** (101MHz ,CHLOROFORM-d) δ = 150.6(-C=O), 137.9(C_{arom}), 135.7(C_{arom}), 134.2(CH_2=CH), 134.0(CH_2=CH), 130.8(C_{arom}), 129.1(C_{arom}), 128.4(C_{arom}), 126.1(C_{arom}), 123.6(C_{arom}), 118.0(CH_2=CH-), 117.7(CH_2=CH), 93.0(PhCHO), 77.9(Ins C), 73.9(Ins C), 73.5(Ins C), 72.2 (CH_2-CH=), 72.1(CH_2-CH=), 70.9(Ins C), 70.4(Ins C), 68.4(Ins C), 58.8 (OCH_3) ppm; **HRMS**: *m*/*z* calcd for $C_{27}H_{30}O_9NH^+$: 512.1915 [M+H^+]; found: 512.1909.

2.5. References

1. B. V. L. Potter, *Comprehensive Medicinal Chemistry*, Vol 4, Pergamon Press **1990**.
2. D. C. Billington, *The Inositol Phosphates: Chemical synthesis and biological significance*. VCH, New York, N.Y. **1993**.
3. Hinchliffe, K.; Irvine, R. *Nature* **1997**, *390*, 123-124.
4. Ferguson, M. A. J.; Williams, A. F. *Annu. Rev. Biochem.* **1988**, *57*, 285.
5. *Phosphoinositides: chemistry, biochemistry and biochemical applications*, K. S. Bruzik, Ed.; ACS symposium series 718.American chemical society, Washington D.C. USA, **1999**.
6. Benjamin, D. I.; Louie, S. M.; Mulvihill, S. M.; Kohnz, R. A.; Li, D. S.; Chan, L. G.; Sorrentino, A.; Bandyopadhyay, S.; Cozzo, A.; Ohiri, A.; Goga, A.; Ng, S.; Nomura, D. K. *Chem. Biol.* **2014**, *9*, 1340−1350.
7. Patassini, S.; Begley, P.; Xua, J.; Church, S. J.; Reid, S. J.; Kim, E. H.; Curtis, M. A.; Dragunow, M.; Waldvogel , H. J.; Snell, R. G.; Unwin, R.D.; Faull, R. L.M.; Cooper, G. J. S. *Biochimica et Biophysica Acta*, **2016**, *1862*, 1650–1662.
8. Chang, H.-H.; Chao, H.-N.; Walker, C. S.; Choong, S.-Y.; Phillips, A.; Loomes, K. M. *Am J Physiol Renal Physiol*, **2015**, 309: F755–F763.
9. Frej, A. D.; Clark, J.; Le Roy, C. I.; Lilla, S.; Thomason, P. A.; Otto, G. P.; Churchill, G.; Insall, R. H.; Claus, S. P.; Hawkins, P.; Stephens, L.; Williams, R. S. B. *Mol. Cell Biol*, **2016**, *36*, 1464 –1479.
10. Swarbrick, J. M.; Cooper, S.; Bultynck, G.; Gaffney, P. R. *J. Org. Biomol. Chem.*
    2009, *7*, 1709–1715.
11. Swarbrick, J. M.; Gaffney, P. R. J. *J. Org. Chem.* **2010**, *75*, 4376–4386.
12. Eisch, J. J.; Rhee, S. G. *J. Am. Chem. Soc.* **1974**, *96*, 7276–7284.
13. Conway, S. J.; Gardiner, J.; Grove, S. J. A.; Johns, M. K.; Lim, Z.-Y.; Painter, G. F.; Robinson, D. E. J. E.; Schieber, C.; Thuring, J. W.; Wong, L. S. M.; Yin, M. X.; Burgess, A. W.; Catimel, B.; Hawkins, P. T.; Ktistakis, N. T.; Stephens, L. R.;
    Holmes, A. B. *Org. Biomol. Chem.* **2010**, *8*, 66–74. and references cited therein.

14. Painter, G. F.; Grove, S. J. A.; Gilbert, I. H.; Holmes, A. B.; Raithby, P. R.; Hill, M. L.; Hawkins, P. T.; Stephens, L. R. *J. Chem. Soc., Perkin Trans. 1* **1999**, 923–935.
15. Gurale, B. P.; Sardessai, R. S., *Carbohydr. Res.* **2014**, *399*,8-14.
16. Gilbert, I. H.; Holmes, A. B.; Pestchanker, M. J.; Young, R. C. *Carbohydr. Res.* **1992**, *234*, 117–130.
17. Gurale, B. P.; Vanka, K.; Krishnaswamy, S.; Shashidhar, M. S. *Tetrahedron,* **2011**, *67*, 7280–7288.
18. Yeh, S. M.; Lee, G. H.; Wang, Y.; Luh, T. Y. *J. Org. Chem.* **1997**, *62*, 8315–8318.
19. Devaraj, S. D.; Shashidhar, M. S.; Dixit, S. S. *Tetrahedron* **2005**, *61*, 529–536.
20. Bruker (2003). *SADABS* (Version 2.05), *SMART* (Version 5.631), *SAINT* (Version 6.45) and *SHELXTL* (Version 6.14). Bruker AXS Inc., Madison, Wisconsin, USA.
21. Sheldrick, G. M. *Acta Cryst.* **2008,** *A64*, 112–122.
22. Farrugia, L. J. *J. Appl. Cryst.* **1997**, *30*, 565–565.
23. (a) Ahlrichs, R.; Bär, M.; Baron, H.-P.; Bauernschmitt, R.; Böcker, S.; Ehrig, M.; Eichkorn, K.; Elliott, S.; Furche, F.; Haase, F.; Häser, M.; Horn, H.; Huber, C.; Huniar, U.; Kattannek, M.; Kölmel, C.; Kollwitz, M.; May, K.; Ochsenfeld, C.; Öhm, H.; Schäfer, A.; Schneider, U.; Treutler, O.; von Arnim, M.; Weigend, F.; Weis, P.; Weiss, H. TURBOMOLE (Version 5.3); Universität Karlsruhe, Karlsruhe, Germany, **2000**; (b) Schäfer, A.; Huber, C.; Ahlrichs, R. *J. Chem. Phys.* **1994**, *100*, 5829–5835; (c) Andrae, D.; Haeussermann, U.; Dolg, M.; Stoll, H.; Preuss, H. *Theor. Chim. Acta* **1990**, *77*, 123–141.
24. (a) Becke, A. D. *Phys. Rev. A*: *At., Mol., Opt. Phys.* **1988**, *38*, 3098–3100; (b) Perdew, J. P. *Phys. Rev. B: Condens. Matter Mater. Phys.* **1986**, *33*, 8822–8824.
25. Schäfer, A.; Horn, H.; Ahlrichs, R. *J. Chem. Phys*. **1992**, *97*, 2571–2577. The resolution of identity (RI), Eichkorn, K.; Treutler, O.; Öhm, H.; Häser, M.; Ahlrichs, R. *Chem. Phys. Lett.* **1995**, *240*, 283–290.
26. Sierka, M.; Hogekamp, A.; Ahlrichs, R. *J. Chem. Phys.* **2003**, *118*, 9136–9148.
27. Klamt, A. *J. Phy. Chem.* **1995**, *99*, 2224–2235.

28. Perrin, D. D.; Armarego, W. L. F. *Purification of Laboratory Chemicals*, 2nd edition, Pergamon Press, Oxford, U.K., 1988.

Appendix I

Appendix I Index

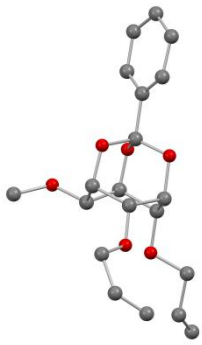

Crystal data table for 2.12		
Empirical formula	$C_{20}H_{24}O_6$	
Formula weight	360.39	
Temperature	296(2) K	
Wavelength	0.71073 Å	
Crystal system	Triclinic	
Space group	P*1*	
Unit cell dimensions	a = 9.803(2) Å	α = 85.714(15)°.
	b = 9.812(2) Å	β = 85.401(16)°.
	c = 19.047(4) Å	γ = 86.484(17)°.
Volume	1818.3(7) $Å^3$	
Z	4	
Density (calculated)	1.317 Mg/m^3	
Absorption coefficient	0.097 mm^{-1}	
F(000)	768	
Crystal size	0.32 x 0.21 x 0.08 mm^3	
Theta range for data collection	2.08 to 28.88°.	
Index ranges	-13<=h<=13, -13<=k<=13, -23<=l<=25	
Reflections collected	29616	
Independent reflections	15203 [R(int) = 0.1627]	
Completeness to theta = 28.88°	96.3 %	
Refinement method	Full-matrix least-squares on F^2	
Data / restraints / parameters	15203 / 3 / 941	
Goodness-of-fit on F^2	1.069	
Final R indices [I>2sigma(I)]	R1 = 0.1422, wR2 = 0.2306	
R indices (all data)	R1 = 0.2370, wR2 = 0.2743	
Absolute structure parameter	-0.6(19)	
Largest diff. peak and hole	0.425 and -0.435 e.$Å^{-3}$	

Crystal data table for 2.15		
Empirical formula	$C_{20}H_{26}O_6$	
Formula weight	362.41	
Temperature	296(2) K	
Wavelength	0.71073 Å	
Crystal system	Orthorhombic	
Space group	P*ccn*	
Unit cell dimensions	a = 11.4462(5) Å	α= 90°.
	b = 16.5302(8) Å	β= 90°.
	c = 20.2606(10) Å	γ = 90°.
Volume	3833.5(3) $Å^3$	
Z	8	
Density (calculated)	1.256 Mg/m^3	
Absorption coefficient	0.092 mm^{-1}	
F(000)	1552	
Crystal size	0.50 x 0.40 x 0.30 mm^3	
Theta range for data collection	2.16 to 30.49°.	
Index ranges	-16<=h<=16, -23<=k<=23, -28<=l<=28	
Reflections collected	32487	
Independent reflections	5840 [R(int) = 0.0393]	
Completeness to theta = 30.49°	99.6 %	
Max. and min. transmission	0.9729 and 0.9554	
Refinement method	Full-matrix least-squares on F^2	
Data / restraints / parameters	5840 / 0 / 238	
Goodness-of-fit on F^2	1.059	
Final R indices [I>2sigma(I)]	R1 = 0.0610, wR2 = 0.1526	
R indices (all data)	R1 = 0.0991, wR2 = 0.1747	
Extinction coefficient	0.0001(2)	
Largest diff. peak and hole	1.245 and -0.558 $e.Å^{-3}$	

Crystal data table for 2.19	
Empirical formula	$C_{27}\ H_{29}\ NO_9$
Formula weight	511.51
Temperature	296(2) K
Wavelength	0.71073 Å
Crystal system	Monoclinic
Space group	P 2_1/c
Unit cell dimensions	a = 14.0160(10) Å α= 90°.
	b = 23.1916(16) Å β= 103.969(4)°.
	c = 8.0892(6) Å γ = 90°.
Volume	2551.7(3) $Å^3$
Z	4
Density (calculated)	1.332 Mg/m^3
Absorption coefficient	0.100 mm^{-1}
F(000)	1080
Crystal size	0.41 x 0.25 x 0.12 mm^3
Theta range for data collection	1.74 to 25.00°.
Index ranges	-16<=h<=16, -27<=k<=27, -9<=l<=9
Reflections collected	36275
Independent reflections	4492 [R(int) = 0.0579]
Completeness to theta = 25.00°	99.8 %
Refinement method	Full-matrix least-squares on F^2
Data / restraints / parameters	4492 / 4 / 372
Goodness-of-fit on F^2	1.355
Final R indices [I>2sigma(I)]	R1 = 0.1235, wR2 = 0.1930
R indices (all data)	R1 = 0.1298, wR2 = 0.1953
Extinction coefficient	0.0012(4)
Largest diff. peak and hole	0.266 and -0.281 $e.Å^{-3}$

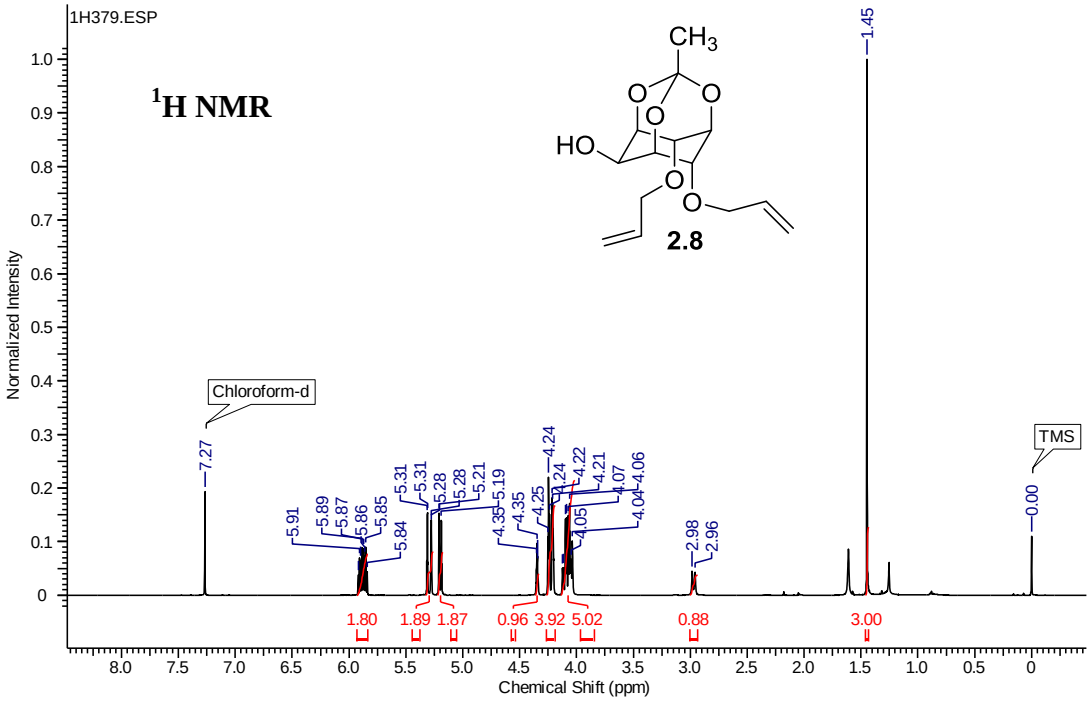
1H379.ESP
1H NMR
CH3
O
O
O
HO
O
O
2.8
1.45
Chloroform-d
7.27
TMS
0.00
5.91
5.89
5.87
5.86
5.85
5.84
5.31
5.31
5.28
5.28
5.21
5.19
4.35
4.25
4.24
4.24
4.22
4.21
4.07
4.06
4.04
4.05
2.98
2.96
1.80
1.89
1.87
0.96
3.92
5.02
0.88
3.00
Normalized Intensity
Chemical Shift (ppm)

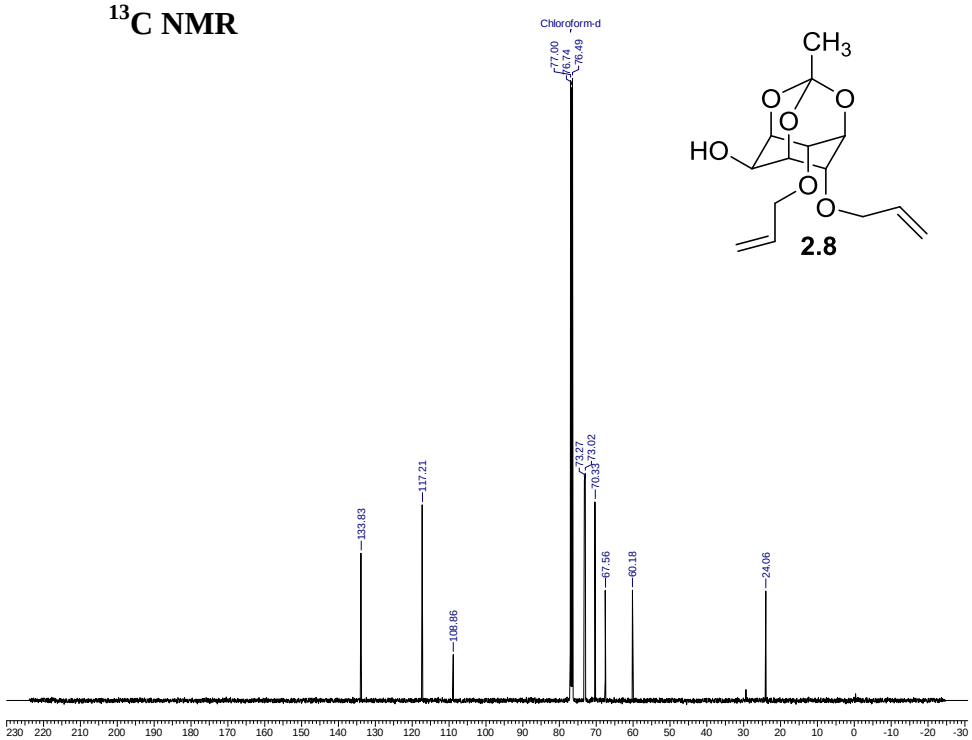
13C NMR
Chloroform-d
77.00
77.32
76.49
CH3
O
O
O
HO
O
O
2.8
133.83
117.21
108.86
73.27
73.02
70.33
67.56
60.18
24.06

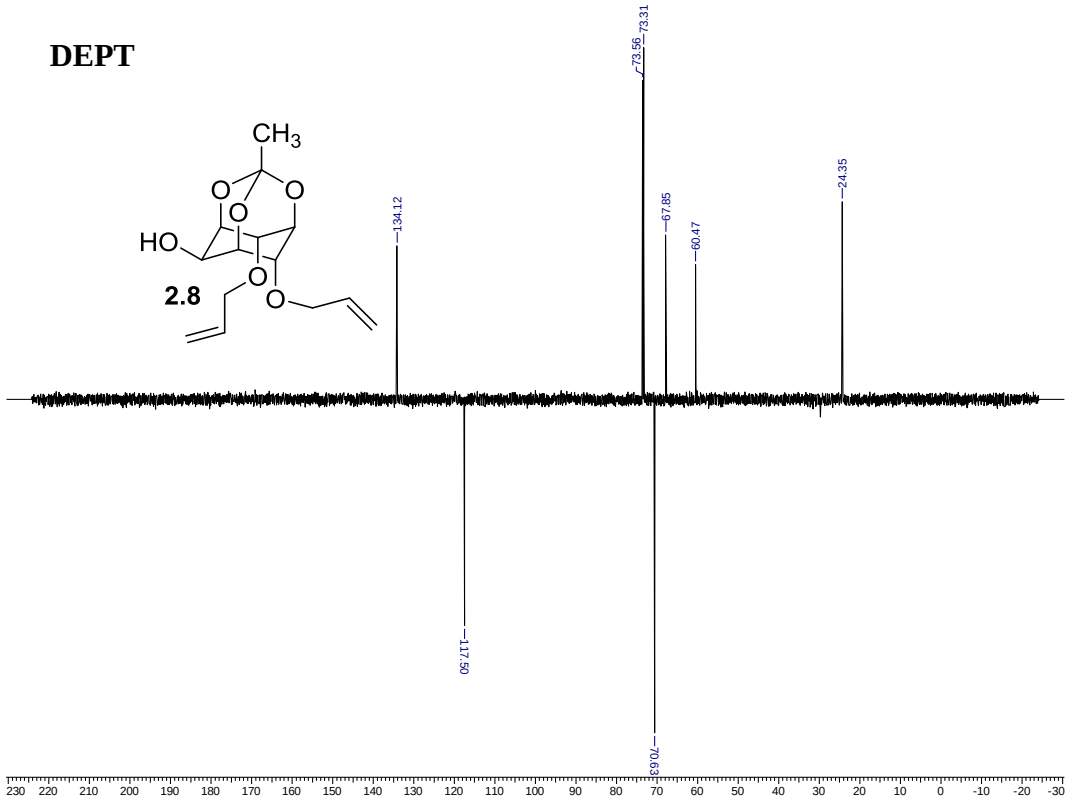
DEPT
CH3
O
O
O
HO
O
O
2.8
134.12
73.56
73.31
67.85
60.47
24.35
117.50
70.63
230 220 210 200 190 180 170 160 150 140 130 120 110 100 90 80 70 60 50 40 30 20 10 0 -10 -20 -30

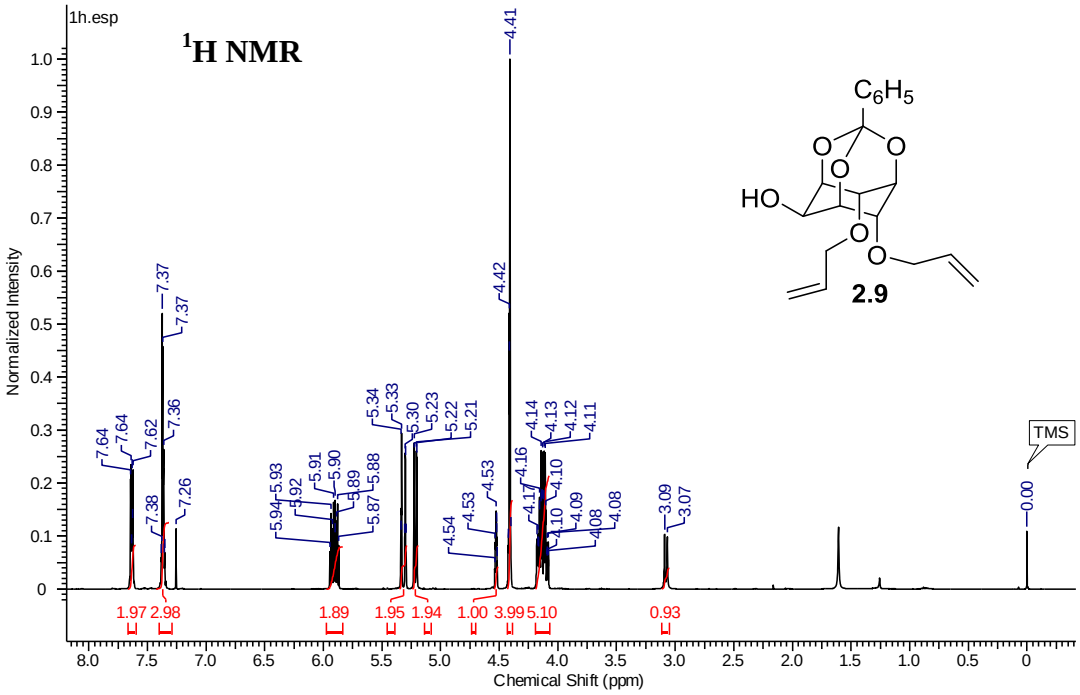
1h.esp
1H NMR
C6H5
O
O
O
HO
O
O
2.9
Normalized Intensity
1.0
0.9
0.8
0.7
0.6
0.5
0.4
0.3
0.2
0.1
0
4.41
4.42
7.37
7.37
7.64
7.64
7.62
7.36
7.38
7.26
5.34
5.33
5.30
5.23
5.22
5.21
5.93
5.92
5.91
5.90
5.89
5.88
5.87
4.53
4.54
4.53
4.16
4.17
4.14
4.13
4.12
4.11
4.10
4.10
4.09
4.08
4.08
3.09
3.07
TMS
0.00
1.97 2.98 1.89 1.95 1.94 1.00 3.99 5.10 0.93
8.0 7.5 7.0 6.5 6.0 5.5 5.0 4.5 4.0 3.5 3.0 2.5 2.0 1.5 1.0 0.5 0
Chemical Shift (ppm)

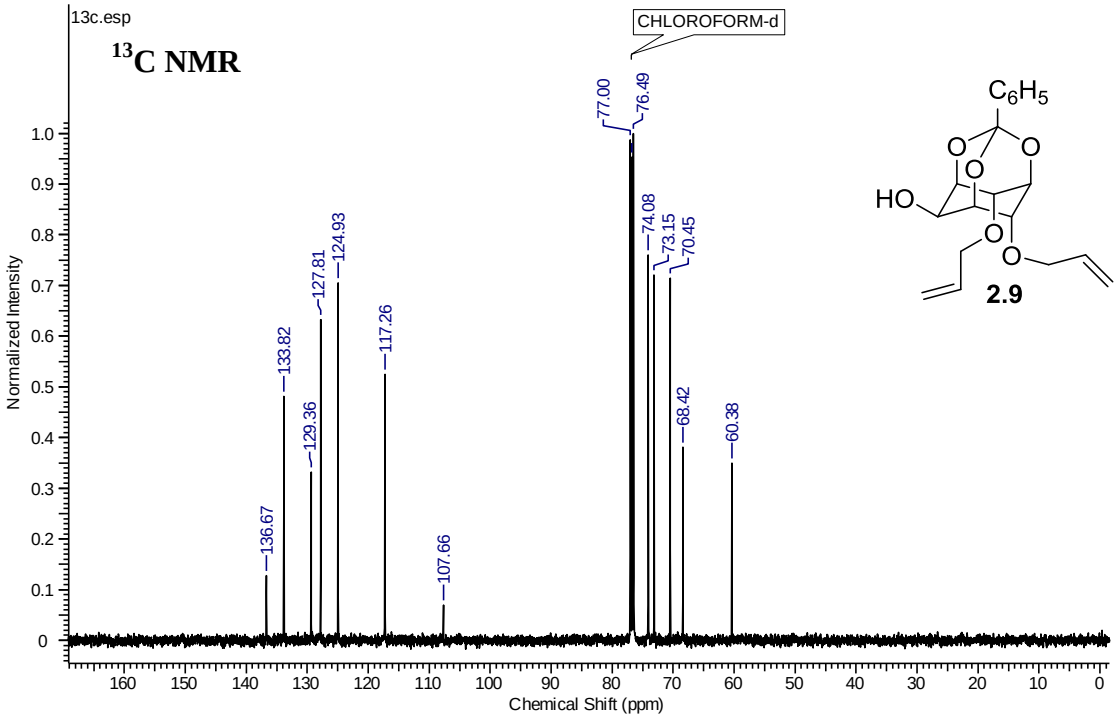
13c.esp
^{13}C NMR
CHLOROFORM-d
77.00
76.49
74.08
73.15
70.45
68.42
60.38
133.82
129.36
127.81
124.93
117.26
136.67
107.66
Normalized Intensity
Chemical Shift (ppm)
C6H5
HO
2.9

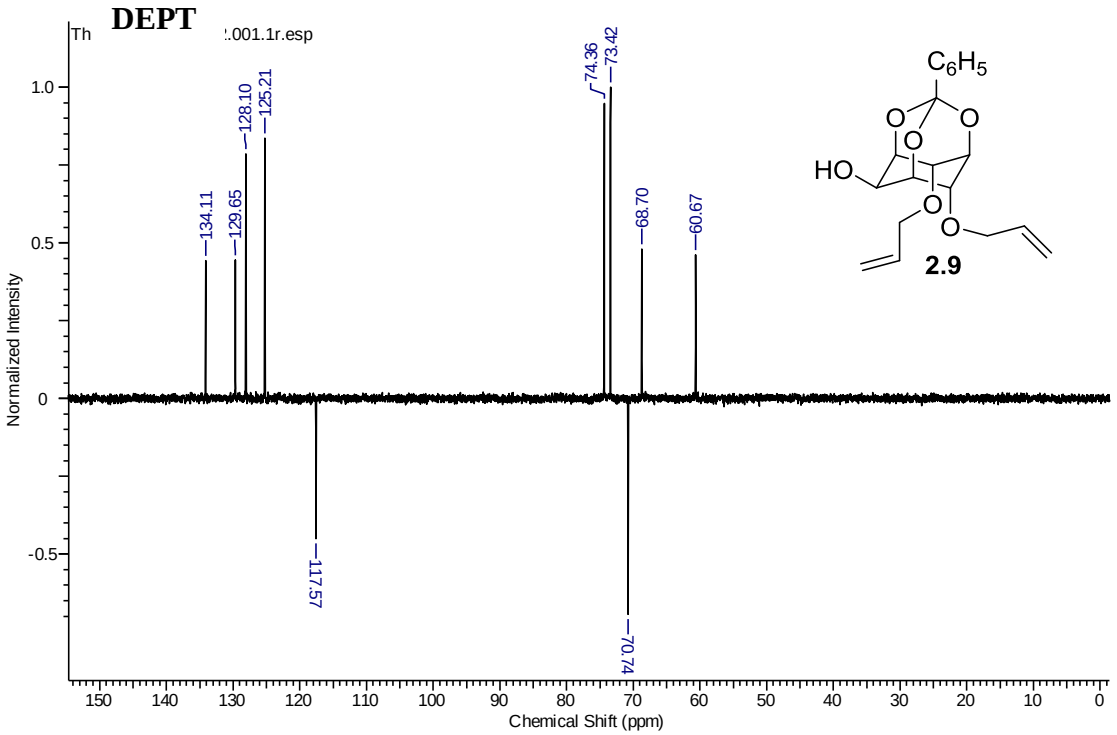
DEPT
Th
.001.1r.esp
74.36
73.42
128.10
125.21
134.11
129.65
68.70
60.67
117.57
70.74
Normalized Intensity
Chemical Shift (ppm)
C6H5
HO
2.9

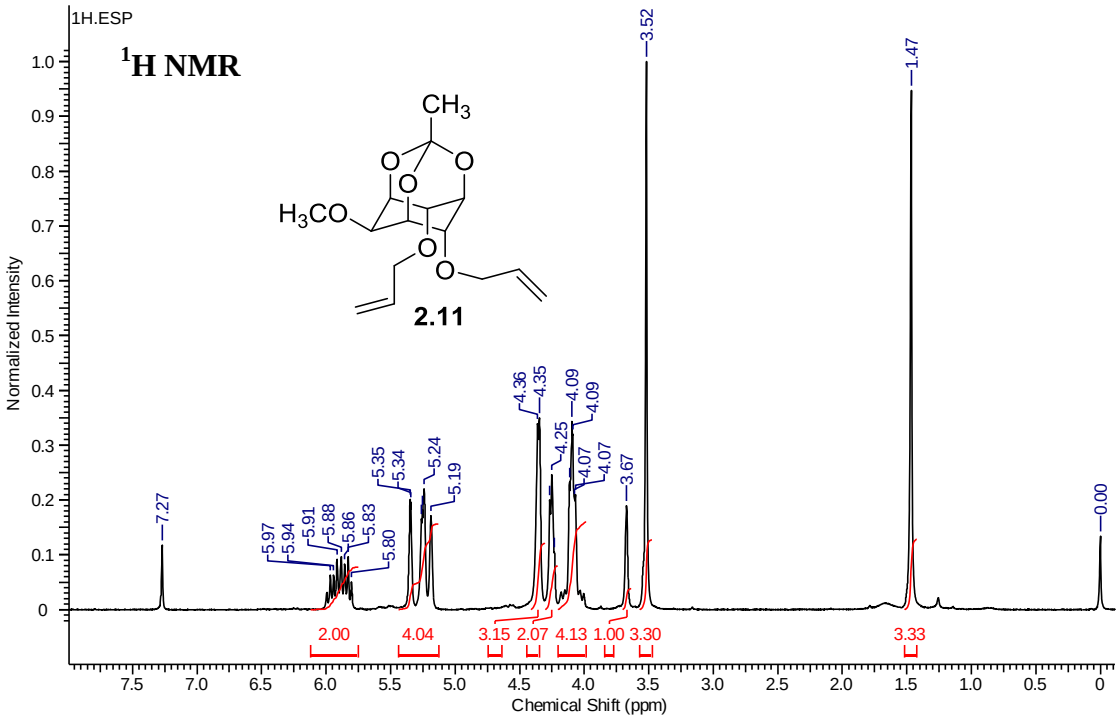
1H.ESP
1H NMR
CH3
O
O
O
H3CO
O
O
2.11
3.52
1.47
0.00
7.27
5.97
5.94
5.91
5.88
5.86
5.83
5.80
5.35
5.34
5.24
5.19
4.36
4.35
4.25
4.09
4.09
4.07
4.07
3.67
2.00
4.04
3.15
2.07
4.13
1.00
3.30
3.33
Normalized Intensity
Chemical Shift (ppm)

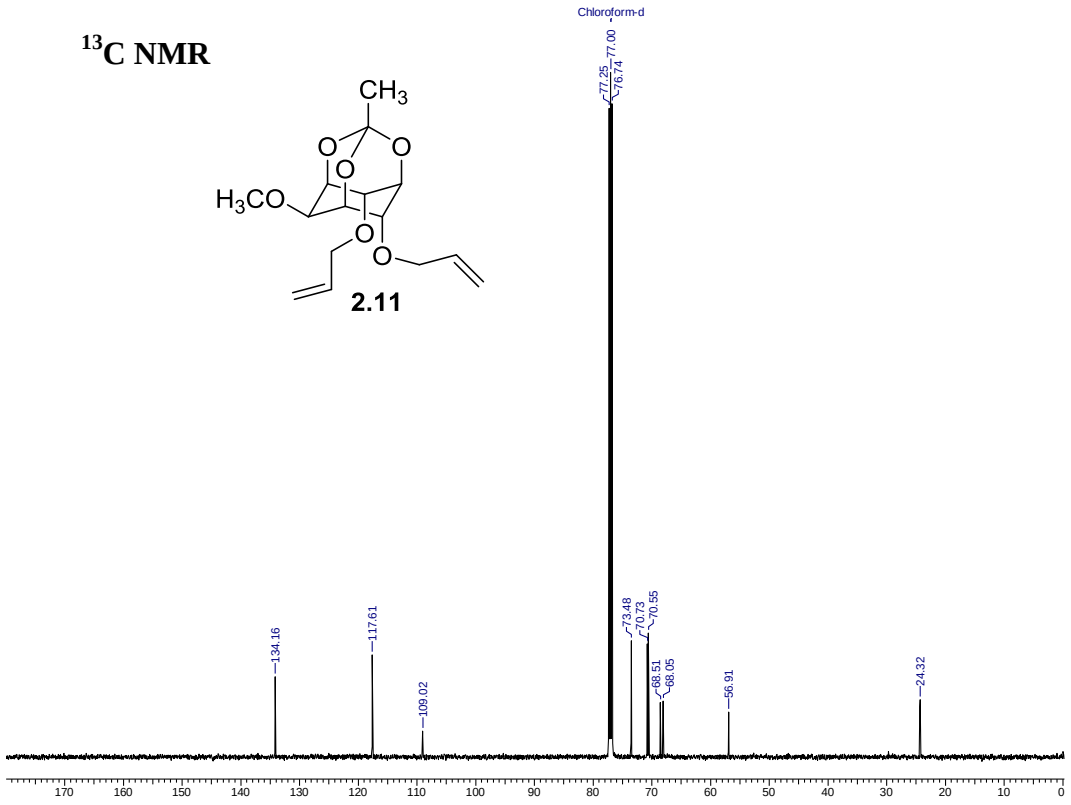
13C NMR
CH3
O
O
O
H3CO
O
O
2.11
Chloroform-d
77.25
77.00
76.74
134.16
117.61
109.02
73.48
70.73
70.55
68.51
68.05
56.91
24.32

DEPT

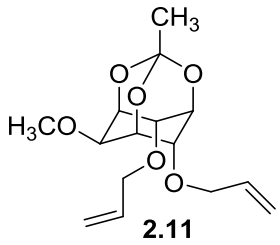

2.11

^{1}H NMR

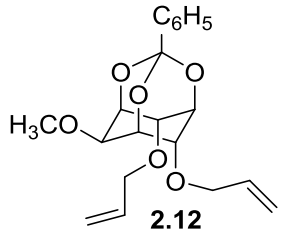

2.12

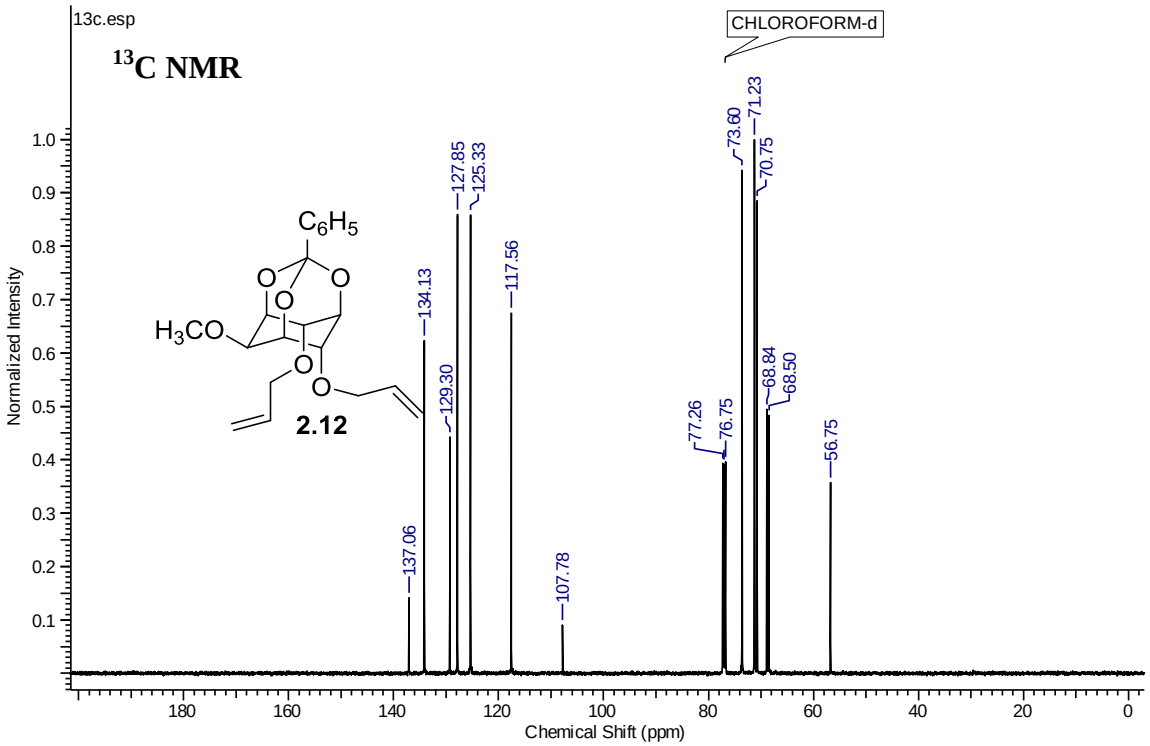
13c.esp
^{13}C NMR
CHLOROFORM-d
Normalized Intensity
Chemical Shift (ppm)
137.06
134.13
129.30
127.85
125.33
117.56
107.78
77.26
76.75
73.60
71.23
70.75
68.84
68.50
56.75
C_6H_5
H_3CO
2.12

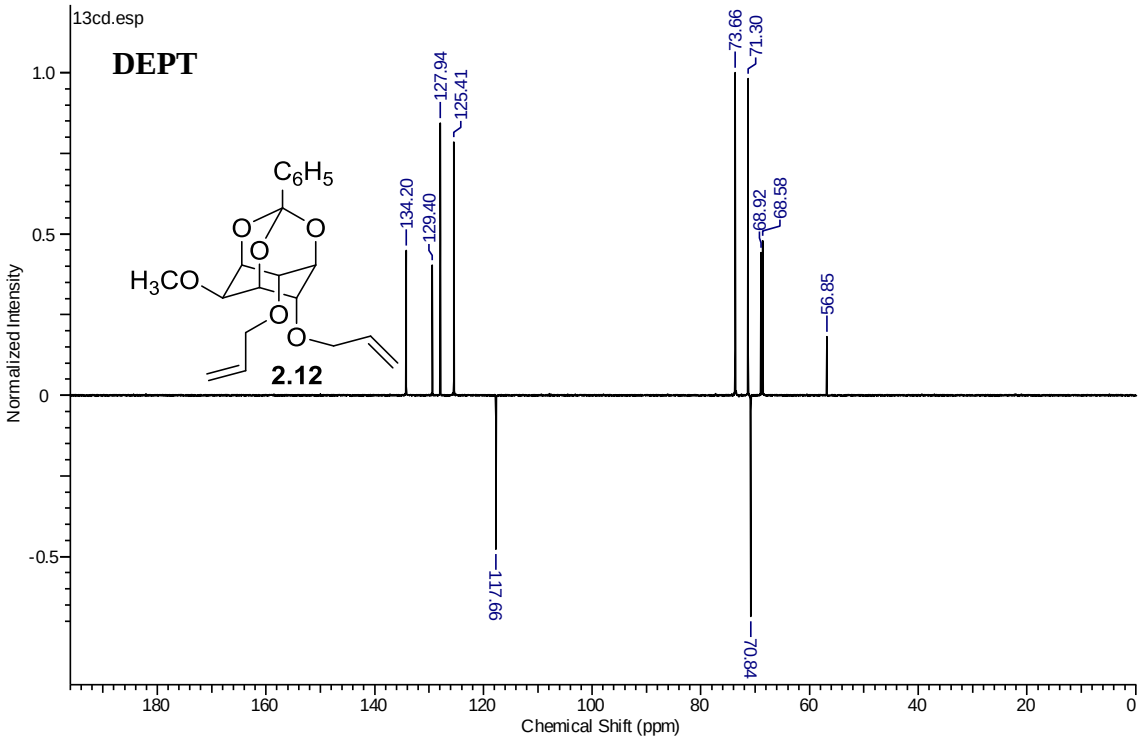
13cd.esp
DEPT
Normalized Intensity
Chemical Shift (ppm)
134.20
129.40
127.94
125.41
117.66
73.66
71.30
70.84
68.92
68.58
56.85
C_6H_5
H_3CO
2.12

^{1}H NMR

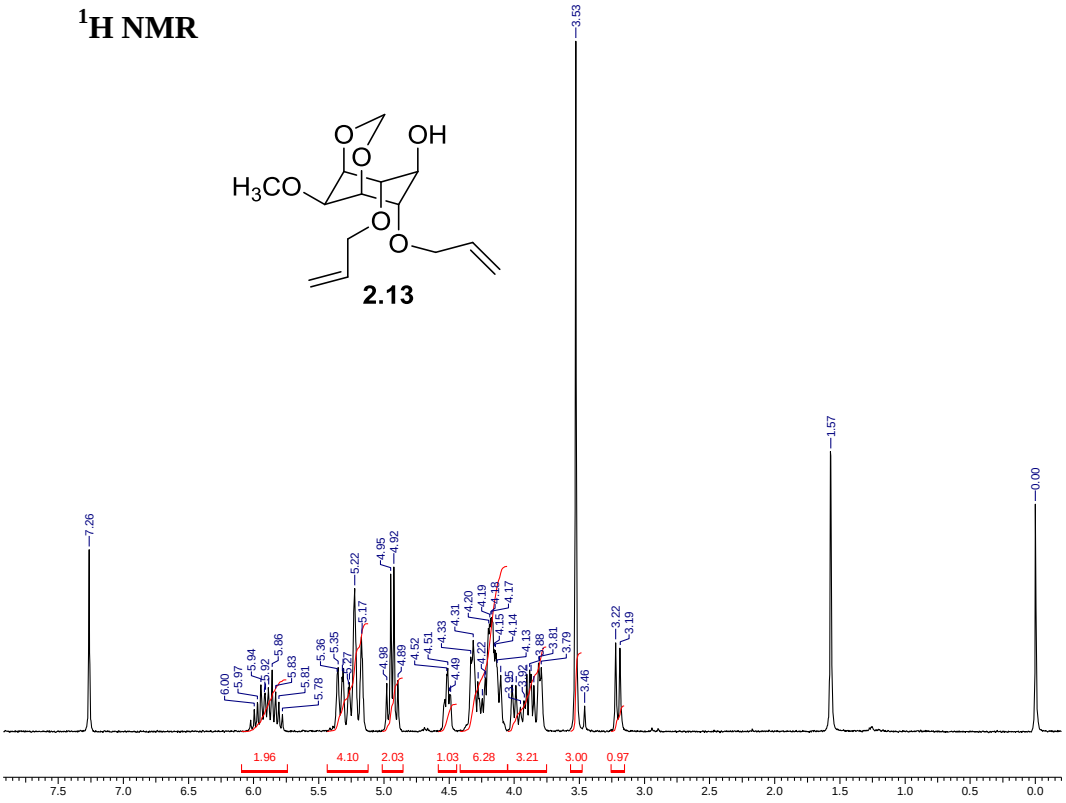
3.53
1.57
0.00
7.26
5.22
4.95
4.92
5.17
5.36
5.35
5.27
5.86
5.94
5.92
5.83
5.81
5.78
6.00
5.97
4.98
4.89
4.52
4.51
4.33
4.49
4.31
4.20
4.19
4.18
4.17
4.15
4.14
4.13
4.22
3.88
3.81
3.79
3.46
3.22
3.19
1.96
4.10
2.03
1.03
6.28
3.21
3.00
0.97

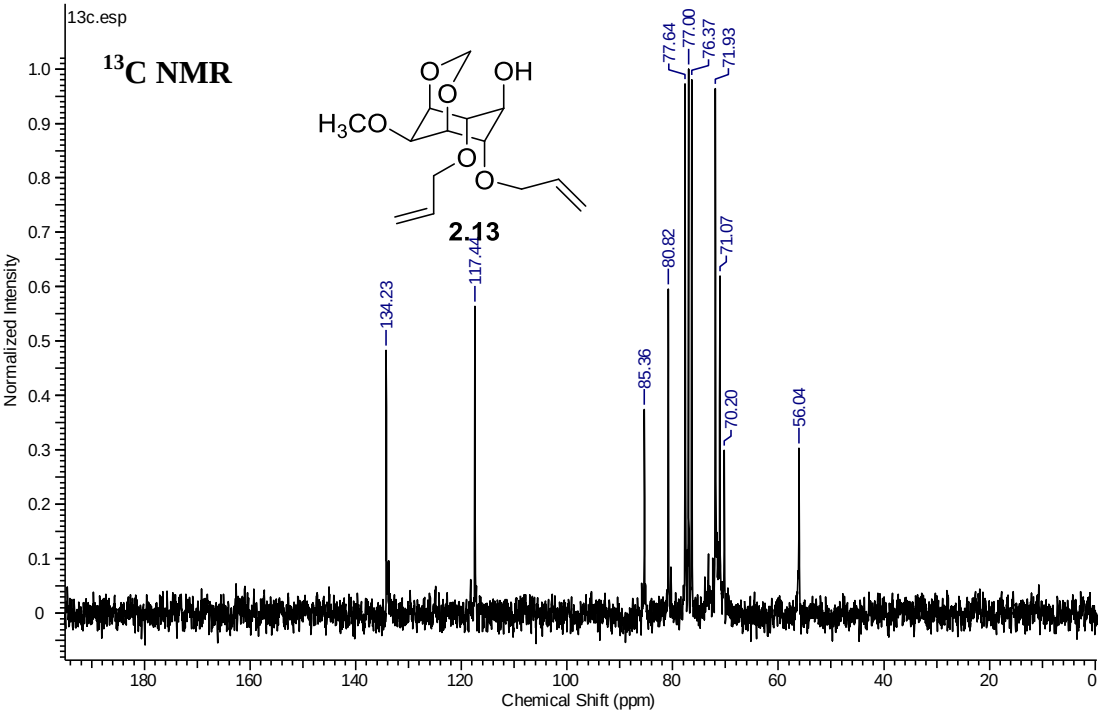
13c.esp
^{13}C NMR
2.13
77.64
77.00
76.37
71.93
80.82
71.07
134.23
117.44
85.36
70.20
56.04
Normalized Intensity
Chemical Shift (ppm)

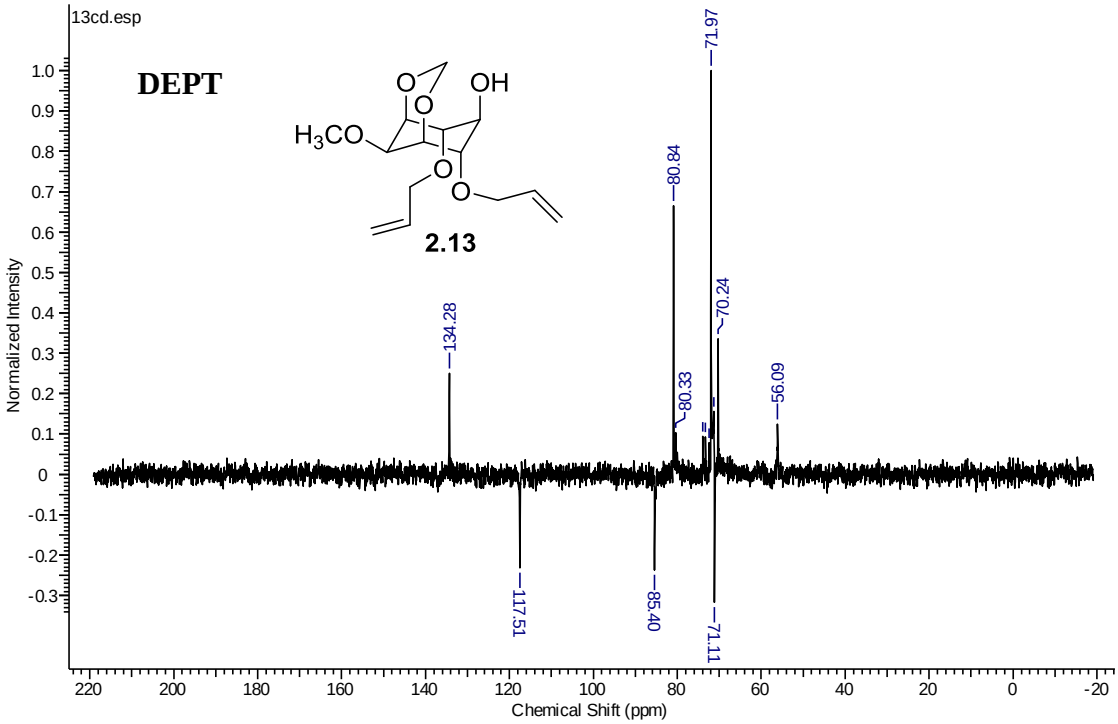
13cd.esp
DEPT
2.13
Normalized Intensity
Chemical Shift (ppm)
71.97
80.84
70.24
134.28
80.33
56.09
117.51
85.40
71.11

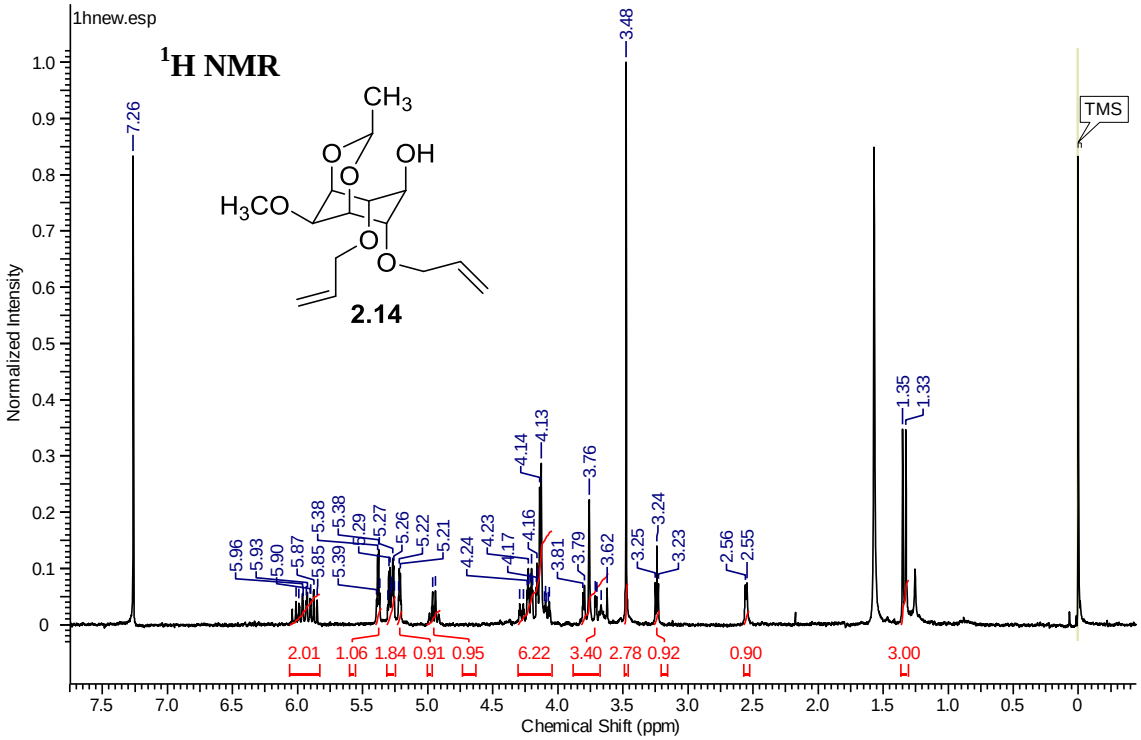
1hnew.esp
1H NMR
2.14
Normalized Intensity
Chemical Shift (ppm)
TMS
7.26
3.48
1.35
1.33
4.13
4.14
3.76
5.38
5.38
5.29
5.27
5.26
5.22
5.21
4.23
4.17
4.16
3.81
3.79
3.62
3.25
3.24
3.23
2.56
2.55
5.96
5.93
5.90
5.87
5.85
5.39
4.24
2.01
1.06
1.84
0.91
0.95
6.22
3.40
2.78
0.92
0.90
3.00

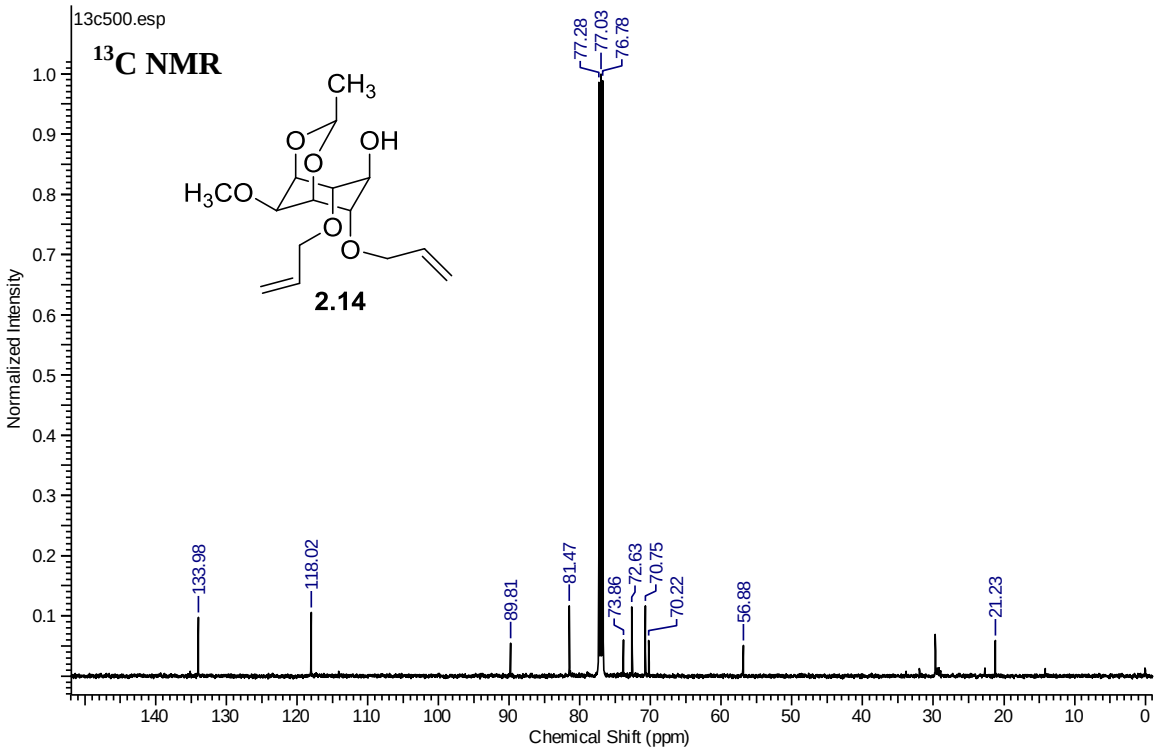
13c500.esp
13C NMR
CH3
O
OH
O
H3CO
O
O
2.14
77.28
77.03
76.78
133.98
118.02
89.81
81.47
73.86
72.63
70.75
70.22
56.88
21.23
Normalized Intensity
Chemical Shift (ppm)

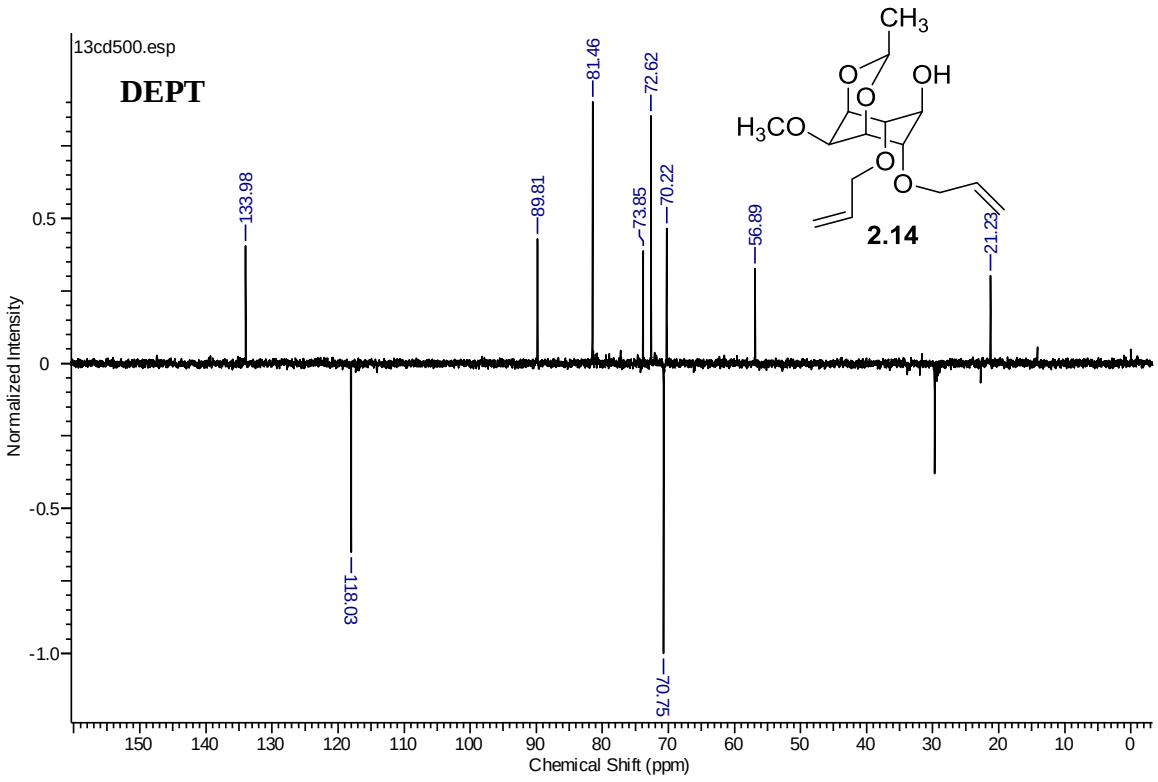
13cd500.esp
DEPT
CH3
O
OH
O
H3CO
O
O
2.14
133.98
89.81
81.46
72.62
73.85
70.22
56.89
21.23
118.03
70.75
Normalized Intensity
Chemical Shift (ppm)

^{1}H NMR

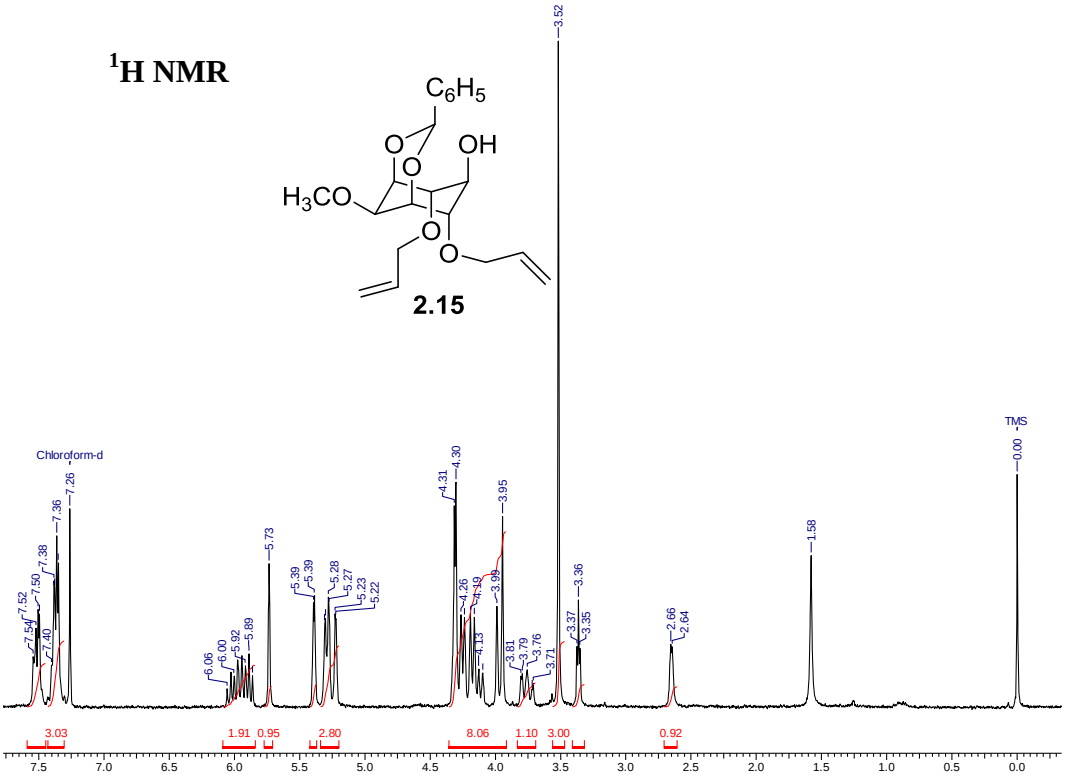

^{13}C NMR

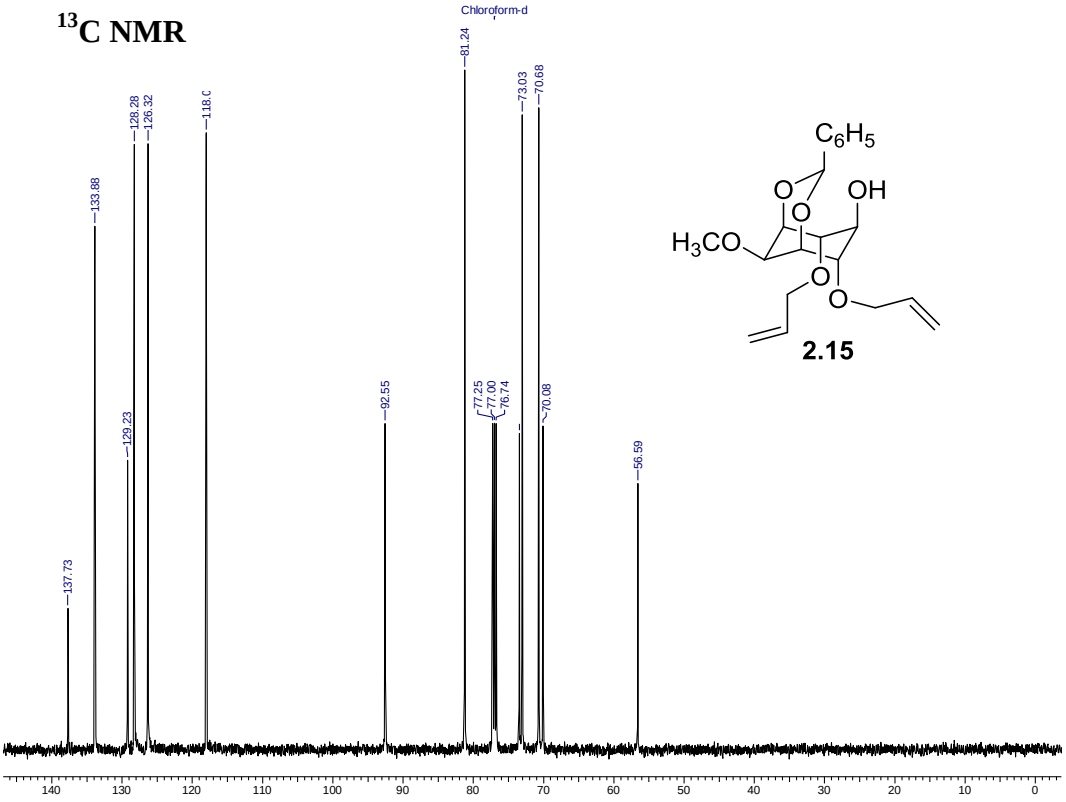

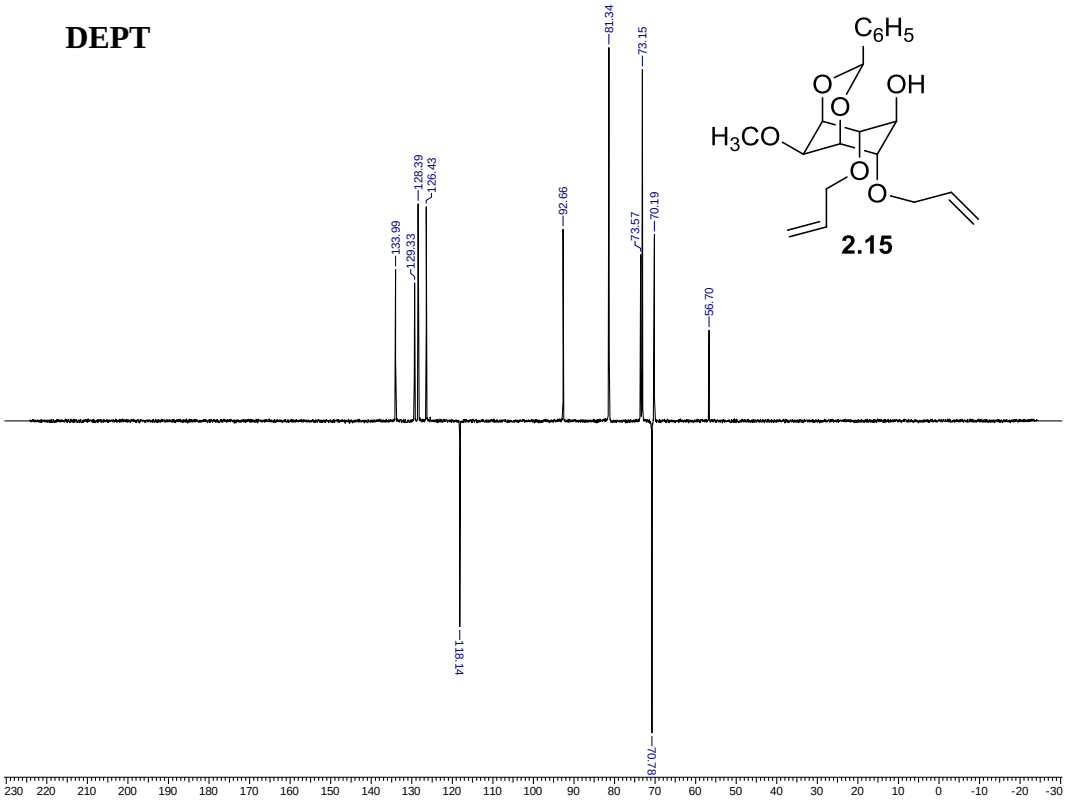
DEPT
C6H5
OH
H3CO
O
2.15
81.34
73.15
128.39
126.43
92.66
73.57
70.19
133.99
129.33
56.70
118.14
70.78

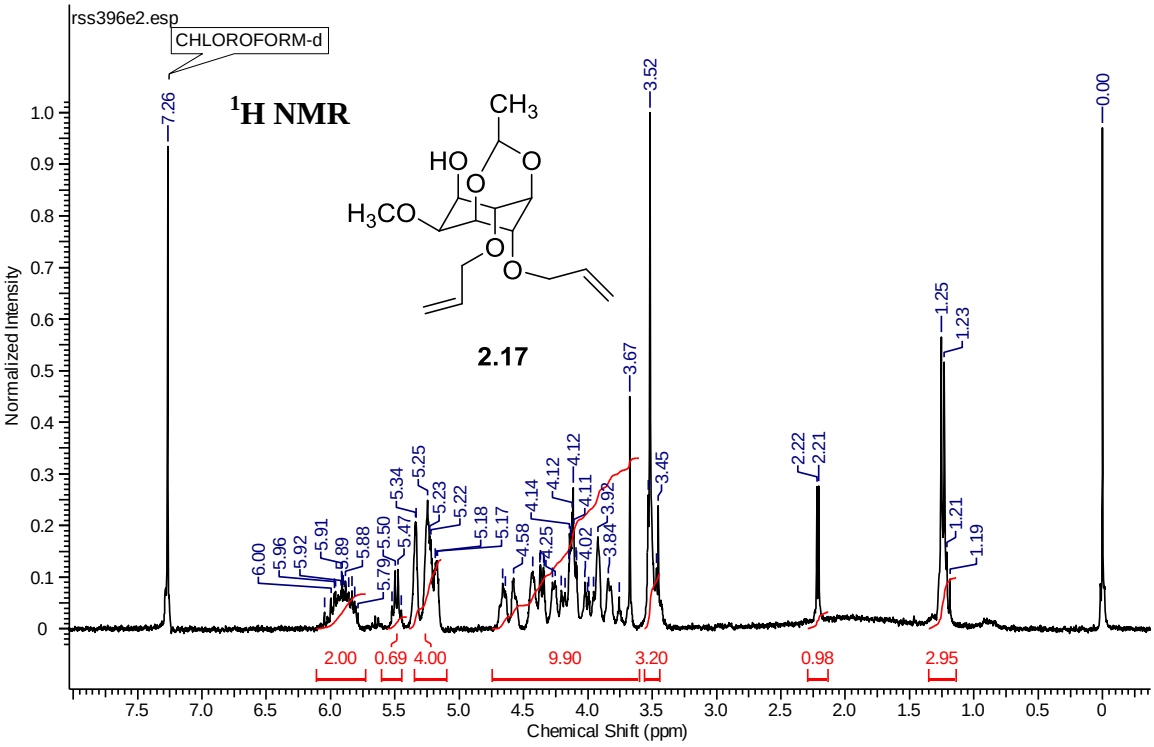
rss396e2.esp
CHLOROFORM-d
1H NMR
CH3
HO
H3CO
2.17
Normalized Intensity
Chemical Shift (ppm)
7.26
3.52
0.00
3.67
3.45
1.25
1.23
2.22
2.21
1.21
1.19
2.00
0.69
4.00
9.90
3.20
0.98
2.95

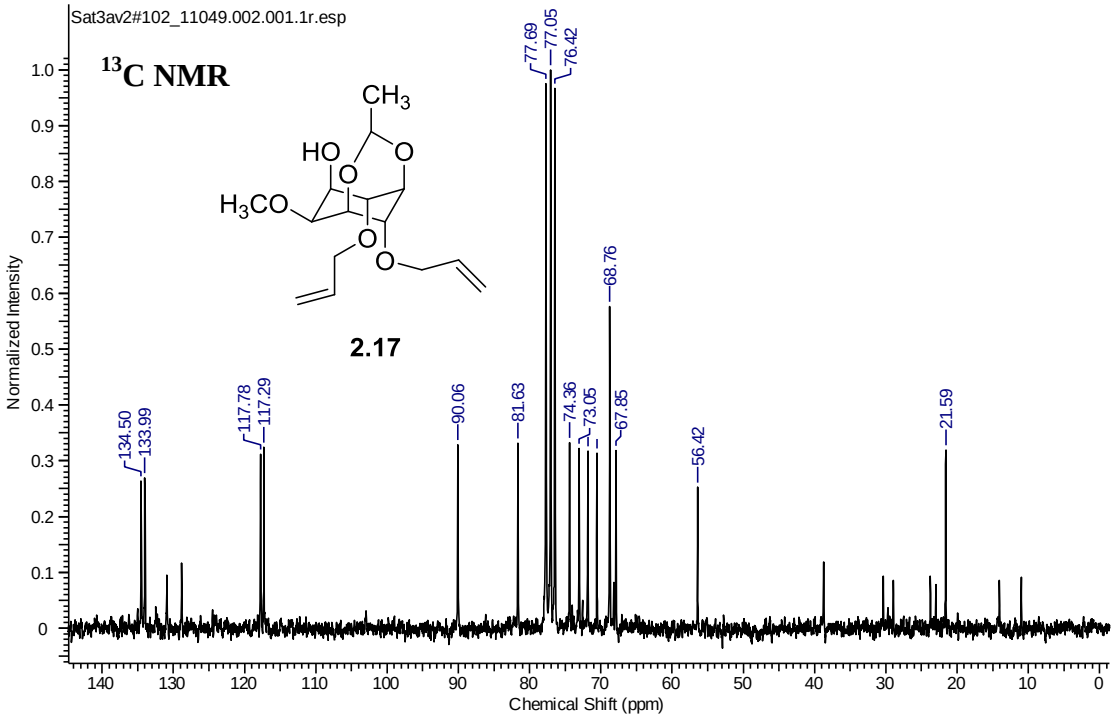
Sat3av2#102_11049.002.001.1r.esp
13C NMR
CH3
HO
O
O
H3CO
O
O
2.17
77.69
77.05
76.42
68.76
117.78
117.29
90.06
81.63
74.36
73.05
67.85
134.50
133.99
56.42
21.59
Normalized Intensity
Chemical Shift (ppm)

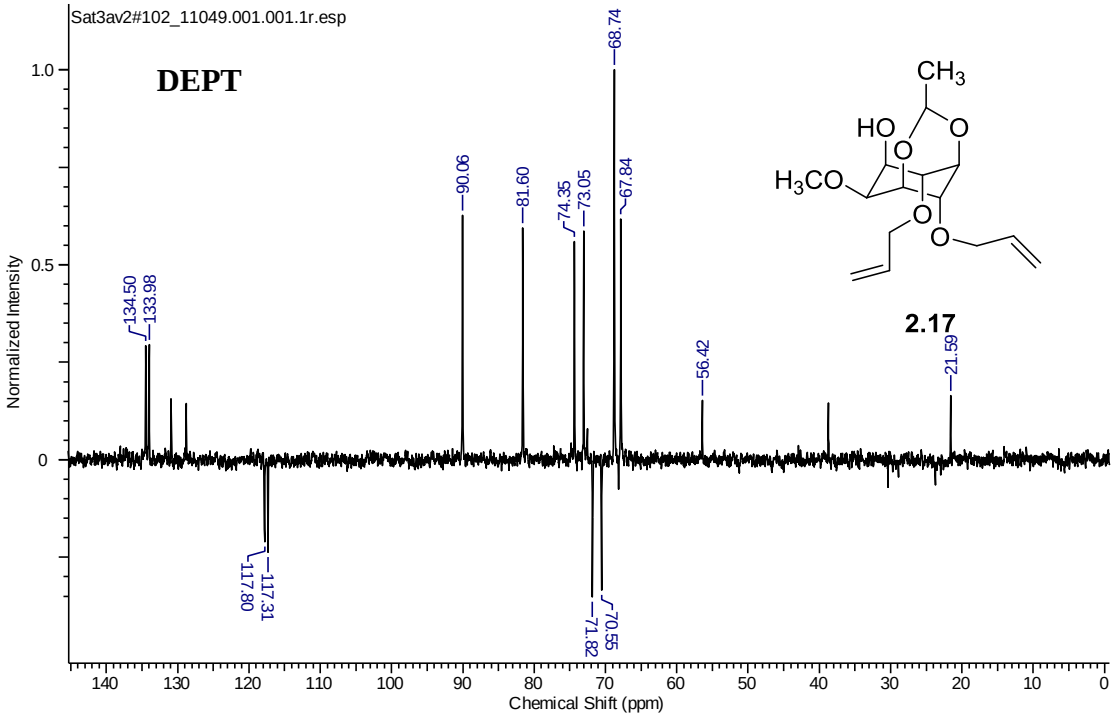
Sat3av2#102_11049.001.001.1r.esp
DEPT
68.74
90.06
81.60
74.35
73.05
67.84
134.50
133.98
56.42
21.59
117.80
117.31
71.82
70.55
CH3
HO
O
O
H3CO
O
O
2.17
Normalized Intensity
Chemical Shift (ppm)

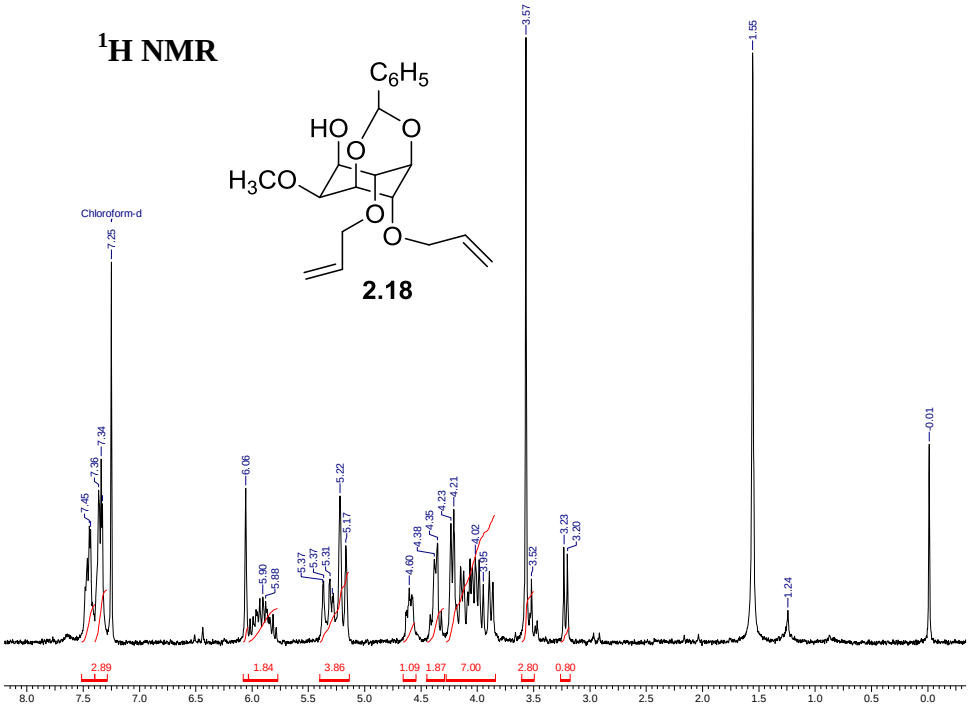
1H NMR
C6H5
HO
O
O
H3CO
O
O
2.18
Chloroform-d
7.25
7.45
7.36
7.34
6.06
5.90
5.88
5.37
5.37
5.33
5.22
5.17
4.60
4.38
4.35
4.23
4.21
4.02
3.95
3.57
3.52
3.23
3.20
1.55
1.24
0.01
2.89
1.84
3.86
1.09
1.87
7.00
2.80
0.80

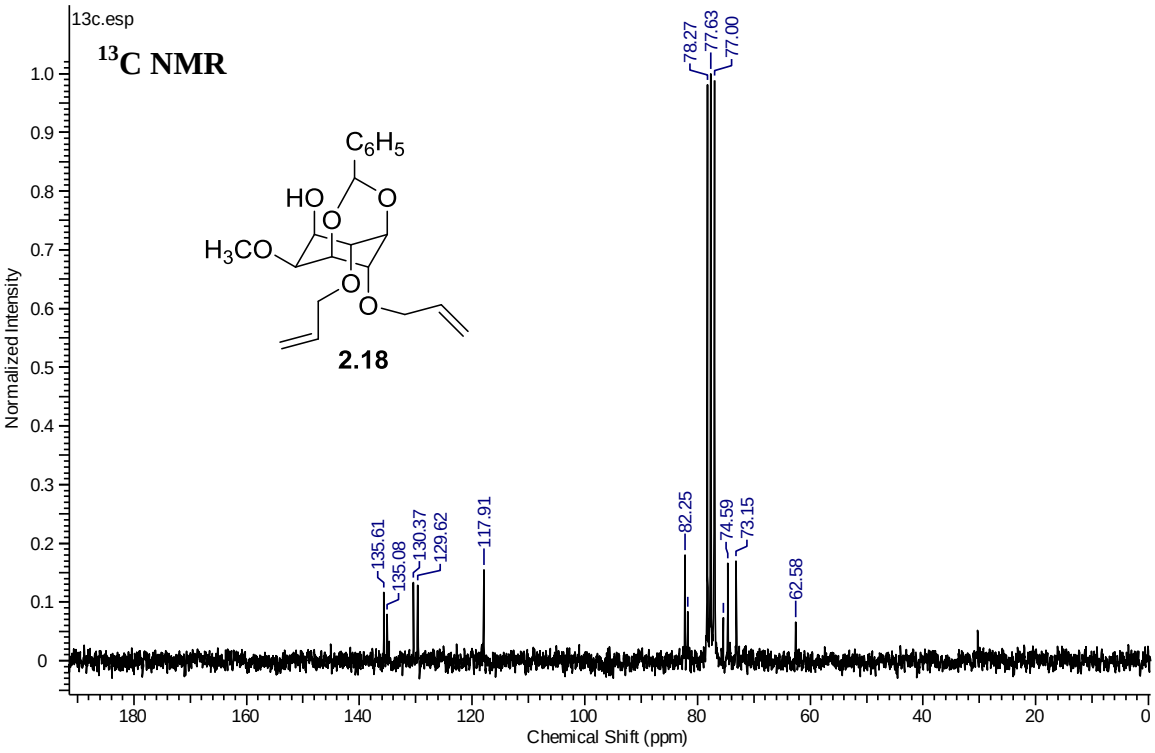
13c.esp
13C NMR
C6H5
HO
O
O
H3CO
O
O
2.18
Normalized Intensity
Chemical Shift (ppm)
78.27
77.63
77.00
135.61
135.08
130.37
129.62
117.91
82.25
74.59
73.15
62.58

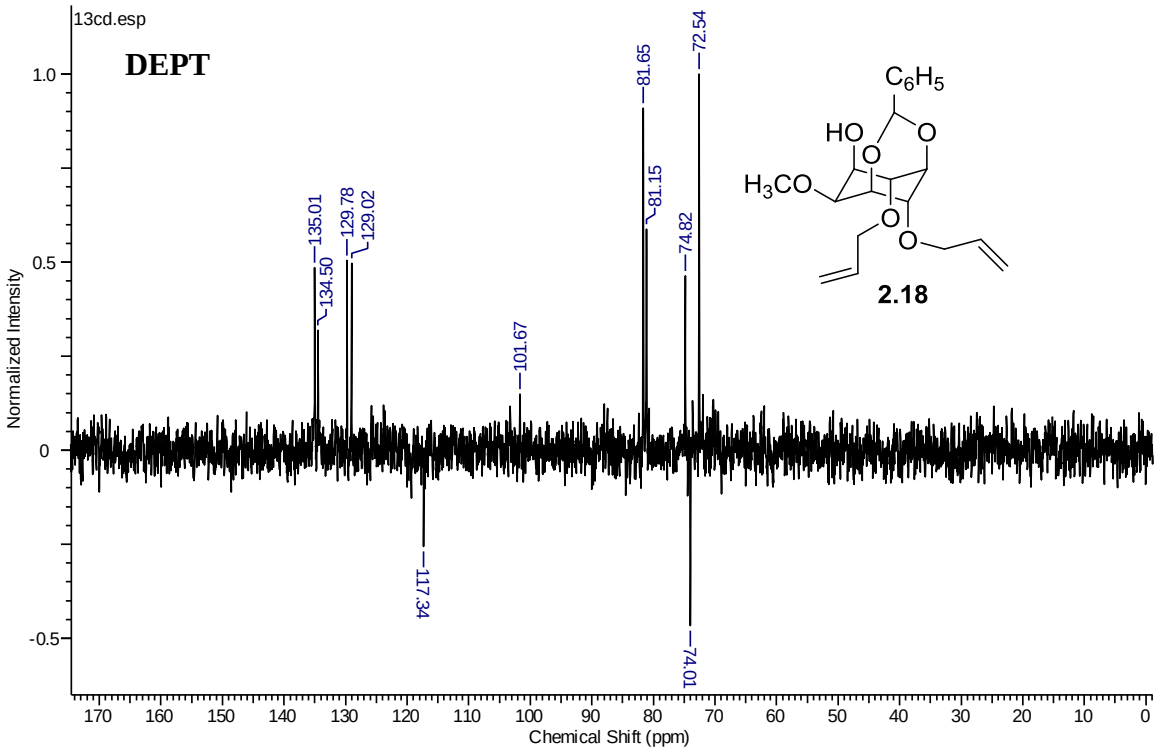
13cd.esp
DEPT
Normalized Intensity
Chemical Shift (ppm)
135.01
134.50
129.78
129.02
101.67
117.34
81.65
81.15
74.82
74.01
72.54
C6H5
HO
O
H3CO
2.18

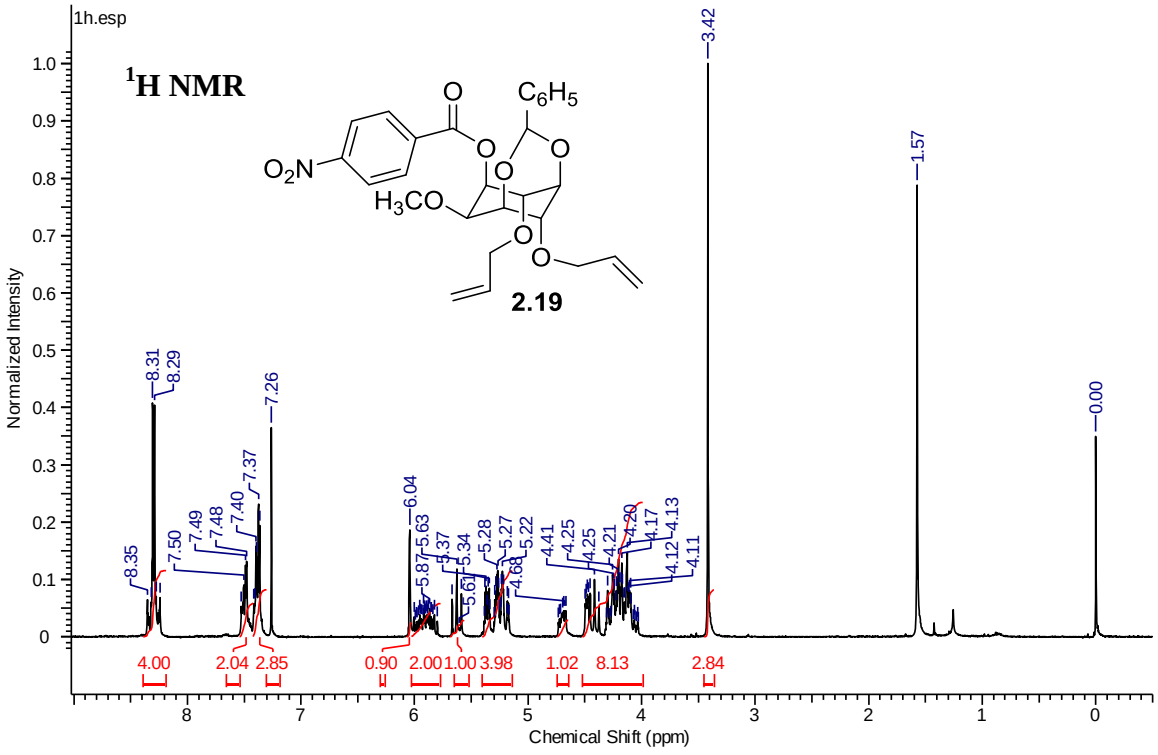
1h.esp
1H NMR
Normalized Intensity
Chemical Shift (ppm)
O2N
C6H5
H3CO
2.19
8.35
8.31
8.29
7.50
7.49
7.48
7.40
7.37
7.26
6.04
5.87
5.63
5.37
5.34
5.28
5.27
5.22
4.68
4.41
4.25
4.21
4.20
4.17
4.13
4.12
4.11
3.42
1.57
0.00
4.00
2.04
2.85
0.90
2.00
1.00
3.98
1.02
8.13
2.84

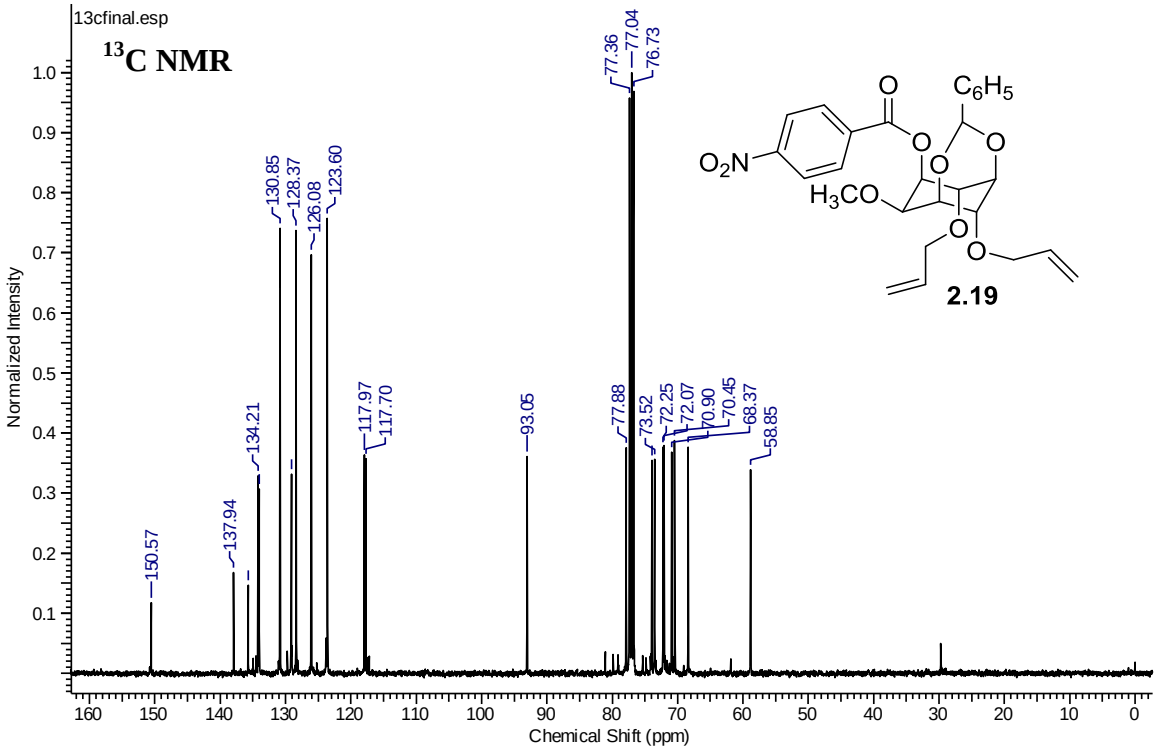
13cfinal.esp
13C NMR
77.36
77.04
76.73
130.85
128.37
126.08
123.60
134.21
137.94
150.57
117.97
117.70
93.05
77.88
73.52
72.25
72.07
70.90
70.45
68.37
58.85
Normalized Intensity
Chemical Shift (ppm)
O2N
H3CO
C6H5
2.19

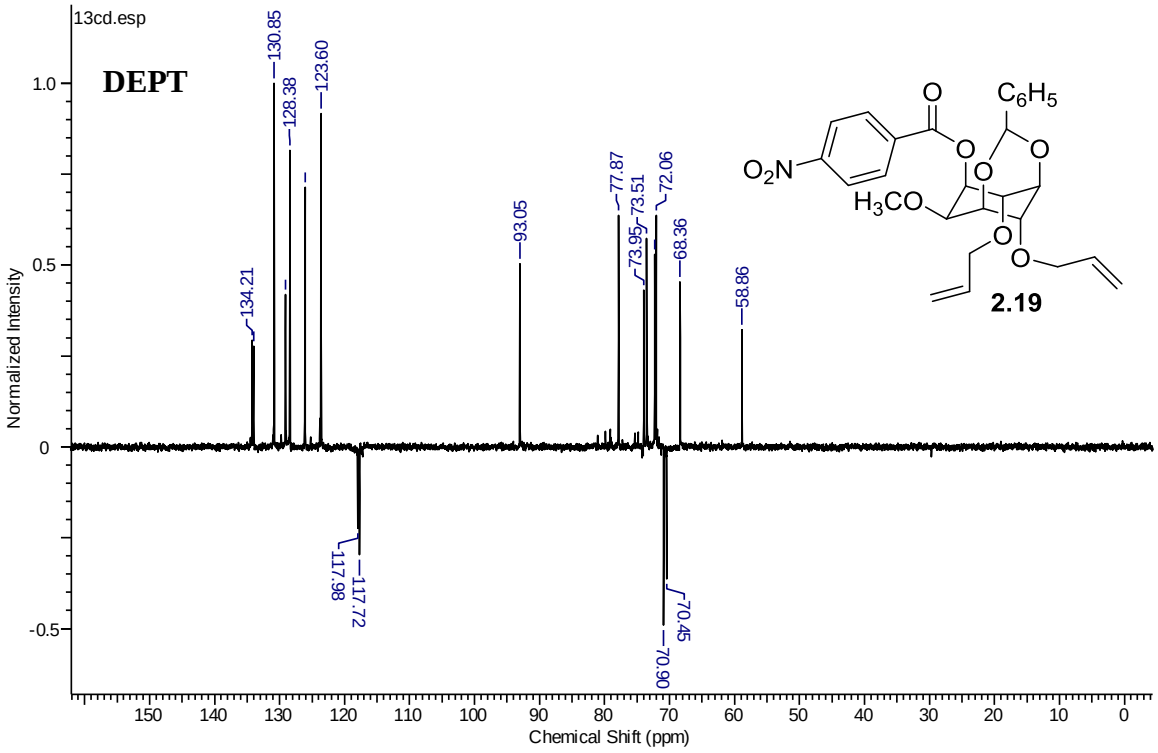
13cd.esp
DEPT
130.85
128.38
123.60
134.21
93.05
77.87
73.51
73.95
72.06
68.36
58.86
117.98
117.72
70.90
70.45
Normalized Intensity
Chemical Shift (ppm)
O2N
H3CO
C6H5
2.19

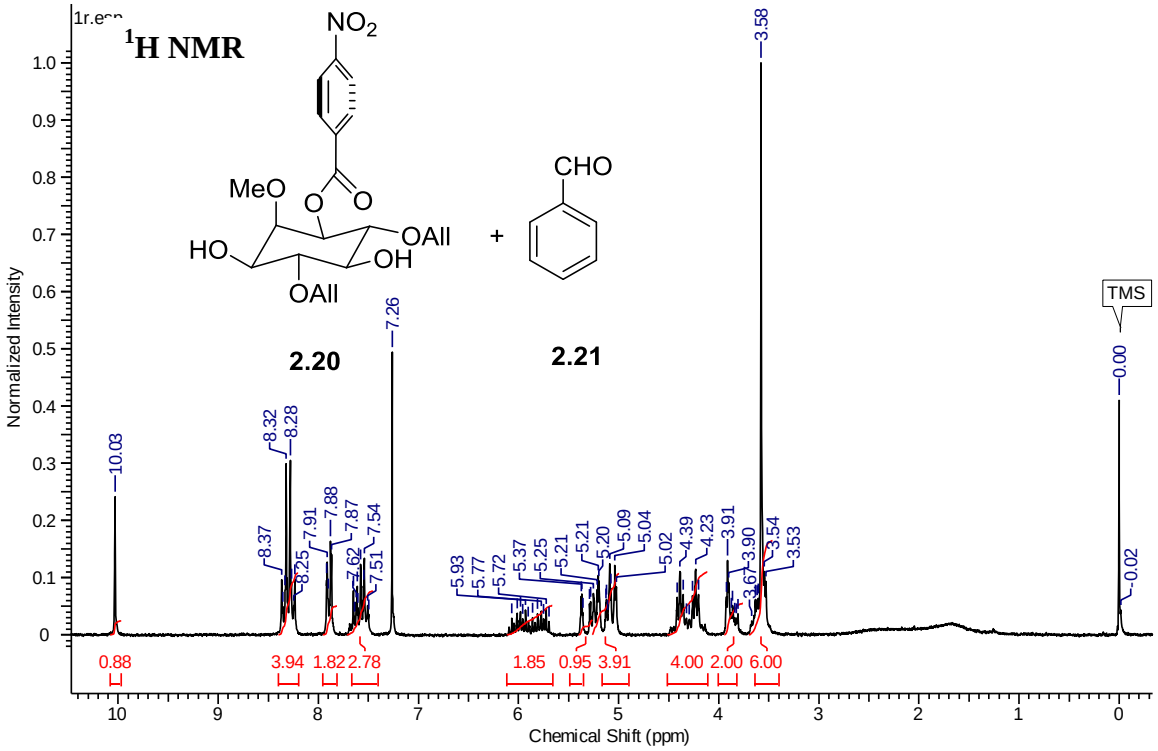
1r.esp
^{1}H NMR
NO2
MeO
O
O
OAll
HO
OH
OAll
+
CHO
2.20
2.21
TMS
Normalized Intensity
Chemical Shift (ppm)
10.03
8.32
8.28
8.37
8.25
7.91
7.88
7.87
7.62
7.54
7.51
7.26
5.93
5.77
5.72
5.37
5.25
5.21
5.21
5.20
5.09
5.04
5.02
4.39
4.23
3.91
3.90
3.67
3.58
3.54
3.53
0.00
0.02
0.88
3.94
1.82
2.78
1.85
0.95
3.91
4.00
2.00
6.00

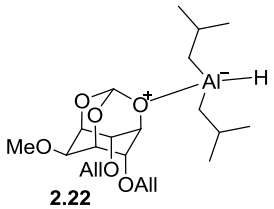

2.22

FINAL HEAT OF FORMATION = -1554.168782

O	0.779496	2.236865	-1.530919	H	-2.053191	6.571104	-0.630963
C	0.088379	1.076579	-1.847276	H	-3.677671	5.871842	1.082161
O	-1.349644	1.249977	-1.513494	H	-4.483815	4.721732	-0.136799
C	-1.939706	2.327933	-2.320438	Al	-2.139739	0.524199	0.260172
C	-1.155161	3.616109	-1.968793	H	-1.095861	-0.717754	0.339971
C	0.315890	3.358246	-2.330945	C	-4.033182	0.192736	-0.322998
C	0.451867	3.044527	-3.822631	C	-1.800163	1.998781	1.580814
C	-0.294472	1.721780	-4.071553	H	-4.443312	1.130585	-0.749200
C	-1.803443	1.874552	-3.782620	C	-4.320700	-0.974734	-1.289765
O	0.200387	0.686271	-3.177065	H	-4.631693	0.042021	0.598966
O	1.836022	2.991451	-4.137835	C	-5.771775	-0.957878	-1.794627
C	2.104841	3.061199	-5.533001	H	-3.663939	-0.870519	-2.175821
O	-2.439037	2.803259	-4.655572	C	-4.001374	-2.326031	-0.637238
C	-3.086312	2.180100	-5.790303	H	-4.187560	-3.163852	-1.327507
C	-4.342760	1.456766	-5.406919	H	-2.952554	-2.376342	-0.309940
C	-4.560899	0.156331	-5.622674	H	-4.637912	-2.481351	0.251441
O	-1.564489	4.774806	-2.682160	H	-5.974498	-1.787603	-2.492357
C	-2.835206	5.326959	-2.276845	H	-6.470501	-1.053755	-0.948618
C	-2.832908	5.837129	-0.865281	H	-6.005121	-0.014155	-2.312468
C	-3.704210	5.457946	0.073911	H	-2.635029	2.726991	1.581587
H	-0.053324	3.845517	-4.394904	C	-1.566637	1.519658	3.029260
H	0.951307	4.207392	-2.053227	H	-0.910273	2.566518	1.250169
H	-1.230340	3.769936	-0.877612	C	-1.210123	2.681819	3.968018
H	-2.995687	2.383601	-2.028753	C	-2.780247	0.750700	3.568220
H	-2.274291	0.879327	-3.856290	H	-0.708202	0.821756	3.024033
H	-0.118319	1.338229	-5.084804	H	-1.013675	2.336471	4.996577
H	3.193713	3.141591	-5.636376	H	-0.316507	3.216197	3.612001
H	1.767325	2.159714	-6.076677	H	-2.036612	3.410965	4.012603
H	1.632016	3.950319	-5.990419	H	-2.620302	0.411173	4.603483
H	-3.309123	3.021611	-6.464107	H	-3.680568	1.388111	3.559097
H	-2.392295	1.498234	-6.316210	H	-3.002727	-0.141884	2.961064
H	-5.106753	2.066241	-4.912536	H	0.433230	0.260721	-1.204263
H	-5.495560	-0.325545	-5.330382				
H	-3.812907	-0.475102	-6.110603				
H	-2.993115	6.154922	-2.985394				
H	-3.650889	4.597747	-2.428597				

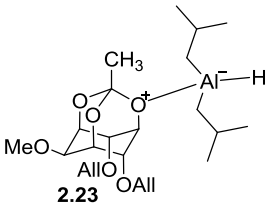

2.23

FINAL HEAT OF FORMATION = -1593.444707

O	0.830584	2.414382	-1.618317	C	1.043416	0.123715	-1.059430
C	0.318194	1.146858	-1.890141	Al	-2.031210	0.449791	0.262264
O	-1.154065	1.140862	-1.515675	H	-1.351471	-1.016568	0.351463
C	-1.889467	2.129523	-2.319112	C	-3.980871	0.503594	-0.245042
C	-1.277027	3.513327	-1.995480	C	-1.397809	1.804703	1.606754
C	0.199315	3.453961	-2.407555	H	-4.302006	1.553507	-0.398590
C	0.325674	3.153189	-3.901550	C	-4.506181	-0.372532	-1.400995
C	-0.241110	1.741813	-4.119513	H	-4.512541	0.205190	0.682528
C	-1.743840	1.691058	-3.783766	C	-5.974508	-0.065833	-1.733842
O	0.409645	0.789217	-3.238545	H	-3.915789	-0.155019	-2.312491
O	1.692376	3.281725	-4.272673	C	-4.330235	-1.866111	-1.097920
C	1.885326	3.427929	-5.674426	H	-4.667157	-2.490222	-1.940660
O	-2.535812	2.524898	-4.624207	H	-3.280682	-2.112897	-0.882454
C	-3.049927	1.848157	-5.793276	H	-4.925179	-2.150073	-0.213728
C	-4.139231	0.870812	-5.464108	H	-6.340833	-0.675835	-2.576574
C	-4.121094	-0.420485	-5.808341	H	-6.618051	-0.275833	-0.863862
O	-1.868437	4.601671	-2.690355	H	-6.112811	0.995083	-1.997139
C	-3.176374	4.988996	-2.222917	H	-2.082609	2.676378	1.600453
C	-3.164045	5.538450	-0.826822	C	-1.276752	1.287732	3.055795
C	-3.935356	5.086464	0.166790	H	-0.418278	2.205000	1.284591
H	-0.304008	3.875318	-4.453448	C	-0.726548	2.360610	4.007958
H	0.726183	4.381592	-2.153860	C	-2.619101	0.753395	3.573561
H	-1.331764	3.657688	-0.901553	H	-0.563023	0.442291	3.060051
H	-2.935744	2.055831	-2.001452	H	-0.604182	1.975791	5.033834
H	-2.077991	0.640382	-3.843704	H	0.251674	2.730507	3.665345
H	-0.039769	1.374864	-5.134911	H	-1.410794	3.224318	4.052414
H	2.958415	3.596477	-5.826909	H	-2.542885	0.398845	4.613239
H	1.591275	2.524911	-6.240957	H	-3.388745	1.542977	3.543868
H	1.323198	4.294360	-6.071721	H	-2.984701	-0.089441	2.964028
H	-3.438470	2.663834	-6.422334	H	2.093053	0.125184	-1.377021
H	-2.237506	1.347464	-6.352659	H	0.983852	0.386623	0.002451
H	-4.987756	1.279184	-4.904353	H	0.605496	-0.867540	-1.213280
H	-4.944645	-1.092383	-5.560417				
H	-3.282465	-0.852278	-6.362124				
H	-3.486960	5.766013	-2.938230				
H	-3.893486	4.152827	-2.308987				
H	-2.472821	6.370406	-0.652315				
H	-3.911856	5.534231	1.161940				
H	-4.627420	4.252567	0.018888				

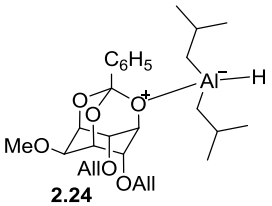

2.24

FINAL HEAT OF FORMATION = -1784.989289

O	0.971138	2.467474	-1.868565	C	1.139684	0.138674	-1.427731
C	0.433501	1.226130	-2.194582	C	1.722119	0.423490	-0.187594
O	-1.037649	1.231388	-1.774291	C	2.366058	-0.589293	0.525141
C	-1.777117	2.276112	-2.496452	C	2.432807	-1.883033	0.002732
C	-1.126400	3.625919	-2.117187	C	1.853184	-2.163934	-1.237465
C	0.334336	3.561036	-2.577400	C	1.206125	-1.157170	-1.953050
C	0.408952	3.341865	-4.088513	H	1.673342	1.436198	0.211865
C	-0.192273	1.955185	-4.364664	H	2.818678	-0.364417	1.492550
C	-1.685172	1.912261	-3.984329	H	2.935963	-2.673568	0.562919
O	0.474322	0.945911	-3.560700	H	1.901611	-3.173749	-1.648923
O	1.765107	3.469776	-4.493282	H	0.750703	-1.370387	-2.919670
C	1.921736	3.677430	-5.891457	Al	-2.071187	0.246386	-0.204890
O	-2.485419	2.796585	-4.763595	H	-1.350845	-1.197829	-0.174265
C	-3.063418	2.172576	-5.932443	C	-3.887228	0.213426	-1.100171
C	-4.138037	1.183559	-5.589850	C	-1.754742	1.491153	1.350108
C	-4.139098	-0.092283	-5.988070	H	-3.737380	0.062245	-2.187336
O	-1.709138	4.768353	-2.727607	C	-4.816628	-0.908675	-0.585869
C	-3.037427	5.097665	-2.268712	H	-4.429230	1.175921	-1.001254
C	-3.088139	5.451926	-0.811836	C	-6.061873	-1.074508	-1.470377
C	-3.876885	4.845671	0.080781	H	-4.256393	-1.861669	-0.621815
H	-0.224847	4.104182	-4.578884	C	-5.230976	-0.669888	0.871905
H	0.889877	4.461990	-2.290621	H	-5.887116	-1.472865	1.242373
H	-1.148017	3.706193	-1.015501	H	-4.359878	-0.614869	1.542883
H	-2.815151	2.205691	-2.150944	H	-5.780582	0.281796	0.966165
H	-2.040654	0.871925	-4.083900	H	-6.709748	-1.894004	-1.117470
H	-0.030038	1.641237	-5.404431	H	-6.660982	-0.148614	-1.470128
H	2.989888	3.859326	-6.062697	H	-5.781700	-1.290841	-2.513243
H	1.345217	4.556734	-6.236318	H	-2.728881	1.893520	1.691755
H	-3.479467	3.015482	-6.505238	C	-1.006610	0.913042	2.569871
H	-2.282751	1.693982	-6.553387	H	-1.200386	2.374345	0.977961
H	-4.955340	1.567958	-4.970224	C	-0.656731	1.999435	3.599556
H	-4.949106	-0.775639	-5.727083	C	-1.806489	-0.213882	3.236790
H	-3.329935	-0.498572	-6.601838	H	-0.056819	0.472703	2.214956
H	-3.315511	5.965372	-2.886454	H	-0.094984	1.588791	4.455006
H	-3.746482	4.283149	-2.499737	H	-0.047665	2.797165	3.145953
H	1.618832	2.797635	-6.488826	H	-1.574210	2.466814	3.994358
H	-2.427203	6.267716	-0.498012	H	-1.272411	-0.631253	4.105025
H	-3.896500	5.146168	1.129564	H	-2.780786	0.160913	3.593075
H	-4.538586	4.023553	-0.207355	H	-1.996195	-1.040201	2.534018

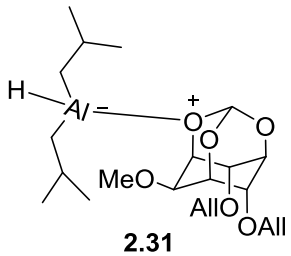

2.31

FINAL HEAT OF FORMATION = -1554.166332

O	1.903024	2.387155	-2.153627	H	0.787355	6.188675	-4.960531
C	1.693291	1.270189	-3.065193	H	-3.112575	3.236977	-6.098143
O	0.518025	0.584078	-2.714905	H	-1.636635	2.442464	-6.709632
C	-0.659954	1.432565	-2.863593	H	-3.977251	0.964792	-5.295519
C	-0.487414	2.601032	-1.864002	H	-3.443267	-0.817305	-6.909542
C	0.800626	3.342405	-2.254434	H	-2.058710	0.212923	-7.604606
C	0.702070	3.864658	-3.689407	H	-3.439991	3.947716	-1.342261
C	0.592644	2.640318	-4.617423	H	-3.096179	2.202508	-1.431970
C	-0.711113	1.860734	-4.339344	H	-2.015601	4.084692	0.795039
O	1.699536	1.729611	-4.381015	H	-2.452207	2.142233	2.245616
O	1.835497	4.680625	-3.948337	H	-3.048272	1.167319	0.777649
C	1.675312	5.538615	-5.072470	H	5.378797	3.847439	-1.249334
O	-1.874702	2.633962	-4.619239	H	4.859051	6.153241	-0.526515
C	-2.423979	2.393562	-5.934171	H	4.096240	1.071342	-1.318467
C	-3.158948	1.087773	-6.013850	H	2.459992	2.826876	1.744248
C	-2.871401	0.111286	-6.880253	H	1.248898	2.030377	0.756911
O	-1.538355	3.555297	-1.869856	H	2.563803	-0.133331	0.934938
C	-2.694493	3.176081	-1.096980	H	4.370618	-0.300418	2.664172
C	-2.422634	3.156794	0.378649	H	4.824190	0.817966	1.361892
C	-2.648687	2.105926	1.172883	H	4.274369	1.455482	2.930303
Al	3.393740	2.387007	-0.667977	H	1.925674	-0.618052	3.308128
C	4.323984	4.127690	-1.062860	H	1.756937	1.126980	3.620781
C	4.294180	5.312814	-0.077316	H	0.654033	0.320140	2.482779
C	4.987492	4.971351	1.248013	H	2.861548	6.709711	0.821075
C	2.327892	2.015683	1.003986	H	2.383943	6.107360	-0.782260
C	2.662366	0.672598	1.686924	H	2.249009	5.049416	0.650505
C	4.112779	0.657728	2.186742	H	5.004748	5.834969	1.931579
C	1.696344	0.352391	2.837427	H	4.468688	4.147462	1.763292
C	2.868014	5.823808	0.165985	H	6.028772	4.655346	1.079735
H	-0.233970	4.448666	-3.768286	H	3.947457	4.460878	-2.048656
H	1.030087	4.155259	-1.555208	H	2.543775	0.598712	-2.915716
H	-0.346537	2.166208	-0.858631				
H	-1.519883	0.798533	-2.611661				
H	-0.698763	0.936738	-4.942468				
H	0.670828	2.927566	-5.674196				
H	2.575382	6.163996	-5.116527				
H	1.591104	4.980832	-6.023595				

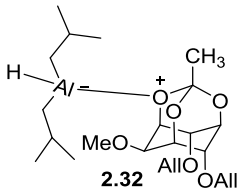

2.32 FINAL HEAT OF FORMATION = -1593.440525

C	1.605189	2.548801	-1.890173	H	-2.393460	2.572914	-3.970261
C	1.139877	1.256783	-2.577585	H	-1.016452	1.597028	-4.546135
C	-0.282728	0.871597	-2.115482	H	-3.560552	0.431135	-3.193483
C	-0.213134	0.697959	-0.591678	H	-3.200493	-1.412200	-4.788302
C	0.306219	1.934225	0.175577	H	-1.674010	-0.566612	-5.433938
O	0.742389	-0.365609	-0.328600	H	-2.193301	4.066785	0.428428
C	2.031411	-0.092411	-0.844591	H	-2.398675	2.315114	0.192666
O	2.016784	0.158087	-2.224794	H	-1.072485	3.591794	2.702823
C	1.696375	2.257640	-0.392972	H	-2.341811	1.852043	3.899017
O	2.565299	1.105806	-0.156407	H	-3.021081	1.224436	2.284163
O	-1.271803	1.837455	-2.463254	H	5.732358	3.233480	0.985338
C	-1.819675	1.651469	-3.786889	H	4.598625	5.189679	2.030734
C	-2.709795	0.447666	-3.883135	H	5.296654	0.388815	0.285491
C	-2.518827	-0.561319	-4.738842	H	3.386163	0.961011	3.631629
C	2.915282	-1.279852	-0.573250	H	2.486086	-0.090179	2.553008
O	2.871250	3.010865	-2.340452	H	4.492267	-1.631675	2.409699
C	2.804865	3.732223	-3.564183	H	6.386923	-1.331688	4.008129
Al	4.240063	1.238500	1.173207	H	6.296442	0.015624	2.854719
C	3.511038	0.261700	2.782831	H	5.710053	0.229966	4.524588
C	4.363577	-0.933478	3.259833	H	4.285113	-2.579659	4.716435
C	3.684786	-1.711728	4.396539	H	3.540558	-1.061262	5.275061
O	-0.461207	3.123964	0.049293	H	2.693393	-2.079181	4.091126
C	-1.761352	3.082097	0.667673	H	2.591152	4.896105	3.468113
C	-1.706740	2.886145	2.154316	H	2.212117	4.556040	1.769583
C	-2.384886	1.941302	2.811862	H	2.428406	3.210429	2.921319
C	4.634985	3.218462	1.139150	H	4.908117	4.507595	4.391901
C	4.301811	4.160642	2.315205	H	4.850378	2.791063	3.929418
C	2.801038	4.207851	2.633564	H	6.187911	3.816447	3.365733
C	5.106035	3.800667	3.570892	H	4.239133	3.637873	0.195113
C	5.767374	-0.481543	3.683801	H	2.507267	-2.135112	-1.124879
H	0.828452	3.323650	-2.028753	H	3.936857	-1.067389	-0.905564
H	2.154675	3.096690	0.138640	H	2.920585	-1.505980	0.499187
H	0.415617	1.640262	1.235276				
H	-1.171125	0.336547	-0.195939				
H	-0.530124	-0.114465	-2.546619				
H	1.205313	1.334131	-3.671300				
H	3.823462	4.078218	-3.778999				
H	2.464794	3.105089	-4.408787				
H	2.135002	4.608881	-3.481374				

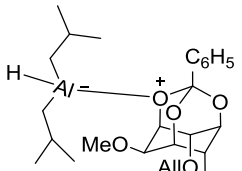

2.33 FINAL HEAT OF FORMATION = -1784.985875

O	1.875809	2.068643	-2.151170	H	-1.960802	2.431889	-6.373392
C	1.252635	0.856151	-2.759009	H	-4.454102	1.567105	-4.732908
O	-0.014826	0.666058	-2.172673	H	-4.374527	-0.401971	-6.212185
C	-0.934255	1.763503	-2.434743	H	-2.860159	0.278319	-7.051261
C	-0.327673	3.013185	-1.758179	H	-2.717943	5.256535	-1.444677
C	1.044180	3.246699	-2.406042	H	-2.986658	3.497411	-1.450095
C	0.895243	3.470068	-3.909637	H	-1.343563	5.006176	0.719881
C	0.334616	2.173433	-4.508115	H	-2.457567	3.425117	2.245673
C	-1.076609	1.871139	-3.959658	H	-3.337489	2.640612	0.805844
O	1.181584	1.053838	-4.145401	H	5.073416	3.917279	-0.881527
O	2.162585	3.840310	-4.437486	H	4.231813	6.149389	-0.235115
C	2.084542	4.464767	-5.713092	H	4.359551	1.084850	-0.998823
O	-2.039799	2.862047	-4.307350	H	1.912946	2.505765	1.702863
C	-2.697532	2.608926	-5.568182	H	1.168962	1.301283	0.660032
C	-3.672508	1.471418	-5.494743	H	3.024094	-0.316302	1.233540
C	-3.633084	0.395275	-6.286341	H	4.509777	0.166967	3.179673
O	-1.063327	4.218481	-1.915390	H	4.805277	1.305713	1.848986
C	-2.280168	4.291012	-1.147197	H	3.862508	1.821504	3.269998
C	-2.046053	4.258471	0.334894	H	2.206688	-0.839530	3.543015
C	-2.638412	3.399371	1.169862	H	1.473346	0.779716	3.650277
Al	3.296959	2.200376	-0.519560	H	0.853354	-0.397281	2.471487
C	3.979676	4.083474	-0.827638	H	2.079870	6.441354	0.974065
C	3.721507	5.246099	0.153820	H	1.804493	5.898166	-0.692052
C	4.322002	4.960585	1.536291	H	1.656104	4.742359	0.658852
C	2.146710	1.645755	1.046819	H	4.190888	5.816882	2.216842
C	2.760298	0.520472	1.906192	H	3.841934	4.085877	2.002781
C	4.056406	0.977489	2.587545	H	5.399767	4.748756	1.463455
C	1.770341	-0.018484	2.949947	H	3.715850	4.397430	-1.855543
C	2.234149	5.601224	0.278051	C	2.125663	-0.344151	-2.485815
H	0.154276	4.278489	-4.054273	C	3.242388	-0.576519	-3.298182
H	1.564121	4.088803	-1.939200	C	4.060558	-1.678887	-3.054504
H	-0.176338	2.773554	-0.690296	C	3.770438	-2.550509	-2.000562
H	-1.885464	1.463035	-1.976149	C	2.655305	-2.317796	-1.191866
H	-1.384454	0.877609	-4.330059	C	1.829892	-1.217103	-1.433126
H	0.345300	2.194163	-5.606169	H	3.467443	0.113298	-4.110817
H	3.104748	4.772290	-5.973301	H	4.933348	-1.853712	-3.685771
H	1.716099	3.780014	-6.499298	H	4.415915	-3.409646	-1.807519
H	1.433256	5.358647	-5.686750	H	2.424146	-2.995274	-0.367701
H	-3.220580	3.551573	-5.791646	H	0.956934	-1.033748	-0.807607

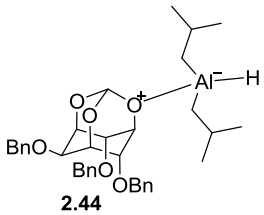

2.44

FINAL HEAT OF FORMATION = -2092.014600

C	5.369917	0.684010	-0.129617	C	-3.952022	0.833679	-3.072564
C	4.651705	-0.390007	0.410875	C	-3.991538	0.596700	-4.597062
C	4.561416	-0.510760	1.806587	C	-2.607512	0.237656	-5.152459
C	5.173437	0.426113	2.640233	C	-4.571366	1.804197	-5.349683
C	5.894640	1.491928	2.090091	C	-5.803987	-1.601180	1.727474
C	5.993178	1.618883	0.703193	H	0.702046	-1.040276	1.390199
C	4.003073	-1.422698	-0.487610	H	2.209582	0.374417	-0.140386
O	2.625888	-1.680460	-0.179649	H	2.228619	-0.508071	-2.593019
C	1.755911	-0.583783	-0.450823	H	0.126412	0.758665	-3.215093
C	1.353514	-0.482467	-1.930997	H	-1.430655	1.501614	-1.424301
C	0.493100	0.778849	-2.173834	H	-1.390719	0.251036	0.745730
C	-0.742347	0.662803	-1.263008	H	-1.178697	-2.592956	-1.859103
C	-0.434040	0.467466	0.233516	H	2.560923	3.290335	-2.592811
C	0.469641	-0.782600	0.349838	H	2.672355	1.696881	-3.376128
O	-1.436031	-0.554525	-1.702516	H	2.087946	1.701797	-5.643946
C	-0.573905	-1.749325	-1.512333	H	0.730536	2.545946	-7.547411
O	0.550074	-1.630075	-2.319568	H	-1.013657	4.283612	-7.160811
O	-0.292416	-1.910419	-0.162033	H	-1.387542	5.175107	-4.863649
O	1.193839	1.986108	-1.902287	H	-0.024352	4.330544	-2.961005
C	1.965925	2.469566	-3.020203	H	-0.980099	1.677375	2.489468
C	1.127139	2.964843	-4.177021	H	0.626053	0.920336	2.652592
C	0.143083	3.944966	-3.969358	H	0.126954	2.717142	4.693752
C	-0.623514	4.414766	-5.036480	H	1.102694	4.843415	5.510920
C	-0.411752	3.916839	-6.327376	H	2.198317	6.415850	3.912024
C	0.565862	2.943940	-6.544331	H	2.308124	5.833271	1.490876
C	1.327479	2.468695	-5.471916	H	1.328948	3.687317	0.673973
O	0.157032	1.647511	0.746398	H	4.492099	-2.400987	-0.366926
C	0.078298	1.752667	2.168402	H	4.128379	-1.124238	-1.545980
C	0.667725	3.065775	2.625686	H	5.443962	0.788659	-1.215797
C	1.283635	3.949031	1.731488	H	6.549492	2.451281	0.267437
C	1.830346	5.150084	2.196322	H	6.375378	2.222892	2.743040
C	1.770145	5.478146	3.552252	H	5.095463	0.323393	3.724495
C	1.155912	4.596861	4.448590	H	3.999537	-1.344730	2.233773
C	0.607965	3.399568	3.986958	H	-3.418019	-2.205126	-2.593434
Al	-3.496667	-0.734992	-1.904210	H	-3.285315	1.696254	-2.867484
C	-4.131809	-0.726990	0.004217	H	-4.656556	-0.265551	-4.791930
C	-5.392079	-1.586143	0.247916	H	-3.935310	2.692332	-5.197743
C	-6.565491	-1.128193	-0.628889	H	-2.645488	0.042832	-6.235845

H	-1.898655	1.068309	-4.991894	
H	-2.198840	-0.659870	-4.663850	
H	-4.337552	0.306731	0.346361	
H	-3.321658	-1.105469	0.655979	
H	-5.152047	-2.626305	-0.041409	
H	-7.462108	-1.745554	-0.462226	
H	-6.832155	-0.081268	-0.408796	
H	-6.321471	-1.188927	-1.702605	
H	-6.676892	-2.250781	1.904519	
H	-4.980754	-1.960272	2.364074	
H	-6.067064	-0.584656	2.064644	

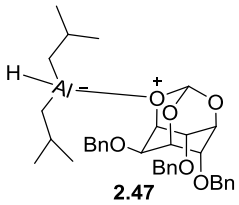

2.47 FINAL HEAT OF FORMATION = -2092.012309

C	5.554052	0.763262	-0.289275	C	-1.772153	-2.053691	2.534781
C	4.943678	-0.463662	0.000633	C	-0.849513	-3.678155	4.225871
C	4.859513	-0.879636	1.339338	C	2.280712	-7.040289	-1.642755
C	5.371684	-0.081506	2.362694	H	1.090796	-1.186103	0.763424
C	5.981509	1.142010	2.062111	H	2.559496	0.367977	-0.652819
C	6.073715	1.562757	0.734161	H	2.558809	-0.275176	-3.178047
C	4.380384	-1.336328	-1.099789	H	0.446862	1.049750	-3.649267
O	2.994036	-1.666628	-0.914074	H	-1.105871	1.569630	-1.781008
C	2.111435	-0.558836	-1.053297	H	-1.023555	0.131956	0.256324
C	1.687276	-0.312751	-2.511102	H	-0.853795	-2.409554	-2.630265
C	0.821909	0.962751	-2.614097	H	2.883865	3.511178	-2.781695
C	-0.402294	0.730992	-1.711826	H	3.015496	1.996955	-3.706710
C	-0.075575	0.407842	-0.242714	H	2.416215	2.167190	-5.962631
C	0.845247	-0.835962	-0.245725	H	1.070193	3.172836	-7.795961
O	-1.095039	-0.436412	-2.241073	H	-0.652765	4.896008	-7.275832
C	-0.272181	-1.568680	-2.238978	H	-1.020177	5.609250	-4.915221
O	0.885632	-1.423551	-2.999431	H	0.330020	4.601455	-3.084059
O	0.080813	-1.921353	-0.864694	H	-0.616196	1.338874	2.114667
O	1.521379	2.139891	-2.226429	H	1.046377	0.707089	2.229181
C	2.299278	2.728270	-3.287394	H	0.421967	2.306325	4.395433
C	1.467209	3.321514	-4.402639	H	1.193975	4.457082	5.355889
C	0.493089	4.292758	-4.119435	H	2.120534	6.233396	3.867776
C	-0.267003	4.853378	-5.146562	H	2.264900	5.832585	1.411902
C	-0.059446	4.455349	-6.472464	H	1.486802	3.664383	0.450058
C	0.907417	3.491326	-6.764522	H	4.887398	-2.312100	-1.122512
C	1.662929	2.925692	-5.732340	H	4.546402	-0.853636	-2.082096
O	0.515394	1.532987	0.378359	H	5.622660	1.097897	-1.328327
C	0.431048	1.524788	1.804543	H	6.544125	2.518127	0.493632
C	0.907064	2.848546	2.355251	H	6.380234	1.766229	2.863739
C	1.427822	3.846613	1.523627	H	5.303128	-0.416565	3.399639
C	1.861958	5.059306	2.069561	H	4.382583	-1.834649	1.573087
C	1.781926	5.285617	3.445095	H	-1.948802	-3.722222	-0.615473
C	1.263008	4.289496	4.279166	H	0.798918	-3.036541	2.053101
C	0.828733	3.079315	3.736885	H	-2.020015	-4.176366	2.497799
Al	-0.391749	-3.843965	-0.160150	H	0.411074	-4.737022	2.073759
C	0.688822	-5.075251	-1.324119	H	-1.710338	-3.497910	4.890316
C	1.767106	-5.965056	-0.671981	H	-0.493960	-4.704478	4.403498
C	2.940036	-5.134939	-0.137133	H	-0.041165	-2.990864	4.528159
C	-0.016775	-3.748748	1.814699	H	-2.633171	-1.854640	3.191815
C	-1.211357	-3.464782	2.748354				

H	-1.001672	-1.296316	2.762450	
H	-2.102324	-1.910871	1.494012	
H	1.160055	-4.497301	-2.143303	
H	-0.051890	-5.726141	-1.827261	
H	1.314585	-6.493415	0.188983	
H	3.699694	-5.771942	0.343111	
H	3.424758	-4.587668	-0.962030	
H	2.606866	-4.387662	0.598431	
H	3.030645	-7.695571	-1.169421	
H	1.457271	-7.674096	-2.005495	
H	2.750399	-6.570667	-2.523046	

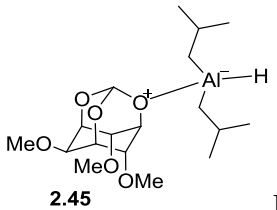

2.45

FINAL HEATOF FORMATION = -1399.535809

C	1.338569	-0.005652	-2.828211	H	0.050506	-2.805581	4.629291
C	1.973914	-0.269522	-1.443665	H	0.277181	-1.198538	3.908077
C	0.817489	-0.477486	-0.452118	H	1.635697	-1.999666	4.737847
C	-0.205476	0.685745	-0.399567	H	1.887929	-2.158395	2.257222
C	-0.733424	0.881781	-1.831387	C	1.911549	-4.151168	3.032624
C	0.427336	1.220834	-2.785601	H	1.249851	-4.861643	3.555274
H	2.085143	0.100208	-3.624846	H	2.244385	-4.629676	2.099813
H	2.539275	-1.218326	-1.504114	H	2.798158	-3.992117	3.666136
H	1.194664	-0.741969	0.544063	C	2.045144	-4.094247	-0.777476
H	-1.042183	0.348051	0.244322	H	2.157027	-3.714322	-1.812634
H	-1.516883	1.649430	-1.845672	H	2.818705	-3.565666	-0.185789
H	0.993684	2.066688	-2.350764	C	2.374186	-5.604144	-0.789188
O	2.806515	0.778895	-0.972429	C	1.464214	-6.366520	-1.762261
C	4.125767	0.735530	-1.520108	H	1.684479	-7.445347	-1.757638
H	4.607577	-0.239476	-1.324567	H	1.611426	-5.999347	-2.791864
H	4.133622	0.925876	-2.607710	H	0.400052	-6.233261	-1.516827
H	4.696341	1.527267	-1.019938	H	2.195776	-6.015879	0.223209
O	0.021265	1.511042	-4.114715	C	3.850329	-5.863795	-1.126630
C	-0.584415	2.791032	-4.262076	H	4.089053	-5.472990	-2.129877
H	-1.569698	2.852531	-3.766745	H	4.087866	-6.940089	-1.120315
H	-0.727630	2.944742	-5.338749	H	4.517486	-5.364914	-0.406952
H	0.064485	3.594009	-3.864390				
C	-1.211357	-3.464782	2.748354				
O	0.296587	1.930116	0.044369				
C	0.699516	1.941474	1.414326				
H	1.649606	1.402789	1.564920				
H	-0.079831	1.502997	2.064567				
H	0.842956	2.994253	1.686561				
O	-1.381197	-0.350158	-2.238672				
C	-0.472900	-1.398987	-2.289057				
O	0.058211	-1.639856	-0.923968				
H	-1.000379	-2.319596	-2.556790				
O	0.580853	-1.200694	-3.171856				
Al	0.230539	-3.540066	-0.103450				
H	-1.071520	-4.114482	-0.882495				
C	-0.044407	-3.065403	1.832904				
C	1.168455	-2.838161	2.758057				
C	0.765985	-2.170341	4.082183				

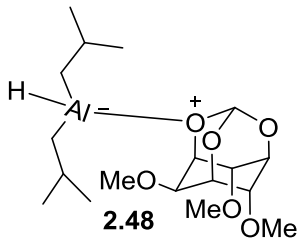

2.48 FINAL HEAT OF FORMATION = -1399.536179

O	-0.069811	-0.171304	-3.146441	C	1.892185	-1.446925	-5.331081
C	0.890150	0.825138	-2.661963	H	2.542888	-0.759009	-4.752830
C	1.585712	0.186888	-1.438284	C	2.373906	-2.892690	-5.085811
C	0.493327	-0.085378	-0.391068	H	2.089799	-1.180258	-6.386825
O	-0.449138	-1.016440	-0.996858	C	-2.804444	1.223649	-7.643580
C	-1.072254	-0.457109	-2.121551	H	-2.509149	-0.830041	-7.102211
C	-0.322662	1.165390	0.020042	C	-3.273782	0.201861	-5.388186
C	-0.949821	1.719607	-1.269966	H	-3.855439	1.091939	-7.950006
C	0.158564	2.107927	-2.268443	H	-2.704923	2.232565	-7.208990
O	-1.801447	0.693759	-1.838524	H	-2.179911	1.189638	-8.549437
O	2.605602	1.001848	-0.881059	H	-4.338539	0.138630	-5.663514
C	3.866928	0.852701	-1.538589	H	-3.056147	-0.636916	-4.709255
O	0.401030	2.221084	0.623937	H	-3.122946	1.137610	-4.825630
C	0.951060	1.894571	1.898814	C	3.789560	-3.128136	-5.633144
O	-0.319353	2.728244	-3.452027	C	2.308451	-3.268207	-3.601089
C	-0.686654	4.093603	-3.273590	H	1.693264	-3.578205	-5.624854
H	1.577661	1.007447	-3.496660	H	4.118902	-4.169875	-5.486132
H	1.994667	-0.790489	-1.754473	H	3.841914	-2.905156	-6.709735
H	0.912340	-0.610225	0.476516	H	4.514625	-2.470839	-5.123744
H	-1.135381	0.816475	0.688528	H	2.611887	-4.313156	-3.432272
H	-1.610013	2.565184	-1.043371	H	2.992120	-2.629411	-3.013925
H	0.881275	2.759852	-1.741782	H	1.291699	-3.142407	-3.197573
H	4.206746	-0.198444	-1.515384				
H	3.835942	1.193184	-2.587974				
H	4.580186	1.475885	-0.985735				
H	-1.001672	-1.296316	2.762450				
H	-1.566593	4.212364	-2.616738				
H	-0.940333	4.478561	-4.268670				
H	0.150818	4.684436	-2.857425				
H	1.805501	1.202815	1.810248				
H	0.185849	1.453233	2.564077				
H	1.304839	2.836326	2.335736				
H	-1.737030	-1.210341	-2.554965				
Al	-0.065957	-1.070151	-5.038930				
H	-0.990009	-2.318625	-4.554297				
C	-0.878118	0.305566	-6.248726				
H	-0.725348	1.302584	-5.791206				
H	-0.273479	0.317789	-7.175554				
C	-2.367401	0.158536	-6.625651				

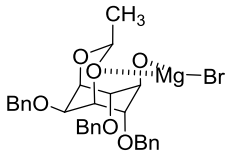

2.50

FINAL HEAT OF FORMATION = -4347.465290

C	1.052987	4.474878	1.672942	H	-1.747376	1.453140	-0.088729
C	0.582586	3.363124	2.383285	C	-0.175127	-3.158862	-1.423723
C	0.797102	3.295863	3.767344	H	3.254525	2.838541	-3.540651
C	1.455770	4.329765	4.435760	H	2.723254	1.281117	-4.213620
C	1.921140	5.438412	3.722626	H	2.305679	1.535879	-6.500644
C	1.722153	5.503890	2.341036	H	1.277053	2.754376	-8.408625
C	-0.193068	2.262882	1.700981	H	0.058741	4.892661	-8.010319
O	0.138291	2.209333	0.309947	H	-0.128188	5.797780	-5.695510
C	-0.704328	1.355371	-0.458439	H	0.914680	4.578961	-3.791457
C	-0.241968	-0.116877	-0.316901	H	-1.282063	2.451282	1.803751
C	1.151420	-0.191831	-0.926621	H	0.018959	1.299790	2.203761
C	0.972617	-0.163323	-2.439945	H	0.445414	2.425376	4.328560
C	0.449375	1.254323	-2.817902	H	1.613197	4.265503	5.514299
C	-0.738430	1.799625	-1.958322	H	2.441349	6.245514	4.241962
O	0.108103	-1.211496	-2.947631	H	2.089796	6.363922	1.777600
C	-0.727553	-1.882637	-2.030331	H	0.901498	4.519121	0.593924
O	-1.240436	-0.948793	-1.020493	H	3.668675	-0.886339	-1.477901
O	-1.961269	1.456296	-2.529509	H	3.546099	-0.113908	0.123371
O	1.910471	-1.282668	-0.400917				
C	3.322718	-1.043855	-0.439176				
C	4.062196	-2.210978	0.164853				
C	3.514203	-2.954044	1.219402				
C	4.233888	-4.006045	1.791084				
C	5.513669	-4.320828	1.325070				
C	6.067899	-3.581377	0.276758				
C	5.342188	-2.538322	-0.303431				
O	1.562996	2.159168	-2.690045				
C	2.368896	2.272451	-3.870183				
C	1.691584	2.986149	-5.022392				
C	1.780181	2.478793	-6.324990				
C	1.201028	3.162347	-7.398670				
C	0.516973	4.359123	-7.175347				
C	0.412550	4.866520	-5.875500				
C	0.999886	4.187525	-4.807416				
H	-0.226113	-0.452373	0.730420				
H	1.651733	0.753756	-0.647988				
H	1.938431	-0.314357	-2.946219				
H	0.076782	1.233905	-3.854814				
H	-0.602488	2.899704	-1.946761				

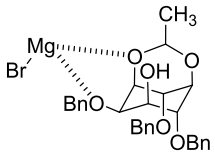

2.56

FINAL HEATOF FORMATION = -4347.490483

C	0.903495	1.150537	-2.512796	H	0.520850	1.044239	-3.541041
C	0.903495	1.150537	-2.512796	H	-0.928988	2.025578	-1.735686
C	0.903495	1.150537	-2.512796	H	-0.840953	0.598490	0.438720
C	0.903495	1.150537	-2.512796	H	3.046690	3.536577	-3.235053
C	0.903495	1.150537	-2.512796	H	3.098624	1.868249	-3.849368
C	0.903495	1.150537	-2.512796	H	2.556207	1.759860	-6.127020
C	0.903495	1.150537	-2.512796	H	1.186100	2.457472	-8.080797
C	0.903495	1.150537	-2.512796	H	-0.597201	4.176819	-7.802549
C	0.903495	1.150537	-2.512796	H	-0.998759	5.193604	-5.561733
C	1.737765	-0.077317	-2.120475	H	0.379346	4.495178	-3.610091
C	2.354802	0.162978	-0.747815	H	-1.286920	2.416664	1.850367
C	1.277392	0.203235	0.389390	H	0.339139	1.923001	2.376307
C	0.028707	1.064967	-0.063541	H	-1.115244	3.898700	3.932020
C	-0.304175	1.138111	-1.577417	H	-0.590410	6.193008	4.713543
O	-1.085322	0.021316	-2.065139	H	0.911981	7.662018	3.366901
C	-0.528420	-1.226604	-1.773754	H	1.879891	6.809730	1.233489
O	0.932450	-1.308285	-2.120464	H	1.350791	4.497582	0.455849
O	0.163457	2.429418	0.356754	H	4.966023	-0.128848	0.266733
C	-0.206566	2.629318	1.718637	H	3.610973	-0.365928	1.425294
C	0.097035	4.045175	2.144495	H	6.328966	-2.119331	-0.451856
C	0.936614	4.874774	1.391288	H	7.131388	-4.404719	0.119023
C	1.226405	6.170584	1.831319	H	5.942586	-5.747614	1.846345
C	0.684757	6.650016	3.026164	H	3.954541	-4.800767	3.009222
C	-0.156597	5.825979	3.781090	H	3.163610	-2.504434	2.453779
C	-0.450027	4.534406	3.340527	H	-1.138362	-2.077308	-3.651186
O	0.946639	-1.076553	0.804463	H	-0.780335	-3.276034	-2.364733
Mg	1.719051	-2.437218	-0.356671	H	-2.285502	-2.318492	-2.296605
Br	1.520008	-4.818016	-0.663626	H	-0.576934	-1.408288	-0.682975
O	3.250539	-0.976548	-0.546930				
C	4.164530	-0.813452	0.587012				
C	4.693826	-2.165507	0.962798				
C	4.032898	-2.926849	1.940877				
C	4.480337	-4.212160	2.256143				
C	5.594607	-4.742417	1.602124				
C	6.261152	-3.989194	0.630168				
C	5.811420	-2.707702	0.309767				
C	-1.224001	-2.293906	-2.578169				
H	1.710681	0.791975	1.229002				
H	2.948723	1.087977	-0.780292				
H	2.533883	-0.282728	-2.851975				

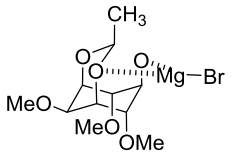

2.51

FINAL HEATOF FORMATION = -3655.000683

C	-0.726042	-1.108298	-2.650251
O	-0.020840	-1.211535	0.949327
C	0.465463	0.061399	0.666743
C	1.716346	-0.026701	-0.263787
C	1.318661	-0.122401	-1.754622
O	0.547423	-1.372955	-1.960008
C	0.495573	1.118481	-2.088148
C	-0.871658	0.944127	-1.425359
C	-0.670265	0.983061	0.109844
O	-1.522216	-0.292208	-1.831478
O	2.576913	1.093085	-0.065482
C	3.941954	0.843601	-0.397355
O	0.477437	1.338408	-3.503483
C	0.128273	2.676674	-3.857928
O	-0.446753	2.372331	0.389569
C	-0.786332	2.748081	1.719808
H	0.836101	0.552511	1.590152
H	2.254448	-0.952380	0.035948
H	2.196715	-0.182910	-2.414320
H	0.995510	1.968249	-1.588933
H	-1.552827	1.767732	-1.685952
H	-1.604111	0.634927	0.588751
C	-1.441972	-2.414703	-2.890761
H	-0.615494	3.829698	1.794466
H	-1.849145	2.531489	1.937447
H	-0.160913	2.238069	2.473377
H	4.501056	1.745096	-0.117879
H	4.339283	-0.017418	0.170713
H	4.092796	0.657631	-1.476326
H	0.224428	2.744230	-4.948484
H	-0.908716	2.928338	-3.574948
H	0.812183	3.404340	-3.385139
Mg	0.140102	-2.612886	-0.280906
H	-2.317561	-2.228518	-3.526198
H	-0.781503	-3.133342	-3.391269
H	-1.818227	-2.865201	-1.957169
H	-0.461929	-0.605094	-3.592133
Br	0.261720	-4.993608	-0.488760

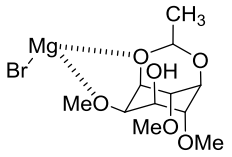

2.57

FINAL HEATOF FORMATION = -3655.010863

O	-1.026804	-0.331953	-2.571748
C	-0.642551	-1.519122	-1.737997
O	-0.555271	-1.220332	-0.374494
C	0.207656	-0.027106	-0.079382
C	-0.720320	1.100673	-0.550474
C	-0.717024	1.013919	-2.078456
C	1.634392	0.026315	-0.685884
C	1.779550	0.451849	-2.198476
O	1.812775	-0.646584	-3.048953
C	0.653939	1.461971	-2.587395
O	2.360100	0.905890	0.187887
C	3.755817	0.621433	0.231362
Mg	0.400174	-0.551015	-4.355143
Br	-0.519898	-1.438725	-6.382301
O	0.615728	1.490241	-4.052467
C	0.010766	2.653202	-4.637320
O	-0.334650	2.430769	-0.234751
C	-0.370123	2.722225	1.162432
H	0.323097	-0.034801	1.011701
H	2.060377	-0.995073	-0.635115
H	2.736121	1.014512	-2.252678
H	0.876324	2.470939	-2.215555
H	-1.517356	1.647421	-2.490774
H	-1.729684	0.887774	-0.148403
C	-1.706899	-2.563855	-1.957235
H	-0.230694	3.806338	1.255185
H	-1.345214	2.444910	1.604016
H	0.441379	2.209910	1.703883
H	4.203701	1.342694	0.926835
H	3.942447	-0.404430	0.599816
H	4.237849	0.732016	-0.755997
H	0.044211	2.508375	-5.723608
H	-1.037871	2.774542	-4.321908
H	0.585722	3.550345	-4.362862
H	-1.806886	-2.784629	-3.028741
H	-1.419727	-3.486676	-1.435036
H	-2.672429	-2.212721	-1.569700
H	0.353659	-1.821959	-2.109673

Chapter 3

Investigations to delineate the role of the 1,3 acetal bridge in inososes for nucleophilic addition to the carbonyl group.

3.1. Introduction

The previous chapters presented the potential of inositol *1,3*-acetals to function as key intermediates for the synthesis of inositol derivatives and the reasons for the differences in observed selectivity during their formation by reductive cleavage of the corresponding *myo*-inositol-1,3,5-orthoester. Inososes are often used as precursors for the preparation of unnatural isomeric inositols (Scheme 1),[1] their derivatives (Scheme 2 and Scheme 3)[2, 3] especially analogs of naturally occurring phoshoinositols (Scheme 4).[4-6]

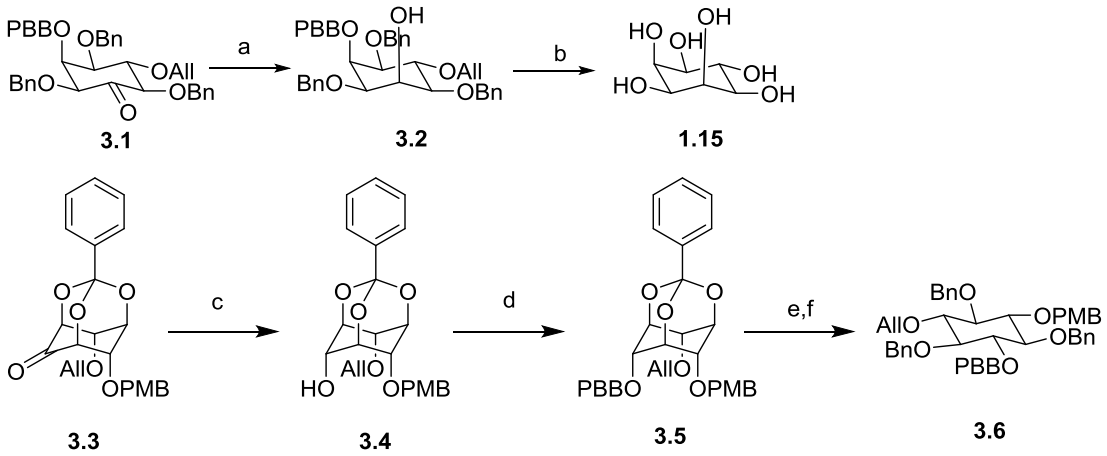

Scheme 1. (a**)** THF, MeOH, $NaBH_4$, 93%; (b) (i) MeOH, H_2O, Pd-C, TsOH, reflux, 92%; (ii)EtOH, THF, TFA, Pd-$(OH)_2$/C, H_2, rt, 94%; (c) THF, MeOH, $NaBH_4$, 90%; (d) DMF, NaH, PBBBr, 94%; (e) CH_2Cl_2, DIBAL-H (5.5 eq., as in Scheme 6, chapter 1); (f) DMF, NaH, BnBr, 68%.

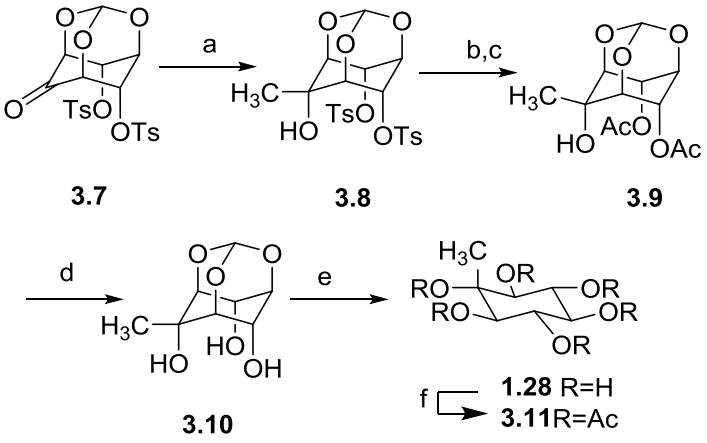

Scheme 2. (a) THF, MeMgI, Et_2O, 0°C–rt, 6 h, 74%; (b) MeOH, NaOMe, 12 h, reflux, 94% ; (c) Pyridine, Ac_2O, RT, 24 h, 95%; (d) MeOH, *iso*-$BuNH_2$, reflux, 12 h, 96%; (e) aq. TFA, 1 h, 100% ; (f) Pyridine, Ac_2O, DMAP, 24 h, 93%.

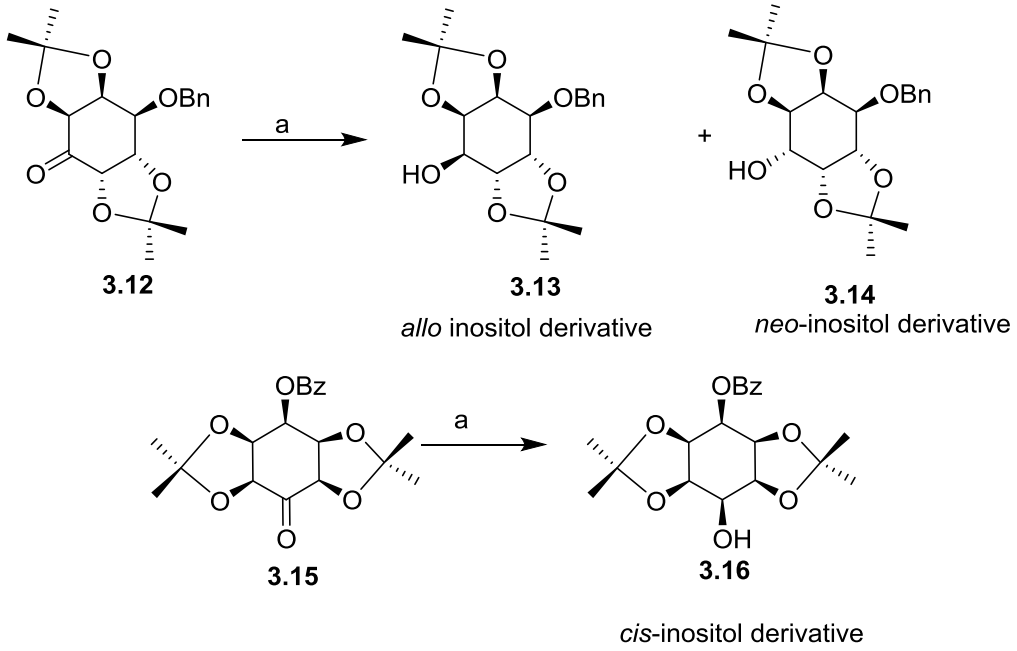

Scheme 3. (a) $NaBH_4$, MeOH, 0 °C, 0.5h 50% for **3.13** , 31% for **3.14** , 89% for **3.16**

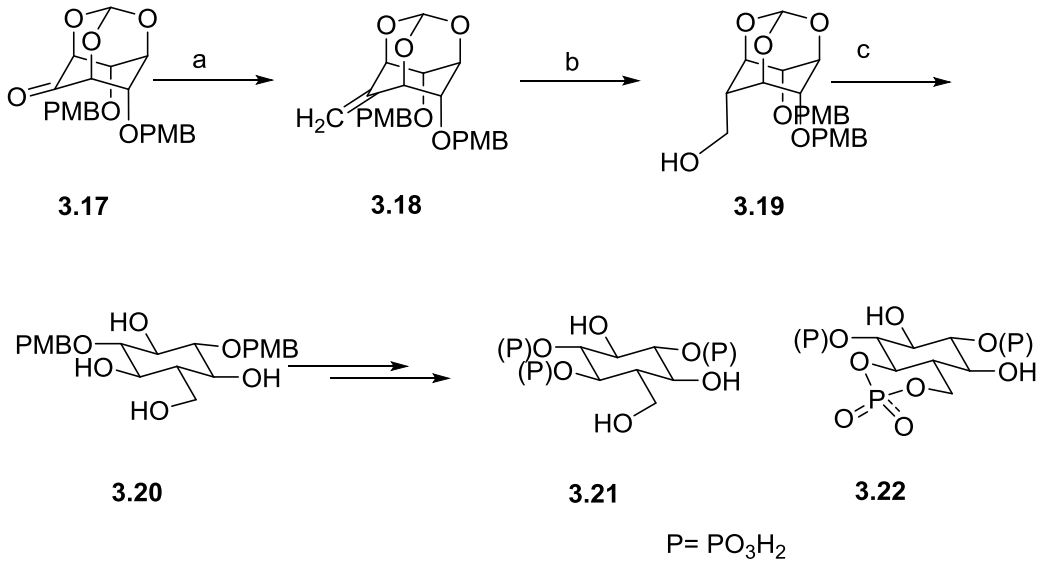

Scheme 4. (a) $MePPh_3Br$, *t*-BuOK, THF, 91%; (b) (i) 9-BBN, THF, 50 °C; (ii) H_2O_2, OH^-, 97% (c) 1M HCl/MeOH, 1:10, 50 °C, 30 min. 87%.

The inososes also serve as precursors for ring substituted derivatives of inositols, some of which occur in nature and are present in several natural products (Chart 1).[2, 7, 8]

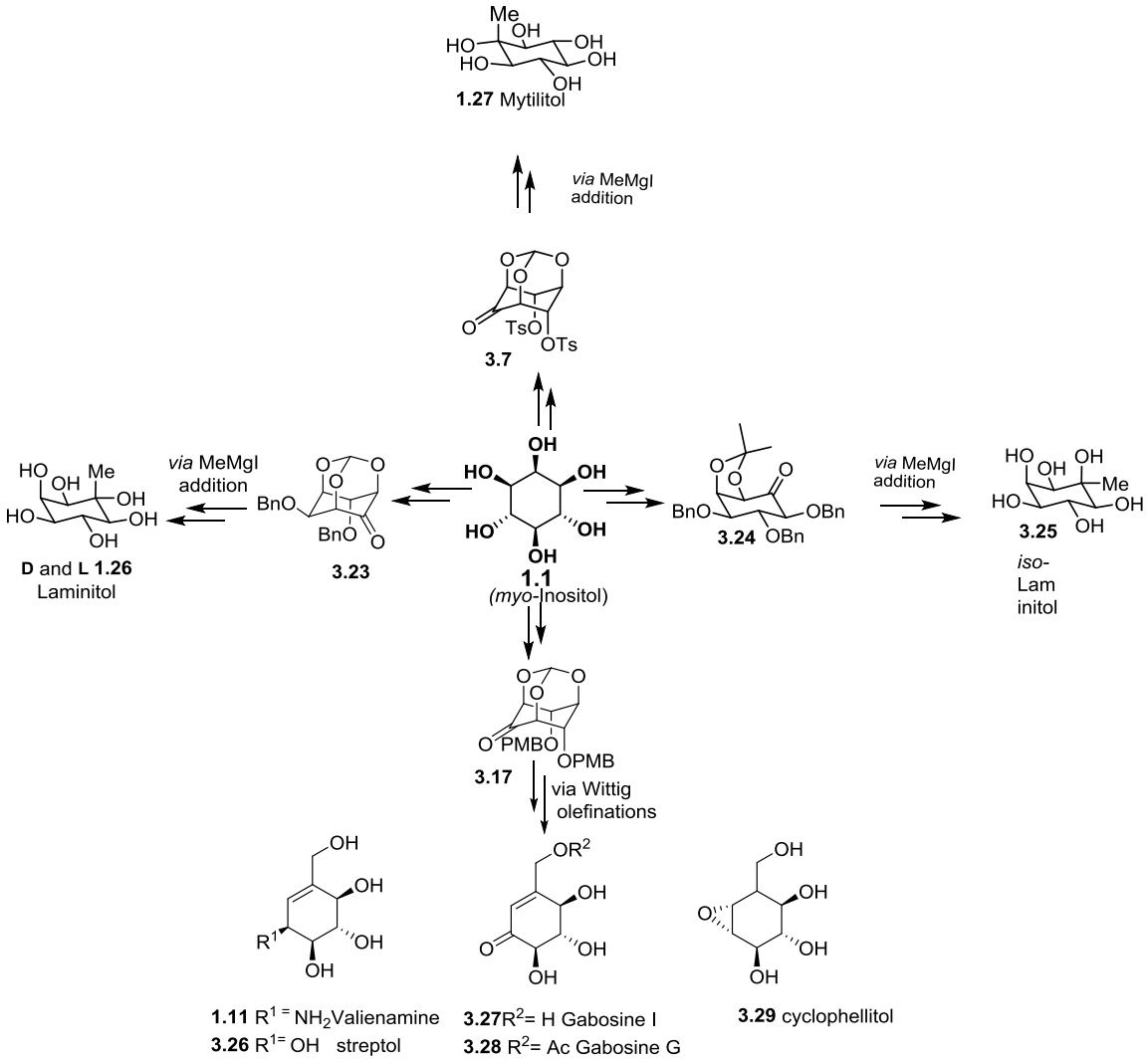

Chart 1. Ring substituted derivatives and natural products of inositols from inosose.

Previous work in our laboratory[9] had suggested that nucleophilic addition to a *myo*-inosose derivative carrying a 1,3-acetal bridge results in the selective formation of the corresponding *neo*-inositol derivative (Scheme 5).

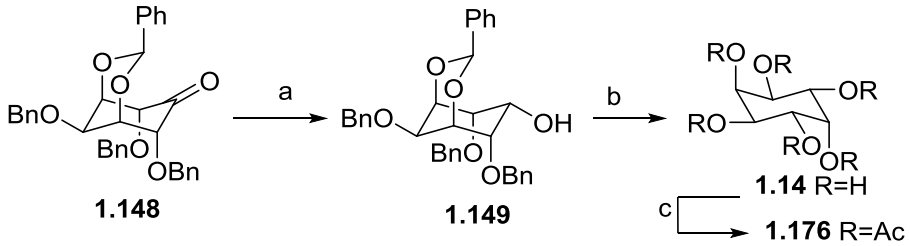

Scheme 5. (a) THF-MeOH, $NaBH_4$, RT, 1 h, 94% ; (b) EtOH, $Pd(OH)_2$-C, H_2 (50 Psi), 6 h, 82%; (c) Ac_2O, pyridine, RT, 4 h, 89%.

Literature reports[10] suggest that in many instances the reaction of inositol derivatives in the presence of metal ions proceed with good selectivity due to the chelation of the metal ion with the reacting inositol derivative (Scheme 5). The inositol orthoester triols (ex. **1.66** and **1.67**) give the dialkylated products (**3.30**-**3.32**) with high selectivity. The results were attributed to the Li^+ ion chelating between the diol.

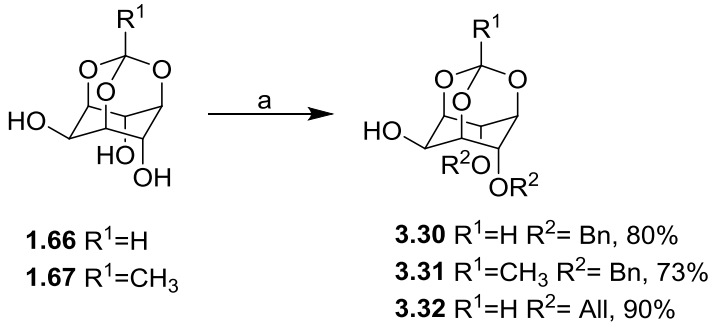

Scheme 6. (a) LiH or BuLi, RT, 22-40h, THF–DMF, BnBr or AllBr

Similarily the *epi*-inosose **3.33**, bearing a β-hydroxy group on reaction with MeMgI resulted in exclusive product formation of **3.34** in high yield; whereas the *scyllo*-inosose **3.35**, lacking an axial hydroxy group gave a mixture of products. The results were ascribed to the formation of a stable chelate **3.38** between the 2 oxygens with the Mg atom that directed the incoming nucleophile to the opposite side of the chelate.[11]

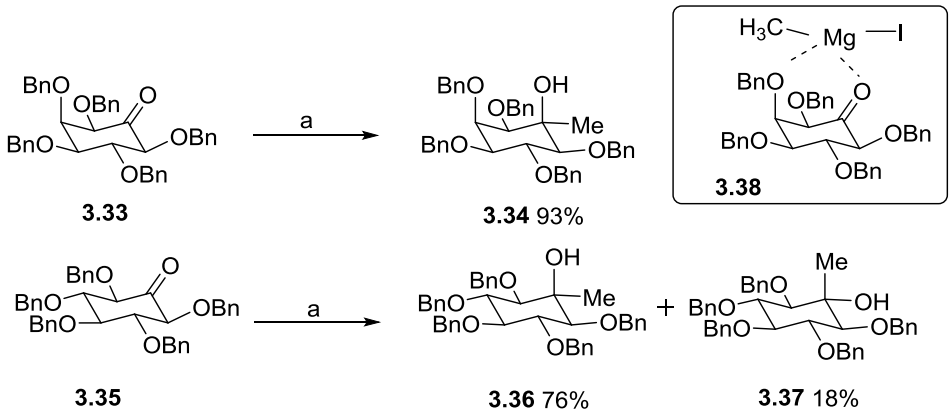

Scheme 7. MeMgI, THF, 0 °C-ambient temp

Hence we undertook the work described in this chapter to understand if the high selectivity observed during reactions of inososes carrying a 1,3-acetal bridge is due to chelation effects or due to any role played by the 1,3-acetal bridge. The latter possibility arises since the presence of 1,3-acetal bridge in an inositol derivative

imparts certain amount of rigidity to the molecule, although not as much rigidity imparted by the presence of an orthoester in *myo*-inositol-1,3,5-orthoesters. Accordingly the rest of this chapter describes and compares the results of sodium borohydride reduction and Grignard reactions of inososes containing a 1,3-acetal and the corresponding inositol derivative devoid of 1,3-acetal bridge.

3.2. Results and Discussion

Previous work in our laboratory had shown that the addition to inositol derived ketones containing a 1,3-acetal bridge led to the formation of the corresponding *neo*-inositol derivative as the single product (Scheme 8) . Since these ketones can in principle exist in three conformations, it was not obvious to conclude that the observed selectivity in product formation was due to the presence of the 1,3-acetal bridge in these molecules.

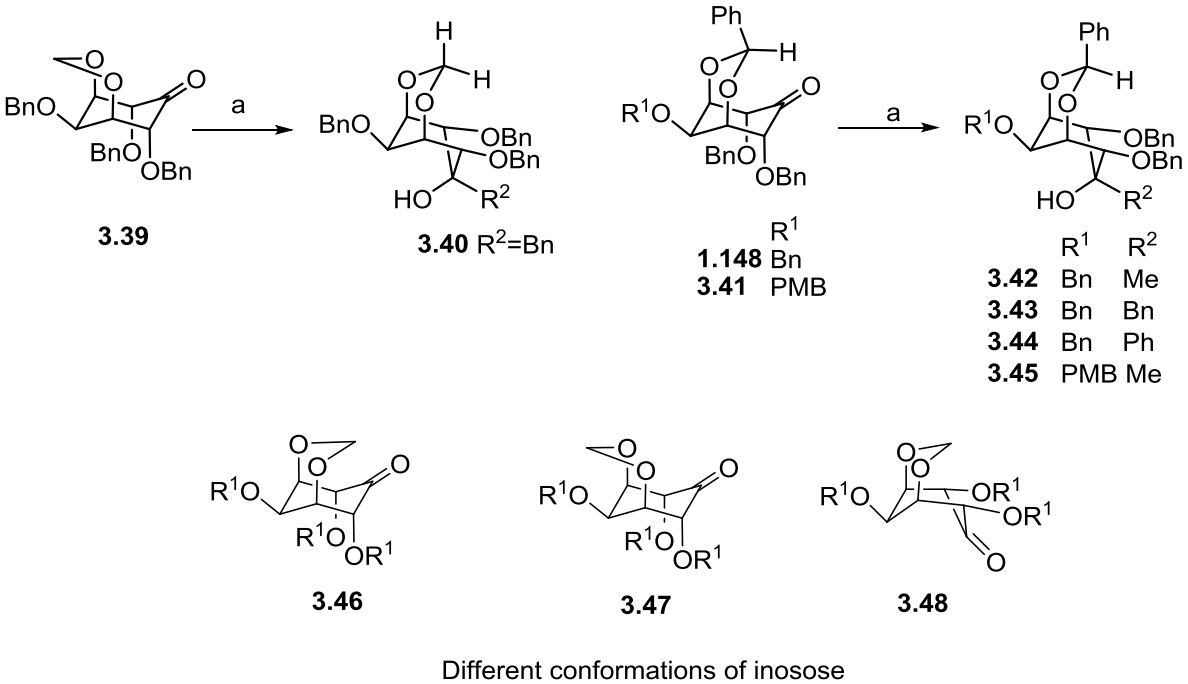

Scheme 8. (a) Diethyl ether, R^2MgBr, -10 °C, 2 h, 90-94%

Hence in order to ascertain the role of the 1,3 acetal bridge, the ketone without the 1,3 acetal bridge was prepared and subjected to hydride reduction as well as Grignard reaction (Scheme 9).

The penta-protected inosose **3.53** was prepared from *myo*-inositol *via* its orthoformate **1.66**. All the three hydroxyl groups in **1.66** were benzylated using sodium hydride and

benzyl bromide. The tribenzyl ether **1.76** was subjected to reductive cleavage with DIBAL-H to release the C5-hydroxyl group. The monohydroxyl derivative **1.150** was converted to its allyl ether **3.49**. Acid hydrolysis of the acetal in **3.49** afforded the diol **3.50**, which was O-benzylated to obtain the pentabenzyl ether **3.51**. Cleavage of the allyl ether followed by oxidation with IBX gave the pentaprotected ketone **3.53** (without the 1,3-acetal bridge).

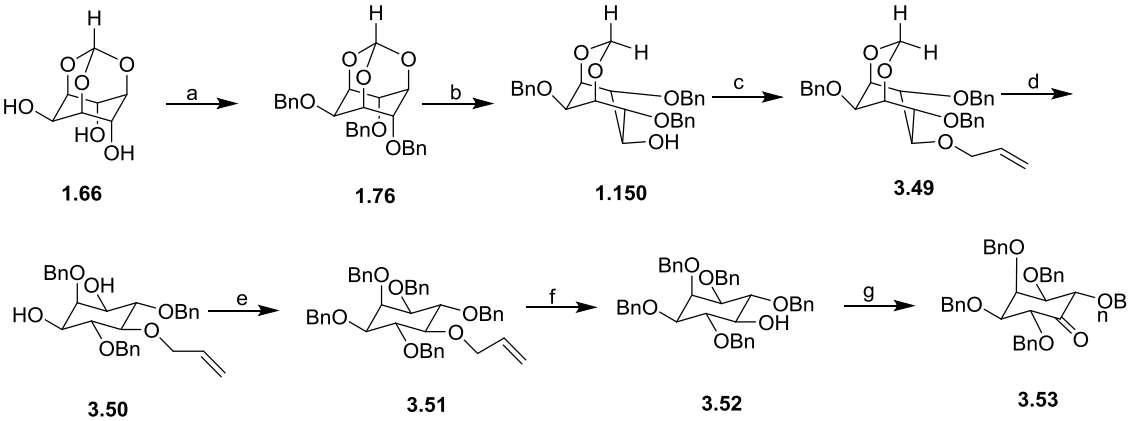

Scheme 9. (a) DMF, NaH, BnBr, RT, 3 h, 92%; (b) DCM, DIBAL-H, 0 °C - RT, 90%; (c) DMF, NaH, AllBr, RT, 3 h, 92%; (d) HCl, MeOH, 12h; (e) DMF, NaH, BnBr, RT, 3 h, 82% over 2 steps; (f) ethanol, anhy. K_2CO_3, $Pd(PPh_3)_4$, reflux, 48h, 86%, (g) EtOAc, IBX, 6h, 96%.

However the cleavage of the allyl ether in the hexaprotected *myo*-inositol derivative **3.51** proved to be a task more onerous than we had anticipated. The steric crowding in the molecule hindered easy access to the allyl group. Various experimental conditions attempted for the cleavage of the allyl ether in **3.51** are shown in Table 1.

Oxidative conditions (entries 1, 2, 5).[12] resulted in a mixture of products, perhaps due to concomitant cleavage of both the allyl and benzyl ethers in **3.51**. Separation of the required product from this mixture did not appear to be practical. The allyl ether in **3.51** could not be isomerized to the corresponding vinyl ether (to enable acid hydrolysis) under strongly basic conditions (entry 4).[13] Isomerization of the allyl ether could however be carried out in the presence of palladium but the yields were low (entries 5 and 6).[14] Better yields were obtained for the cleavage of the allyl ether in **3.51** in the presence of palladium chloride in acetic acid, but the yields were not consistent (entry 7).[15]The allyl ether in **3.51** also resisted cleavage with sodium borohydride in the presence of lithium chloride as well as with *N*-bromosuccinimide.[16, 17] Fortunately, the allyl ether in **3.51** could be cleaved with $Pd(PPh_3)_4$ to obtain the C5-alcohol **3.52** in good isolable yield.

Table 1. A summary of the attempts to cleave the allyl group in **3.51**

Sr. No	**CONDITIONS**	**RESULTS** (Yields are with respect to **3.51**)	**REFERENCE**
1.	*i*-PrOH, 20% $Pd(OH)_2$(0.2eq), Pd/ C (10%) (0.2eq), reflux 19h	Complex mixture indicating debenzylation	12
2.	i-PrOH, 20% $Pd(OH)_2$(0.2eq), reflux 2h	Complex mixture indicating debenzylation	12
3.	CH_3COCH_3: H_2O, (10:1), N-bromosuccinimide (1.2eq), 70 minutes 0-5 °C	Complex mixture indicating debenzylation	16
4.	a) DMSO, potassium *tert*-butoxide, 20h, 100 °C , b) H+,Acetone ,	No reaction	13
5.	MeOH+H_2O, Pd/C (10%), 0.3eq p-TSA	55% isolated from a complex mixture	14
6.	*i* -PrOH, Pd/C (10%), 0.3eq p-TSA	40%, isolated from a complex mixture	Modification of ref 14
7.	$PdCl_2$ (1.5) NaOAc (6eq) 95% AcOH, temperature varied from RT-100 C, 6h to 42h .	60- 80% yield but inconsistent results.	15
8.	LiCl (2.2eq), $NaBH_4$ (1.1eq), 0 to RT , 24 h.	No reaction	17

Crystals of the allyl ether **3.51** as well as the pentabenyl ether **3.52** suitable for single crystal X-ray diffraction studies could be obtained after arduous trials to shed light on them (Figure 1). The molecular structure of **3.51** in its crystal revealed crowding of the benzyl ethers near the allyl ether moiety. Hence it is likely that the heavy substitution in **3.51** masks the allyl ether and prevents its facile cleavage.

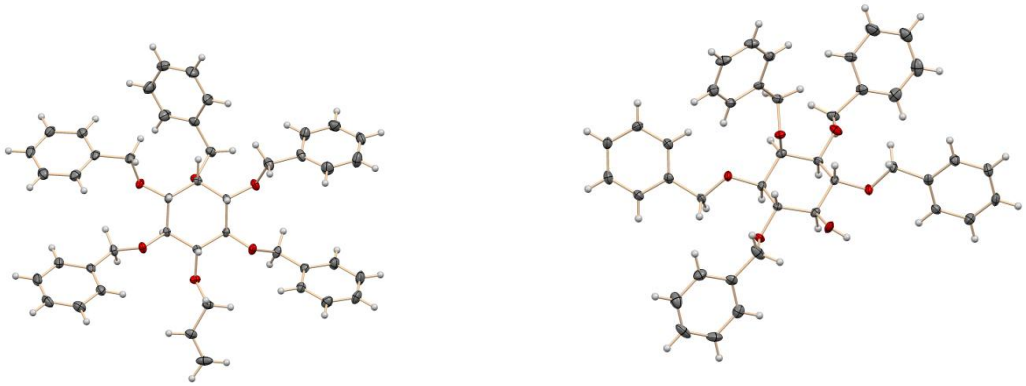

(a) (b)

Figure 1. ORTEP of (a) **3.51** (b) **3.52**. Thermal ellipsoids are drawn at 50% probability level. Hydrogen atoms are depicted as small spheres of arbitrary radii.

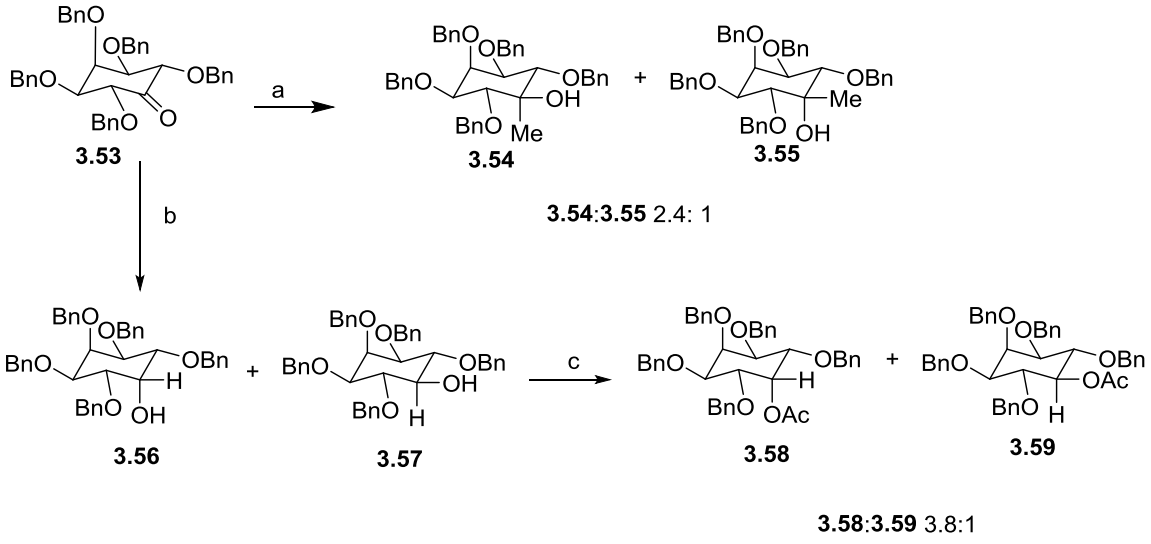

Scheme 10. (a) Toluene, MeMgI, RT, 1h, (b) MeOH, $NaBH_4$, reflux, 24h; (c) Pyridine, Ac_2O, DMAP, 48h, RT.

Grignard reaction of the *myo*-inososе derivative **3.53** gave a mixture of the corresponding *myo*- and *neo*-inositol derivatives. The mixture of the products was analysed by ^1H NMR spectroscopy.

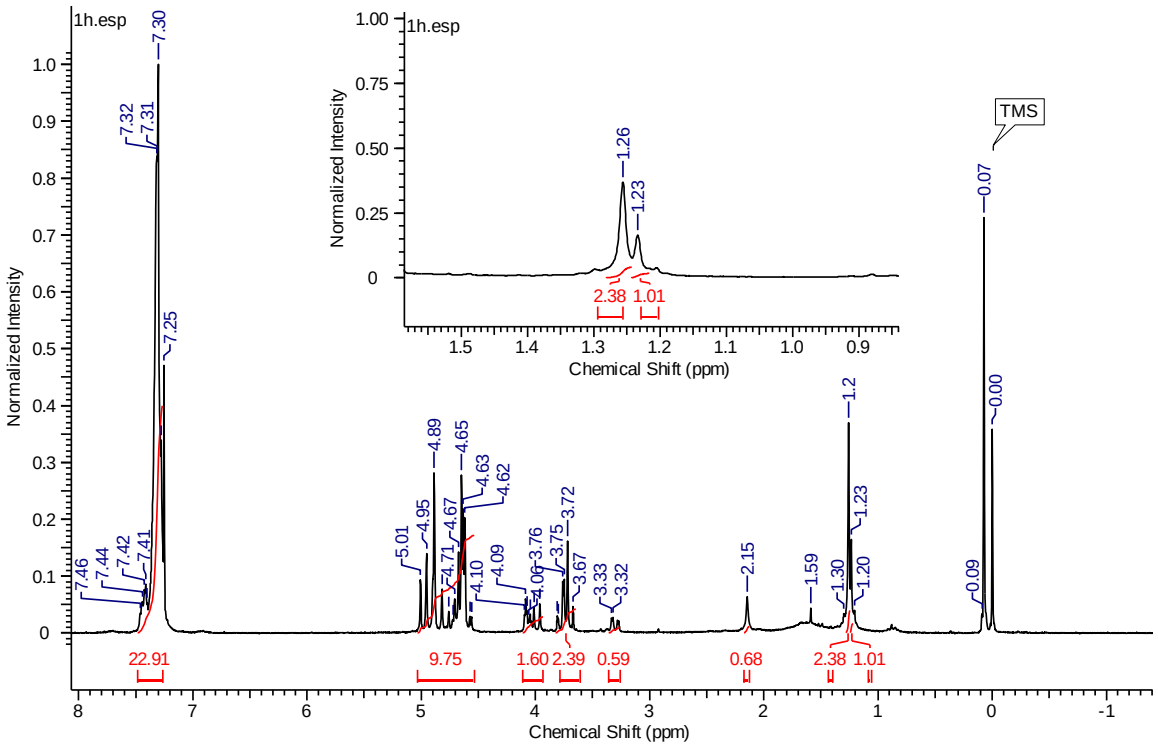

Figure 2. ^{1}H NMR spectrum of mixture of **3.54** and **3.55** in ($CDCl_3$).

From previous reports [11] in our laboratory it was clear that the axial methyl group appears downfield relative to the methyl group at the equatorial position (in inositol derivatives). The spectrum (Figure 2) shows two peaks, at δ1.26 corresponding to the axial methyl group and the other at δ1.23 corresponding to the equatorial methyl group. Although this assignment is not confirmed by other supporting data, it is sufficient to show that a mixture of two isomeric products resulted on C-methylation of the inososе **3.53**.

Hydride reduction of the *myo*-inososе derivative **3.53** gave a mixture of the corresponding *myo*- and *neo*-inositol derivatives (Scheme 10).

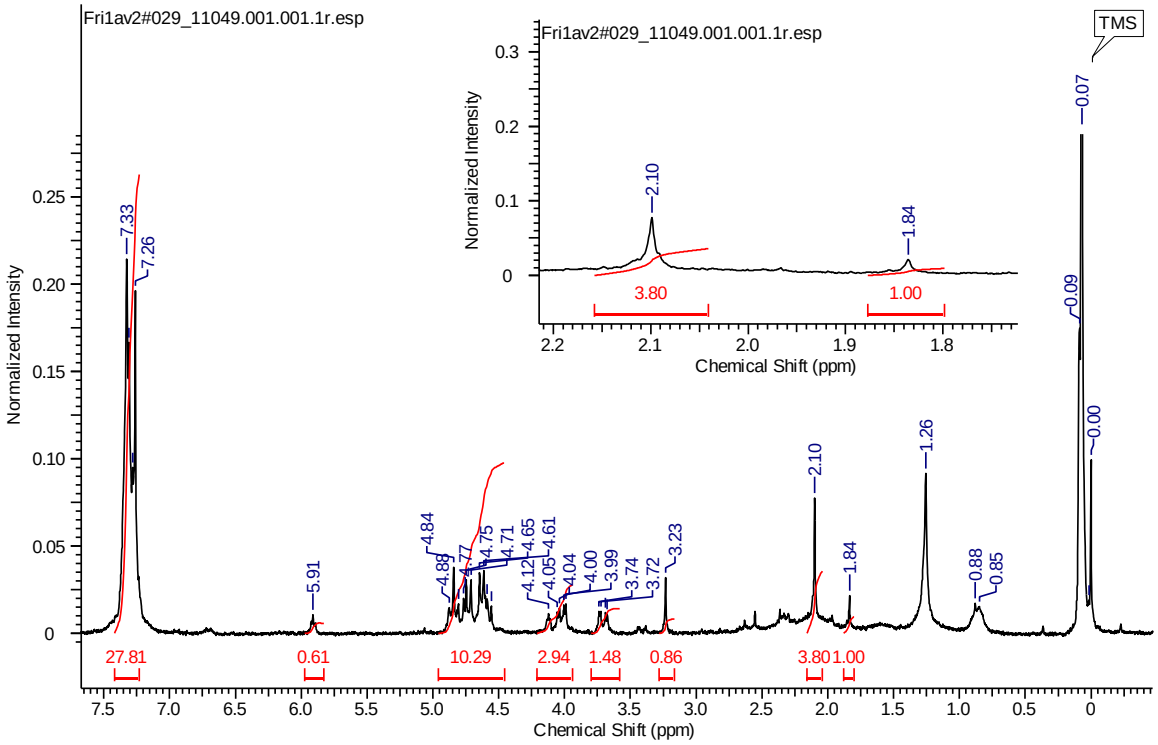

Figure 3. ^{1}H NMR spectrum of mixture of **3.58** and **3.59** in ($CDCl_3$)

The axial acetate protons (*neo*-isomer **3.58**) also appears downfield at δ2.10 whereas the equitorial acetate protons (*myo*-isomer **3.59**) appears at δ1.84.[18] (Figure 3)The results described above (on comparison with earlier reports)[18] as in Scheme 10 conclusively established the role of the acetal bridge in directing selective addition to the carbonyl group. However it is not unlikely that chelation of the metal ion (in the reducing agent or the Grignard reagent) with the inososе containing the 1,3-acetal bridge contributes to control the selectivty in these nucleophilic addition to the inososе carbonyl group. Since this aspect cannot be easily ascertained by experiment, we carried out DFT calculations on certain model systems to get better insight into this aspect.

A comparison of the result of hydride reduction of inososes and other cyclohexanones containing a β-hydroxyl group (or its protected derivative) revealed that the selectivity towards the formation of the 1,3-diaxial alcohol was better when the β-substituent was in the axial orientation.[18] The equatorial orientation of the β-substituent generally led to decrease in the selectivity towards the formation of the 1,3-diaxial diol.

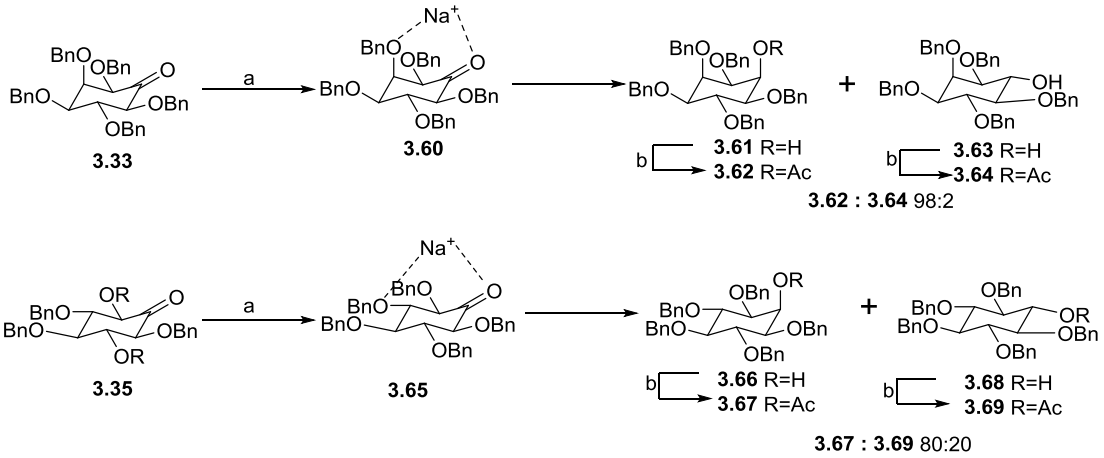

Scheme 11. (a) $NaBH_4$, DCM/MeOH, 0 °C-RT , 30 min; (b) pyridine, Ac_2O, DMAP, reflux, 20 h.

Earlier reports on the complexation of inositols with metal ions reveal that the cyclitols which have a sequence of three hydroxyl groups in the axial-equatorial-axial arrangement (as in *epi*-inositol) are better at forming metal ion complexes.[19-21]These results taken together implied the possibility of the complexation of the metal ion in the hydride reducing agent with the hydroxyl ketone being a factor in deciding the observed selectivity (as in the scheme 11). When the β-substituent is equatorial, the intramolecular distance between oxygen atoms seems to be relatively large and hence the stability of the resulting chelate is relatively less, leading to loss of selectivity during product formation. Hence, a computational study was undertaken on model systems as shown in Scheme 12. The starting hydroxyl ketone, all the possible chelated intermediates were geometry optimized using DFT calculation. The results are tabulated in Figure 4.

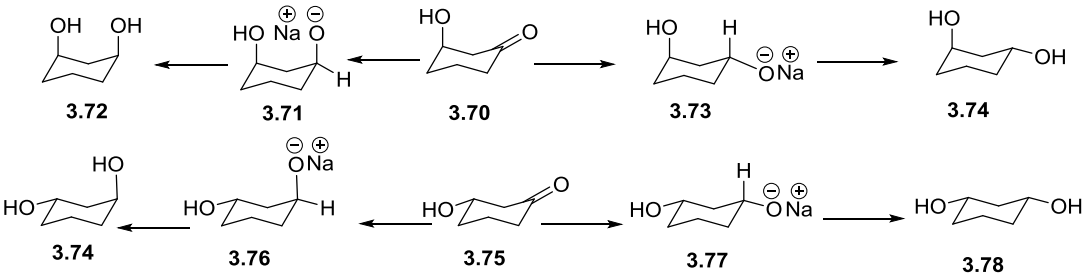

Scheme 12. Hydride reduction of the 3-hydroxy ketones **3.70** and **3.75**

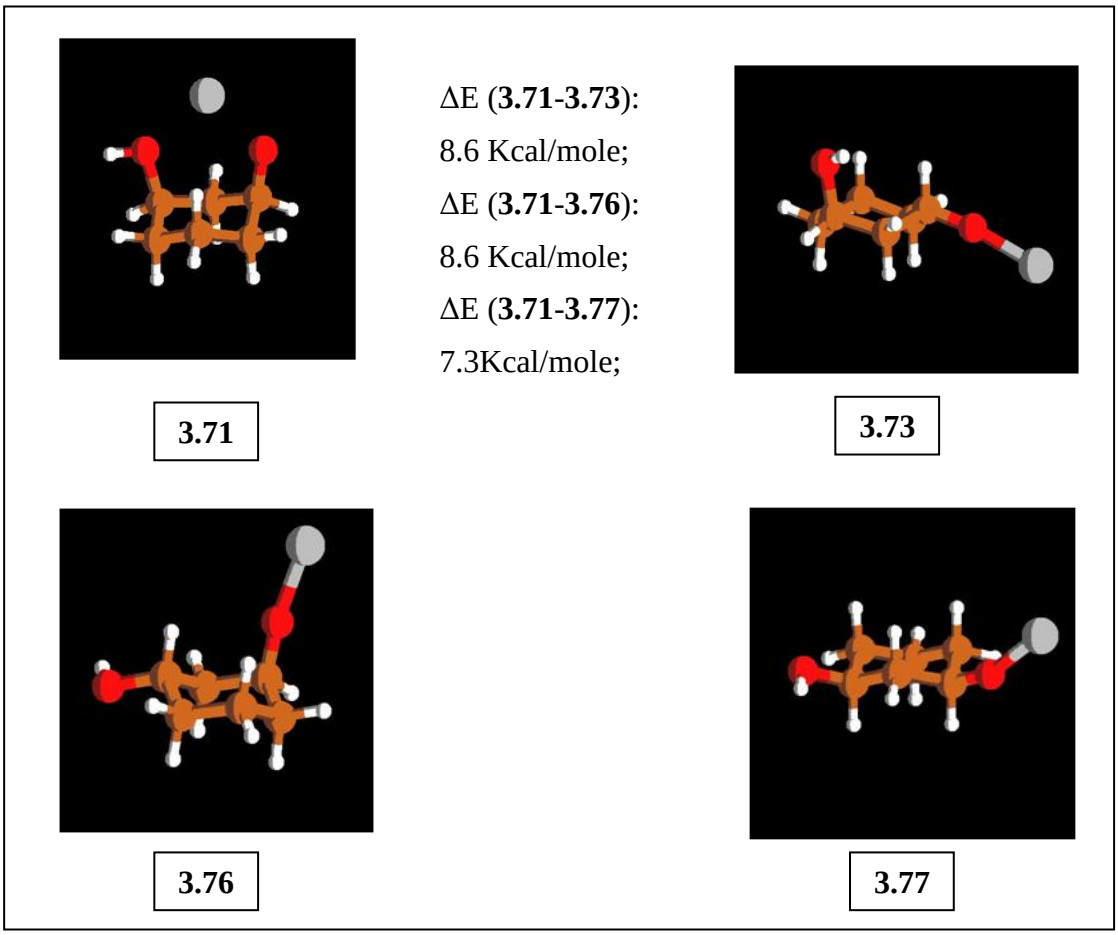

Figure 4. The optimized geometries for the intermediate Na^+ complexes **3.71**, **3.73**, **3.76** and **3.77**. The energy difference ΔE represents the relative stability of the complexes.

Hence the stability and therefore the probability of the involvement of the chelate **3.71** is higher as compared to **3.73**, **3.76**, and **3.77**.

Grignard reaction of protected *epi*- and *scyllo*-inososes with methyl magnesium iodide (Scheme 7) resulted in the formation of the C-methyl *epi*-inositol derivative and a diastereomeric mixture of C-methyl *myo*- and *scyllo*-inositol derivatives respectively.[11]

The product selectivity observed in these reactions are similar to those obtained for the hydride reduction of the inososes (Scheme 11). These results suggest that the orientation of the β-hydroxyl group in inososes affect the stereochemistry of addition of carbon nucleophile to the carbonyl group in inososes. Hence a similar study of geometry optimization was undertaken with regard to Grignard reaction on model systems shown in Scheme 13. The results are shown in Figure 5.

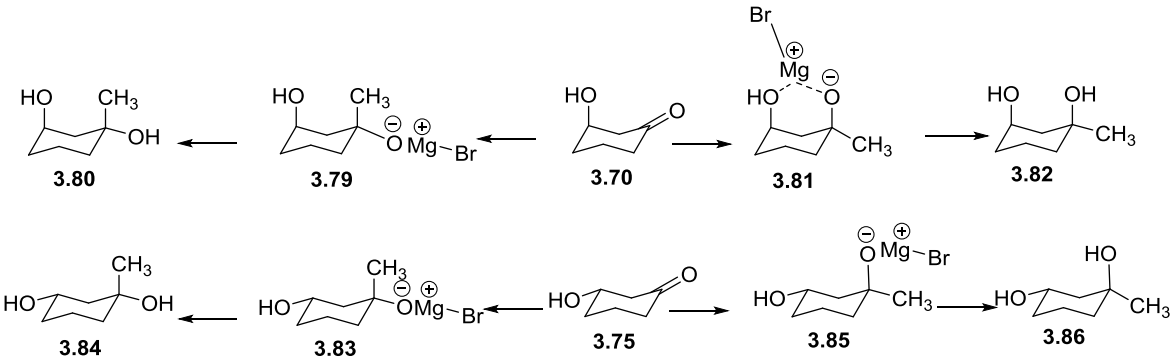

Scheme 13 . Grignard addition to the 3-hydroxy ketones **3.70** and **3.75**

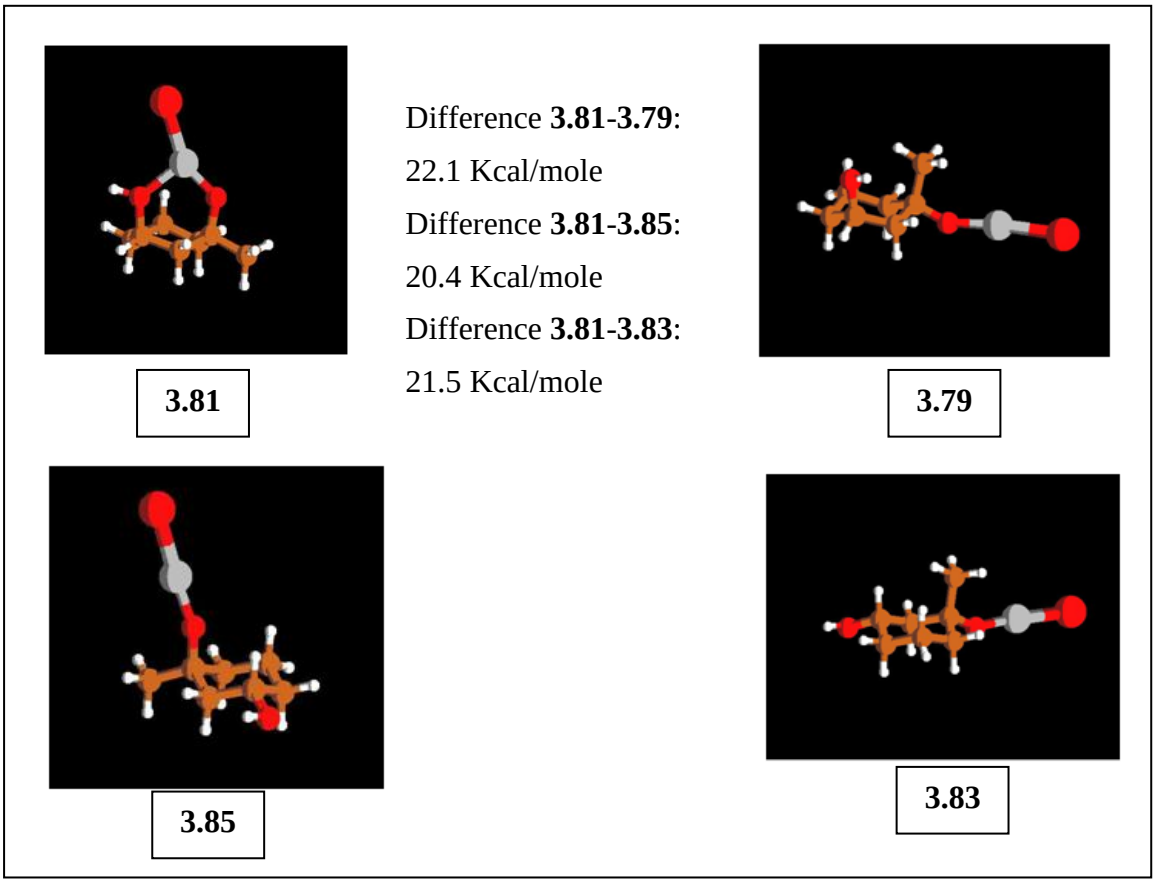

Figure 5. The optimized geometries for the MeMgBr complexes **3.81**, **3.79**, **3.85**, and **3.83**. The energy difference ΔE represents the relative stability of the isomeric complexes.

The stability and probability of the involvement of the chelates **3.81** during the Grignard reaction is higher as compared to **3.79**, **3.83** and **3.85**.

Results of the DFT calculations support the involvement of metal ion chelates during the sodium borohydride reduction and the Grignard reaction of inososes containing the 1,3-acetal bridge (since in these ketones an axial β-alkoxyl moiety is present).

This could be a major factor in deciding the stereoselectivity of nucleophilic addition to these inososes. The findings of the computational study are in concurrence with the experimental results. Hence it is likely that the observed selectivity in the reaction of inososе derivatives containing the1,3-acetal bridge is a consequence of conformational change forced by the 1,3-acetal bridge (which places an axial alkoxyl group β- to the reacting keto group as in **3.39**, Scheme 8).

3.3. Conclusions

A comparative study of the hydride reduction and Grignard reaction of inososes with and without the *1,3*-acetal bridge reveals the role played by the acetal bridge in directing the product selectivity. Hence inositol derivatives with the *1,3*-acetal bridge could be superior intermediates in synthetic protocols aiming to prepare inositol derivatives.

3.4. Experimental

3.4.1. X-ray Data (Collection, Structure Solution and Refinement)

For compound **3.51 s**ame as in the subsection **2.4.1** (Chapter 2).

X-ray intensity data measurements of **3.52** were carried out on a Bruker D8 VENTURE Kappa Duo PHOTON II CPAD diffractometer equipped with Incoatech multilayer mirrors optics. The intensity measurements were carried out with Mo micro-focus sealed tube diffraction source (Mo-Kα = 0.71073 Å). The X-ray generator was operated at 50 kV and 1.4 mA. A preliminary set of cell constants and an orientation matrix were calculated from three sets of 12 frames. Data were collected with *Z* scan width of 0.5° at different settings of *M* and *Z* with a frame time of 30 secs keeping the sample-to-detector distance fixed at 5.00 cm. The X-ray data collection was monitored by APEX3 program (Bruker, 2016).[22] All the data were corrected for Lorentzian, polarization and absorption effects using SAINT and SADABS programs (Bruker, 2016). SHELX-97 was used for structure solution and full matrix least-squares refinement on F^2.[23]

3.4.2 Computational details

Same as in the subsection **2.4.2** (Chapter 2).

3.4.3 General Experimental Methods

Same as in the subsection **2.4.3** (Chapter 2).

1,3-*O*-Methylidene-2,4,6-tri-*O*-5-*O*-allyl-*myo*-inositol (3.49): To an ice cooled solution of 4.835 g (10.4 mmoles) of **1.150** was in 6 mL DMF , 1.123 g (46.8 mmoles) of sodium hydride and 4 mL (46.8 mmoles) of allyl bromide was added and stirred subsequently for 3 hour at ambient temperature. Ice was added to the reaction mixture and solvents were removed under reduced pressure and the residue worked up with ethyl acetate, dried over anhydrous sodium sulphate. The solvent was removed under reduced pressure to obtain **3.49**. The crude product was purified by column chromatography (eluent 15% ethyl acetate in light petroleum, silica 100-120 mesh) to afford **3.49** (4.793 g, 92 % yield) as a gum. TLC *Rf* = 0.5 in 20% ethyl acetate in light petroleum).

Data for **3.49**: **IR** (Chloroform): *v* 3100–2900 cm^{-1}; **^{1}H NMR** (200MHz ,$CDCl_3$) δ = 7.44 - 7.25 (m, 15 H), 6.04 - 5.74 (m, 1 H), 5.33 - 5.05 (m, 3 H), 4.82 (d, *J* = 5.6 Hz, 1

H), 4.74 - 4.51 (m, 6 H), 4.26 (s, 2 H), 4.13 m, 2 H), 3.91 (d, *J* = 5.6 Hz, 2 H), 3.84 (t, *J* = 2.0 Hz, 1 H), 3.55 (t, *J* = 5.6 Hz, 1 H) ppm; **^{13}C NMR** (50MHz , $CDCl_3$) δ = 137.8(C_{arom}), 135.0(C_{arom}), 128.5(C_{arom}), 127.9(C_{arom}), 127.9(C_{arom}), 117.1 (CH_2), 85.5 (CH_2), 82.1(Ins C), 80.0 (Ins C), 72.6 (Ins C), 72.1 (*C*H_2), 71.9 (*C*H_2), 71.0 (*C*H_2O), 70.3 (Ins C) ppm; **HRMS**: *m*/*z* calcd for $C_{31}H_{35}O_6$: 503.2434 [*M*+H^+]; found: 503.2433.

1,2,3,4,6-penta-*O*-benzyl-5-allyl-*myo*-inositol (3.51):The acetal **3.49** (1.964 g, 3.8 mmoles) was dissolved in MeOH (12 mL) and conc. HCL (7 mL) and refluxed for 12 h. The acid was neutralized with solid $NaHCO_3$, the solvent was removed under reduced pressure to yield **3.50**. The solvents were removed in vacuo and the compound was dried thoroughly to exclude moisture. The cakey white solid was then used in the next step without further purification as **3.50** was observed to be water soluble on preliminary trials of this reaction. To the crude diol **3.50** in dry DMF (15 mL), NaH (0.3782 g, 9.455 mmol), benzyl bromide (1.1 mL, 9.455 mmol), were added at 0° C and then stirred at RT for 2 h. Ice was added to the reaction mixture and solvents were removed under reduced pressure and the residue worked up with ethyl acetate, dried over anhydrous sodium sulphate. The solvent was removed under reduced pressure to obtain **3.51**. The crude product was purified by column chromatography (eluent 15 % ethyl acetate in light petroleum, 100-200 mesh) to afford **3.51** (1.864 g, 82%)as a solid. TLC *Rf* = 0.3 (in 25% ethyl acetate in light petroleum.) TLC *Rf* = 0.3 (in 20% ethyl acetate in light petroleum.)

Data for **3.51**: **M.p**. 87-89 °C (Crystallized from chloroform and benzene);**IR** (Chloroform): *v* 3350 cm-^{1}; **^{1}H NMR** (200MHz ,$CDCl_3$) δ = 7.46 - 7.19 (m, 26 H), 6.12 - 5.81 (m, 1 H), 5.35 - 5.06 (m, 2 H), 4.94 - 4.75 (m, 6 H), 4.72 - 4.50 (m, 4 H), 4.35 (d, *J* = 5.6 Hz, 2 H), 4.10 - 3.92 (m, 3 H), 3.40 - 3.22 (m, 3 H) ppm; **^{13}C NMR** (50MHz , $CDCl_3$) δ = 138.9(C_{arom}), 138.4(C_{arom}), 135.3(CH_2=*C*H), 128.3 (C_{arom}), 128.1 (C_{arom}), 127.7 (C_{arom}), 127.5(C_{arom}), 127.3 (C_{arom}), 116.5 (CH_2), 83.5 (Ins C), 81.6 (Ins C), 80.8 (Ins C), 75.9 (CH_2), 74.6 (CH_2), 74.4 (Ins C), 74.1 (CH_2), 72.8 (CH_2) ppm. **HRMS:** *m*/*z* calcd for $C_{44}H_{47}O_6^+$: 671.3367 [*M*+H^+]; found: 671.3371.

1,2,3,4,6-penta-*O*-benzyl-*myo*-inositol (3.52): To a solution of **3.51** (0.112g, 0.167mmoles) and 0.276g (2mmol) of anhydrous potassium carbonate in degassed ethanol (3 mL) , tetrakis triphenylphosphine palladium was added in 2 parts (0.045g

each time), 8 hours apart. The reaction mixture was refluxed for 48 hours. solvents were removed under reduced pressure and the residue worked up with 2N HCl, ethyl acetate and dried over anhydrous sodium sulphate. The solvent was removed under reduced pressure to obtain **3.52**. The crude product was purified by column chromatography (eluent 7% ethyl acetate in light petroleum, silica 100-120 mesh) to afford **3.52** (0.092 g, 86 % yield) as a white solid. TLC *Rf* = 0.3 in 15% ethyl acetate in light petroleum. 0.006 g of starting material was isolated.

Data for **3.52**:**M.p.** 182-185 °C (crystallised from benzene and dichloromethane); **IR** (Chloroform): 3360 cm^{-1}.;**^{1}H NMR** (200MHz,$CDCl_3$) δ = 7.48 - 7.27 (m, 25 H), 5.01 - 4.55 (m, 10 H), 4.17 - 3.83 (m, 3 H), 3.62 - 3.28 (m, 3 H), 1.97 (s, 1H, OH, D_2O exhangeable) ppm;**^{13}C NMR** (50MHz, $CDCl_3$) δ = 138.9 (C_{arom}), 138.8 (C_{arom}), 138.3 (C_{arom}), 128.3 (C_{arom}), 128.0 (C_{arom}), 127.7(C_{arom}), 127.6 (C_{arom}), 127.4 (C_{arom}), 81.1 (Ins C), 80.7 (Ins C), 75.4 (CH_2), 75.1(Ins C), 74.5(Ins C), 74.2(CH_2), 72.6 (CH_2) ppm; **HRMS**: *m*/*z* calcd for $C_{41}H_{43}O_6^+$: 631.3054 [M+H^+]; found: 631.3054

1,2,3,4,6-penta-*O*-benzyl-*myo*-inososse (3.53): To a solution of **3.52 (**0.355 g, 0.5628 mmoles) in 3 mL ethyl acetate 0.472 g (1.688 mmoles) of 2-iodoxy benzoic acid was added. The resulting solution was refluxed for 6 h. The reaction mixture was filtered through sintered glass funnel over celite and washed with ethyl acetate. The combined filtrate and washings were evaporated under reduced pressure to obtain to obtain **3.53**. The crude product was purified by column chromatography (eluent 10 % ethyl acetate in light petroleum, 100-200 mesh) to afford **3.53** 0.341g (96%) as a white solid. TLC *Rf* = 0.3 (in 20% ethyl acetate in light petroleum.)

Data for **3.53**: **M.p.** 150-152 °C; **IR** (Chloroform): 1733 cm^{-1}; **^{1}H NMR** (200MHz , $CDCl_3$) δ = 7.48 - 7.27 (m, 25 H), 4.99 - 4.86 (m, 4 H), 4.84 - 4.72 (m, 2 H), 4.70 - 4.52 (m, 6 H), 4.13 (s, 1 H), 3.47 (m, 2 H) ppm; **^{13}C NMR** (50MHz ,$CDCl_3$) δ = 203.7(C=O), 138.5 (C_{arom}), 138.2 C_{arom}), 137.9 (C_{arom}), 128.4 (C_{arom}), 128.4 (C_{arom}), 128.3 (C_{arom}), 128.1 (C_{arom}), 127.7 (C_{arom}), 127.7 (C_{arom}), 83.1 (Ins C), 79.4 (Ins C), 76.0 (Ins C), 75.0(CH_2), 73.7(CH_2), 73.5(CH_2) ppm; **HRMS**: *m*/*z* calcd for $C_{41}H_{41}O_6^+$: 629.2901 [M+H^+]; found: 629. 2898.

Reaction of methyl magnesium iodide with 3.53: To a cooled (0 °C) solution of the 0.060g (0.09 mmoles) **3.53** in dry toluene 2 mL was added a solution of MeMgI (6mmol). in diethyl ether and stirred for 1 h. The reaction mixture was diluted with

diethyl ether, washed with saturated solution of ammonium chloride, water, followed by brine and dried over anhydrous sodium sulphate. The solvent was removed under reduced to give a mixture of alcohols (**3.54** and **3.55**) 0.056 g (91%), which was analyzed by ^{1}H-NMR spectroscopy.

Reduction of 3.53 with $NaBH_4$: 0.007 g (0.0477 mmoles) $NaBH_4$ was added to a solution of 0.037 g (0.058 mmoles) of **3.53** in mixture of 1mL dichloromethane and 0.25 mL methanol and refluxed for 24 h. The reaction was quenched by adding aqueous ammonium chloride solution. The resulting mixture was concentrated under reduced pressure and the residue was worked up with ethyl acetate. The solid obtained was acetylated without further purification using pyridine 1mL , acetic anhydride (0.5mL) and DMAP (0.010 g)) at room temperature for 48 h. The reaction mixture was quenched by adding few pieces of ice, solvent was removed under reduced pressure and the residue obtained was worked up with ethyl acetate to obtain a mixture of acetates (**3.58** and **3.59**) 0.041 g (93%) which was analyzed by ^{1}H-NMR spectroscopy.

3.5. References

1. Jagdhane, R. C.; Shashidhar, M. S. *Eur. J. Org. Chem.* **2010**, 2945–2953.
2. Sarmah, M. P.; Shashidhar, M. S.; Sureshan, K. M.; Gonnade, R. G.; Bhadbhade, M. M. *Tetrahedron*, **2005**, *61*, 4437–4446.
3. Mohanrao, R.; Asokan, A.; Sureshan, K. M. *Chem. Commun*., **2014**, *50*, 6707-6710.
4. Riley, A. M.; Murphy, C. T.; Lindley, C. J.; Westwick, J.; Potter, B. V. L. *Bioorg. & Med. Chem. Lett.* **1996**, *6*, 2197-2200.
5. Riley, A. M.; Murphy, C. T.; Lindley, C. J.; Westwick, J.; Potter, B. V. L. *Bioorg. & Med. Chem. Lett.* **1996**, *6*, 2197-2200.
6. Riley, A. M.; Guédat, P.; Schlewer, G.; Spiess, B.; Potter, B. V. L. *J. Org. Chem.* **1998**, *63*, 295-305.
7. Gigg, J.; Gigg, R. *Carbohydrate Research* **1997**, *299*, 77.
8. Mondal, S.; Prathap, A.; Sureshan K. M. *J. Org. Chem.* **2013**, *78*, 7690−7700.
9. Murali, C.; Gurale, B. P.; Shashidhar, M. S. *Eur. J. Org. Chem.* **2010**, 755–764.
10. Devaraj, S.; Shashidhar, M. S.; Dixit, S. S. *Tetrahedron*, **2005**, *61*, 529–536.
11. Jagdhane, R.C.; Patil, M. T.; Krishnaswamy, S. *Tetrahedron* **2013**, *69*, 5144-5151.
12. Mart, A; Shashidhar, M. S. *Tetrahedron* **2012**, *68*, 9769-9776.
13. Gigg, J.; Gigg, R. *J. Chem. Soc. C* **1966**, 82-86.
14. Boss, R.; Scheffold, R. *Angew. Chem. Int. Ed.* **1976**, *15*, 558–559.
15. Smith III, A. B.; Fukui, M.; *Vaccaro,* H. A.; Empfield. J. R. *J. Am. Chem. Soc.* **1991**, *113*, 2071–2092.
16. RajaRam, S.; Chary, K. P.; Salahuddin, S.; Iyengar, D. S. *Synthetic Commun.* **2002**, *32*, 133–137.
17. Dim, R. R.; Melgarejo, C. R. Lopez-Espinosa, M. T. P.; Cubero, I. I. *J. Org. Chem.* **1994**, *59*, 7928-7929.
18. Patil, M. T.; Krishnaswamy, S.; Sarmah, M. P.; Shashidhar, M. S. *Tetrahedron Lett.* 2011, ***52***, 3756-3758.
19. Angyal S. J.; Davis, K. P. *J. Chem Soc. D Chem. Commun*. **1971**, 500-501.
20. Angyal S. J. *Pure Appl. Chem*. **1973**, *35*, 131-146.

21. Angyal S. J. *Aust. J. Chem*. **1972**, 25, 1957-1966.
22. Bruker (2016). *APEX3*, *SAINT* and *SADABS*. Bruker AXS Inc., Madison, Wisconsin, USA.
23. Sheldrick, G. M. *Acta Cryst*. **2008**, *A64*, 112 – 122.

Appendix II

Appendix II Index

Crystal data table for 3.51	
Empirical formula	$C_{44}H_{46}O_6$
Formula weight	670.81
Temperature	100(2) K
Wavelength	0.71073 Å
Crystal system	Monoclinic
Space group	P 21/n
Unit cell dimensions	a = 14.9056(3) Å D= 90°.
	b = 8.8063(2) Å E= 97.4800(10)°.
	c = 27.5973(7) Å J= 90°.
Volume	3591.68(14) Å^3
Z	4
Density (calculated)	1.241 Mg/m^3
Absorption coefficient	0.081 mm^{-1}
F(000)	1432
Crystal size	0.480 x 0.220 x 0.100 mm^3
Thetarange for data collection	2.430 to 26.999°.
Index ranges	-19<=h<=19,-11<=k<=11,-35<=l<=35
Reflections collected	93548
Independent reflections	7792 [R(int) = 0.0256]
Completeness to theta = 25.242°	99.3 %
Absorption correction	Semi-empirical fromequivalents
Max. and min. transmission	0.992 and 0.962
Refinement method	Full-matrix least-squares on F^2
Data / restraints / parameters	7792 / 13 / 478
Goodness-of-fit on F^2	1.062
Final R indices [I>2sigma(I)]	R1 = 0.0422, wR2 = 0.1065
R indices (all data)	R1 = 0.0450, wR2 = 0.1088
Extinction coefficient	n/a
Largest diff. peak and hole	0.748 and-0.289 e.Å^3

Crystal data table for 3.52	
Empirical formula	$C_{41} H_{42} O_6$
Formula weight	630.74
Temperature	296(2) K
Wavelength	0.71073 Å
Crystal system	Monoclinic
Space group	P 21/c
Unit cell dimensions	a = 15.817(3) Å D= 90°.
	b = 8.6655(15) Å E= 96.536(12)°.
	c = 24.054(4) Å J= 90°.
Volume	3275.5(10) Å^3
Z	4
Density (calculated)	1.279 Mg/m^3
Absorption coefficient	0.085 mm^{-1}
F(000)	1344
Crystal size	0.420 x 0.310 x 0.110 mm^3
Theta range for data collection	2.020 to 24.997°.
Index ranges	-18<=h<=15,-9<=k<=10,-28<=l<=28
Reflections collected	23154
Independent reflections	5678 [R(int) = 0.1068]
Completeness to theta = 24.997°	98.5 %
Absorption correction	Semi-empirical from equivalents
Max. and min. transmission	0.991 and 0.965
Refinement method	Full-matrix least-squares on F^2
Data / restraints / parameters	5678 / 246 / 465
Goodness-of-fit on F^2	1.024
Final R indices [I>2sigma(I)]	R1 = 0.0648, wR2 = 0.1349
R indices (all data)	R1 = 0.1064, wR2 = 0.1534
Extinction coefficient	0.0050(9)
Largest diff. peak and hole	0.525 and -0.477 e.Å^{-3}

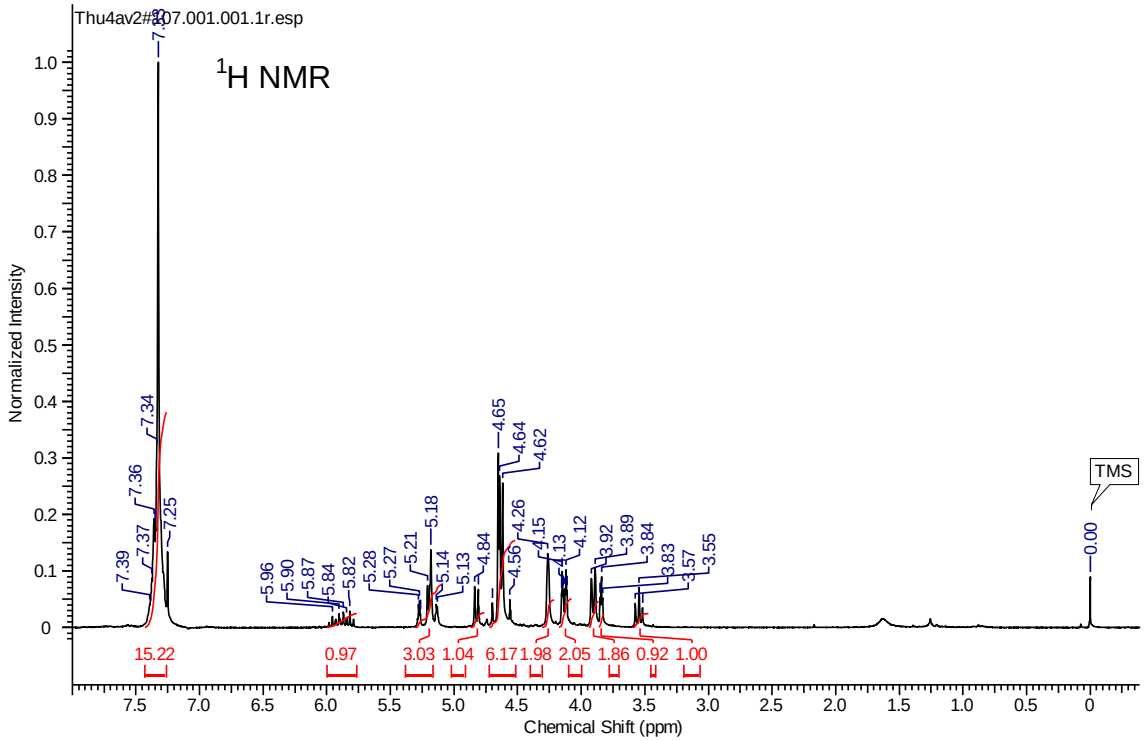
Thu4av2#207.001.001.1r.esp
1H NMR
Normalized Intensity
Chemical Shift (ppm)
TMS
15.22
0.97
3.03
1.04
6.17
1.98
2.05
1.86
0.92
1.00

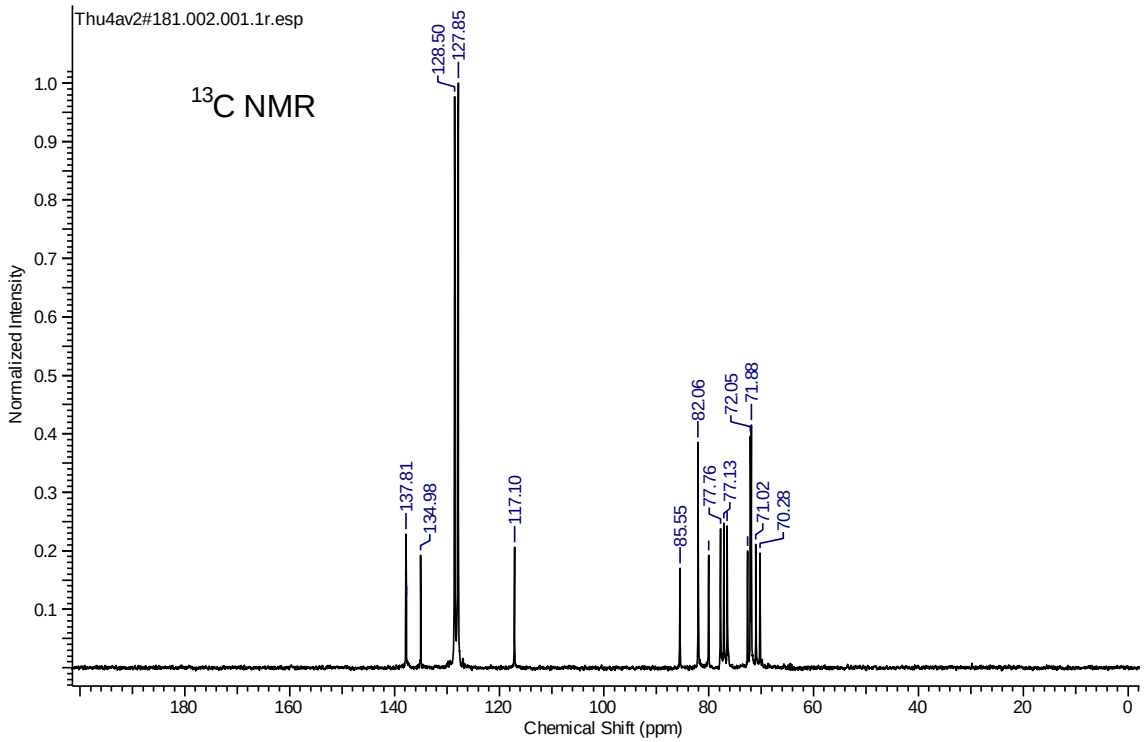
Thu4av2#181.002.001.1r.esp
13C NMR
Normalized Intensity
Chemical Shift (ppm)

DEPT

^{1}H NMR

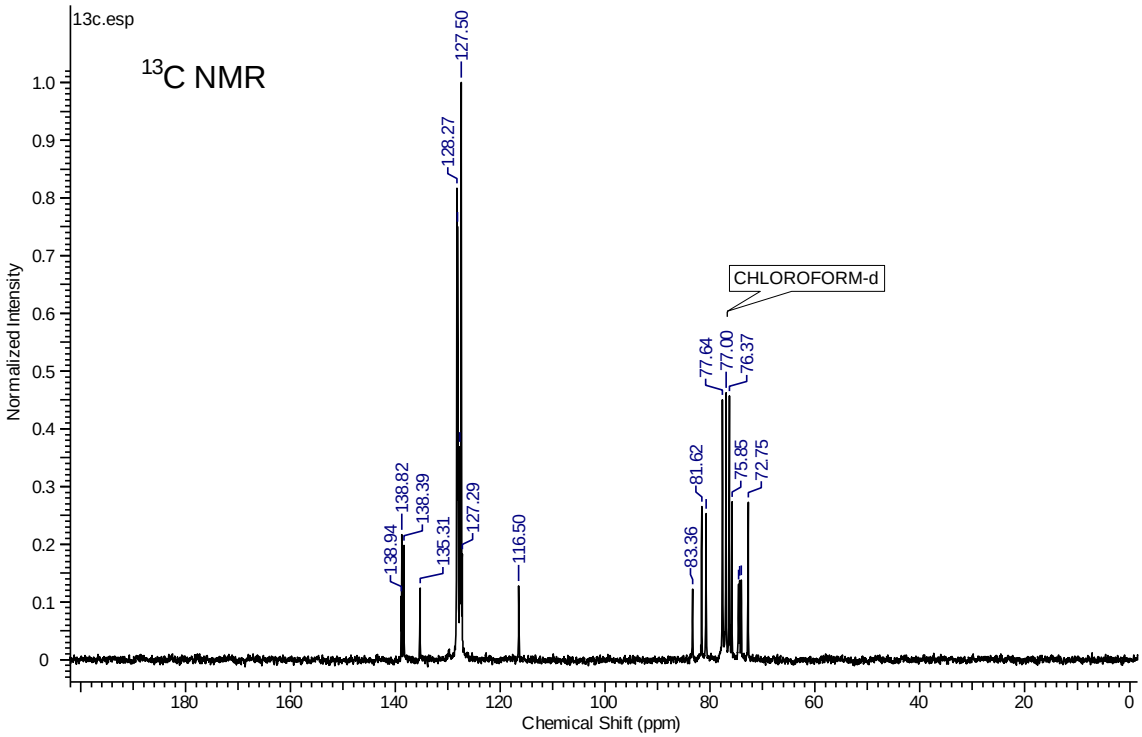
13c.esp
^{13}C NMR
127.50
128.27
CHLOROFORM-d
77.64
77.00
76.37
81.62
75.85
72.75
138.82
138.39
138.94
135.31
127.29
116.50
83.36
Normalized Intensity
Chemical Shift (ppm)

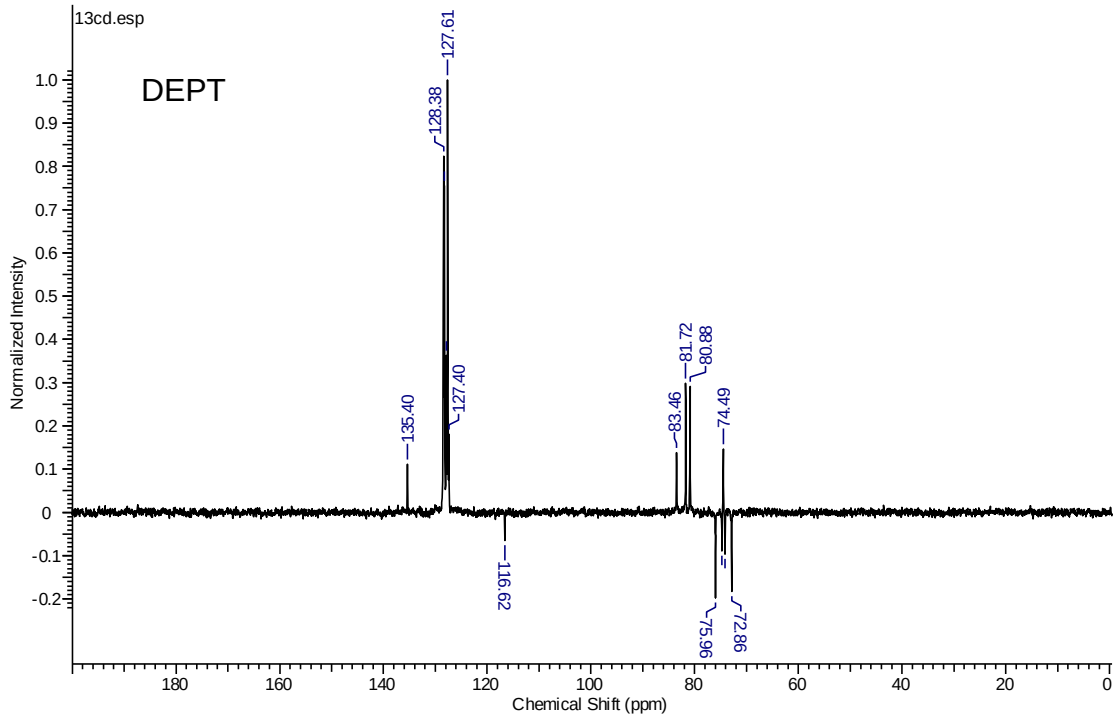
13cd.esp
DEPT
127.61
128.38
127.40
135.40
81.72
80.88
83.46
74.49
116.62
75.96
72.86
Normalized Intensity
Chemical Shift (ppm)

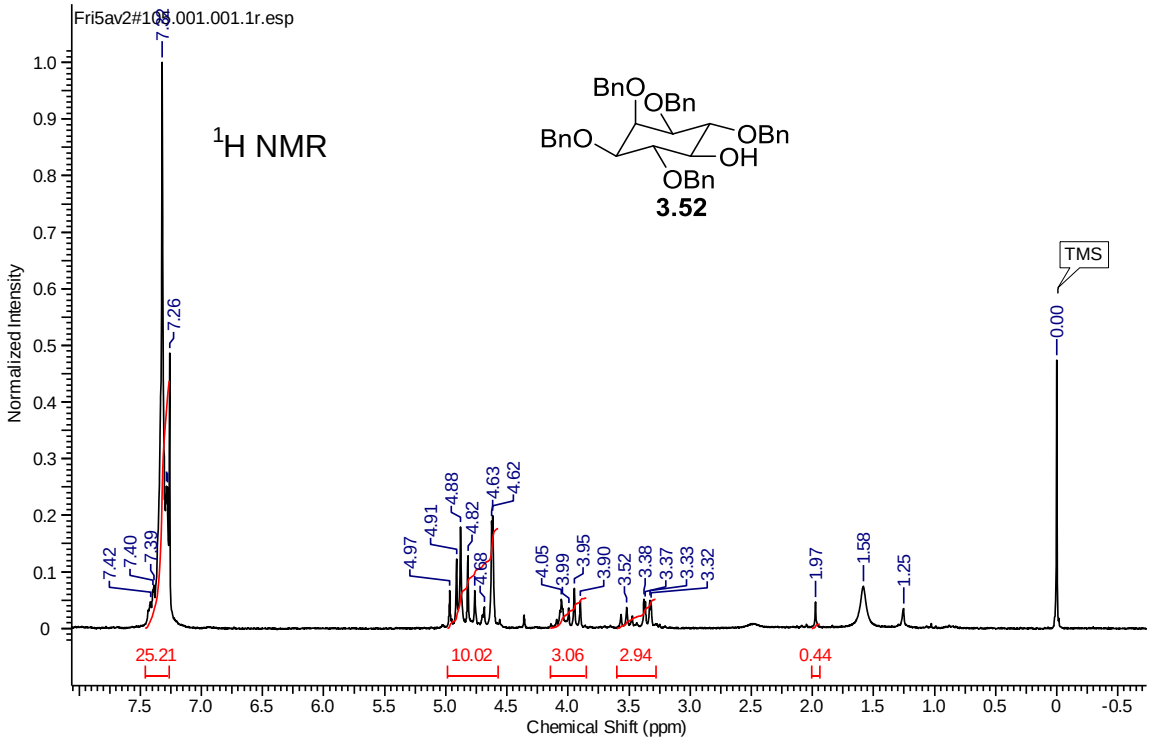
Fri5av2#105.001.001.1r.esp
^{1}H NMR
BnO
OBn
BnO
OBn
OH
OBn
3.52
TMS
Normalized Intensity
Chemical Shift (ppm)
7.42
7.40
7.39
7.26
4.97
4.91
4.88
4.82
4.68
4.63
4.62
4.05
3.99
3.95
3.90
3.52
3.38
3.37
3.33
3.32
1.97
1.58
1.25
0.00
25.21
10.02
3.06
2.94
0.44

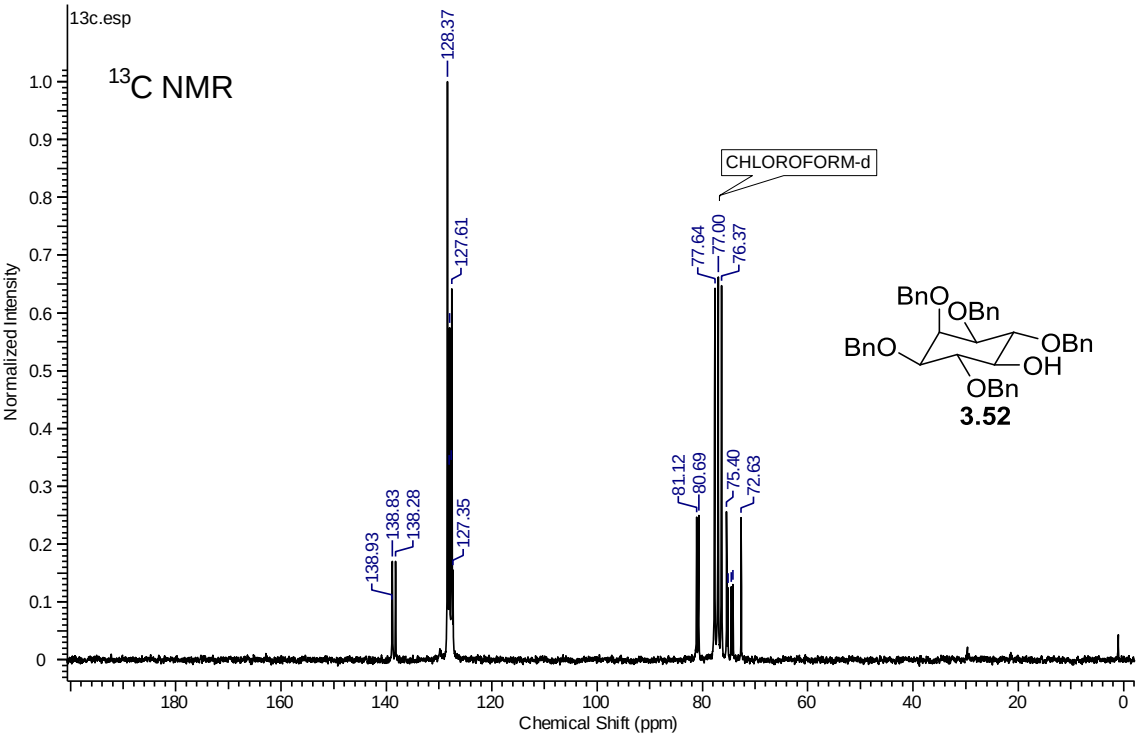
13c.esp
^{13}C NMR
CHLOROFORM-d
BnO
OBn
BnO
OBn
OH
OBn
3.52
Normalized Intensity
Chemical Shift (ppm)
128.37
127.61
127.35
138.93
138.83
138.28
77.64
77.00
76.37
81.12
80.69
75.40
72.63

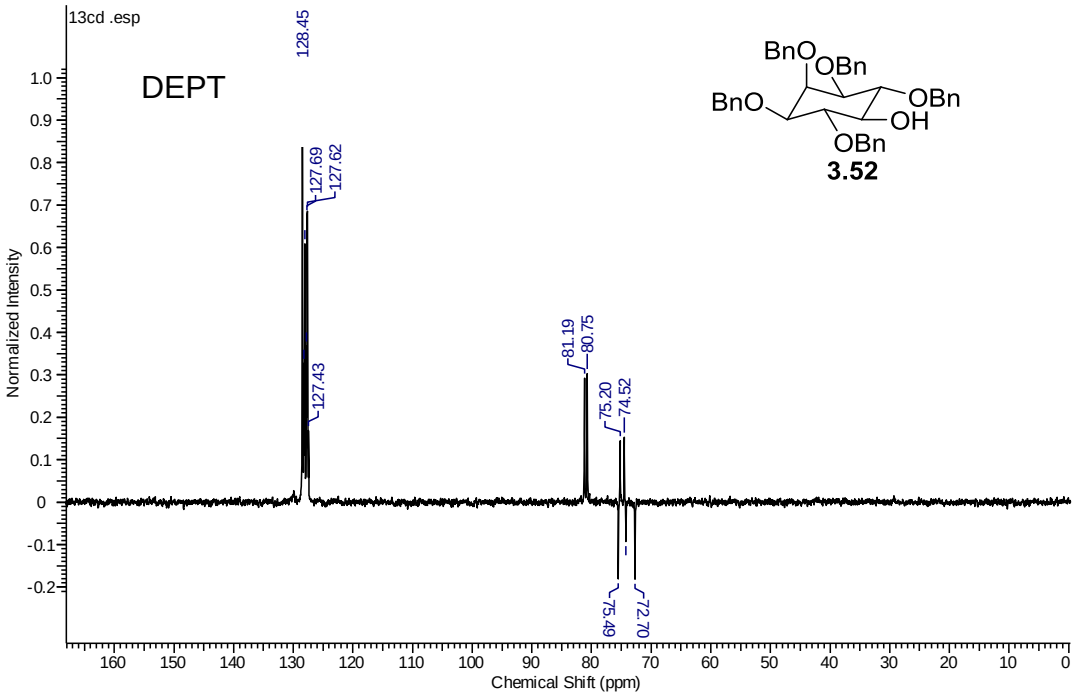
13cd .esp
DEPT
128.45
127.69
127.62
127.43
81.19
80.75
75.20
74.52
75.49
72.70
Normalized Intensity
Chemical Shift (ppm)
BnO
OBn
BnO
OBn
OH
OBn
3.52

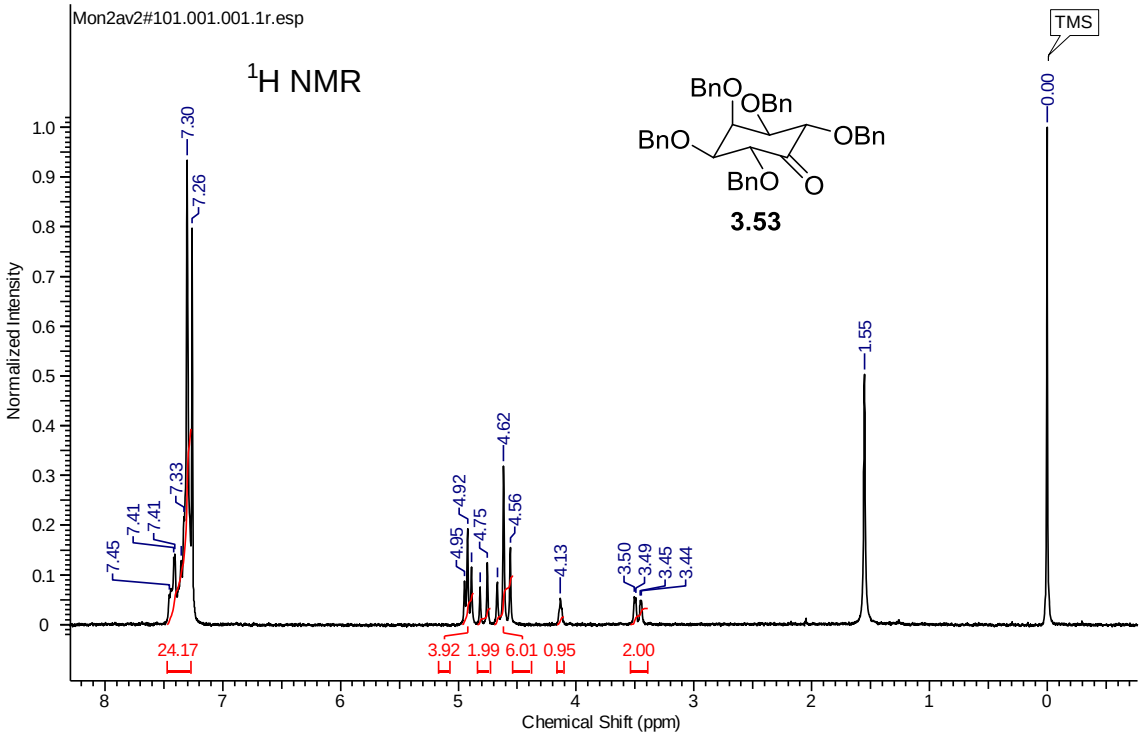
Mon2av2#101.001.001.1r.esp
1H NMR
TMS
0.00
7.30
7.26
7.45
7.41
7.41
7.33
4.95
4.92
4.75
4.62
4.56
4.13
3.50
3.49
3.45
3.44
1.55
24.17
3.92
1.99
6.01
0.95
2.00
Normalized Intensity
Chemical Shift (ppm)
BnO
OBn
BnO
OBn
BnO
O
3.53

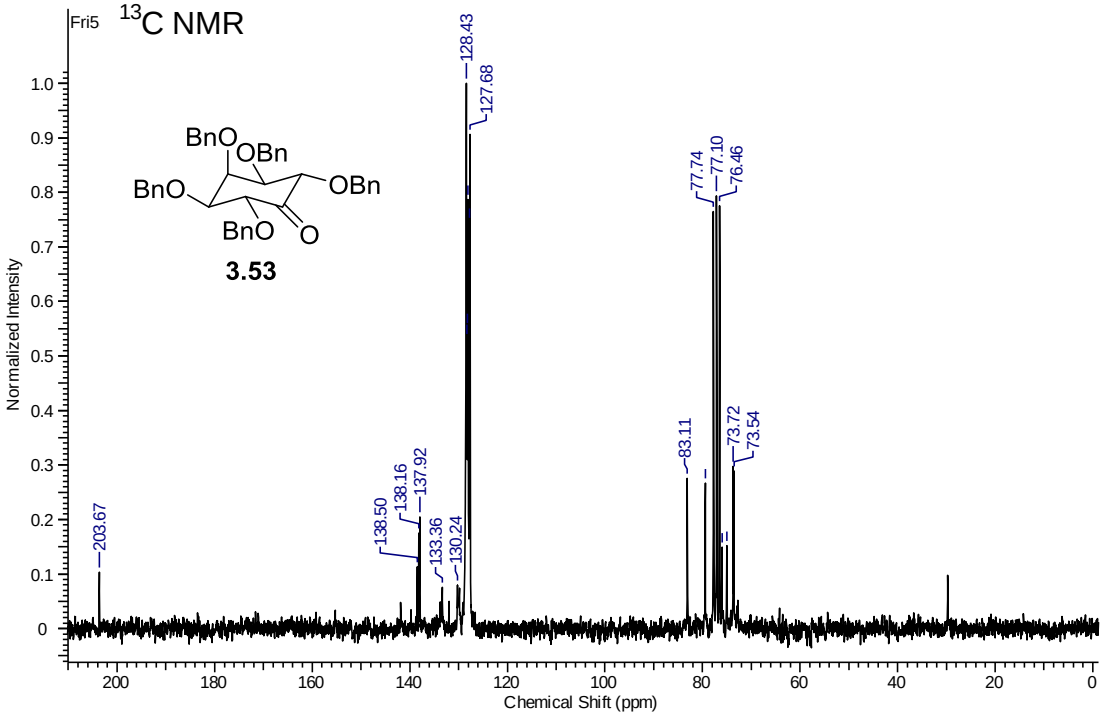
Fri5
13C NMR
BnO
OBn
BnO
OBn
BnO
O
3.53
Normalized Intensity
Chemical Shift (ppm)
128.43
127.68
77.74
77.10
76.46
83.11
73.72
73.54
203.67
138.50
138.16
137.92
133.36
130.24

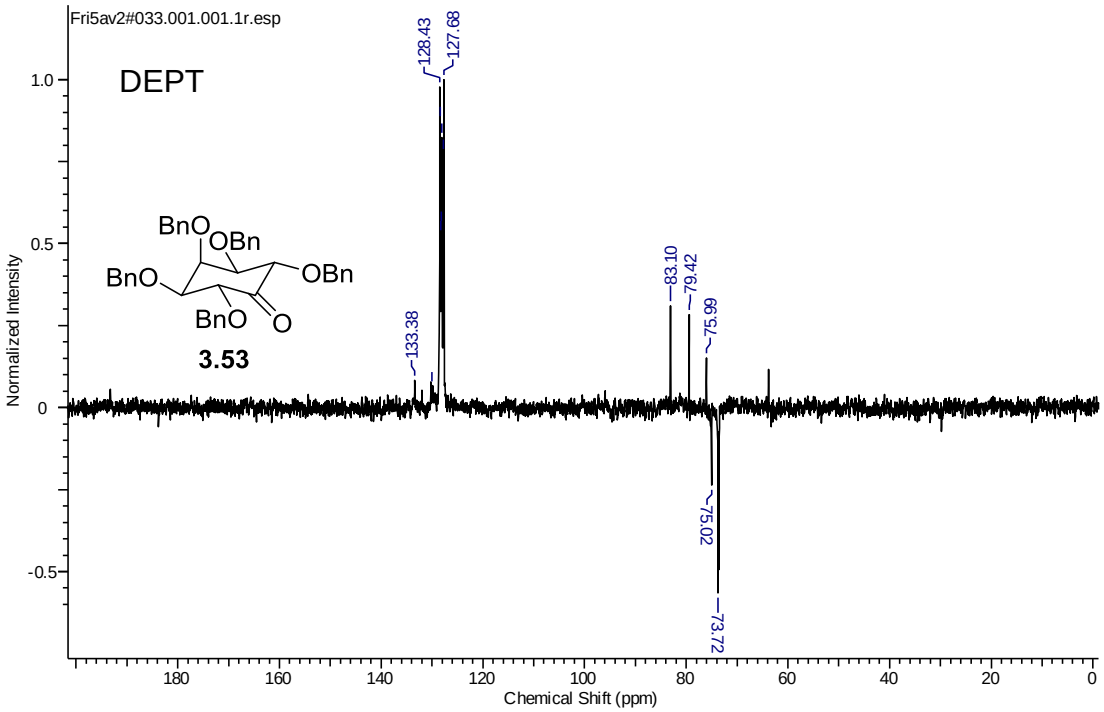
Fri5av2#033.001.001.1r.esp
DEPT
BnO
OBn
BnO
OBn
BnO
O
3.53
Normalized Intensity
Chemical Shift (ppm)
128.43
127.68
133.38
83.10
79.42
75.99
75.02
73.72

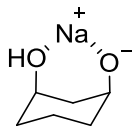

3.71

FINAL HEAT OF

FORMATION = -547.566506

C	-0.881879	-1.169990	1.539983
C	-0.229488	0.106994	1.00127
C	1.176701	0.341129	1.56485
C	1.147222	0.365113	3.09460
C	0.650285	-0.992642	3.671274
C	-0.763302	-1.282665	3.062063
O	1.558743	-1.999848	3.483624
Na	1.309934	-3.476187	2.059826
O	-0.293187	-2.366722	0.896338
H	-0.225790	0.084963	-0.104666
H	-0.882169	0.952334	1.2[illegible]2
H	1.850695	-0.470481	1.242348
H	1.587589	1.278055	1.15614
H	2.154899	0.546583	3.49761
H	0.496623	1.191746	3.44117
H	0.455402	-0.810168	4.762539
H	-1.095266	-2.284381	3.386158
H	-1.496715	-0.565953	3.478361
H	-1.952128	-1.178788	1.263520
H	-0.443794	-2.261441	-0.058839

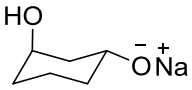

3.73

FINAL HEAT OF

FORMATION = -547.552748

C	-0.012637	-2.529617	1.075124
C	-0.741882	-1.264893	1.545379
C	-0.057166	0.069495	1.161166
C	1.416196	0.012891	1.623274
C	2.161362	-1.212490	1.077454
C	1.460605	-2.513791	1.486434
O	-0.744490	1.149091	1.666158
Na	-1.203928	2.739544	2.763149
O	-0.046251	-2.672681	-0.365483
H	1.913944	0.948247	1.315303
H	1.416719	-0.002986	2.731314
H	2.196988	-1.159643	0.022920
H	3.206838	-1.224234	1.428009
H	1.962830	-3.388657	1.043288
H	1.508771	-2.634495	2.583031
H	-0.498304	-3.418858	1.527746
H	-1.778659	-1.257239	1.161005
H	-0.823867	-1.287246	2.647693
H	-0.026366	0.105075	0.042650
H	-0.932276	-2.394405	-0.653467

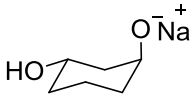

3.76

3.77

FINAL HEAT OF FORMATION = -547.553471

FINAL HEAT OF FORMATION = -547.554577

C	-0.842026	-1.105170	1.490294
C	-0.076829	0.116457	0.993155
C	1.367917	0.103639	1.511348
C	1.404993	0.010580	3.040139
C	0.653059	-1.246316	3.545781
C	-0.803894	-1.192161	3.014307
O	1.285184	-2.415755	3.194383
Na	2.417003	-4.008005	2.870029
H	-0.107236	0.148201	-0.108111
H	-0.599744	1.019676	1.355787
H	1.899613	-0.768701	1.093147
H	1.901712	1.001596	1.159149
H	2.445351	-0.041003	3.401670
H	0.950601	0.919511	3.476945
H	0.581798	-1.143683	4.667000
H	-1.327953	-2.103989	3.351408
H	-1.338617	-0.319182	3.431666
O	-2.192784	-1.010719	0.979369
H	-2.714668	-1.678001	1.458127
H	-0.358305	-2.013890	1.081067

C	-0.758656	-1.190359	1.414443
C	-0.035563	0.125780	1.129203
C	1.391408	0.094347	1.665095
C	2.159397	-1.111894	1.106939
C	1.424050	-2.429025	1.388528
C	-0.025471	-2.435124	0.851107
O	-0.699865	1.261458	1.7301
O	-0.699055	-3.600384	1.120625
Na	-1.366087	-5.182171	2.125152
H	1.899367	1.039326	1.414809
H	1.341219	0.035027	2.766275
H	2.283167	-0.990754	0.015586
H	3.176335	-1.136559	1.530561
H	1.963047	-3.283034	0.445949
H	1.374242	-2.608376	2.479747
H	-1.779012	-1.170133	0.990697
H	-0.857383	-1.317061	2.508153
H	-1.640126	1.189584	1.490132
H	0.009365	0.275496	0.029728
H	0.058043	-2.275937	-0.256919

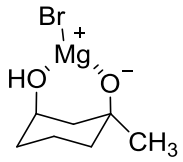

3.81

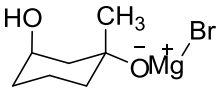

3.79

FINAL HEAT OF FORMATION = -3198.496588

FINAL HEAT OF FORMATION = -3198.461376

C	-0.158878	-2.412648	0.970299	C	0.198920	-2.508380	1.237462
C	-0.782146	-1.088500	1.427280	C	-0.578453	-1.355120	1.871138
C	0.111193	0.117096	1.135210	C	-0.224210	-0.010889	1.213902
C	1.551611	-0.091832	1.601548	C	-0.265188	0.034609	-0.333323
C	2.195306	-1.431074	1.140314	C	0.520703	-1.176232	-0.885958
C	1.247075	-2.591083	1.546261	C	0.077842	-2.518220	-0.289814
O	0.134225	0.406758	-0.323813	O	-1.981272	-1.684653	1.761492
C	3.552452	-1.605105	1.836902	O	0.391056	1.210973	-0.752626
O	2.397472	-1.439833	-0.247461	H	0.434472	-1.180656	-1.984774
H	1.691822	-3.531484	1.187061	H	1.584535	-0.999868	-0.652496
H	1.187450	-2.655337	2.648249	H	-0.963992	-2.738665	-0.571473
H	-0.109107	-2.450140	-0.131963	H	0.690966	-3.332434	-0.707471
H	-0.810742	-3.248022	1.268076	H	-0.160841	-3.454696	1.669576
H	-1.778252	-0.935267	0.977668	H	1.259478	-2.403514	1.523444
H	-0.938252	-1.114537	2.520353	H	-0.310997	-1.293733	2.944642
H	-0.300630	1.023105	1.607940	H	-0.872784	0.789671	1.617940
H	2.177791	0.749078	1.257889	H	0.806231	0.248401	1.508173
H	1.535247	-0.042009	2.703834	C	-1.706572	0.041051	-0.864806
H	-0.724938	0.763383	-0.608708	H	-2.483639	-0.937580	2.130179
H	4.011325	-2.545242	1.498399	H	-1.692492	0.117471	-1.963735
H	4.225713	-0.782707	1.553132	H	-2.268954	-0.857903	-0.577317
H	3.463222	-1.630273	2.934526	H	-2.247528	0.914068	-0.460179
Mg	1.472015	-0.528249	-1.567728	Mg	0.223817	2.934959	-1.250506
Br	0.963567	-0.009966	-3.845759	Br	0.236135	5.216056	-1.875049

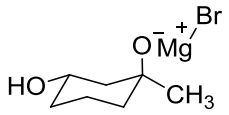

3.85

FINAL HEAT OF

FORMATION = -3198.464009

C	-0.789319	-0.965593	1.795295
C	-0.059127	0.167257	1.070926
C	1.439790	0.111589	1.341735
C	2.014985	-1.258666	0.963550
C	1.280522	-2.391344	1.686581
C	-0.242723	-2.364725	1.419282
O	-0.524158	1.462285	1.499437
O	-0.476730	-2.596694	0.051409
H	1.941440	0.920188	0.788258
H	1.601164	0.308217	2.164508
H	1.922725	-1.411259	-0.124838
H	3.090484	-1.293718	1.197707
H	1.668858	-3.372419	1.367618
H	1.454513	-2.310566	2.773961
C	-0.945990	-3.444295	2.252381
H	-1.866958	-0.937848	1.551899
H	-0.690533	-0.802766	2.882151
H	-1.489331	1.478490	1.376650
H	-0.227625	0.051638	-0.018058
Mg	-1.091705	-3.321730	-1.456514
Br	-1.864140	-4.135651	-3.533295
H	-2.029825	-3.426330	2.056912
H	-0.558800	-4.438855	1.980717
H	-0.790654	-3.299409	3.332625

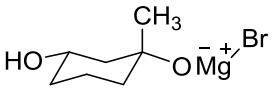

3.83

FINAL HEAT OF

FORMATION = -3198.462314

C	-0.438865	-1.395605	1.458060
C	0.278607	-0.113821	0.973650
C	1.580927	0.190520	1.709650
C	1.350794	0.263460	3.221163
C	0.692664	-1.018896	3.747175
C	-0.607700	-1.323499	2.993390
O	2.079650	1.432207	1.176633
O	-1.714185	-1.431221	0.866243
H	2.309275	0.443245	3.739550
H	0.703258	1.133527	3.425835
H	1.395469	-1.864125	3.647557
H	0.488024	-0.920010	4.824833
H	-1.052950	-2.268286	3.346889
H	-1.344685	-0.527987	3.193478
H	0.468562	-0.185242	-0.108886
H	-0.409680	0.732595	1.128569
H	2.316038	-0.614466	1.501523
C	0.341178	-2.655689	1.049594
H	-0.201852	-3.554520	1.381486
H	0.436216	-2.689621	-0.050631
H	1.355162	-2.700349	1.470571
Mg	-3.025889	-2.308470	0.011840
H	2.893017	1.650059	1.664800
Br	-4.849400	-3.336306	-1.082613

Chapter 4
Achieving molecular stability of racemic 4-*O*-benzyl-*myo*-inositol-1,3,5-orthoformate through crystal formation

This chapter is published in: Bardessar, R.; Krishnaswamy, S.; Shashidhar, M. S. *CrystEngComm*, 2012, 14, 8010-8016. DOI: 10.1039/C2CE26199E

4.1. Introduction

4-*O*-substituted-*myo*-inositol-1,3,5-orthoesters are versatile intermediates for the preparation of biologically relevant inositol derivatives.[1-4] In particular, racemic 4-*O*-benzyl-*myo*-inositol-1,3,5-orthoformate (4.1) has been utilized for the synthesis of phosphoinositols and their analogs (Scheme 1).[3,5,8]

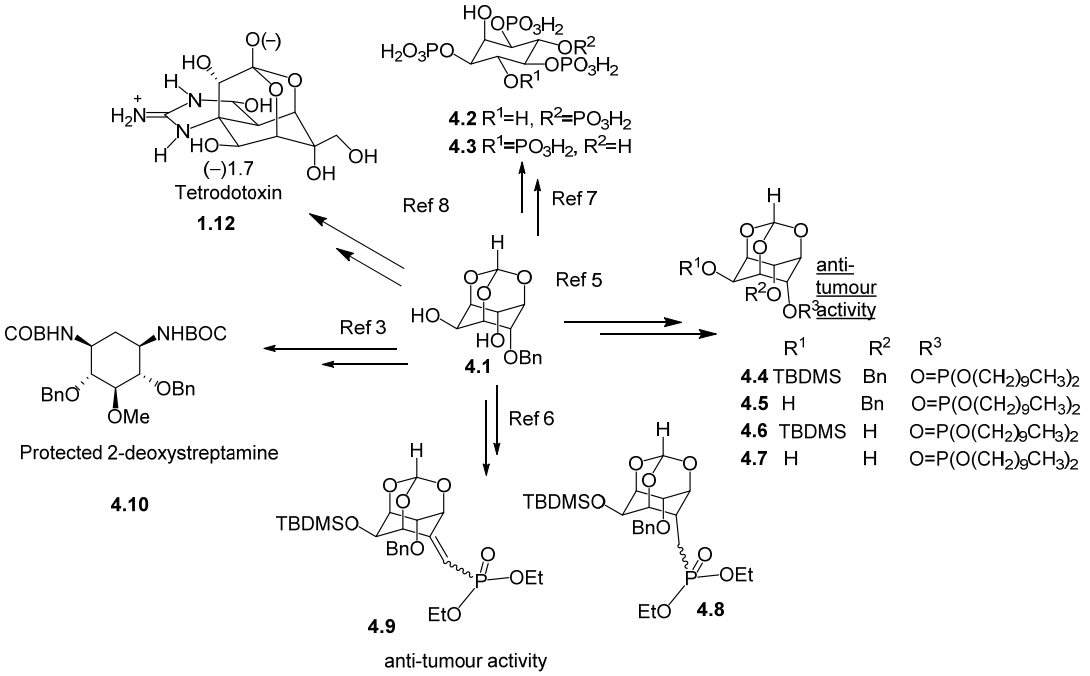

Scheme 1 Synthetic utility of the benzyl ether 4.1.

We had to prepare, store and use relatively larger amounts of the benzyl ether 4.1 as a part of an ongoing study on the chemistry of inositols.[9]

It was known as seen in Scheme 2 (ref 1), that the reaction of the triol 1.66 with alkyl halides in the presence of lithium derived bases (LiH, BuLi) gave selectively the 4,6-diaxial ether.[10] Whereas the same reaction in the presence of sodium hydride led to a mixture of 2,4- and 4,6-di-*O*-alkyl derivatives.[11] This was thought to be because of the involvement of lithium chelates (4.14) which are expected to be relatively more stable than the corresponding sodium chelates (4.15) owing to the smaller size of the lithium cation and its better co-ordination capacity.

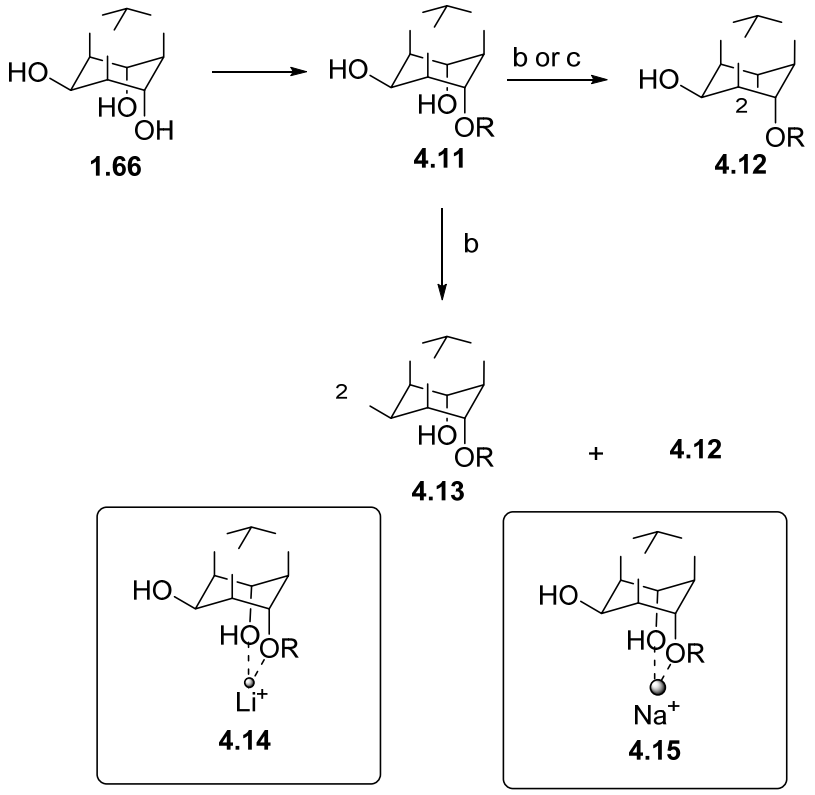

Scheme 2(a) DMF, NaH, R^1X; b) THF, n-BuLi, R^2X, DMF; c) DMF, LiH, R^2X.

Hence, we wondered whether the relative selectivity to favor the formation of unsymmetrical diethers (4.13) during this O-alkylation reaction could be influenced by added alkali metal salts especially cesium salts, which have larger ionic radii (and hence disfavor the formation of symmetrical chelates similar to lithium chelate). To investigate this we carried out alkylation of the benzyl ether 4.1 in the presence of sodium hydride and cesium and lithium salts (Scheme 3). The products were then acetylated and the mixture of acetates was analyzed by NMR spectroscopy to determine the relative regioselectivity. However the results showed that there was no appreciable effect of the added salts on this O-alkylation reaction.

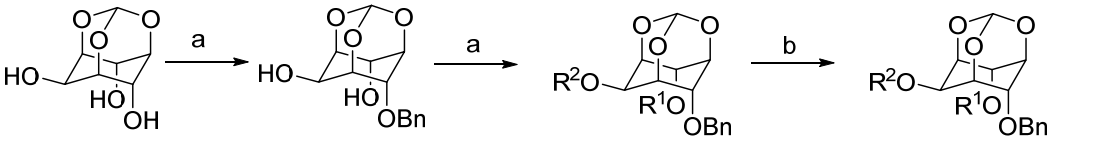

Scheme 3a) DMF, NaH, BnBr, CsF or LiBr; b) Ac_2O, pyridine.

We also carried out alkylation of the racemic mono benzyl ether 4.1 in the presence of dibutyltinoxide.[12] However these attempts were not successful in improving the regioselectivity towards the formation of the unsymmetrical diethers 4.13.

During these investigations, we were intrigued to realize that the racemic benzyl ether 4.1 was stable when stored as a solution in common organic solvents, but did not stay pure when stored as a gum at ambient temperature. However storing the benzyl ether 4.1 in solution was inconvenient over long periods of time. A survey of the literature revealed that, while the physical state of the racemic benzyl ether 4.1 at ambient conditions was mentioned as a gum in some reports[11, 13], most other reports did not mention the physical state (or the purity) of the sample used for further synthetic transformations. It was also surprising to note that while many 4-O-substituted-*myo*-inositol-1,3,5-orthoesters existed as solids or crystalline compounds under ambient conditions,[7, 14] racemic benzyl ether 4.1 was never reported as a solid.

Table 1 : Physical state of racemic 4-O-substituted-*myo*-inositol-1,3,5-orthoesters under ambient conditions

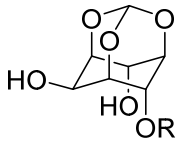

Compound no	R^1	Nature	Reference
4.20	THP	Solid	15
4.21	Lauryl	Solid	16
4.22	p-Allylbenzyl	Solid	17
4.23	OPO(Bn)2	Crystalline solid	18
4.24	Ac	Crystalline solid	16
4.25	Piv	Crystalline solid	
4.26	Bz	Crystalline solid	
4.27	Allyl	Gum	11

Hence we scrutinized the samples of the racemic benzyl ether 4.1 stored over varying periods of time (days to years) and observed that some samples of the benzyl ether 4.1 exhibited partial degradation while a few other samples had turned into solids. Subsequently, we could arrive at experimental conditions to obtain good crystals of the racemic benzyl ether 4.1 which prevented molecular degradation on storage. The results of this investigation showed that the orthoformate 4.1 undergoes cleavage to the corresponding formyl ester in the gummy state, while it is inert in crystalline and

solution states. We had earlier reported[19] an interesting instance of the epimerization of inositol 1,3-bridged acetals, which occurred only in the molten state, but not in the solid and solution states.

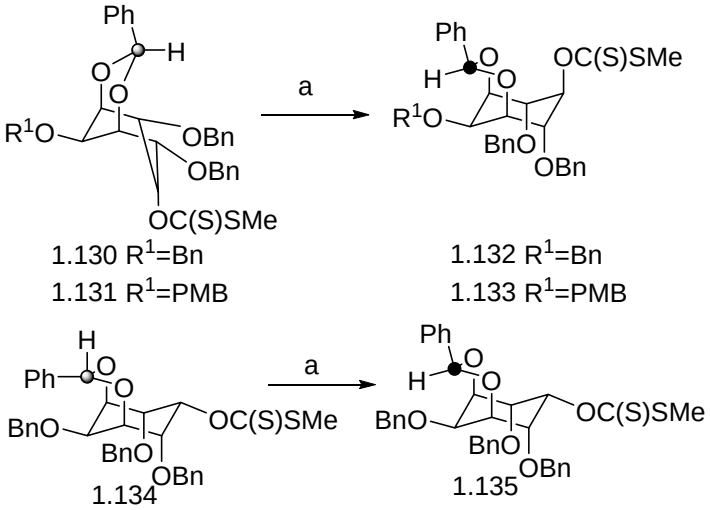

Scheme 4: Epimerization of *myo*-inositol derived 1,3-acetals. (a) 120 °C, 12 h for 1.130, 1.131 and 30 h for 1.134.

Encountering such instances of variation of the stability of molecules in different phases reiterates the importance of the effect of molecular aggregation on observed properties attributed to individual molecules. Accordingly, the rest of this chapter presents results of detailed investigations carried out to understand the stability of racemic **4.1**.

4.2. Results and discussion

Monobenzyl ethers **4.1**, **4.28**, **4.29** of *myo*-inositol orthoesters **1.66**, **1.67** and **1.68** were prepared (Scheme 5) and the stored samples were analyzed for purity / presence of impurities. The stability of orthoacetate **4.28** and orthobenzoate **4.29** benzyl ethers were also looked into, since comparisons and controls were deemed necessary to interpret the results of experiments carried out with the orthoformate **4.1**.

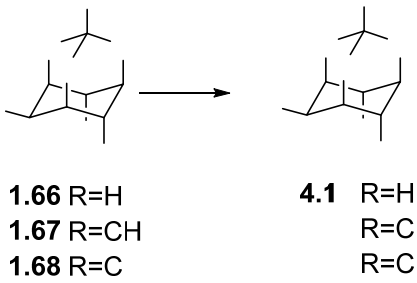

Scheme 5: Synthesis of racemic 2-benzyl-*myo*-inositol-1,3,5-orthoesters. (a) DMF, NaH, benzyl bromide (BnBr), 2 h, 80-90%.

The benzyl ether 4.1 was always obtained as a gum (4.1A) and the samples were usually stored at low temperature (0 to -20 ºC) or as solution in dichloromethane. Racemic 4.1 mostly remained as a gum on storage for few weeks (4.1B) or turned into a solid (sample 4.1C) on storage for long periods of time. The sample 4.1C had different solubility characteristics in common organic solvents compared to the gum (sample 4.1A) from which these solids formed. For example, sample 4.1A was completely soluble in dichloromethane and methanol, while the sample 4.1C was sparingly soluble in dichloromethane but completely soluble in methanol. Some of the samples of racemic 4.1 which had been stored for long periods of time revealed the presence of well defined crystals (form I and form II see below for details). Interestingly, the solubility characteristics of these crystals were similar to those of the gums (sample 4.1A) from which crystals had formed. Hence, we systematically analyzed the samples of racemic O-benzyl ethers 4.1, 4.29, 4.30 of myo-inositol-1,3,5-orthoesters.

Investigation of stored samples of 4.1.

The FT-IR spectra (Figures 1-4) of the gummy sample 4.1B (i.e. 4.1A stored up to 4 weeks,) and the amorphous solid sample 4.1C, (i.e. 4.1A stored from several months up to 2 years,) revealed peaks between 1710 and 1730 cm^{-1}, suggesting the presence of a carbonyl group, although the racemic benzyl ether 4.1 is devoid of carbonyl groups. The FT-IR spectrum of freshly prepared samples of 4.1 (sample 4.1A) however, did not indicate the presence of carbonyl group. Heating (120-130 °C) sample 4.1A also led to the formation of a mixture of products similar to the samples of 4.1 stored for long periods of time (sample 4.1B or 4.1C), as revealed by a comparison of the IR spectrum (Figure 4).

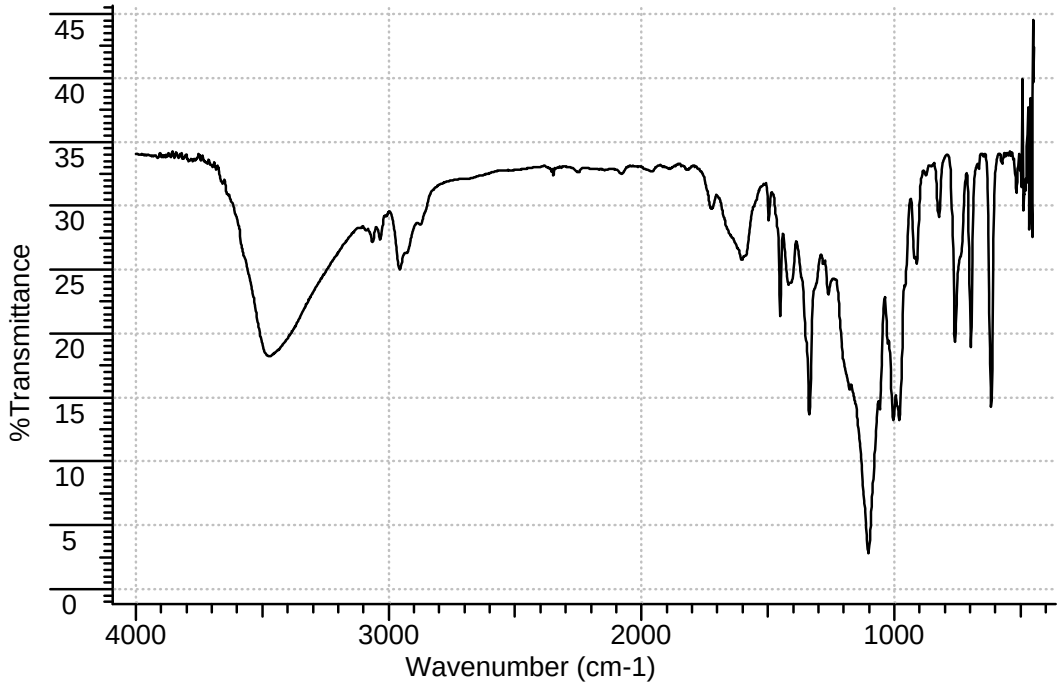

Figure 1. IR spectrum of the freshly prepared racemic benzyl ether.

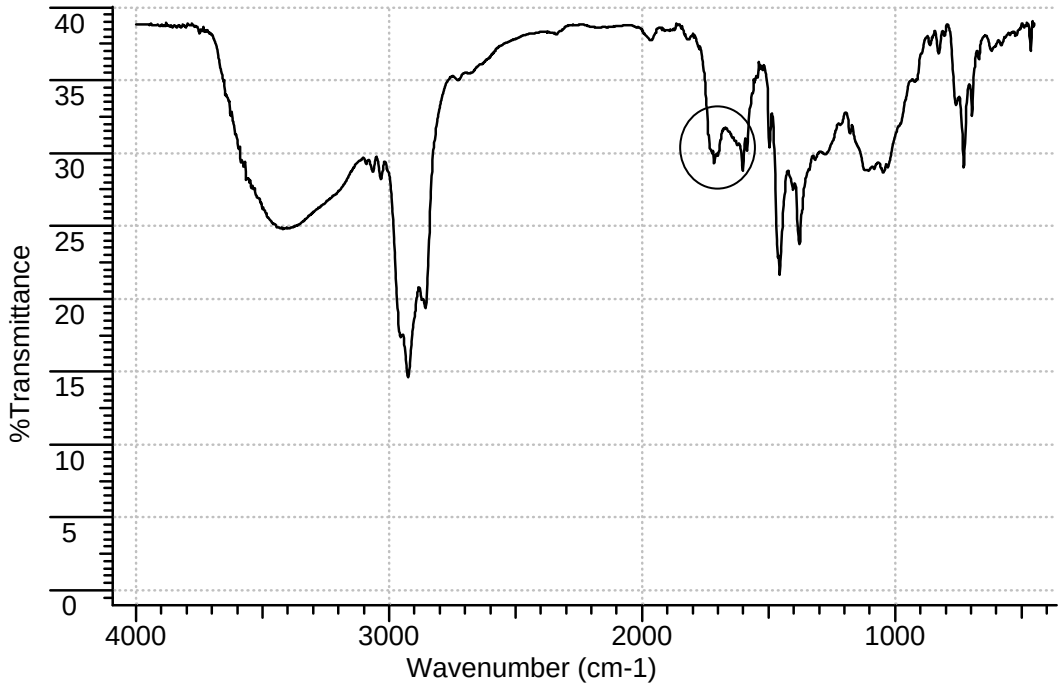

Figure 2. IR spectum of the sample.

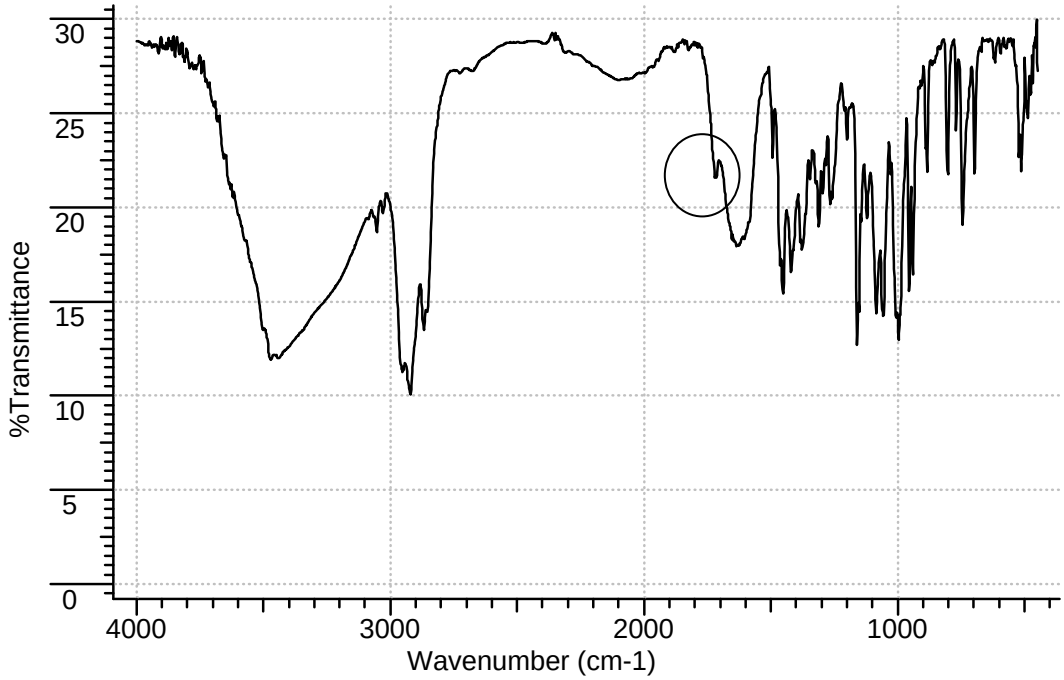

Figure 4.3. IR spectum of sample 1C.

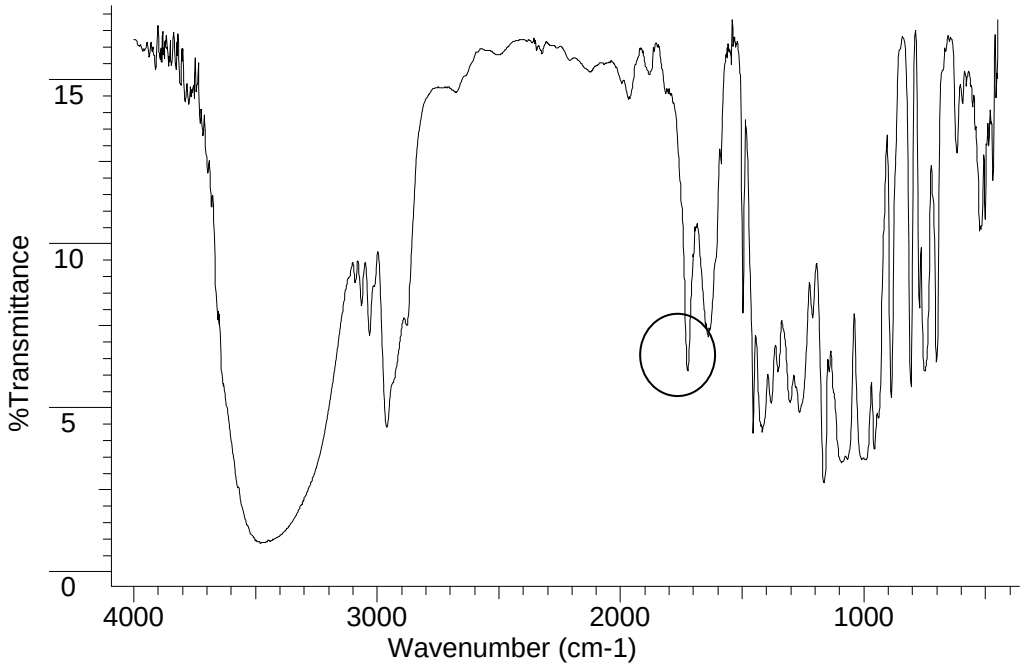

Figure 4.4. IR spectum of the sample 1A heated for several hours.

A comparison of the ^{1}H NMR spectra of the same sample of 4.1A (freshly prepared gum), 4.1B (gum stored at ambient temperature), 4.1D (samples of 4.1 stored below -10 °C for more than 2-3 weeks) indicated the appearance of broad signals in 4.1B which were not present in 4.1A and 4.1D, (indicating the formation of esters of inositol, see Figure 5-7).

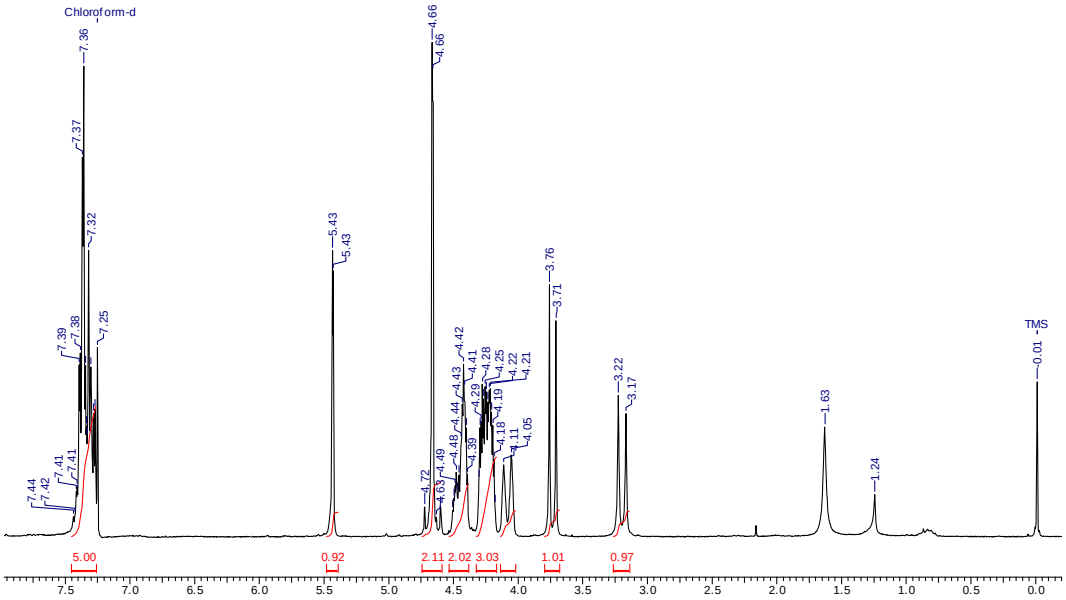

Figure 5. ^{1}H NMR spectrum (in $CDCl_3$) of 4.1A.

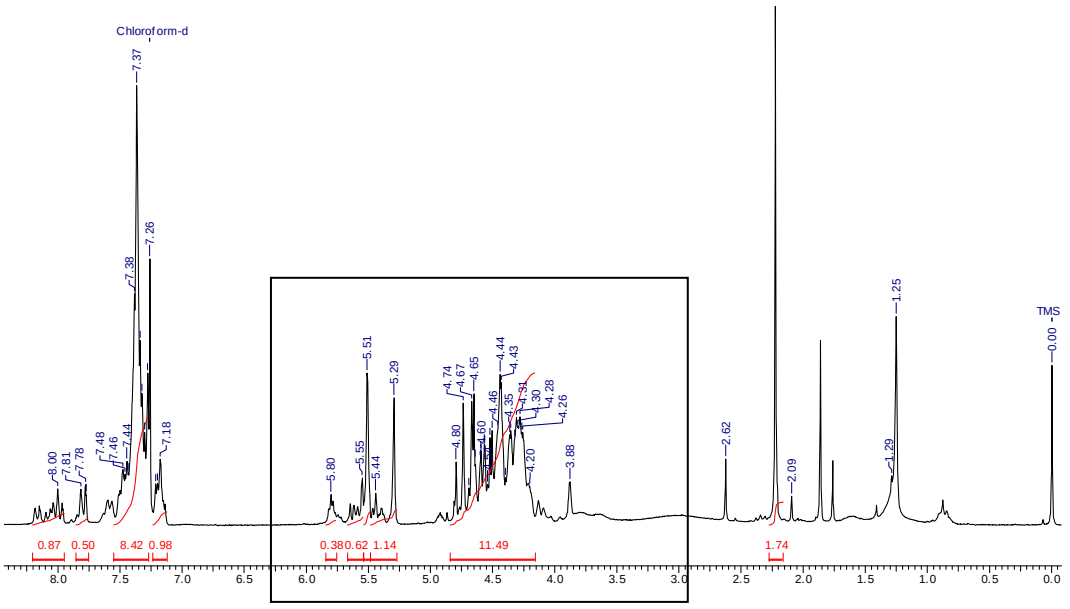

Figure 6. ^{1}H NMR spectrum (in $CDCl_3$) of 4.1B the region of signal broadnening is demarcated by a box.

Broadening of signals was also observed due to the formation of mixture of inositol derivatives. The ^{1}H NMR spectra and the PXRD patterns (Figure 7-9)of the solid samples **4.1D** and **4.1E** (**4.1**stored at -20 °C for 12 h to obtain a solid, done in order to reproduce the crystals Form I) were very similar to that of Form I crystals, indicating that the they were in fact microcrystalline forms of the latter crystals.

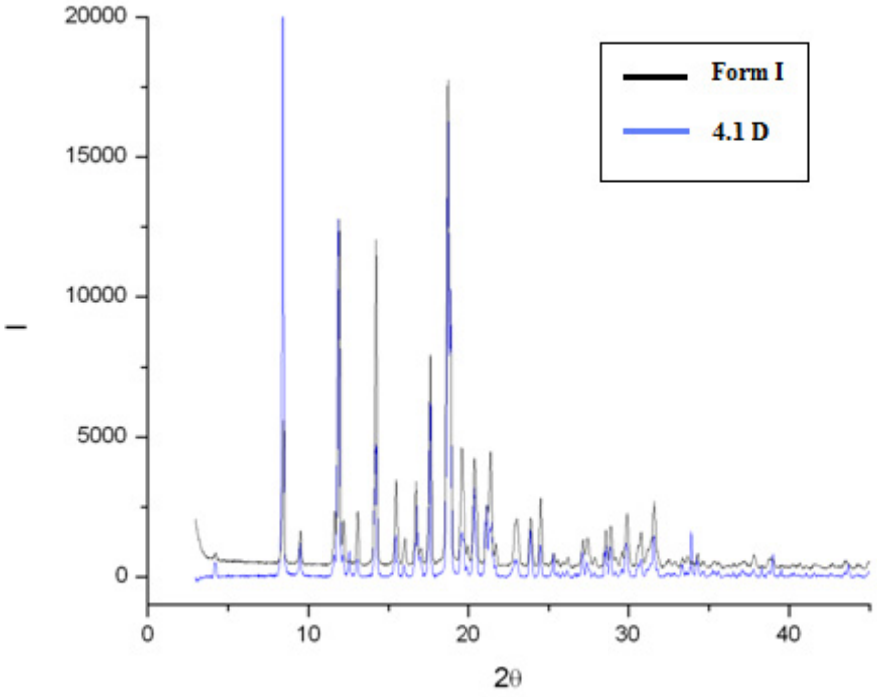

Figure 7. PXRD patterns for crystals of (a) black-Form I. and (b) blue – sample **4.1D**

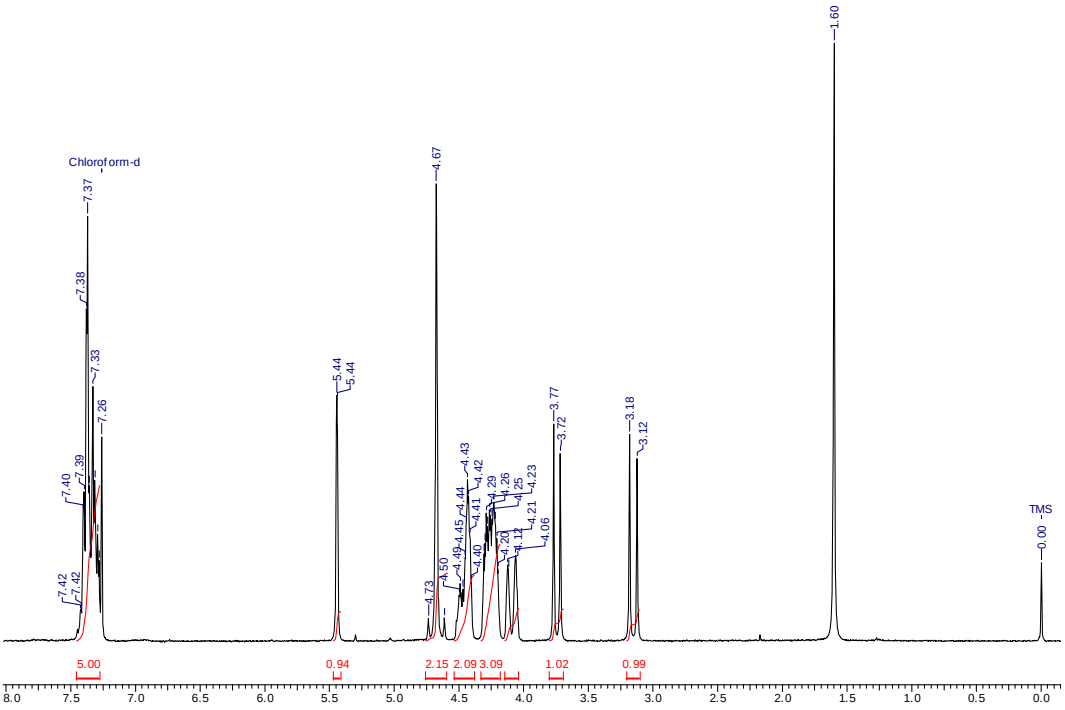

Figure 8. ^{1}H NMR spectrum (in $CDCl_3$) of 4.1D.

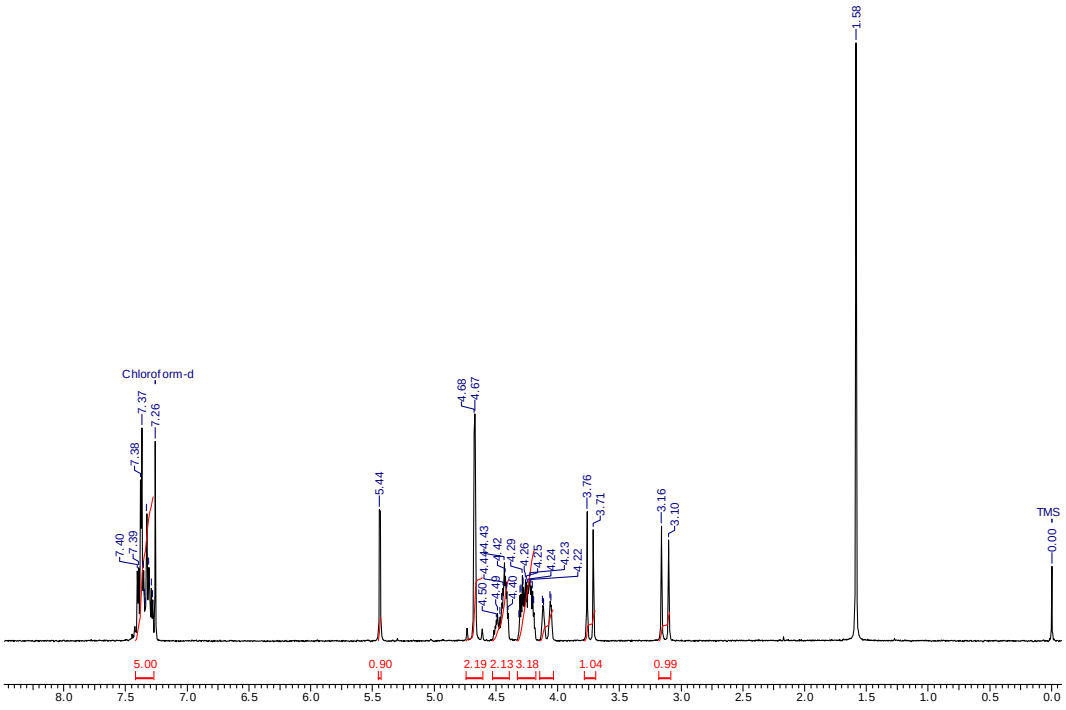

Figure 9. ^{1}H NMR spectrum (in $CDCl_3$) of racemic 4-*O*-benzyl-*myo*-inositol 1,3,5-orthoformate (Form I crystals).

Chromatographic purification of the sample 4.1C yielded small quantities of a polar component along with the pure benzyl ether 4.1. However, the FT-IR spectra of both these compounds did not reveal the presence of a carbonyl group. Acetylation of the polar component yielded a penta-acetate, whose structure was established to be 4.31

(Scheme 6) based on its spectral data. Hence, the precursor of 4.30 isolated after chromatography from the sample 4.1C must be racemic 2-benzyl-myo-inositol (4.30). This explains the insolubility of solid sample 4.1C in non-polar solvents such as dichloromethane and its solubility in polar solvents like methanol, as mentioned earlier.

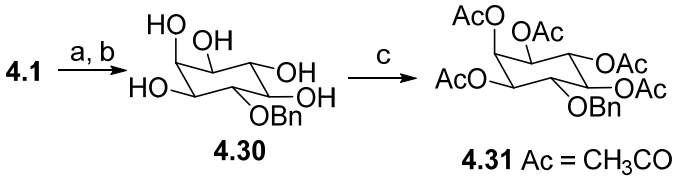

Scheme 6. (a) Store for several months or heat at 130 °C for 12 h; (b) chromatography; (c) pyridine, acetic anhydride, ambient temperature, 48 h

Investigation on samples of the orthoacetate 4.28 and orthobenzoate 4.29

The results described above however did not account for the presence of carbonyl group (as indicated in their IR spectra, Figures 1-4) in stored samples of 4.1. Hence we also examined the samples of the racemic benzyl ethers 4.28 and 4.29 of myo-inositol-1,3,5-orthoacetate and orthobenzoate.[20] The benzyl ethers 4.28 and 4.29 which were obtained as gums, were heated and IR and NMR spectra of the resulting samples were analyzed. A comparison of the IR spectra of the orthoesters 4.28 and 4.29, before and after heating showed an increase in intensity of the peak due to the ester carbonyl group. (Figure 10-13). The ^{1}H NMR spectra (Figure 14-17) of the same samples also indicated the appearance of signals between δ5 and δ6, which indicated the formation of esters (acetates and benzoates, Scheme 7) of inositol. Broadening of signals could also be due to the formation of mixture of inositol derivatives. Analysis of older samples of the racemic benzyl ethers 4.28 and 4.29 by IR spectroscopy also showed the presence of carbonyl group in them, as observed in aged samples of 4.1 (Figure 18 and Figure 19).

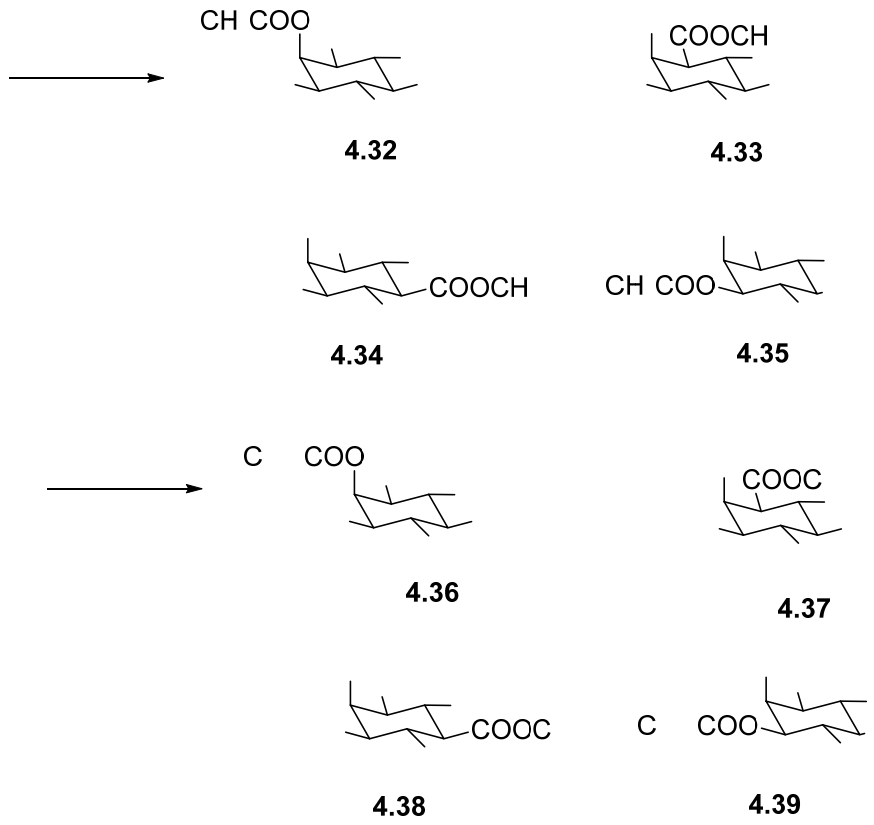

Scheme 7. Formation of esters from 4.28 and 4.29 (a) Store for several months or heat for 12 h.

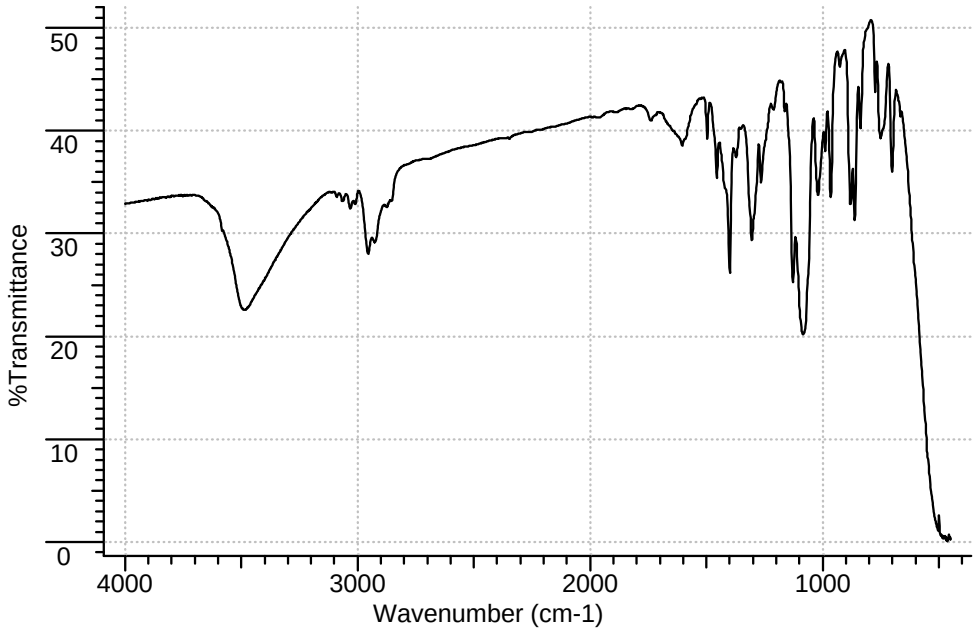

Figure 10. IR spectra of racemic 4-O-benzyl-myo-inositol 1,3,5-orthoacetate (4.28) freshly prepared (in $CDCl_3$)

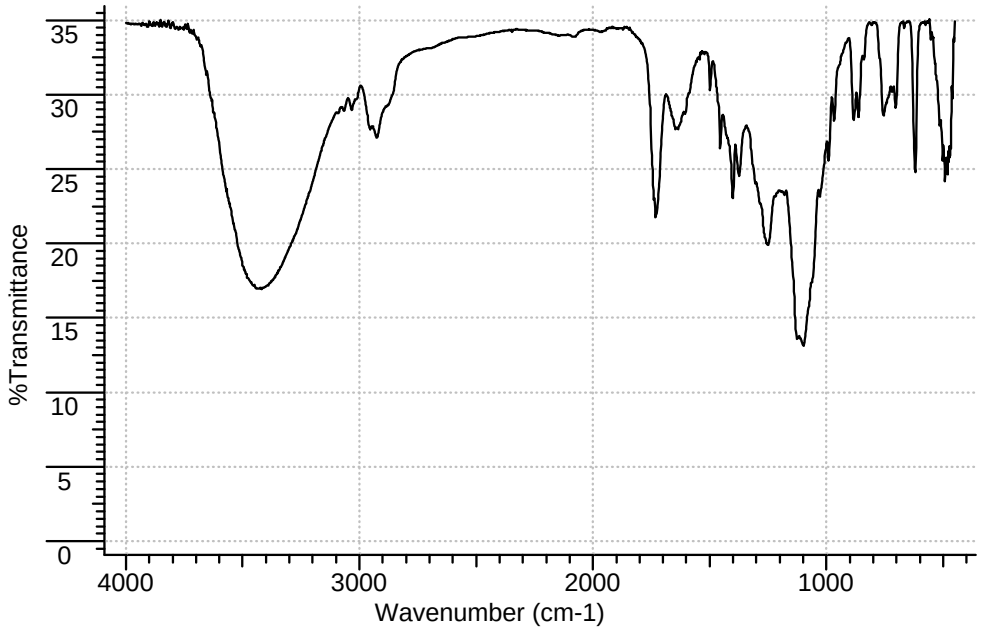

Figure 11. IR spectra of racemic 4-*O*-benzyl-*myo*-inositol 1,3,5-orthoacetate (**4.28**) heated at 120 °C for 6 hours (Nujol):

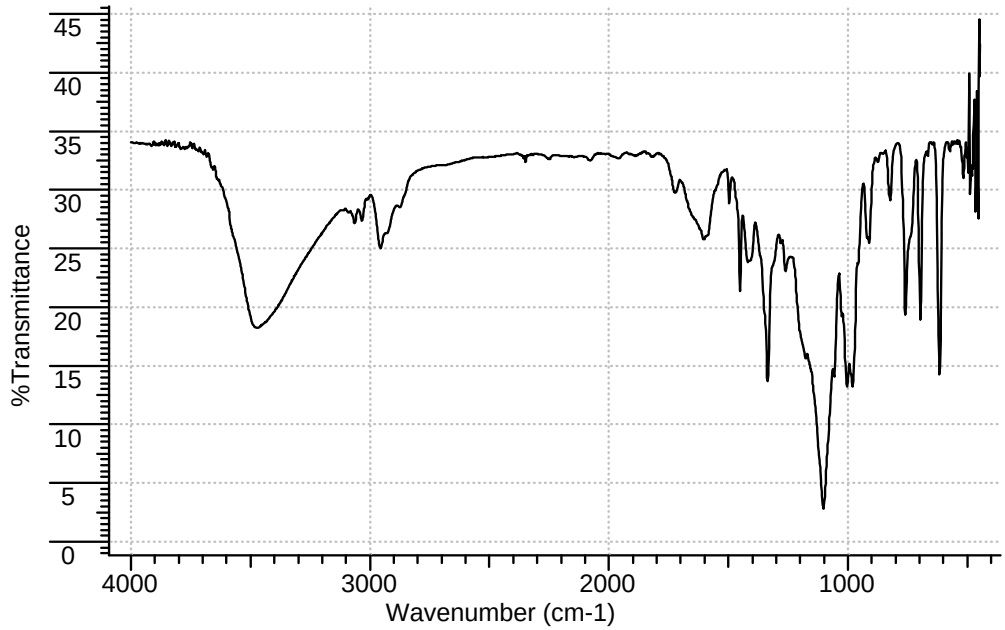

Figure 12. IR spectra of racemic 4-*O*-benzyl-*myo*-inositol 1,3,5-orthobenzoate (**4.29**) freshly prepared (in $CDCl_3$)

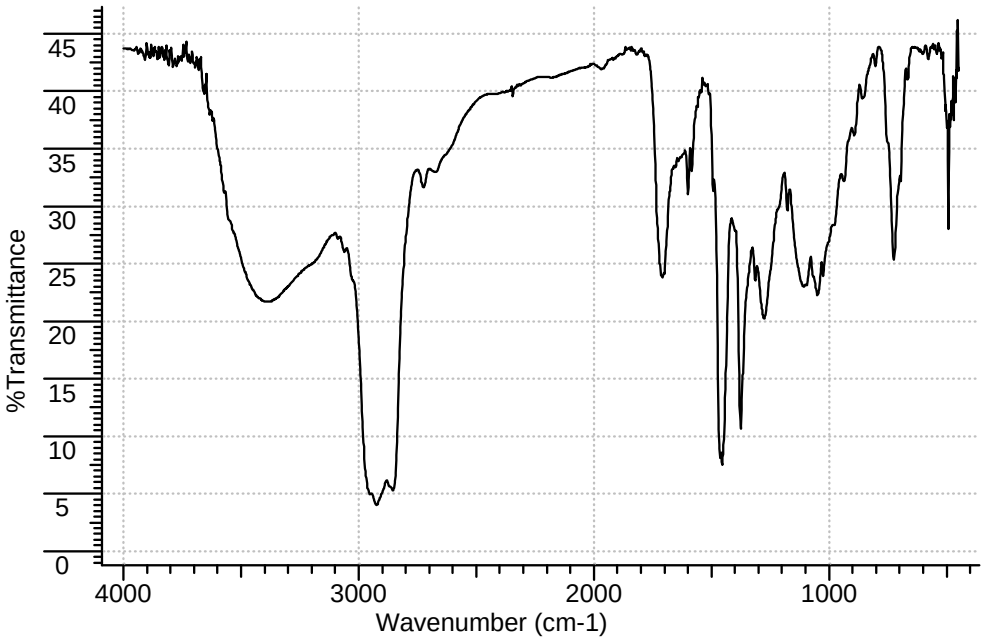

Figure 13. IR spectra of racemic 4-*O*-benzyl-*myo*-inositol 1,3,5- orthobenzoate (4.29) heated at 120 °C for 6 hours (Nujol):

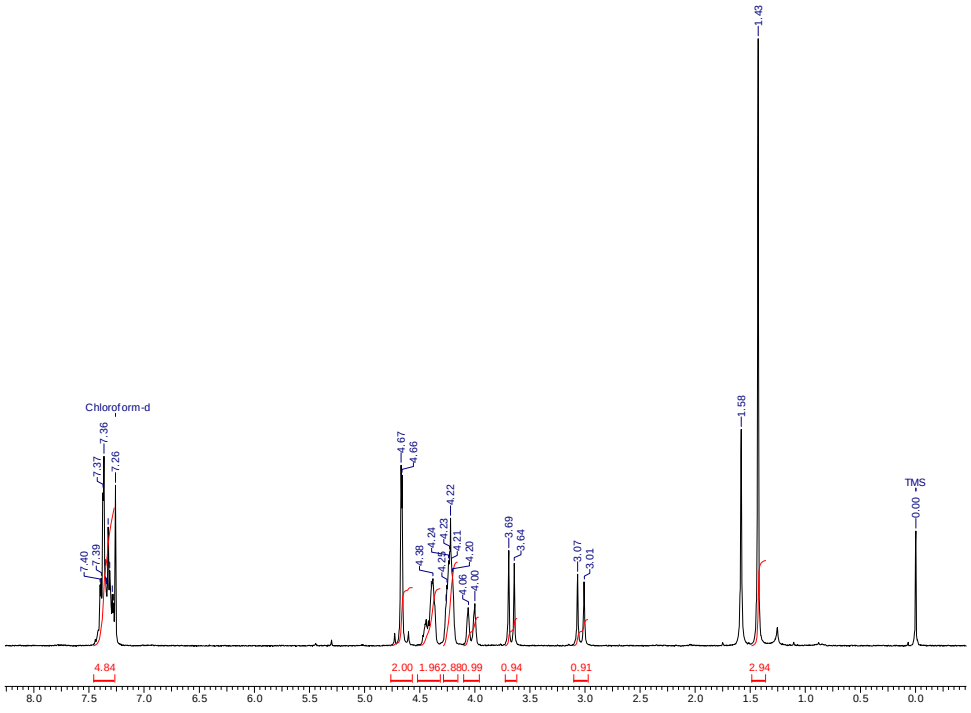

Figure 14. ^{1}H NMR spectrum (in $CDCl_3$) of racemic 4-*O*-benzyl-*myo*-inositol 1,3,5-orthoacetate (4.28).

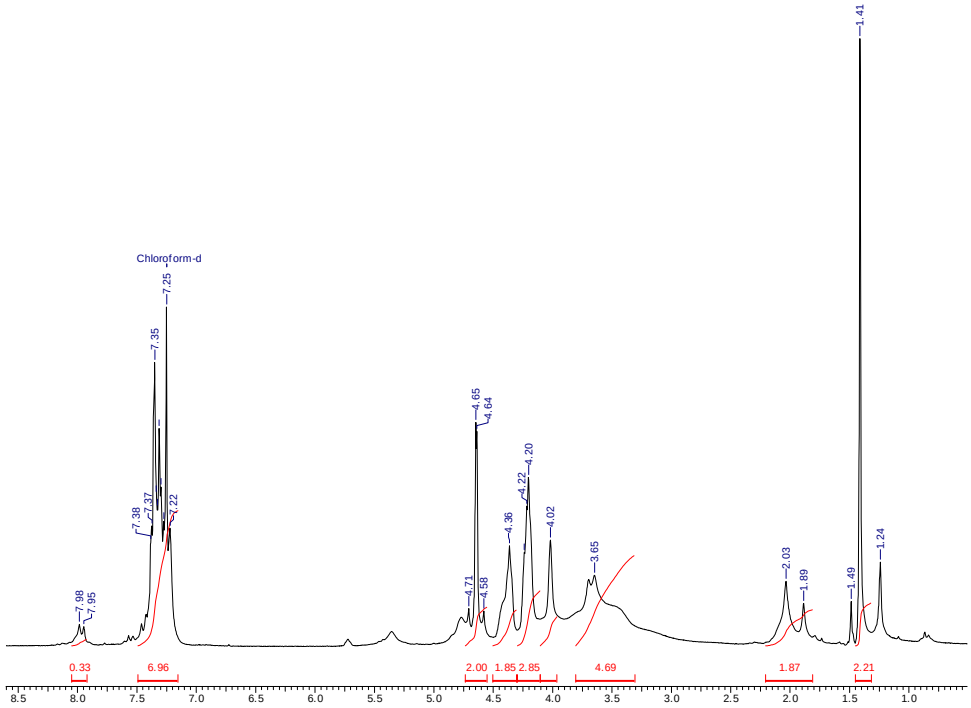

Figure 15. ^{1}H NMR spectrum (in $CDCl_3$) of heated sample of racemic 4-*O*-benzyl-*myo*-inositol 1,3,5-orthoacetate (4.28).

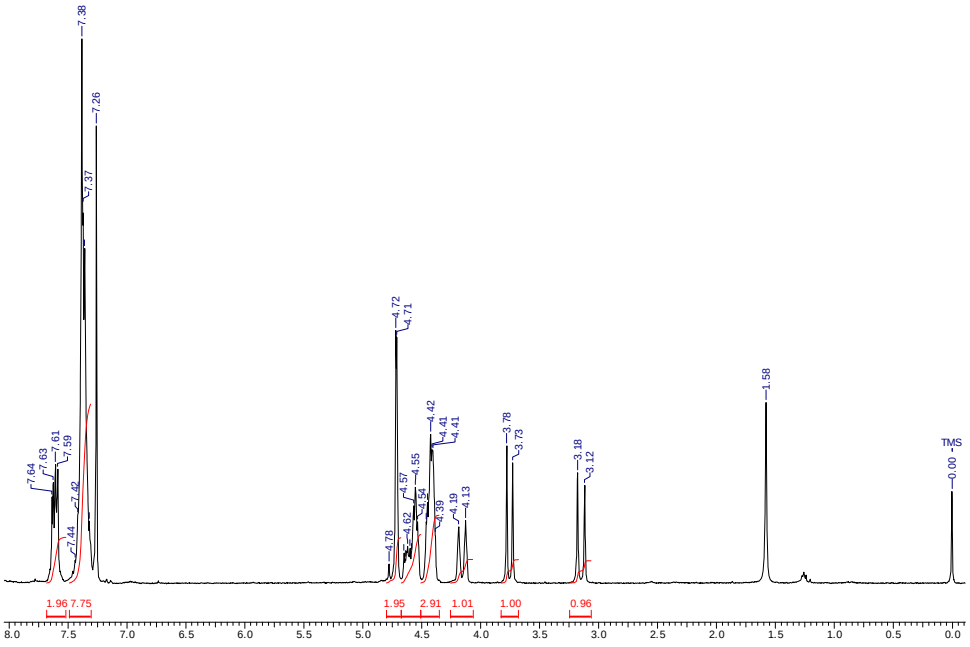

Figure 16. ^{1}H NMR spectrum ($CDCl_3$) of racemic 4-*O*-benzyl-*myo*-inositol 1,3,5-orthobenzoate (4.29).

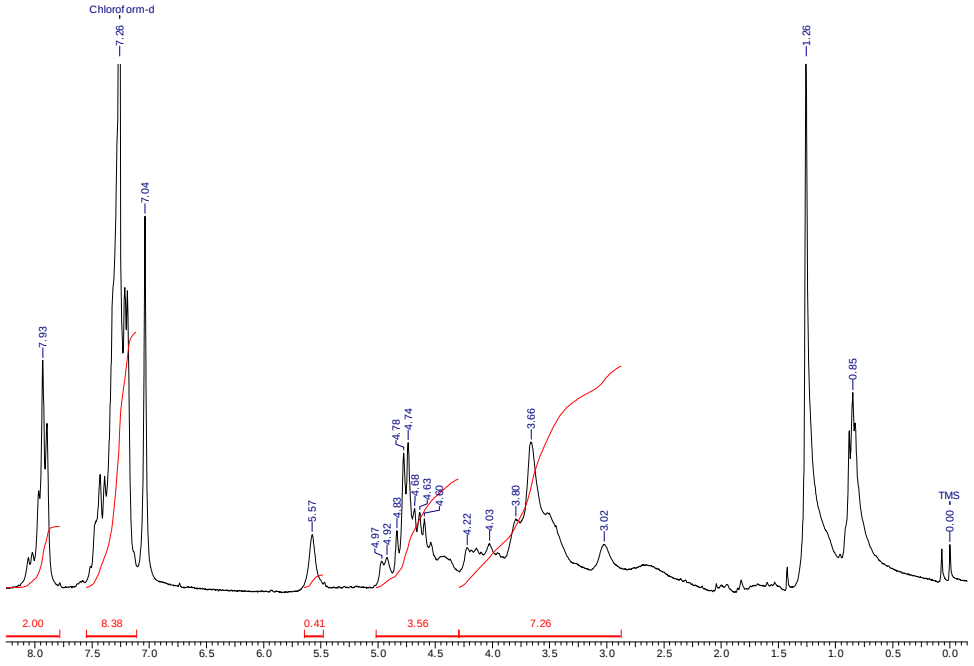

Figure 17. ^{1}H NMR spectrum ($CDCl_3$) of heated sample of racemic 4-O-benzyl-*myo*-inositol 1,3,5-orthobenzoate (4.29)

.

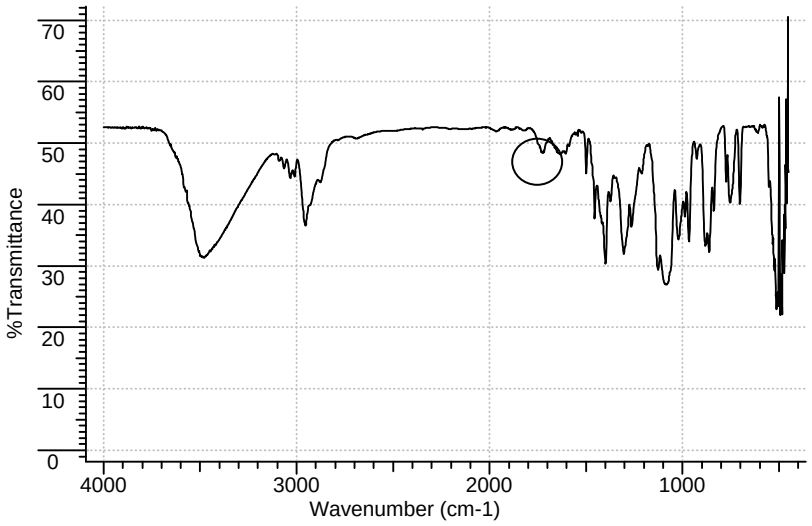

Figure 18. IR spectra of racemic 4-O-benzyl-*myo*-inositol 1,3,5-orthoacetate (4.28) stored at ambient temperature for a month

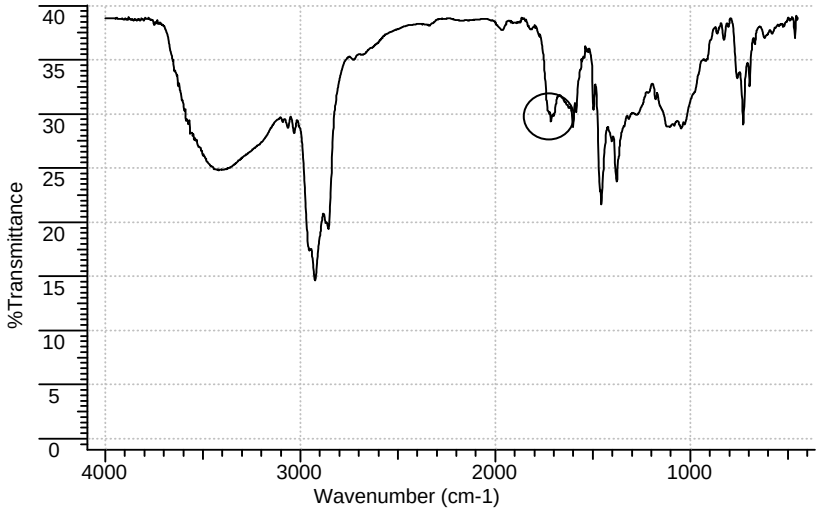

Figure. 19 IR spectra of racemic 4-O-benzyl-myo-inositol 1,3,5-orthobenzoate (4.29) stored at ambient temperature for a month

From a comparison of the results obtained by the analysis of the samples of the benzyl ethers 4.1, 4.28 and 4.29, we could infer that the orthoformate 4.1 gets converted to the corresponding formate esters which are labile in the gum (perhaps due to absence of water) but hydrolyze during work-up or chromatography to the corresponding pentol 4.30. Esters of formic acid are known to be far more labile to hydrolysis as compared to other carboxylic acid esters.[21] It is pertinent to mention here that the instability of myo-inositol orthoesters has previously been exploited for the regioselective acylation of the C2-hydroxyl group.[22]

4.2a. Crystallization and crystal structure of the racemic benzyl ether 4.1

Two of the samples of 4.1 (1A) stored for extended periods of time had led to the formation of plate-like (form I) and block-shaped crystals (form II, Figure 20) embedded in the gum. However, slow rate of crystallization (a period of 3 to 4 weeks for form I and 3 to 4 months for form II) initially, prevented us from developing a consistent procedure for obtaining crystals of 4.1. However, we were able to obtain form I crystals of 4.1 consistently by first cooling the gummy sample to -20 ºC to obtain a solid (microcrystalline - sample 4.1E) and its subsequent crystallization from dichloromethane – light petroleum mixture. Our attempts to crystallize the freshly prepared gummy samples of 4.1 (without solidifying by cooling to -20 ºC) in the same solvent system failed. Also, we could not obtain form II crystals of 4.1 reproducibly.

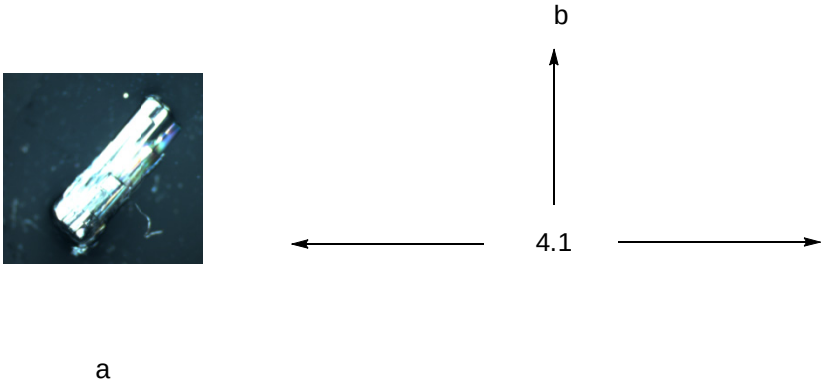

Figure 20. Photomicrographs of solid samples of 4.1 (b) amorphous solid (sample 4.1C); (a) Form I crystals; (c) Form II crystals.

The crystals of form I belong to the orthorhombic space group Pbca with an enantiomorphic pair of independent molecules in the asymmetric unit (Figure 21a), while form II crystals are monoclinic, space group $P2_1/c$ (Figure 21b).

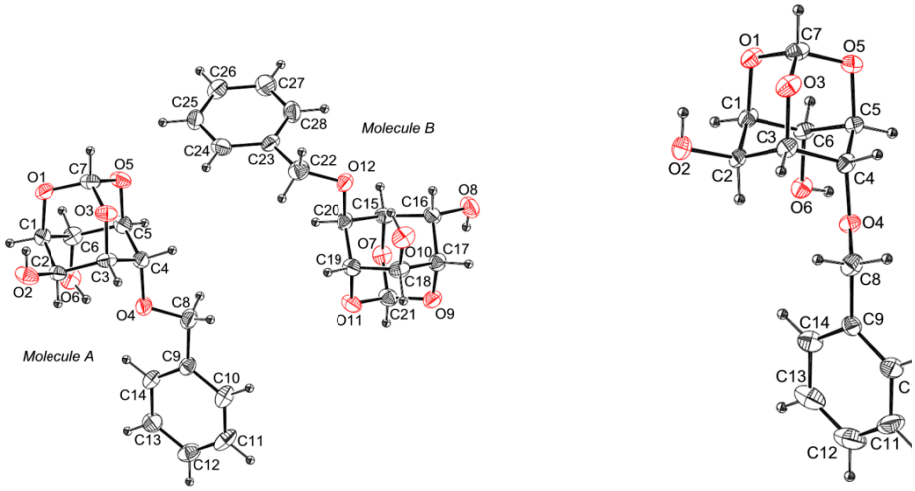

Figure 21: Representative ORTEP of molecules in (a) form I and (b) form II crystals. Thermal ellipsoids are drawn at 30% probability and hydrogen atoms are depicted as small spheres of arbitrary radii.

The two symmetry-independent molecules in the crystal structure of form I show significant difference in the torsion angle associated with the 4-O-benzyl group, C4-O4-C8-C9 (~97°) while the torsional differences associated with the hydroxyl groups

C1-C2-O2-H2' (~6°) and C1-C6-O6-H6' (~12°) are small (Figure 22a). The molecular overlap of form I (molecule A) and form II reveals conformational changes in the C6-hydroxyl group and the benzyl group (Figure 22b); the difference in torsional angles C1-C6-O6-H6' and C4-C8-C9 being ~86° and 9° respectively. The torsional angle differences for the C6-hydroxyl and C4-benzyl groups in the molecular overlay of the form I (molecule B) and form II crystals (Figure 22c) are ~74° and 106° respectively. These conformational changes drive the molecular association in the dimorphs. The calculated powder X-ray diffraction patterns of the dimorphs also reveal the structural differences between the two forms (see Appendix).

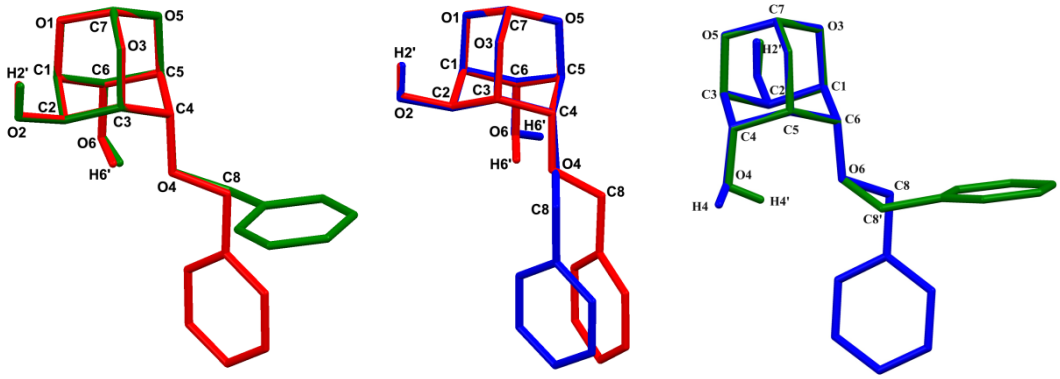

Figure 22: The overlap of molecules in (a) the asymmetric unit of form I crystals (red and green) (b) form I (molecule A, red) and form II crystals (blue) (c) form I (molecule B, green) and form II crystals (blue) which show the conformational differences in the functional groups. C-H H-atoms are omitted for the sake of clarity.

Vasella and co-workers[23] investigated the intramolecular hydrogen bonding in 1 by an analysis of their FT-IR spectra in CCl_4 and DMSO solutions. A strong intramolecular hydrogen bond was observed between the C6-hydroxyl group and the oxygen atom O4 (O6-H6'···O4) while the C2–OH group exhibited weaker hydrogen bonding with the orthoester oxygen atoms O1 and O3 in solution. In the crystalline state the hydrogen bonding between the C6-hydroxyl group and the C4-oxygen atom is intramolecular in form I (paralleling that in solution) and intermolecular in form II crystals. The identical orientation of the C2-hydroxyl group in the dimorphs results in similar hydrogen bonding interactions, with the axial hydroxyl group of a glide-related molecule (O2-H2'···O6, in case of molecule A in form I and molecules in form II crystals) or a screw related molecule (O8-H8'···O10, in case of molecule B in form I) forming an O-H···O linked molecular chain (Figure 23).

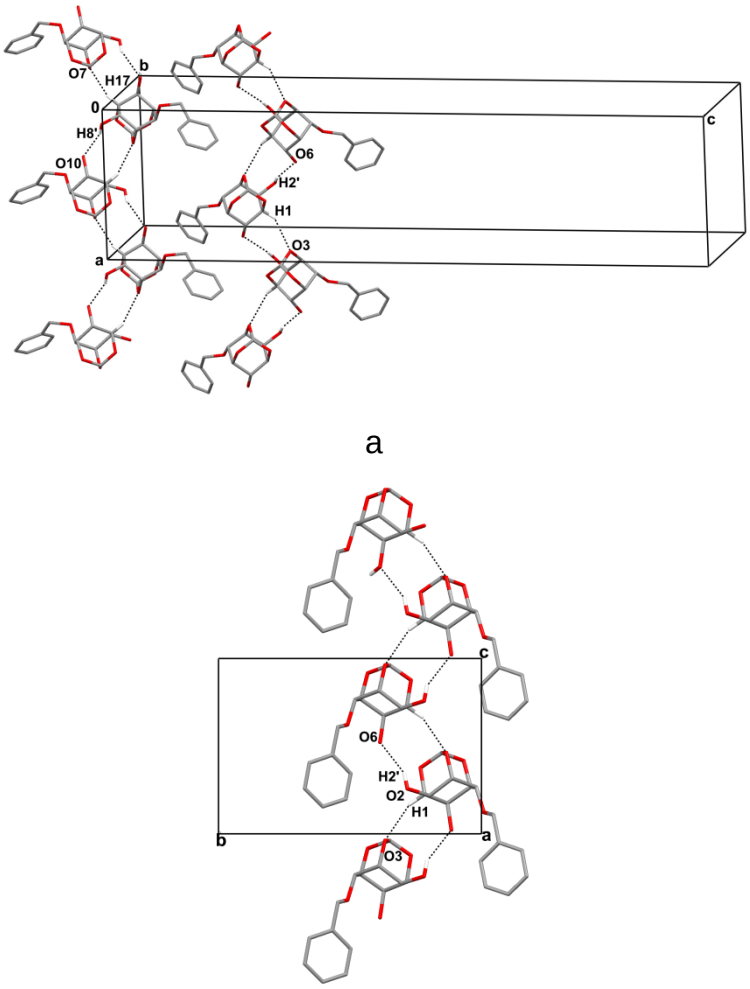

Figure 23. Intermolecular O-H···O hydrogen bonding in crystals of 4.1 (a) form I, consisting of separate chains of glide and screw related molecules along the a-axis and (b) form II, glide related molecules associated along the c-axis. Dotted lines represent O-H···O and C-H···O interactions. H-atoms not involved in hydrogen bonding are omitted for the sake of clarity.

Identical supporting C-H···O interactions between inositol ring proton and the orthoformate oxygen atom (C1-H1···O3 and C17-H17···O7, Figure 23) along the molecular chains are also observed in both the forms. In form I crystals, adjacent chains of glide related molecules (molecule A) are linked by a pair of short and linear C-H···O interactions (C7-H7···O2 and C2-H2···O5) while chains of screw related molecules (molecule B) are linked by moderately strong C15-H15···O11 contacts along the b-axis (Figure 24a). Adjacent molecular chains are connected by weak C11-H11···O9 interactions along the c-axis. In form II crystals the O-H···O bonded molecular chains are linked along the b-axis by short and linear O6-H6'···O4 and C4-H4···O3 contacts (Table 2) and weak C8B-H8B···O1 interactions (Figure 24b).

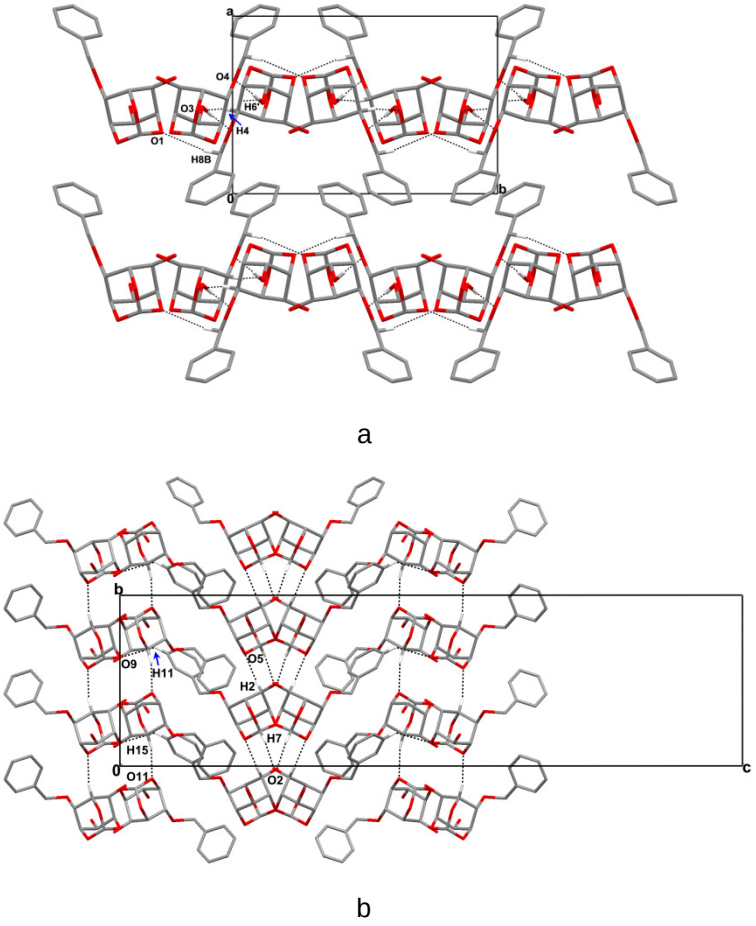

Figure 24. Molecular packing in crystals of 4.1 (a) form I: chains of glide and screw related molecules along the b-axis are linked by C-H···O interactions and (b) form II: chains of glide related molecules are linked by O-H···O and C-H···O interactions. Dotted lines represent hydrogen bonding interactions. Adjacent chains along the c-axis are linked by C11-H11···O9 contacts. H-atoms not involved in hydrogen bonding are omitted for the sake of clarity. The blue arrows indicate the atoms referred to by the atom labels.

Thus, strong intramolecular O-H···O interactions observed in solutions of 4.1 are carried over to the crystals of form I, which also exhibit a faster rate of crystallization than the form II crystals. The dimorphs exhibit similar patterns of O-H···O hydrogen bonding involving the C2-hydroxyl groups forming molecular chains, however the conformational differences in the C6-hydroxyl and C4-benzyl groups in the dimorphs result in dissimilar modes of packing in their crystals.

4.3. Conclusions

Analysis of the samples of racemic 4-*O*-benzyl-*myo*-inositol-1,3,5-orthoformate (4.1) stored for longer periods of time revealed the reason for its slow rate of crystallization and helped us to develop a reproducible procedure to obtain well defined crystals of a compound until now reported as a gum. The results suggest that the products formed on cleavage of the orthoformate during storage prevent the crystallization of 4.1 and

hence, it exists as a gum or turns to an amorphous solid on storage. Comparison of the structures of the dimorphs obtained show that conformational flexibility in even a small functional group such as the hydroxyl group can result in dissimilar molecular arrangement in the crystal lattice, leading to conformational dimorphs.[24, 25]

The enhanced molecular stability for 4.1, imparted by the crystal lattice as compared to the gummy state implies distinction in the molecular aggregation and intermolecular interactions in different states, resulting in an improved stability of molecules in the crystalline state.[19,26,27] There are several instances of small organic molecules exhibiting enhanced reactivity in the crystalline state, relative to solution or molten states, owing to proper orientation of the reactive functional groups in crystals.[28]

Such systems are valuable in organic synthesis and in understanding the reaction mechanisms. The results described in this chapter demonstrate the opposite, in that the molecules are imparted higher stability (or lower reactivity) in their crystal as compared to the gummy state. This aspect is of relevance in the context of understanding the stability of small molecules such as drugs and drug intermediates, which require storage over longer periods of time, without compromising on their purity and pharmaceutical performance. The latter could deteriorate due to changes in content or composition resulting from lack of molecular stability.

4.4. Experimental

Analysis of the samples of racemic 4-*O*-benzyl-*myo*-inositol 1,3,5-orthoformate (4.1)

Samples of the racemic benzyl ether **4.1** obtained as a gum (sample **4.1A**) by a reported[11] procedure, were stored (in sealed containers out of contact with air) for various periods of time and analyzed by IR and NMR spectroscopy

4.1B: **4.1A** was stored in a sealed flask at room temperature for a few days.

4.1C: Samples of **4.1A** stored in the refrigerator for upto a year.

The sample **4.1C** (0.09 g) on thin layer chromatographic analysis indicated the presence of two compounds. Column chromatography (silica 60-120 mesh, eluent, 1:1 ethyl acetate: hexane) of this sample yielded gummy **4.1** (0.051 g) and an amorphous solid **4.30** (0.017 g).

Acetylation of **4.30**: 0.017g **4.30** was acetylated using acetic anhydride (0.08 mL, 0.915 mmol) in pyridine (1 mL) for 48 h at ambient temperature. The solvents were evaporated under reduced pressure and the residue was dissolved in ethyl acetate and washed with dil. HCl, water and brine, the organic layer was dried over anhydrous sodium sulphate. Removal of the solvent under reduced pressure gave the known[29,30] penta acetate **4.31** (0.02 g, 67 % as a white flaky solid. M.p. 159-160 °C lit.[29] M.p. 162-164 °C.

4.1D: **4.1A** was stored below -10 °C for more than 2-3 weeks to form a shiny solid (sample).

Crystallisation of **4.1**

A freshly prepared gummy sample of **4.1** (sample **4.1A**, 0.5 g) was stored at -20 °C for 12 h to obtain a solid (sample **4.1E** M.p. 84-86 °C). It was dissolved in dichloromethane (4-5 mL). To this solution, light petroleum (boiling range 60-80°C) was added drop-wise till turbidity appeared and persisted. Minimum amount of dichloromethane was then added drop-wise till a clear solution was obtained. The mouth of the container was covered with perforated aluminium foil and the solution was allowed to stand at ambient temperature. Fine plates (Form I crystals) appeared in 5-6 h; complete crystallization took 48 h. M.p. 86-88°C. Our attempts to crystallize freshly prepared gummy sample **4.1A**, without storing at -20 °C failed.

Although we were able to observe the formation of form II crystals (M.p. 90 °C) in some of the stored samples of **4.1A**, we could not develop a procedure to obtain these

crystals consistently, perhaps due to long duration (several months during which 4.1 progressively decomposes to result in samples of varied purity) necessary for the formation of these crystals.

Synthesis of racemic 4-*O*-benzyl-*myo*-inositol 1,3,5-orthoacetate (4.28)

To an ice-cooled solution of *myo*-inositol 1,3,5-orthoacetate (4.27, 0.75 g, 3.72 mmol) in dry DMF (15 mL), sodium hydride (0.16 g, 4.09 mmol, 60% suspension in mineral oil) was added, followed by benzyl bromide (0.48 mL, 4.09 mmol). The reaction mixture was stirred at room temperature for 80 min, and then quenched with ice. The solvent was removed under reduced pressure and the residue was diluted with ethyl acetate. The organic layer was washed with dil. HCl, followed by brine, dried over anhydrous sodium sulphate and concentrated. The gum obtained was flash column chromatographed (230-400 mesh silica gel; eluent, 1:3 ethyl acetate : light petroleum) to obtain 4.28 (0.627 g, 58%) as a pale yellow gum. Crystals of racemic 4.28 could be obtained by slow evaporation of dichloromethane solution at ambient temperature, M.p. 90-94^{o}C. However, the crystals were small and sticky, resulting in poor quality X-ray diffraction data. Data for 4.28: IR ($CHCl_3$): 3484 cm^{-1}; ^1H NMR ($CDCl_3$, 200MHz): 7.44-7.27 (m, 5H), 4.67 (dd, J_1 = 11.6 Hz, J_2 = 13.4 Hz, 2H), 4.45-4.38 (m, 2H), 4.26-4.20 (m, 3H), 4.03 (m, 1H), 3.66 (d, J = 10.2 Hz, 1H, 2-OH exchangeable), 3.04 (d, J = 11.9 Hz, 1H, 6-OH exchangeable), 1.43 (s, 3H) ppm; ^{13}C NMR ($CDCl_3$, 50.32 MHz): 135.9 (C_{arom}), 128.9 (C_{arom}), 128.8 (C_{arom}), 128.1 (C_{arom}), 108.7 (CH_3CO), 75.3 (Ins C), 74.0 (Ins C), 73.0 (CH_2), 72.8 (Ins C), 67.7 (Ins C), 67.4(Ins C), 59.8 (CH_3), 24.1(CH_3); Elemental analysiscalcd (%) for $C_{15}H_{20}O_6$ (294.1103): C 61.22, H 6.16, found: C 61.14 , H 6.04 %.

Synthesis of racemic 4-*O*-benzyl-*myo*-inositol 1,3,5-orthobenzoate (4.29)

To an ice-cooled solution of *myo*-inositol 1,3,5-orthobenzoate (4.26 (0.768g, 2.15 mmol) in dry DMF (10 mL), sodium hydride (0.094 g, 2.36 mmol, 60% suspension in mineral oil) was added, followed by benzyl bromide (0.28 mL, 2.36 mmol). The reaction mixture was stirred at room temperature for 80 min, and then quenched with ice. The solvent was removed under reduced pressure and the residue was diluted with ethyl acetate. The organic layer was washed with dil. HCl, followed by brine, dried over anhydrous sodium sulphate and concentrated. The gum obtained was flash column chromatographed (230-400 mesh silica gel; eluent, 1:5 ethyl acetate : light petroleum) to obtain 4.29 (0.64 g, 84 %) as a white solid. Data for 4.29: Mp. = 86-88

°C; IR (CHCl3): CO 3600 cm^{-1}; ^{1}H NMR ($CDCl_3$, 200 MHz): / 7.58-7.63 (m, 2H, Ar H), 7.25-7.49 (m, 8H, Ar H), 4.70 (q, 2H, CH_2, J = 12 Hz), 4.50-4.62 (m, 2H, Ins H), 4.35-4.46 (m, 3H, Ins H), 4.15 (d, 1H, Ins H, J = 10 Hz), 3.75 (d, 1H, OH, J =10 Hz,), 3.14 (d, 1H, OH, J = 11 Hz) ppm; ^{13}C NMR ($CDCl_3$, 50.3 MHz): / 136.6 (C_{arom}), 135.9 (C_{arom}), 129.8 (C_{arom}), 129.0 (C_{arom}), 128.2 (C_{arom}), 127.1 (C_{arom}), 125.2 (C_{arom}), 107.5 ($PhCO_2$), 76.1 (Ins C), 74.1(Ins C), 73.6 (Ins C), 73.2 (CH_2), 68.2(Ins C), 67.8(Ins C), 60.0(Ins C) ppm. HRMS: m/z calcd for $C_{20}H_{21}O_6Na^+$: 379.1152 [M+ Na^+]; found: 379.1152

Crystallographic details

Single-crystal X-ray intensity measurements for crystals of 4.1 (form I and form II) were recorded at ambient temperature on a Bruker SMART APEX single crystal X-ray CCD diffractometer with graphite-monochromatized (Mo-K = 0.71073 Å) radiation. The X-ray generator was operated at 50 kV and 30 mA. Diffraction data were collected with a scan width of 0.3° at different settings of (0, 90, 180 and 270°) keeping the sample-to-detector distance fixed at 6.145 cm and the detector position (2) fixed at -28°. The X-ray data acquisition was monitored by SMART program.[31]. All the data were corrected for Lorentz-polarization effects using SAINT programs.[31] A semi-empirical absorption correction (multi-scan) based on symmetry equivalent reflections was applied using the SADABS[31] program. Lattice parameters were determined from least-squares analysis of reflections. The structures were solved by direct methods and refined by full-matrix least squares, based on F^2, using SHELX-97 software package[32].

All H atoms were placed in geometrically idealized positions (with C-H = 0.98 Å for inositol ring H atoms and orthoformate H atoms H7 and H21; C-H = 0.93 Å for aromatic H atoms; C-H = 0.97 Å for methylene H atoms) and constrained to ride on their parent atoms with U_{iso}(H) = 1.2U_{eq}(C). The O-bound H atoms were located in difference Fourier maps and refined isotropically. The refined O-H distances were in the range 0.77(3)–0.91(6) Å. In the form I crystals, the hydroxyl bond length O6-H6' was restrained to 0.86(3) Å using the DFIX command. Molecular and packing diagrams were generated using ORTEP-3[33] and Mercury CSD 2.3[34] respectively. Geometrical calculations were performed using SHELXTL and PLATON[34].

The geometrical parameters for H-bonding interactions. crystallographic data are summarized in Table 1 and Table 2. (Appendix)

4.5. References

1. Potter, B. V. L.; Lampe, D. Angew. Chem. Int. Ed. Engl. 1995, 34, 1933–1972.
2. Sureshan, K. M. ; Shashidhar, M. S.; Praveen, T.; Das, T. Chem. Rev. 2003, 103, 4477-4503.
3. Kim, S.; Lee, C. Cheong, Bull. Korean Chem. Soc. 2004, 25, 1578-1580.
4. Kilbas, B.; Balci, M. Tetrahedron 2011, 67, 2355–2389.
5. Song, F.; Zhang, J.; Zhao, Y.; Chen, W.; Lib, L.; Xi, Z. Org. Biomol. Chem. 2012, 10, 3642-3654.
6. Song, F.; Zhang, J.; Cui, Q., Wang, T.; Chen, W.; Li, L.; Xi Z. Tetrahedron Lett. 2012, 53, 1102–1104.
7. Baudin, G.; Glänzer, B. I.; Swaminathan, K. S.; Vasella, A. Helv. Chim. Acta 1988, 71, 1367-1378.
8. Sato, K.; Akai, S. I.; Sugita, N.; Ohsawa, T.; Kogure, T.; Shoji, H.; Yoshimura, J. J. Org. Chem., 2005, 70, 7496-7504.
9. Devaraj, S.; Jagdhane, R. C.; Shashidhar, M. S. Carbohydr. Res. 2009, 344, 1159–1166 and references cited therein.
10. Devaraj, S.; Shashidhar, M. S.; Dixit, S. S. Tetrahedron 2005, 61, 529–536.
11. Billington, D. C.; Baker, R.; Kulagowski, J. J.; Mawer, I. M.; Vacca, J. P.; deSolms, S. J.; Huff, J. R. J. Chem. Soc. Perkin Trans. 1 1989, 1423–1429.
12. Reginato, G.; Ricci, A., Roelens, S., Scapecchi, S. J. Org. Chem 1990, 55, 5132-5139.
13. Murali, C.; Shashidhar, M. S.; Gonnade, R. G.; Bhadbhade, M. M. Chem. Eur. J. 2009, 15, 261–269.
14. Padiyar, L. T.; Wen, Y.; Hung, S. Chem. Commun. 2010, 46, 5524–5526.
15. Das, T.; Shashidhar, M. S. Carbohydr. Res. 1998, 308, 165-168.
16. Sureshan, K. M.; Shashidhar, M. S. Tetrahedron 2009, 65, 2703-2710.
17. Iemma, F.; Trombino, S.; Puoci, F.; Di, G.; Spizzirri, U. G.; Muzzalupo, R.; Picci, N. Macromol. Biosci. 2005, 5, 1049–1056.
18. Billington, D. C.; Baker, R. J. Chem. Soc., Chem. Commun. 1987, 1011-1013.
19. Gurale, B. P.; Krishnaswamy, S.; Kumar , V.; Shashidhar, M. S. Tetrahedron 2011, 67, 7280–7288.

20. Murali, C.; Shashidhar, M. S.; Gopinath, C. S. Tetrahedron 2007, 63, 4149-4155.
21. Taft Jr., R. W. J. Am. Chem. Soc. 1952, 74, 3120–3128.
22. Uhlmann, P.; Vasella, A. Helv. Chim. Acta 1992, 75, 1979–1994.
23. Bernet, B.; Vasella, A. Helv. Chim. Acta 2000, 83, 995–1021.
24. Ibberson, R. M.; Parsons, S.; Allen, D. R.; Bell, A. M. T. Acta Crystallogr. Sect B 2008, 64, 573-582.
25. Krishnaswamy, S.; Gonnade, R. G.; Bhadbhade, M. M.; Shashidhar, M. S. Acta Crystallogr. Sect., C 2009, 65, o54-o57.
26. Beristain, M. F.; Fomine, S.; Ogawa, T. Mol. Cryst. Liq. Cryst. 2006, 447, 251-263.
27. Kaupp, G. J. Phys. Org. Chem. 2008, 21, 630-643.
28. Krishnaswamy, S.; Shashidhar , M. S.; Bhadbhade, M. CrystEngComm. 2011, 13, 3258–3264 and references cited therein.
29. Podeschwa, M. A. L.; Plettenberg, O.; Altenbach, H. Eur. J. Org. Chem. 2005, 3116-3127.
30. Gigg, J.; Gigg, R.; Payne, S.; Conant, R. J. Chem. Soc., Perkin Trans 1 1987, 423-429.
31. Bruker 2003. SADABS Version 2.05, SMART Version 5.631 and SAINT Version 6.45. Bruker AXS Inc., Madison, Wisconsin, USA.
32. Sheldrick, G. M. Acta Crystallogr., Sect. A: Found. Crystallogr. 2008, 64, 112–122.
33. Farrugia, L. J. J. Appl. Crystallogr. 1997, 30, 565-566.
34. Macrae, C. F.; Edgington, P. R.; McCabe, P.; Pidcock, E.; Shields, G. P.; Taylor, R.; Towler, M.; van de Streek, J. J. Appl. Crystallogr. 2006, 30, 453–457.

Appendix III

Appendix III Index

Table 1 Geometrical parameters for H-bonding interactions.

Form	D-H···A	D-H (Å)	H···A (Å)	D···A (Å)	D-H···A (°)
I	O2- + ¶ Â Ã Â 2	0.77(3)	2.21(3)	2.910(3)	152(3)
	O6- + ¶ Â Â Â 2	0.86(3)	2.10(3)	2.802(3)	139(3)
	O8- + ¶ Â Âii Â 2	0.81(4)	2.25(3)	3.004(3)	155(4)
	O10- + ¶ Â Â Â	0.88(4)	2.05(4)	2.804(3)	143(4)
	C1- + Â Âiii Â 2	0.98	2.58	3.380(3)	139
	C2- + Â Âiv Â 2	0.98	2.48	3.459(3)	174
	C7- + Â Âv Â 2	0.98	2.22	3.193(4)	170
	C11- + Â Âvi Â 2	0.93	2.57	3.296(4)	136
	C15- + Â Â Âvii 2	0.98	2.42	3.366(3)	164
II	O2- + ¶ Â Âviii Â 2	0.84(6)	2.08(5)	2.839(4)	151(6)
	O6- + ¶ Â Âix Â 2	0.91(7)	1.92(7)	2.824(4)	175(6)
	C1- + Â Âx Â 2	0.98	2.44	3.364(5)	158
	C4- + Â Âxi Â 2	0.98	2.55	3.495(4)	161

*Intramolecular interaction

Symmetry codes: (i) x ±½, y, -z + ½; (ii) ½ +x, ½ - y, -z; (iii) x + ½, y, -z + ½; (iv) ±x + 3/2, y + ½, z; (v) ±x + 1, y ±½, -z + ½; (vi) ±x, -y + 1, -z; (vii) ±x + ½, y ±½, z; (viii) x, -y + ½, z + ½; (ix) ±x + 1, -y, -z; (x) x. ±y + ½, z ±½; (xi) ±x + 1, -y, -z + 1.

Table 3: Crystallographic data for dimorphs of 4.1

	Form I	Form II
Chemical formula	$C_{14}H_{16}O_6$	$C_{14}H_{16}O_6$
M_r	280.27	280.27
Temperature (K)	297(2)	297(2)
Morphology	Plate	plate
Crystal size	0.22 × 0.12 × 0.07	0.17 × 0.15 × 0.0
Crystal system	Orthorhombic	Monoclinic
Space group	Pbca	$P2_1/c$
a/Å	10.460(5)	10.4043(17)
b/Å	11.536(5)	13.720(2)
c/Å	42.364(19)	10.3515(17)
./ °	90	90
E/°	90	118.031(3)
/ °	90	90
V/Å^3	5112(4)	1304.3(4)
Z	16	4
D_{calc} (g cm^{-3})	1.457	1.427
P(mm^{-1})	0.115	0.112
F(000)	2368	592
T_{min}	0.975	0.981
T_{max}	0.992	0.991
h,k, l (min, max)	(-11, 12), (-13, 13), (-46, 50)	(-12, 12), (-16, 16), (-9, 12)
Reflns collected	24154	6531
Unique reflns	4500	2307
Observed reflns	2952	1591
R_{int}	0.0616	0.0583
No. of parameters	377	189
GoF	1.024	1.224
R_1[I > 2 V(I)]	0.0513	0.0852
wR_2[I > 2 V(I)]	0.1163	0.1454
R_1_all data	0.0867	0.1280
wR_2_all data	0.1343	0.1581
û U$_{max}$ û U$_{min}$ (e Å^{-3})	0.45,-0.26	0.20,-0.21
CCDC No.	848918	848919

^{1}H NMR

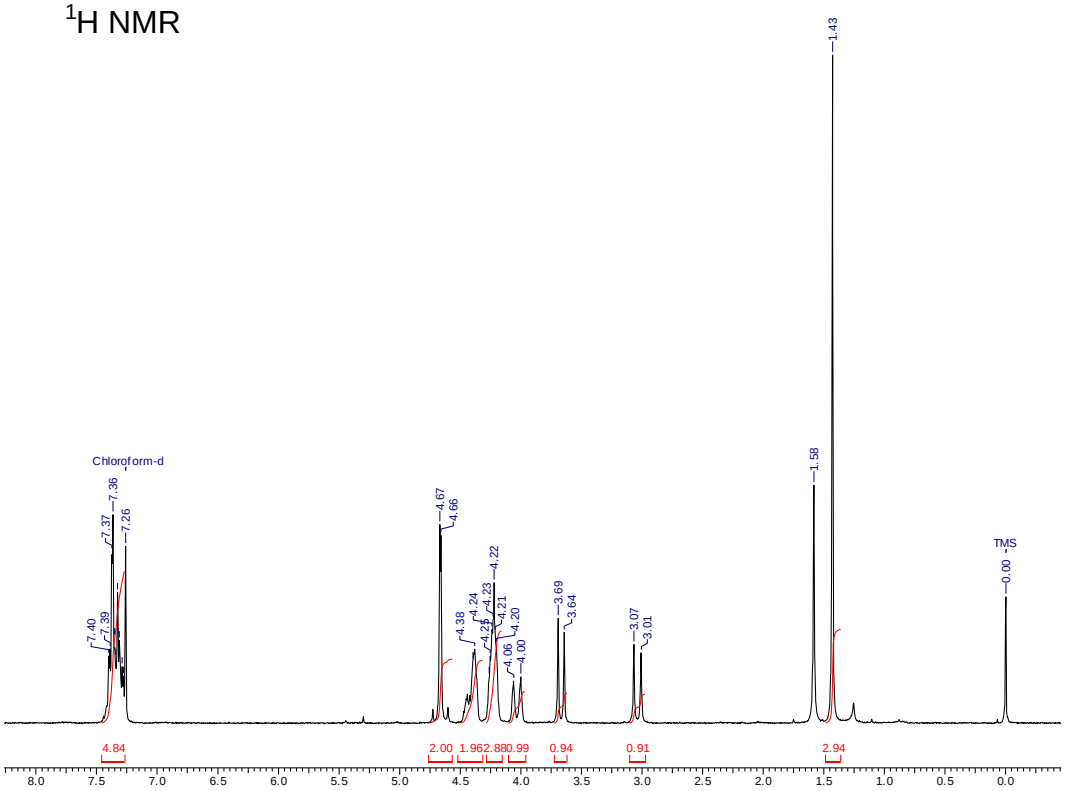
Chloroform-d
7.40
7.39
7.37
7.36
7.26
4.67
4.66
4.38
4.24
4.23
4.22
4.21
4.20
4.06
4.00
3.69
3.64
3.07
3.01
1.58
1.43
TMS
0.00
4.84
2.00
1.96
2.88
0.99
0.94
0.91
2.94

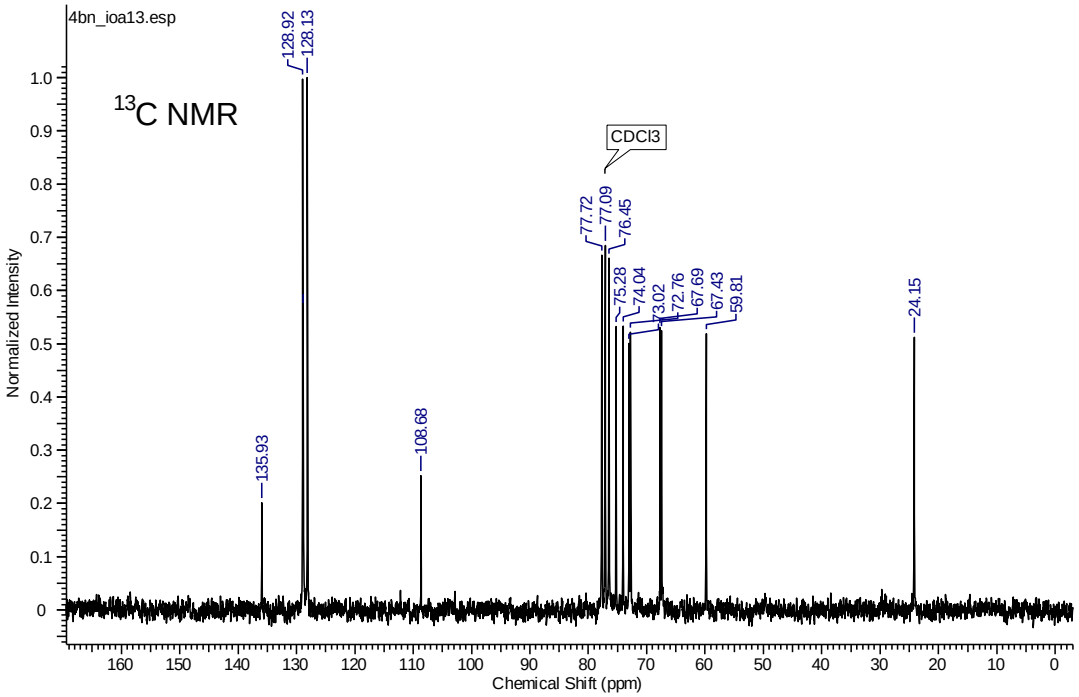
4bn_ioa13.esp
^{13}C NMR
Normalized Intensity
Chemical Shift (ppm)
CDCl3
128.92
128.13
135.93
108.68
77.72
77.09
76.45
75.28
74.04
73.02
72.76
67.69
67.43
59.81
24.15

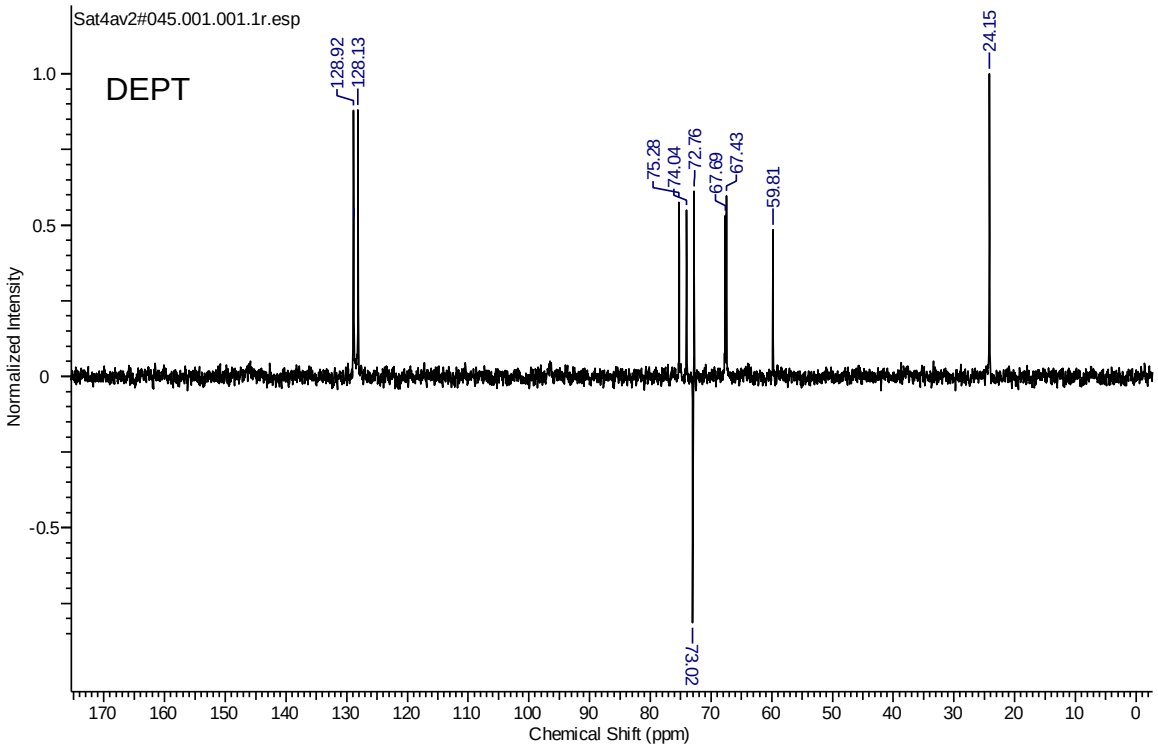
Sat4av2#045.001.001.1r.esp
DEPT
128.92
128.13
24.15
75.28
74.04
72.76
67.69
67.43
59.81
73.02
Normalized Intensity
Chemical Shift (ppm)

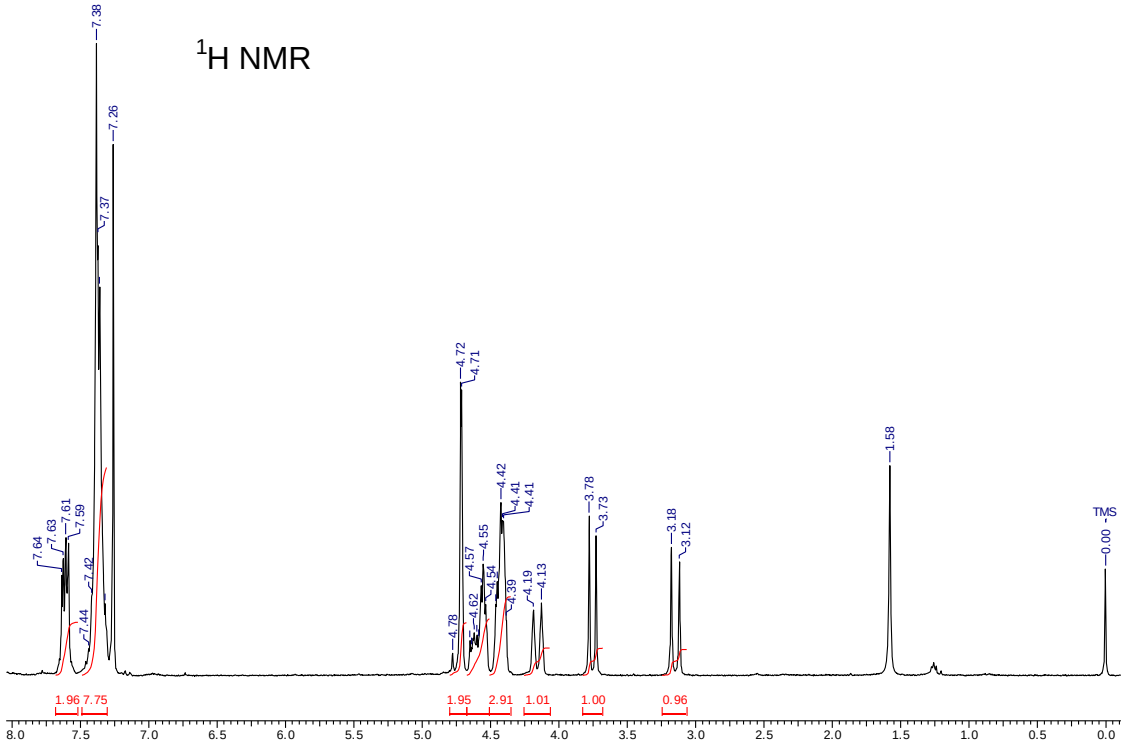
1H NMR
7.38
7.26
7.37
7.64
7.63
7.61
7.59
7.42
7.44
4.72
4.71
4.42
4.41
4.41
4.57
4.55
4.54
4.62
4.39
4.19
4.13
4.78
3.78
3.73
3.18
3.12
1.58
TMS
0.00
1.96 7.75
1.95
2.91
1.01
1.00
0.96

^{13}C NMR

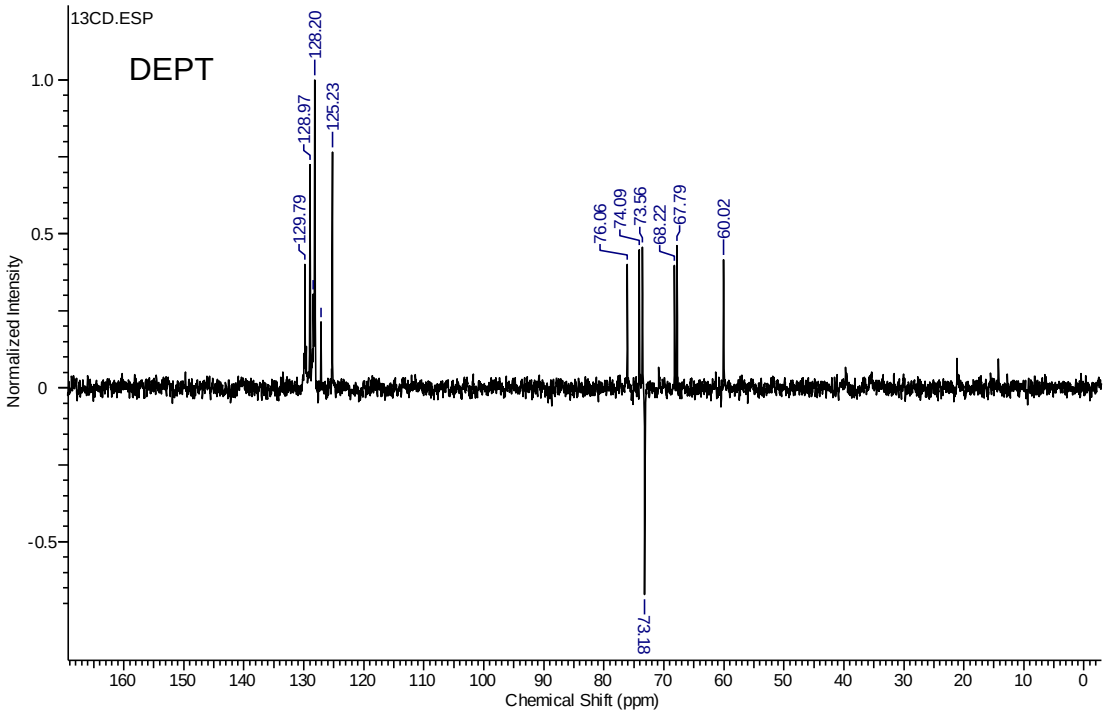
13CD.ESP
DEPT
128.20
128.97
125.23
129.79
76.06
74.09
73.56
68.22
67.79
60.02
73.18
Normalized Intensity
1.0
0.5
0
-0.5
160
150
140
130
120
110
100
90
80
70
60
50
40
30
20
10
0
Chemical Shift (ppm)